

EXPERIMENTAL AND COMPUTATIONAL STUDY OF A SCALED REACTOR  
CAVITY COOLING SYSTEM

A Dissertation

by

RODOLFO VAGHETTO

Submitted to the Office of Graduate and Professional Studies of  
Texas A&M University  
in partial fulfillment of the requirements for the degree of

DOCTOR OF PHILOSOPHY

Chair of Committee,	Yassin A. Hassan
Committee Members,	Kalyan Annamalai
	Maria D. King
	William H. Marlow
Head of Department,	Yassin A. Hassan

December 2013

Major Subject: Nuclear Engineering

Copyright 2013 Rodolfo Vaghetto

## ABSTRACT

The Very High Temperature Gas-Cooled Reactor (VHTR) is one of the next generation nuclear reactors designed to achieve high temperatures to support industrial applications and power generation. The Reactor Cavity Cooling System (RCCS) is a passive safety system that will be incorporated in the VHTR, designed to remove the heat from the reactor cavity and maintain the temperature of structures and concrete walls under desired limits during normal operation and accident scenarios. A small scale (1:23) water-cooled experimental facility was scaled, designed, and constructed in order to study the complex thermohydraulic phenomena taking place in the RCCS during steady-state and transient conditions. The facility represents a portion of the reactor vessel with nine stainless steel coolant risers and utilizes water as coolant. The facility was equipped with instrumentation to measure temperatures and flow rates and a general verification was completed during the shakedown. A model of the experimental facility was prepared using RELAP5-3D and simulations were performed to validate the scaling procedure. The overall behavior of the facility met the expectations. The steady-state condition was achieved and the facility capabilities were confirmed to be very promising in performing additional experimental tests, including flow visualization, and produce data for code validation. The experimental data produced during the steady-state run were successfully compared with the simulation results obtained using RELAP5-3D, confirming the capabilities of the system code of simulating the thermal-hydraulic phenomena occurring in the reactor cavity.

## ACKNOWLEDGEMENTS

The project was funded by the Nuclear Energy University Program (NEUP) and the US Department of Energy (DOE).

The author would like to acknowledge the technical collaboration with other universities and institutions:

- University of Wisconsin, Madison: Prof. M. Corradini and his students.
- University of Idaho: Prof. A. Tokuhiro and his students.
- Argonne National Laboratory: Dr. T. Wei.

## NOMENCLATURE

ANL	Argonne National Laboratory
CFD	Computational Fluid Dynamics
D	Diameter
DCC	Depressurized Conduction Cooldown
DOE	Department Of Energy
GFR	Gas-cooled Fast Reactor
GT-MHR	Gas Turbine-Modular Helium Reactor
HS	Heat Structure
IAEA	International Atomic Energy Agency
ID	Inner Diameter
INL	Idaho National Laboratory
IRUG	International RELAP5 Users Group
L	Length
LFR	Lead-cooled fast reactor
LOCA	Loss of Coolant Accident
LWR	Light Water Reactor
MHTGR	Modular High Temperature Gas-Cooled Reactor
MSR	Molten Salt Reactor
NEUP	Nuclear Energy University Program
NSTF	Natural Convection Shutdown Heat Removal Test Facility

OD	Outer Diameter
PCS	Power Conversion System
PRV	Pressurized Reactor Vessel
PWR	Pressurized Water Reactor
RCCS	Reactor Cavity Cooling System
SCS	Shutdown Cooling System
SCWR	Supercritical-water-cooled reactor
SFR	Sodium-cooled fast reactor
SS	Stainless Steel
S-S	Steady-State
TC	Thermocouple
USB	University Science Building
VHTR	Very High Temperature Gas-Cooled Reactor

## TABLE OF CONTENTS

	Page
ABSTRACT .....	ii
ACKNOWLEDGEMENTS .....	iii
NOMENCLATURE .....	iv
TABLE OF CONTENTS .....	vi
LIST OF FIGURES .....	x
LIST OF TABLES .....	xvii
CHAPTER I INTRODUCTION .....	1
CHAPTER II PURPOSE .....	15
CHAPTER III RESEARCH APPROACH .....	17
III.1 Phase 1: Data Collection and Literature Review .....	17
III.2 Phase 2: Scaling Approach.....	18
III.3 Phase 3: Facility Design and Material Selection.....	18
III.4 Phase 4: RELAP5-3D Model Preparation.....	19
III.5 Phase 5: Facility Design Completion, Vendor Selection, and Construction.....	20
III.6 Phase 6: Instrumentation Selection and Installation .....	21
III.7 Phase 7: Facility Shakedown.....	22
III.8 Phase 8: Analysis of the Experimental Data and Comparison with Simulations.....	23
CHAPTER IV PHASE 1: DATA COLLECTION AND LITERATURE REVIEW.....	24
CHAPTER V PHASE 2: SCALING APPROACH .....	33
V.1 Number of Risers.....	38
V.2 Pipes Dimensions .....	39
V.3 Materials.....	39
V.4 Panel Configuration.....	40
V.5 Panel-to-Vessel Distance.....	42
V.6 Water Tank Scaling.....	44

	Page
CHAPTER VI PHASE 3: FACILITY DESIGN AND MATERIALS SELECTION	46
VI.1 Reactor Cavity Assembly Design	47
VI.1.1 Reactor Vessel	48
VI.1.2 RCCS Cooling Panel	51
VI.1.3 Cavity Walls	53
VI.1.4 Manifolds	54
VI.2 Water Tank Design and Elevation	56
VI.3 Primary Structure and Scaffold Design	59
VI.3.1 Primary Structure	59
VI.3.2 Scaffold	60
VI.4 Pipeline Design	62
VI.5 Secondary Heat Removal System Design	64
CHAPTER VII PHASE 4: RELAP5-3D MODEL PREPARATION AND PRELIMINARY ANALYSIS	66
VII.1 RELAP5-3D Nodalization	68
VII.1.1 Heat Structures	71
VII.1.2 Pipelines and Tank	71
VII.1.3 Reactor Cavity	71
VII.1.4 Radiation View Factors	76
VII.1.5 Risers' Heat Structures Settings	79
VII.2 Steady-State Scaling Laws Confirmation	81
VII.3 Transient Simulations	84
VII.3.1 Simulation Results: System Time Response	86
VII.3.2 Simulation Results: Flow Regimes	89
VII.3.3 Simulation Results: Flow Rate and Two-Phase Flow Oscillations	91
VII.3.4 Simulation Results: Cavity Energy Balance	96
VII.4 Sensitivity Analysis	97
VII.4.1 Sensitivity Analysis of the Water Tank Nodalization	98
VII.4.2 Sensitivity Analysis of the Top Manifold Nodalization	101
VII.4.3 Water Tank Liquid Level Sensitivity Analysis	105
CHAPTER VIII PHASE 5: FACILITY DESIGN COMPLETION, VENDOR SELECTION, AND CONSTRUCTION	110
VIII.1 Reactor Cavity	111
VIII.1.1 Risers' Panel	111
VIII.1.2 Reactor Vessel	118
VIII.1.3 Electric Heaters and Controller	121
VIII.2 Manifolds	125

	Page
VIII.3 Water Tank .....	128
VIII.4 Pipeline and Pipe Connections .....	135
VIII.4.1 The Downcomer .....	136
VIII.4.2 The Bottom Section .....	140
VIII.4.3 The Upward Pipeline .....	141
VIII.4.4 The Top Section .....	143
VIII.4.5 Other Connections .....	144
VIII.5 Structures .....	145
VIII.5.1 Primary Support Structure .....	146
VIII.5.2 Scaffolding .....	150
VIII.5.3 Secondary Support Structures .....	153
 CHAPTER IX PHASE 6: INSTRUMENTATION SELECTION AND INSTALLATION .....	 162
IX.1 Measurement of the Temperature .....	164
IX.1.1 Temperature of the Walls .....	164
IX.1.2 Temperature of the Coolant .....	168
IX.2 Measurement of the Coolant Flow Rate .....	173
IX.3 Data Acquisition System .....	177
 CHAPTER X PHASE 7: FACILITY SHAKEDOWN .....	 179
X.1 Step 0: Facility Preparation .....	179
X.1.1 Refill and Drain System .....	180
X.1.2 Secondary Heat Removal System .....	182
X.2 Step 1: Leak Tests (Room Temperature) .....	186
X.3 Step 2: Leak Tests (Final Steady-State Temperature) .....	186
X.4 Step 3: Empty Test (Heat Flux Verification) .....	187
X.5 Step 4: Thermal Insulation Installation .....	189
X.5.1 Insulation of the Reactor Cavity .....	190
X.5.2 Insulation of the Pipeline .....	197
X.5.3 Insulation of the Water Tank .....	201
X.6 Step 5: Final Tests and Test Repeatability .....	203
X.7 Step 6: RELAP5-3D Model Refinement and Comparison with Shakedown Tests .....	 215
 CHAPTER XI PHASE 8: ANALYSIS OF THE EXPERIMENTAL DATA AND COMPARISON WITH SIMULATIONS .....	 220
XI.1 Experimental Procedure .....	221
XI.2 Test Results – Main Parameters .....	223
XI.3 Test Results – Other Parameters .....	231

	Page
XI.4 RELAP5-3D Simulations and Comparison with the Experimental Data .....	236
CHAPTER XII ISSUES RESOLUTION PLAN .....	243
XII.1 Issues Directly Inherent to the Experimental Facility .....	244
XII.1.1 Flanged Connections.....	244
XII.1.2 Pipe-to-Pipe Connections .....	248
XII.2 Issues Related to the Support Structures .....	250
XII.3 Issues in the Facility Instrumentation .....	254
XII.3.1 Thermocouple Probes .....	254
XII.3.2 Thermocouple Wires.....	255
XII.4 Other Issues to Be Addressed .....	256
CHAPTER XIII CONCLUSIONS.....	257
REFERENCES.....	260
APPENDIX A – SCAFFOLDING CAPACITY VERIFICATION.....	266
APPENDIX B – ANCHORS CAPACITY VERIFICATION .....	272
APPENDIX C – SOLIDWORKS STRUCTURE ANALYSIS .....	273
APPENDIX D – HEATERS SPECIFICATIONS .....	277
APPENDIX E – EPOXY PAINT MATERIAL SAFETY DATASHEETS .....	279
APPENDIX F – PIPING LAYOUT CALCULATIONS .....	287
APPENDIX G – RISERS’ PANLE WELDING CERTIFICATE .....	291
APPENDIX H – EPOXY GLUE SPECIFICATIONS .....	296
APPENDIX I – PROJECT SAFETY ANALYSIS (PSA) .....	297

## LIST OF FIGURES

	Page
Figure 1. Carbon Emissions History and Projections. ....	2
Figure 2. 50-year Ahead Carbon Emission Projections. ....	3
Figure 3. Evolution of Nuclear Energy Systems. ....	4
Figure 4. Generation IV Nuclear Systems [7] (1: GFR; 2: VHTR; 3: SCWR; 4: SFR; 5: LFR; 6: MSR). ....	7
Figure 5. Air-Cooled RCCS - General Atomic Design [8]. ....	10
Figure 6. Water-Cooled RCCS - AREVA Design [13]. ....	11
Figure 7. Typical RCCS Configuration. ....	13
Figure 8. GT-MHR Reactor Building Layout and Internals [3]. ....	26
Figure 9. Schematic and Main Dimensions of the Reactor Pressure Vessel. ....	28
Figure 10. Comparison of Reactor Pressure Vessel Sizes ....	29
Figure 11. GT-MHR Vessel and Cavity Dimensions ....	30
Figure 12. Typical Reactor Cavity Internals and RCCS Layout. ....	31
Figure 13. Shield Configuration. ....	40
Figure 14. Fin Configuration (Selected) ....	41
Figure 15. Pitch Configurations (Top: Selected; Bottom: Alternative) ....	42
Figure 16. Reactor Cavity Floor Plan. ....	43
Figure 17. Reactor Vessel (Front View) ....	49
Figure 18. Reactor Vessel (Back View). ....	50

	Page
Figure 19. RCCS Panel .....	52
Figure 20. Manifold.....	55
Figure 21. Water Tank .....	58
Figure 22. Scaffold and Elevations .....	61
Figure 23. Experimental Facility Overview.....	63
Figure 24. Secondary Heat Removal System Schematic.....	65
Figure 25. RELAP5-3D Nodalization Diagrams (A: Symmetric Version; B: Asymmetric Version).....	69
Figure 26. Cavity Nodalization and Heat Structures Arrangement.....	72
Figure 27. Heat Transfer Mechanisms in the Cavity .....	73
Figure 28. NEVADA Input Geometry .....	77
Figure 29. Risers' Heat Structure Definition.....	79
Figure 30. Scaling Validation Method - Flow Chart.....	82
Figure 31. Tank Nodalization for Transient Analysis.....	85
Figure 32. Tank Void Fractions .....	88
Figure 33. Coolant Mass Flow Rate.....	92
Figure 34. Mass Flow Oscillations.....	93
Figure 35. Water Temperature (Central Pipe, Heated Section, Volume 20503).....	95
Figure 36. Temperature Oscillations (Central Pipe, Heated Section, Volume 20503). ...	96
Figure 37. Primary Coolant Mass Flow Rate.....	99
Figure 38. Secondary Coolant Mass Flow Rate.....	99

	Page
Figure 39. Primary Coolant Temperature (Cavity Outlet).....	100
Figure 40. New Top Manifold Nodalization.....	102
Figure 41. Risers' Flow Rate and Manifold Collapsed Liquid Level.....	103
Figure 42. Flow Direction (Snapshots).....	104
Figure 43. Water Tank Nodalization and Initial Liquid Levels.....	105
Figure 44. Water Tank Collapsed Liquid Level.....	106
Figure 45. Time to Liquid Level at the Jet Elevation.....	108
Figure 46. Time to Tank Depletion.....	109
Figure 47. Risers' Panel Drawing and Specifications.....	112
Figure 48. Risers' Panel as Fabricated.....	114
Figure 49. Risers' Panel Top Plate.....	115
Figure 50. Risers' Panel at the End of the Welding Process.....	116
Figure 51. Risers' Panel Final Configuration.....	117
Figure 52. Reactor Vessel Drawing.....	119
Figure 53. Reactor Vessel.....	120
Figure 54. Raw Materials.....	121
Figure 55. Electric Radiant Heaters (Front View).....	122
Figure 56. Electric Radiant Heaters (Back View).....	123
Figure 57. Heaters Controller Panel.....	124
Figure 58. Manifolds' Drawing.....	126
Figure 59. Glass Manifold (Top).....	127

	Page
Figure 60. Water Tank Modifications .....	130
Figure 61. Tank Windows.....	131
Figure 62. Tank Windows - Final Configuration.....	132
Figure 63. Tank View - Internals.....	134
Figure 64. Tank Supporting Frame.....	135
Figure 65. Downcomer - Upper Section.....	137
Figure 66. Polycarbonate Flanged Connection.....	138
Figure 67. Stainless Steel - Polycarbonate Connection.....	139
Figure 68. Bottom Section.....	140
Figure 69. Upward Pipe.....	142
Figure 70. Top Section.....	144
Figure 71. Vertical Posts before Installation.....	147
Figure 72. Main Support Structure - Lower Working Deck.....	148
Figure 73. Main Support Structure - Upper Working Deck.....	149
Figure 74. Scaffolding – Dimensions (British Units).....	151
Figure 75. Scaffold Flooring.....	153
Figure 76. Tank Support.....	154
Figure 77. Tank Support Installment.....	155
Figure 78. Vertical Pipes Support Structure.....	156
Figure 79. Horizontal Support Columns.....	157
Figure 80. Top Manifold Supports.....	158

	Page
Figure 81. Vessel and Heaters Supports.....	159
Figure 82. Risers' Panel Support. ....	161
Figure 83. Instrumentation Layout.....	163
Figure 84. Risers' Panel Thermocouples Layout.....	165
Figure 85. Thermocouple Holes Locations. ....	166
Figure 86. Thermocouple Wires on the Risers' Panel (Front).....	167
Figure 87. Risers Thermocouples Fittings. ....	169
Figure 88. Thermocouples Configuration - Risers Panel (Back).....	170
Figure 89. Other Thermocouple Probes Locations. ....	171
Figure 90. Magnetic Flow Meter. ....	175
Figure 91. Ultrasonic Flow Meter. ....	176
Figure 92. Data Acquisition System. ....	178
Figure 93. Refill and Draining System.....	181
Figure 94. Schematic Configuration of the Proposed Heat Removal System. ....	183
Figure 95. Heat Removal System - Final Installation. ....	185
Figure 96. Dry test - Temperature Profile (Row 5). ....	188
Figure 97. Microtherm Panels in the Reactor Cavity.....	191
Figure 98. Cavity Insulation - Heaters Side Panels Preparation. ....	192
Figure 99. Cavity Insulation - Heaters Side Complete Microtherm Panels Intallation..	193
Figure 100. Silica Mats Installation in the Reactor Cavity. ....	195
Figure 101. Cavity Final Insulation Installment (Side View). ....	196

	Page
Figure 102. Cavity Final Insulation Installment (Top View).....	197
Figure 103. Polyurethane Pipe Insulation. ....	198
Figure 104. Polyurethane Pipe Insulation Installation. ....	199
Figure 105. Insulation of the Secondary Heat Removal Pipeline. ....	200
Figure 106. Water Tank Insulation. ....	202
Figure 107. Coolant Volumetric Flow Rate (Run 1 and Run 2). ....	205
Figure 108. Coolant Volumetric Flow Rate and Heaters Power (Run 3). ....	207
Figure 109. Rhodamine Injection Technique. ....	209
Figure 110. Flow Visualization at the Bottom Manifold. ....	210
Figure 111. Coolant Cavity Inlet and Outlet Temperatures (Run 3).....	211
Figure 112. New Hose Clamp Connections (Top Manifold). ....	213
Figure 113. Constant Pressure Hose Clamps - Final Configuration. ....	214
Figure 114. Cavity Heat Structure Nodalization - Original (Left), New (Right).....	216
Figure 115. Shakedown Experimental Data and RELAP-3D Simulation Results.....	218
Figure 116. Water Inlet and Outlet Cavity Temperatures and RELAP5-3D New Model Prediction. ....	219
Figure 117. Secondary Coolant Temperatures. ....	225
Figure 118. Coolant Cavity Temperatures. ....	227
Figure 119. Water Tank Coolant Temperatures. ....	229
Figure 120. Primary Coolant Volumetric Flow Rate. ....	230
Figure 121. Risers' Probes Layout.....	232

	Page
Figure 122. Risers' Coolant Temperatures (wp = water probe). .....	233
Figure 123. Risers' Coolant Temperature Rise (Row 5 - Row 1). .....	235
Figure 124. Secondary Heat Removal Nodalization. ....	237
Figure 125. Secondary Coolant Temperature. ....	238
Figure 126. Cavity Inlet Coolant Temperature. ....	239
Figure 127. Cavity Outlet Coolant Temperature. ....	240
Figure 128. Main Coolant Volumetric Flow Rate.....	241
Figure 129. Tank Outlet Flange Modification (Original: Left; Modified: Right).....	246
Figure 130. Upward Pipe Mid-Section Flange Modification (Original: Left; Modified: Right) .....	247
Figure 131. Upward Pipe Top Flange Modification (Original: Left; Modified: Right)	248
Figure 132. Manifold-to-Panel Connection Replacement (Original: Top; Modified: Bottom). ....	249
Figure 133. Welded Braces (Corner). ....	251
Figure 134. Welded Braces (Top).....	252
Figure 135. Tension Cables Layout. ....	253

## LIST OF TABLES

	Page
Table 1. Scaling Factors .....	36
Table 2. Thermal Power .....	37
Table 3. Experimental Facility Design Basic Characteristics .....	46
Table 4. Tank Characteristics .....	57
Table 5. Legend of Figure 7. ....	64
Table 6. Cavity Heat Structures Summary .....	75
Table 7. Radiation View Factors .....	78
Table 8. Steady-State Risers Inlet/Outlet Temperatures Summary .....	83
Table 9. Flow Regimes in the Risers .....	90
Table 10. Flow Regimes in other Components. ....	91
Table 11. Cavity Energy Balance .....	97
Table 12. Water Tank Nodalization Sensitivity - Summary. ....	101
Table 13. Original Water Tank - Dimensions .....	128
Table 14. Parts Dimensions (British Units). ....	152
Table 15. Thermocouples Summary. ....	172
Table 16. Shakedown Tests Procedure. ....	204
Table 17. Test Conditions. ....	221
Table 18. Experiment Initial Conditions. ....	223
Table 19. Project Resolution Summary .....	259

# CHAPTER I

## INTRODUCTION

The global greenhouse gas emissions, constantly grown since the pre-industrial times, have increased approximately 70% between 1970 and 2004. With the current climate change mitigation policies and practices, the global greenhouse gas emissions will continue to grow, contributing to the earth's long lasting climate changes which may impact temperatures, precipitation rates, sea level, ice and snow cover surface, storm frequency and intensity, and desertification [1].

Figure 1 presents the carbon emissions trend within a 100-year period (from 1955 to 2055) [2].

As the figure shows, carbon emissions from fossil fuel burning are projected to double in the next 50 years, keeping the world on course to more than triple the atmosphere's carbon dioxide concentration from its pre-industrial level. This path (black dashed line) is predicted to lead to significant global warming by the end of this century.

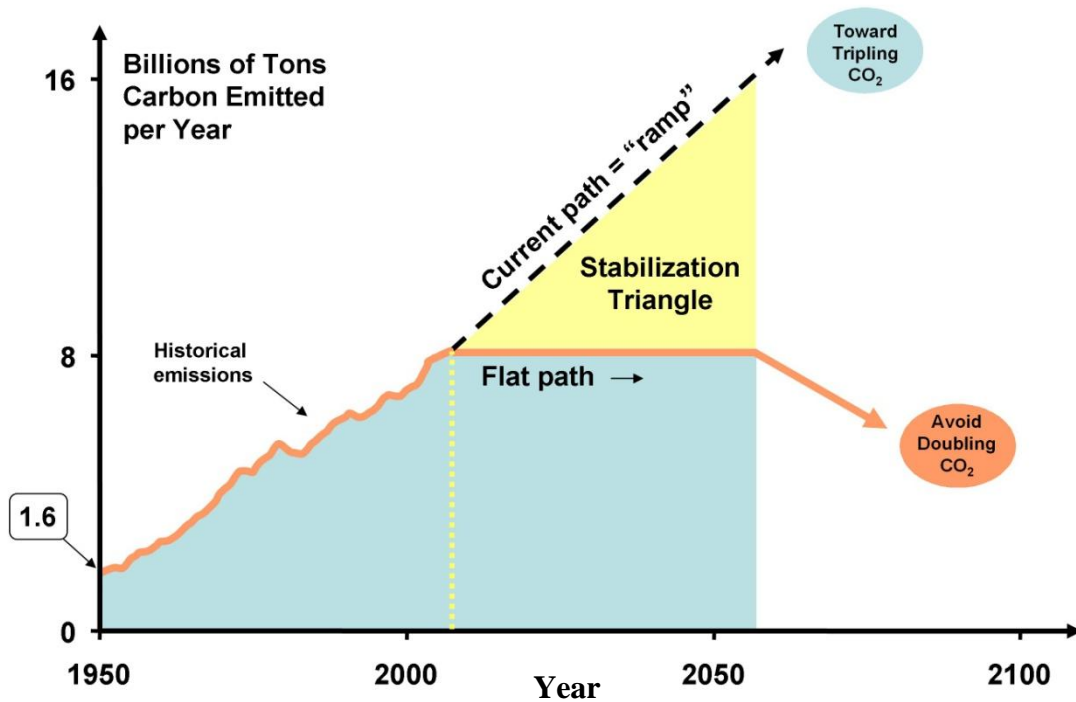


**Figure 1. Carbon Emissions History and Projections.**

The flat path, followed by emissions reductions later in the century, is predicted to limit CO<sub>2</sub> rise to less than a doubling and skirt the worst predicted consequences of climate change.

Keeping emissions flat for 50 years will require trimming projected carbon output by roughly 8 billion tons per year by 2060, keeping a total of 200 billion tons of carbon from entering the atmosphere (yellow triangle). This carbon saving is sometimes referred as the stabilization triangle [2,3].

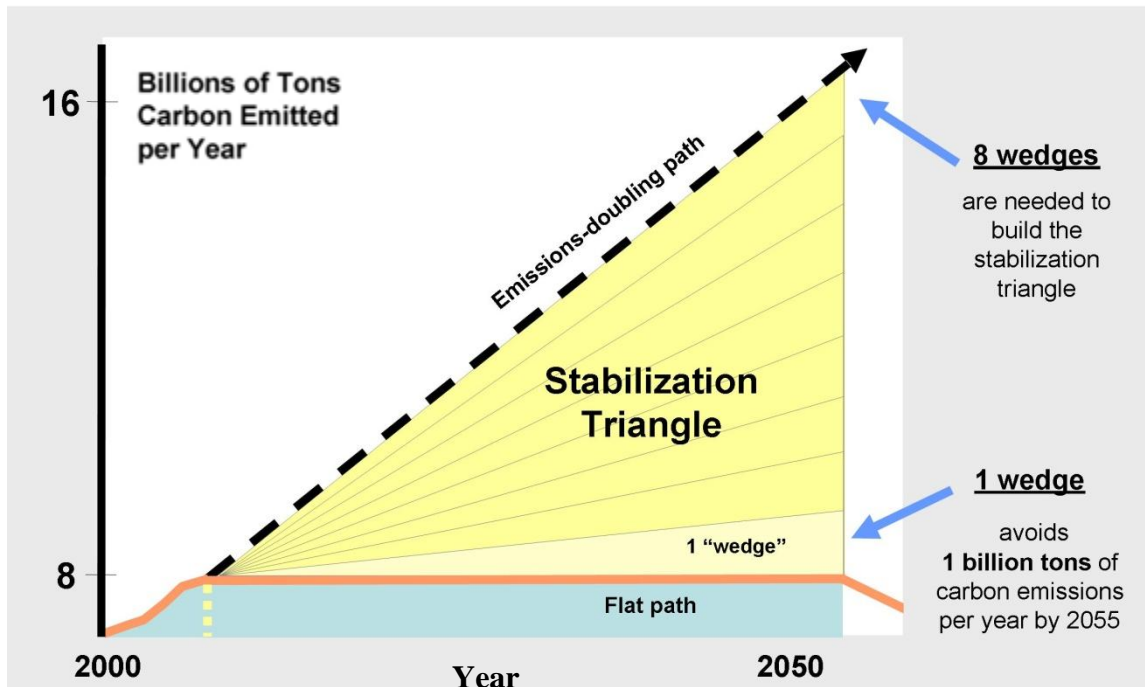


**Figure 2. 50-year Ahead Carbon Emission Projections.**

The stabilization triangle can be subdivided in eight wedges, each one equivalent to a reduction of approximately 1 billion tons of carbon emissions per year. As Figure 2 shows, eight wedges are required to stabilize the carbon emissions to the current rate (orange path).

The nuclear energy can be part of the future, sustainable sources of energy but the contribution for a “nuclear wedge” would require adding approximately 700 GW to the current nuclear power installation, which corresponds to tripling the number of the nuclear power plants currently in operation [3]. “...*The global pace of nuclear power plant construction from 1975 to 1990 would yield a wedge, if it continued for 50 years.*”

*Substantial expansion in nuclear power requires restoration of public confidence in safety and waste disposal, and international security agreements governing uranium enrichment and plutonium recycling...”.*

Most of the commercial nuclear power plants in operation around the world are Light Water Reactors (LWRs) which belong to the Generation II and III nuclear power plants (Figure 3). There are currently 359 LWRs in operation, in over 27 countries, producing a total energy of 328.4 GWe. The global nuclear capacity shares approximately 16% of the global electricity [4].

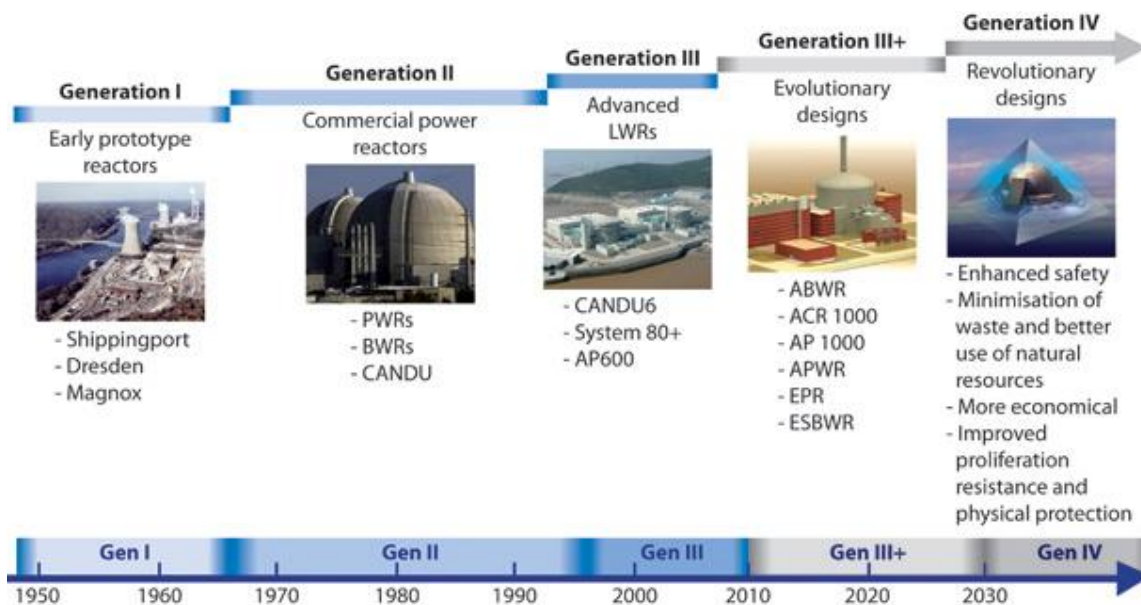


**Figure 3. Evolution of Nuclear Energy Systems.**

To explore new opportunities, the U.S. Department of Energy's Office of Nuclear Energy has engaged governments, industry, and the research community worldwide in a wide ranging discussion on the development of next generation nuclear energy systems known as "Generation IV."

Different technology goals have been defined for the Generation IV systems, which can be grouped in four broad areas: sustainability, economics, safety and reliability, and proliferation resistance and physical protection. [5].

**Sustainability.** Generation IV nuclear energy systems will provide sustainable energy generation that meets clean air objectives and provides long-term availability of systems and effective fuel utilization for worldwide energy production. These types of nuclear energy systems will minimize and manage their nuclear waste and notably reduce the long-term stewardship burden, thereby improving protection for the public health and the environment.

**Economics.** Generation IV nuclear energy systems will have a clear life-cycle cost advantage over other energy sources, and a level of financial risk comparable to other energy projects.

**Safety and Reliability.** Generation IV nuclear energy systems operations will excel in safety and reliability (very low likelihood and degree of reactor core damage), eliminating the need for offsite emergency response.

**Proliferation Resistance and Physical Protection.** Generation IV nuclear energy systems will increase the assurance that they are very unattractive and the least

desirable route for diversion or theft of weapons-usable materials, and provide increased physical protection against acts of terrorism.

Six systems with different technologies and features (Figure 4) were selected and introduced to the Generation IV technology roadmap [6]:

- Gas-cooled fast reactor (GFR), featuring a fast-neutron-spectrum, helium-cooled reactor and closed fuel cycle;
- Very-high-temperature reactor (VHTR), a graphite-moderated, helium-cooled reactor with a once-through uranium fuel cycle;
- Supercritical-water-cooled reactor (SCWR), a high-temperature, high-pressure, water-cooled reactor that operates above the thermodynamic critical point of water;
- Sodium-cooled fast reactor (SFR), featuring a fast-spectrum, sodium-cooled reactor and closed fuel cycle for efficient management of actinides and conversion of fertile uranium;
- Lead-cooled fast reactor (LFR), a fast-spectrum, lead/bismuth eutectic liquid-metal-cooled reactor and a closed fuel cycle for efficient conversion of fertile uranium and management of actinides;
- Molten salt reactor (MSR), producing fission power in a circulating molten salt fuel mixture with an epithermal-spectrum reactor and a full actinide recycling fuel cycle.

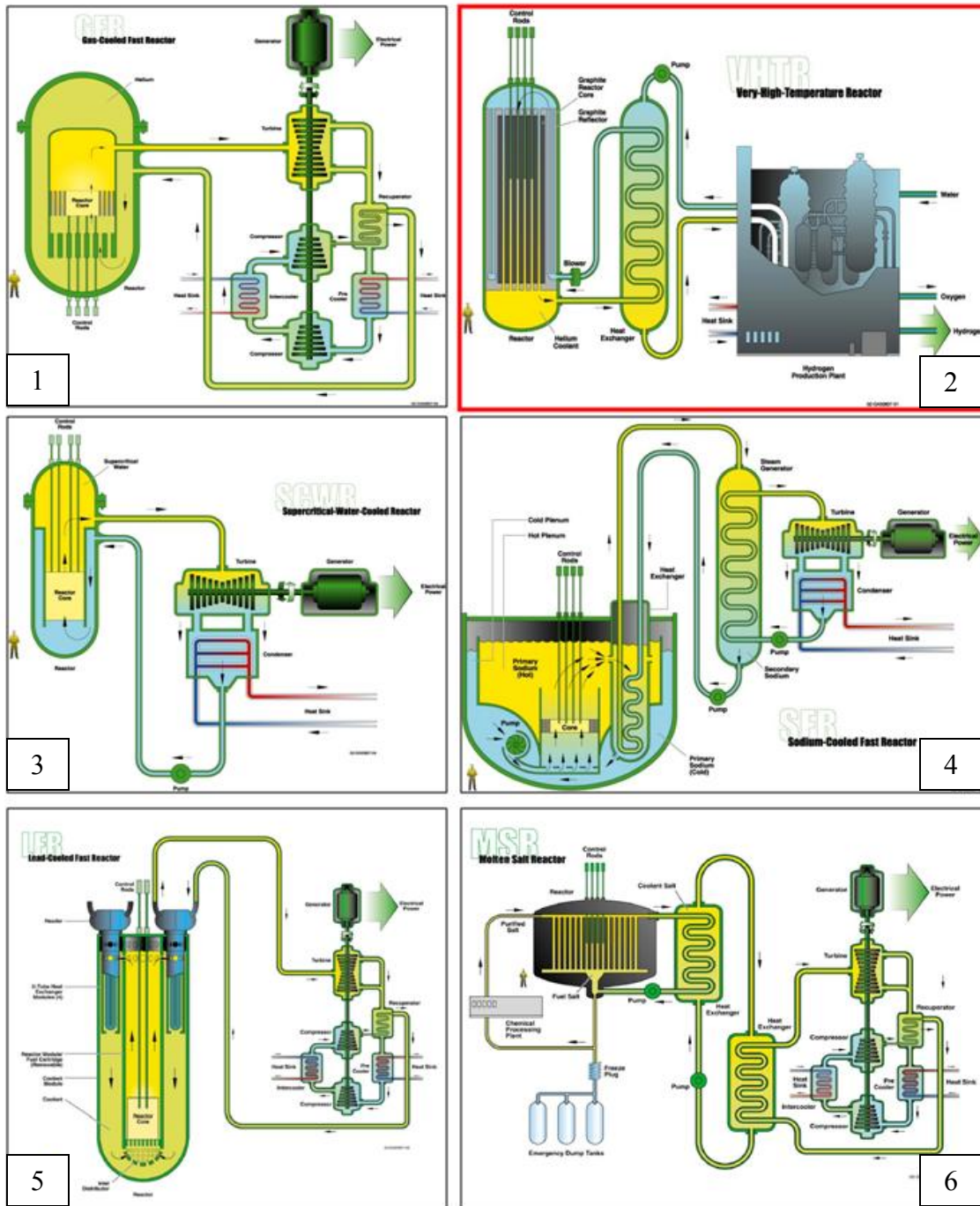


**Figure 4. Generation IV Nuclear Systems [7]  
(1: GFR; 2: VHTR; 3: SCWR; 4: SFR; 5: LFR; 6: MSR).**

The Very-High-Temperature Reactor (VHTR), one of the six nuclear systems mentioned above (red box in Figure 4), is a graphite-moderated, helium-cooled reactor with a thermal neutron spectrum. The VHTR is designed to be a high efficiency system, which can supply electricity and process heat to a broad spectrum of high-temperature and energy-intensive processes. The VHTR offers the potential for the cogeneration of electricity and hydrogen, alongside process heat applications. As the basic technology for VHTR systems has already been established in high temperature gas reactor plants, the design is an evolutionary development. Thus, the VHTR offers a high-efficiency electricity production and a broad range of process heat applications, while retaining the desirable safety characteristics in normal as well as off-normal events. Solutions to adequate waste management will be developed. The basic technology for the VHTR has been well established in former High Temperature Gas Reactors plants, such as the US Fort Saint Vrain and Peach Bottom prototypes, and the German AVR and THTR prototypes. The technology is being advanced through near- or medium-term projects lead by several plant vendors and national laboratories, including the Next Generation Nuclear Power (NGNP) project in the United States.

The reference reactor is a 600 MWth core connected to an intermediate heat exchanger to deliver process heat. The reactor core can be a prismatic block core or a pebble-bed core according to the fuel particles assembly. Fuel particles are coated with successive material layers, high temperature resistant, then formed either into fuel compacts embedded in graphite block for the prismatic block-type core reactor, or formed into graphite coated pebbles. The reactor supplies heat with core outlet

temperatures up to 1,000 degrees Celsius, which enables such applications as hydrogen production or process heat for the petrochemical industry.

Due to the high temperatures reached in the system, some components designed for standard steam-cycle plants must be modified or revised to operate under such temperature conditions [8].

Passive heat removal systems are one of the primary technological goals of the Generation IV program [9], since they can guarantee their functionality also in the event of an accident, when power is lost, requiring no human intervention. Natural circulation is in fact one of the most promising passive heat removal mechanisms, already implemented in new reactor systems of the latest generations (III and III+).

The Reactor Cavity Cooling System (RCCS) is a new safety system designed for the next generation of nuclear power plants and it will be incorporated into proposed reactor designs for VHTR. This system was conceived to guarantee the integrity of the fuel, the reactor vessel and the structures inside the reactor cavity by removing heat from the Pressurized Reactor Vessel (PRV) during both normal operation and accident scenarios. Two different reactor cavity cooling system designs are currently under discussion. The design proposed by General Atomic [10, 11] is a natural convection, air-based cooling system with no pumps, circulators, valves, or other active components, and is designed to operate continuously in all modes of plant operation (Figure 5).

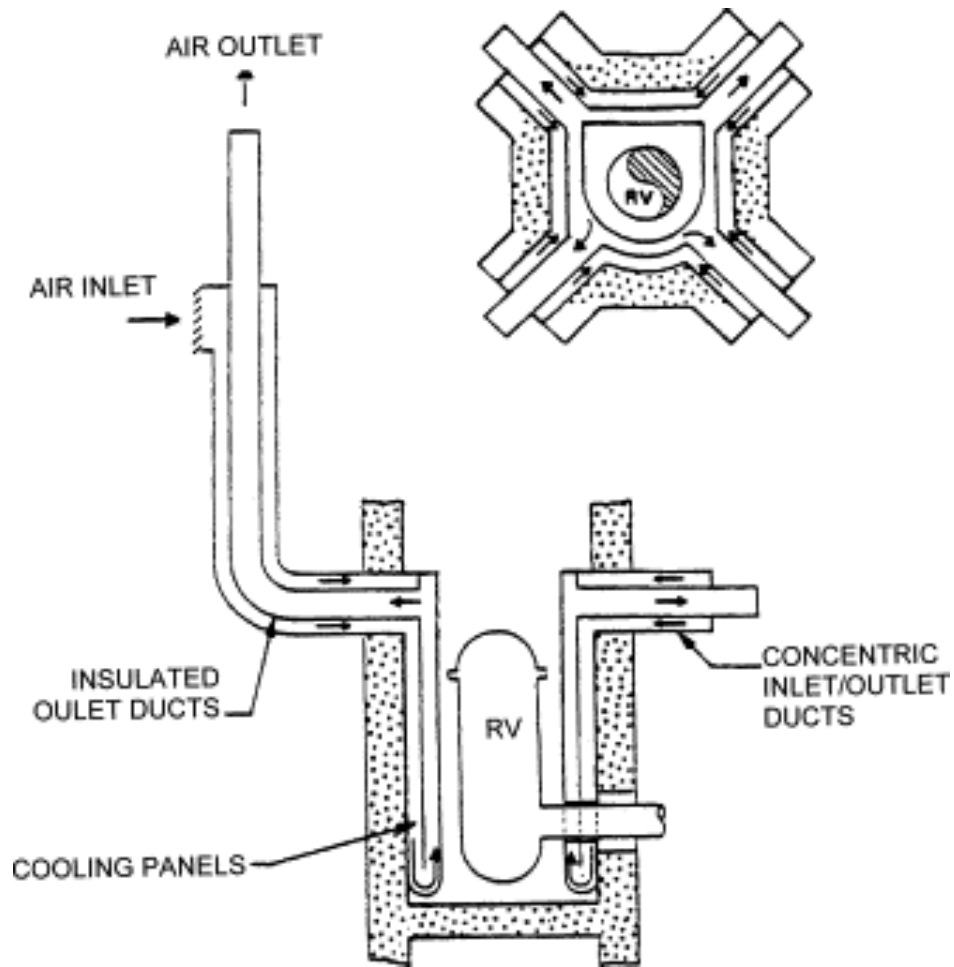


**Figure 5. Air-Cooled RCCS - General Atomic Design [8].**

The second configuration, proposed by AREVA [12], is a constant flow, water-based cooling system that operates at low-temperature and low pressure (Figure 6). Water temperatures are below 30°C during normal active operation, reaching the boiling point only during emergency passive operation.

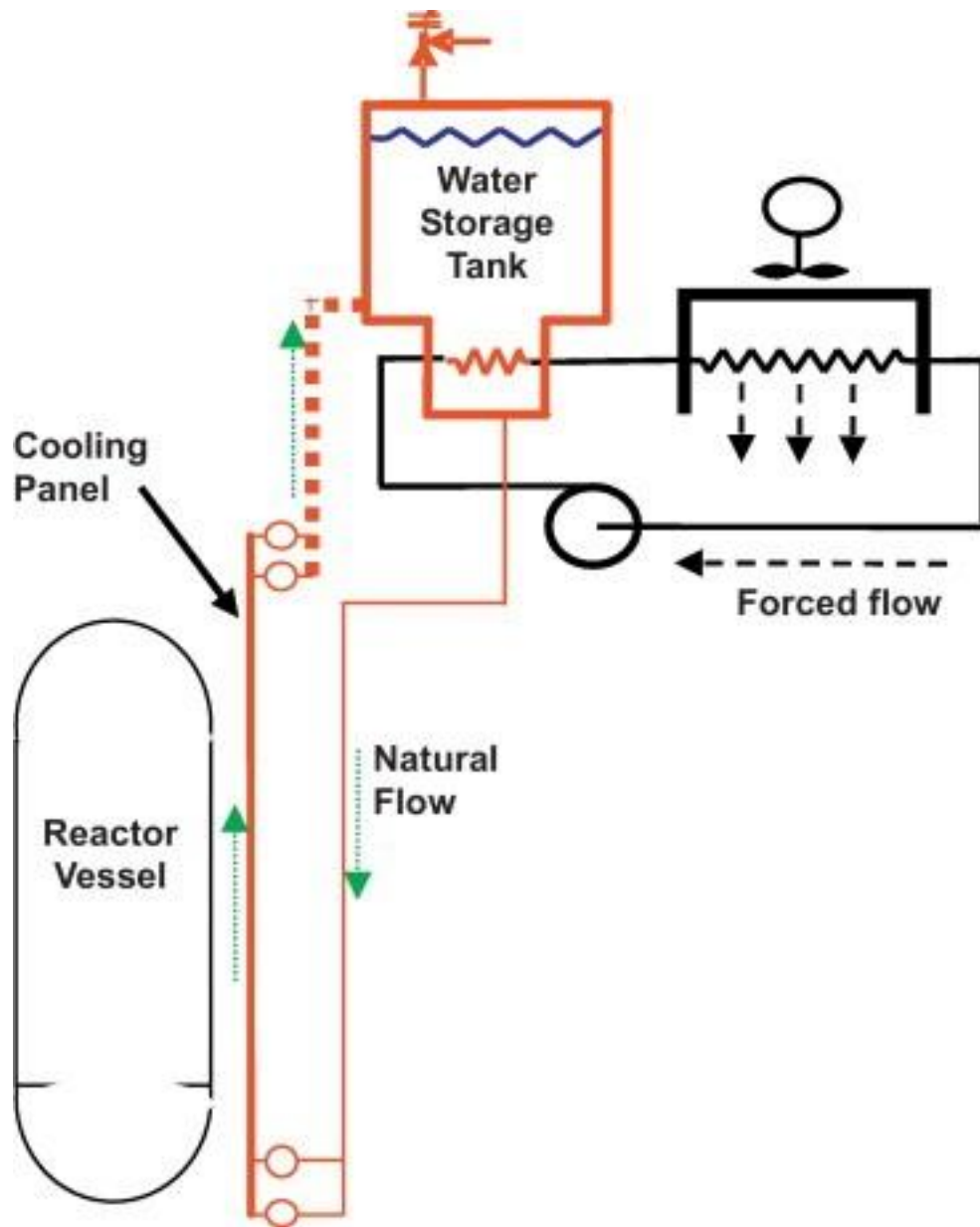
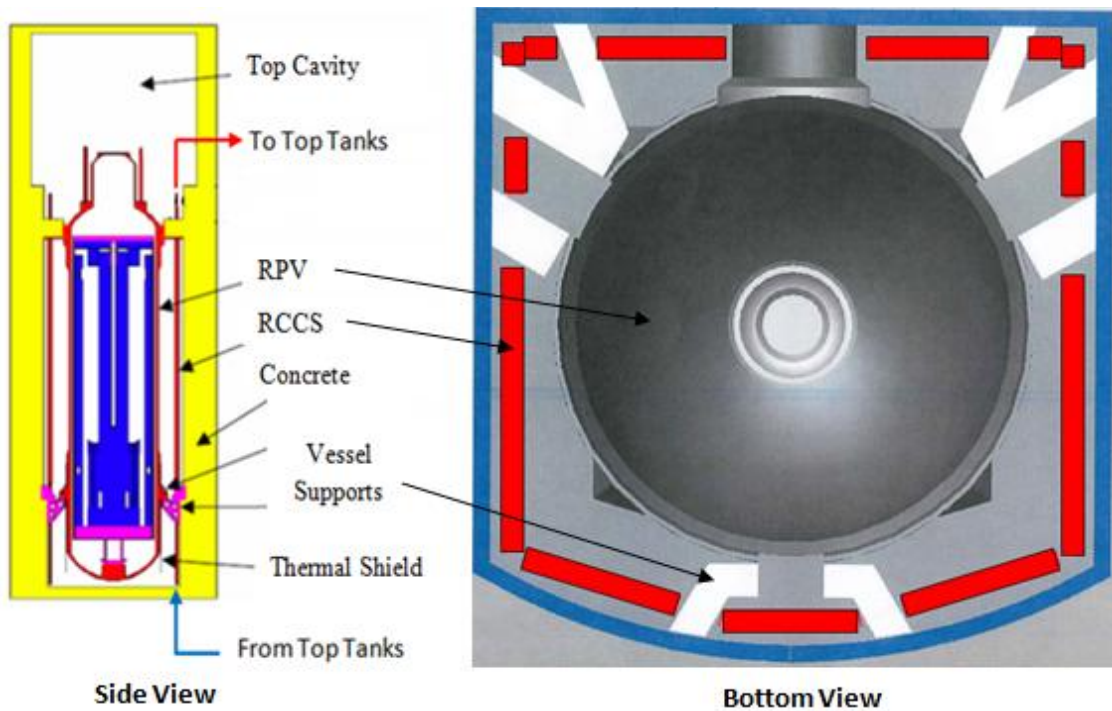


Figure 6. Water-Cooled RCCS - AREVA Design [13].

In this case the RCCS can operate both in active mode, by removing the heat from the water in the tanks via active systems, or passive mode by boiling the water for approximately 72 hours. The heat removed from the reactor cavity through water circulation is released into the atmosphere by an active secondary heat removal system.

In both configurations, since the reactor vessel is not thermally insulated, a small portion of the heat produced in the core is released into the reactor cavity. The heat is transferred by conduction through the vessel wall and released to the RCCS coolant, flowing upward through vertical risers, by convection within the air of the reactor cavity and radiation between the outer vessel surface and the riser's walls. The coolant coming from different risers is collected in horizontal headers or upper plena. In the air-cooled configuration, the air is then discharged into the atmosphere through the outlet chimneys. In the water-cooled configuration, water reaches the water tanks, mixes with cold water and comes back into the loop. As mentioned above, the RCCS is used during normal operation and during accident scenarios, when the Power Conversion System (PCS) and the Shutdown Cooling System (SCS) may not be available, to maintain the temperature of concrete, vessel, and core within the design limits. The RCCS is designed to guarantee the removal of about 0.7MW (1% of the thermal power generation) during normal operation and up to 1.5MW in case of accident [14]. The system's heat removal effectiveness is strongly affected by different factors including geometry (riser length and dimensions, number of risers, wall thickness, total elevation change), physical properties of the materials (emissivity, thermal conductivity, heat capacitance) and thermal conditions (temperatures throughout the system).

A typical layout of the components inside the cavity of a VHTR is shown in Figure 7.



**Figure 7. Typical RCCS Configuration.**

The reactor cavity walls are lined by stainless steel vertical pipes (risers) which surround the Reactor Pressurized Vessel (RPV). The risers are organized in panels (red lines in Figure 7, right). The cooling system consists of twenty-five cooling panels each one containing nine risers. Since the majority of the heat in the cavity is transferred by

radiation [15] the riser panels may include additional features to enhance the radiation heat transfer. These include stainless steel fins, welded along the side of two adjacent risers, and shield, and additional thin panel welded on the back of the risers wall.

A water-cooled RCCS experimental facility was scaled down, designed and built in order to conduct analyses of the thermal-hydraulic behavior of the coolant in the system under normal operation (steady-state) and during accident scenarios.

The experimental data produced will be used to study the thermal-hydraulic behavior of the coolant under different operating conditions, such as normal operation (steady-state) and accident scenarios (transient, two-phase).

The data will be also used to validate computer codes such as system codes (RELAP5-3D) or Computational Fluid Dynamics (CFD) codes.

## CHAPTER II

### PURPOSE

The U.S. Department of Energy's (DOE) Office of Nuclear Energy has engaged governments, industry, and the research community worldwide in a wide ranging discussion on the development of next generation nuclear energy systems. In particular the DOE and the Nuclear Energy University Program (NEUP) has sponsored a specific research activity to study the thermal-hydraulic phenomena of the RCCS and to prove its potential capability to remove the heat from the reactor cavity during the normal operation and in case of accidents. In the framework of such research activity, the Department of Nuclear Engineering of Texas A&M University is actively cooperating with other universities and institutions in the United States to conduct a dedicated computational and experimental research activity to support the study of the RCCS behavior under different conditions.

The objectives of this research activity are summarized in the following bullets:

1. Scale down, design, build, and shakedown a small scale water-cooled RCCS experimental facility to support the analysis of the thermal-hydraulic behavior of the coolant in the system and its cooling capabilities;
2. Conduct scaled test to study the thermal-hydraulic behavior of a water-cooled RCCS under steady-state conditions;

3. Identify and analyze specific phenomena occurring during the single-phase stage of the experiments;
4. Develop and refine computational models (systems codes and Computational Fluid Dynamics codes) to analyze these phenomena;
5. Produce experimental data to be used for computational codes validation.
6. Identify possible technical issues and technique to fix them, also in preparation for the two-phase (accident) stage.

The contribution of the present project to this research activity specifically focuses on two main topics:

**Experimental:** Scaling, designing, building and operating a small-scale water-cooled RCCS to be used to conduct single-phase (steady-state) and two-phase (transient) experiments;

**Computational:** Selecting a system code, developing and refining a dedicated model to conduct the simulations of the full-scale power plant and the experimental facility.

## CHAPTER III

### RESEARCH APPROACH

As mentioned in Chapter II, the main purpose of the present project is to design, build, and shakedown the RCCS experimental facility which will be used to conduct the single-phase (steady-state) and two-phase (transient) experiments. To successfully achieve this scope, the entire project will be fractioned in eight phases, listed below.

#### **III.1 Phase 1: Data Collection and Literature Review**

This preliminary phase will play an important role in defining the reference features of the experimental facility. Most of the full-scale power plant features, information, and drawings will be provided by Argonne National Laboratory (ANL), which has developed the conceptual RCCS design. The provided information will be also integrated with openly available literature. Even though the experimental facility will use water as coolant, due to lack of information of the AREVA design, the General Atomic Modular HTGR (MHTGR) cavity design will be assumed as the main reference, where the air-cooled duct array will be replaced with the water-cooled vertical pipes (risers).

### **III.2 Phase 2: Scaling Approach**

The scaling procedures will follow the one developed and adopted by similar experimental facilities. One of the most important parameters, the length scale factor,  $l_R$ , defined as the ratio of the characteristic length of the experimental facility and the characteristic length of the full-scale power plant, will be customized based on:

- The characteristic length chosen for the other experimental facilities built by other universities and institutions participating to the project;
- The laboratory space available at Texas A&M University;
- Other technical limiting factors.

The selection of the scaling factor for this experimental facility will subsequently affect all the other scaling parameters (in particular the power scaling factor).

### **III.3 Phase 3: Facility Design and Material Selection**

The design of the experimental facility will be driven by the defined scaling laws but modifications may be required due to engineering limitations, assuming that these modifications will not induce distortion. Particular attention will be dedicated to the material selection to preserve some of the features of the full-scale plant and to accommodate specific features of the experimental facility. These materials may include:

- Stainless steel. Used for some of the components in the reactor cavity such as vessel and risers, it will preserve some of the features of the full-scale plant such as surfaces emissivity and thermal conductivity.
- Glass and polycarbonate and/or acrylic. These materials may be selected for selected regions of the facility to allow flow visualization which will be one of the most important features of this experimental facility, standing very high, high, and medium/low temperatures respectively.
- Steel, aluminum and other metals. These materials will be adopted mainly for structural purposes.

Due to the expected overall dimensions, the relatively high temperatures, and the different materials adopted (that may be interconnected), particular attention will be dedicated on selecting joints, connectors and other components to allow for differential thermal expansion, and reduce mechanical and thermal stresses that may damage the components of the facility.

#### **III.4 Phase 4: RELAP5-3D Model Preparation**

RELAP5-3D is one of the system codes that have been designated for the analysis of the VHTRs. While MELCOR has been selected by other participating Universities, the selection of the RELAP5-3D system code has been driven by different factors:

- The system code has been largely used for analysis of water systems. Including natural circulation phenomena.
- Strong partnership with Idaho National Laboratory (INL) where RELAP5 was designed and still maintained. This will help facilitating the resolution of possible technical issues.
- The computer code is currently available at the Nuclear Engineering Department.

During this phase, the simulation results will help:

- Identify thermal-hydraulic phenomena that may require a special experiment configurations to be observed and/or analyzed;
- Obtain preliminary estimations of the main thermal-hydraulic parameters of the full-plant and the experimental facility;
- Validate the scaling laws;
- Select proper instrumentation and define/optimize its layout
- Prepare the base for the final model to be used for the final simulations that will be compared with the experimental results.

### **III.5 Phase 5: Facility Design Completion, Vendor Selection, and Construction**

The design of each component of the experimental facility, the selection of the materials to be adopted, the instrumentation to be installed and its layout will be finalized during this phase based on the founding and results of the previous phases (3

and 4). Based on specific features and characteristics, some of the components of the facility will be custom manufactured. For these components, a dedicated manufacturer selection process may be required. Once materials and single are purchased and available, the construction will begin.

### **III.6 Phase 6: Instrumentation Selection and Installation**

This phase will include the selection of the instrumentation that will be necessary to acquire the data during the experimental activity. The instrumentation will include:

- K-type thermocouples to measure the temperatures of the risers walls at different locations
- K-type thermocouple probes to measure the temperature of the water at different locations of the facility, including risers and water tank
- Flow meters to measure the flow of the coolant in selected locations.

The installation of the selected instrumentation will be performed during and after the facility assembly and will consider required calibration based on the vendor specifications.

### **III.7 Phase 7: Facility Shakedown**

After the instrumentation and the other components are verified after their installation, the facility will be turned on and selected parameters will be immediately monitored and recorded order to:

- Confirm that all the electric components and instrumentation are working properly and safely;
- The natural circulation is established;
- The experimental data are properly recorded;
- The overall behavior of the facility meets the expectations and the results give the confidence that the experimental activity may be started without any additional modification.

The results collected during this phase may help refining the RELAP5-3D model in preparation for the simulations of the experimental cases defined in the following phase.

### **III.8 Phase 8: Analysis of the Experimental Data and Comparison with Simulations**

A test activity will be defined including the experimental runs to be performed. The tests to be performed will be intended to produce experimental results that may be possible to achieve only with the specific features of this experimental facility (such as risers flow and temperature analysis and flow visualization), and comparable with the simulation results.

The data collected during the experimental activity will be analyzed and compared with simulations performed with system codes (RELAP5-3D) and with CFD codes.

Each of the phases will be described in details in the next chapters.

## CHAPTER IV

### PHASE 1: DATA COLLECTION AND LITERATURE REVIEW

Preliminary research on the available literature and other documentation was performed in order to collect general information about plant design, including plant and reactor layouts, connections between the reactor vessel and the steam generator or turbine, and other reactor cavity penetrations that should be accounted for the RCCS design. It will be shown that most of the available publications and documentation refer to the air-cooled RCCS and to power plant designs which will use this version of the cooling system. The type of information and the approach adopted when searching and collecting the required documentation, can be summarized as follow:

- Introductory publications to the Generation IV nuclear reactors and Gas-Cooled Reactors.
- Overview of the plant and its main features (power, layout, temperatures, dimensions).
- Drawings of the reactor cavity interiors including reactor vessel
- Detailed description of dimensions, materials, and working conditions of the RCCS (air or water-cooled).
- Existing Experimental Facilities and Similar Scaling Approaches.

A paper presented by General Atomic, Inc. in October 1992 during the IAEA Workshop on High Temperature Applications of Nuclear Energy in Japan [16], provides an overview of the High Temperature Gas-Cooled Reactor project scope and describes

some of the main features of the power plants. The paper put in evidence the potentiality of the reactor to be used not only for electricity production but to support industrial processes such as coal conversion, thanks to the high temperatures of the coolant reached during normal operation. Preliminary data regarding the reactor thermal power and the operating coolant temperatures are also available in the paper. The first comprehensive description of the Gas Turbine-Modular Helium Reactor (GT-MHR, a design of the gas-cooled reactor where the reactor coolant directly goes to the turbine) is provided in the conceptual design report prepared by General Atomic in 1996 [10]. Idaho National Laboratory (INL), actively working on the HTGR project, has recently published detailed reports where important information of the power plant can be found. A survey of materials research and development conducted by INL on VHTR [17] was found to be a good source of information for the reactor building and cavity layout. Figure 8 shows the GT-MHR reactor building, providing an insight of the reactor cavity and pipeline arrangement.

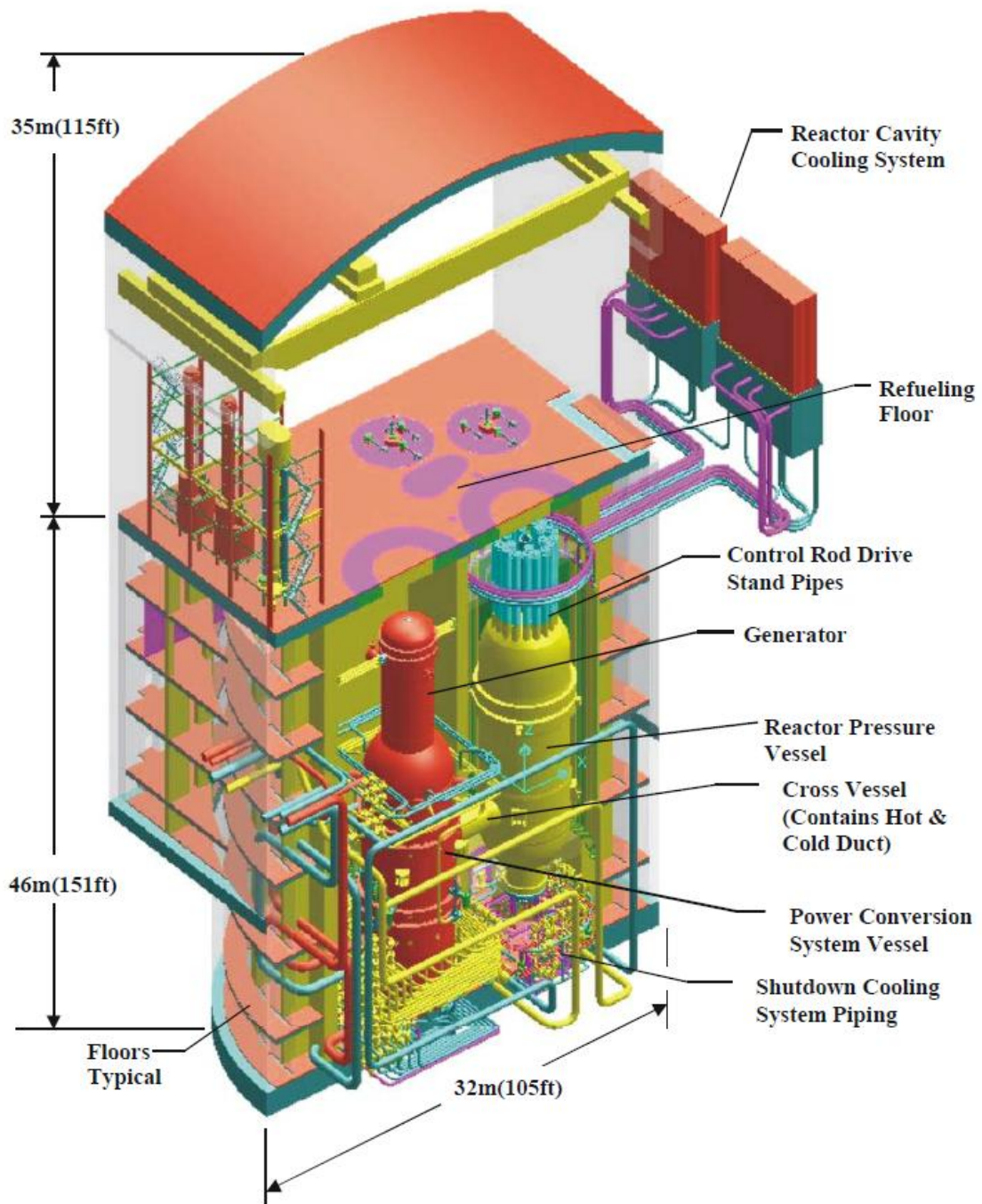
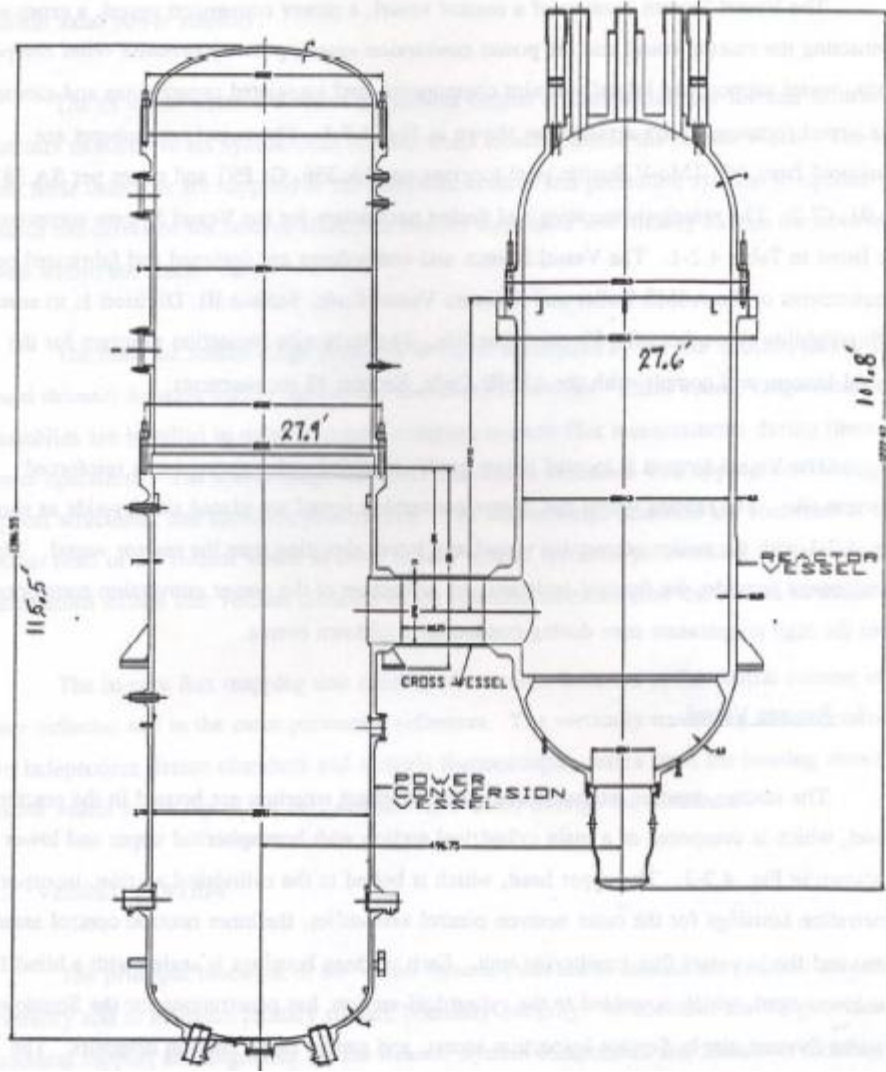
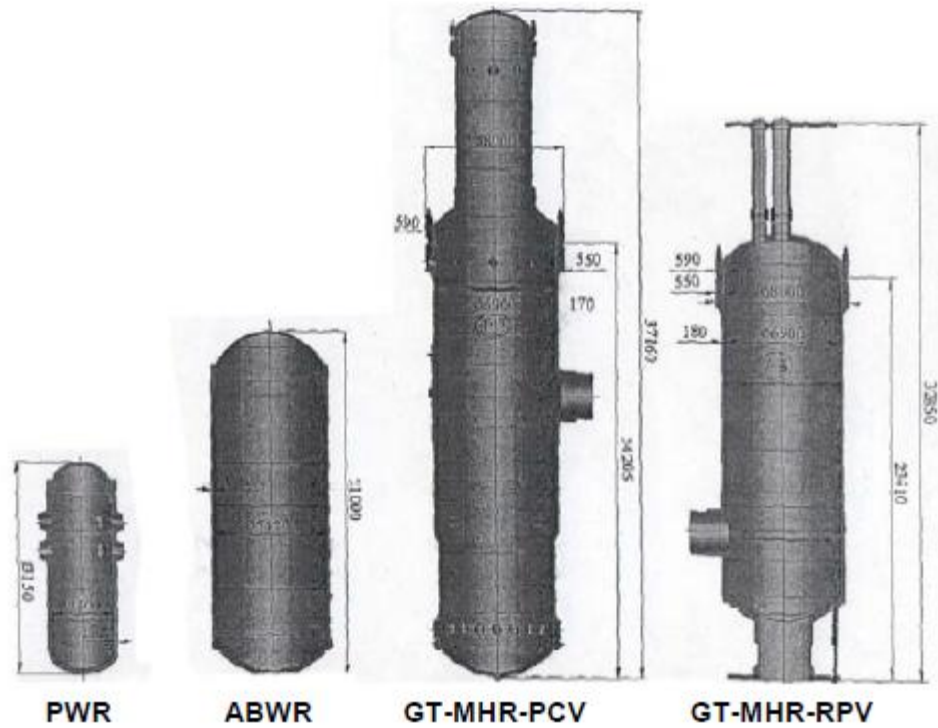


Figure 8. GT-MHR Reactor Building Layout and Internals [3]

The entire reactor confinement structure is under ground level. The reactor vessel (yellow vessel in Figure 8), is located inside the reactor cavity and connected to the power conversion vessel (red vessel in the same figure) through an annular duct. The RCCS (air-cooled design) is also visible in Figure 8. Cooling panels line up the cavity walls surrounding the reactor vessel. The panels are connected to external chimneys through which the air is discharged in the atmosphere. Dimensions of the reactor vessel are shown in Figure 9. As one can see, the reactor vessel is slender with a vertical length approximately four times larger than the vessel diameter and a corresponding aspect ratio much larger than the existing Light Water Reactor Vessels. A comparison of the dimensions of the GT-MHR Reactor Pressure Vessel (RPV), Power Conversion Vessel (PCV), Pressurized Water Reactor (PWR), and Advanced Boiling Water Reactor (ABWR) vessels is presented in Figure 10.



**Figure 9. Schematic and Main Dimensions of the Reactor Pressure Vessel**



**Figure 10. Comparison of Reactor Pressure Vessel Sizes**

More accurate details of the reactor cavity and vessel dimensions were found in recent publications on VHTGR [18, 19]. Figure 11 shows a schematic representation of the GT-MHR and provides the main dimensions of the reactor cavity and pressure vessel. These dimensions were selected for the scaling of the experimental facility that will be described in Chapter V.

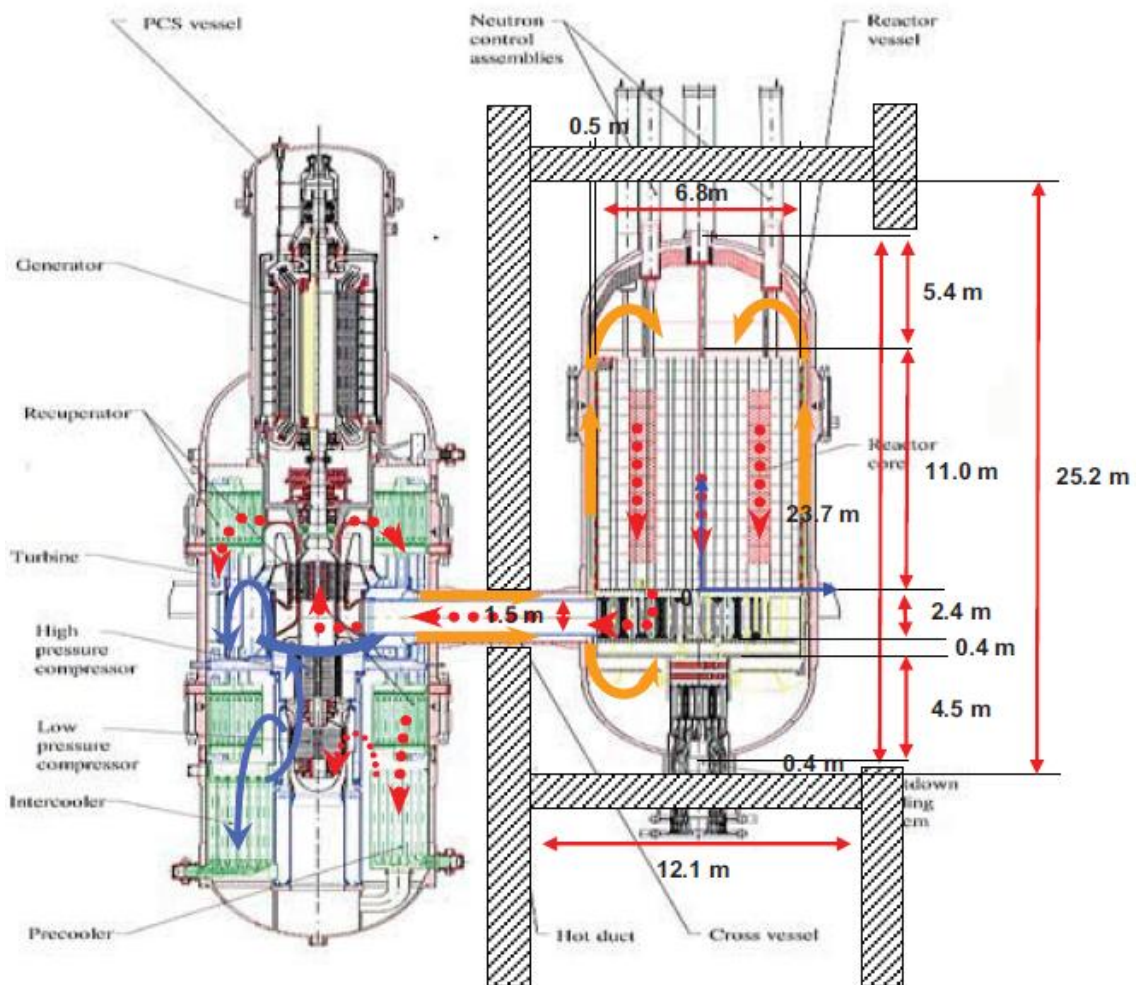


**Figure 11. GT-MHR Vessel and Cavity Dimensions**

Although a specific design for the water-cooled RCCS has not yet been selected, the information collected for the air-cooled design allowed defining the main features of the RCCS design under consideration. One of the most important characteristics of the RCCS, in evidence in the reactor cavity cooling system design description [20], is the

definition of the riser's layout to account for the penetrations in the cavity walls (reactor supports, coolant inlet/outlet line, others) as shown in Figure 12. As it shown in the figure, the reactor cavity is broken up into distinct regions due to the presence of the vessel supports (white radial shapes in the bottom view), and cross duct penetration. Approximately ten to fifteen regions of the walls were identified which require *physically distinct riser's panels*. This configuration may allow a more uniform heat removal from the reactor cavity, minimizing the 'hot spots' in the cavity walls.

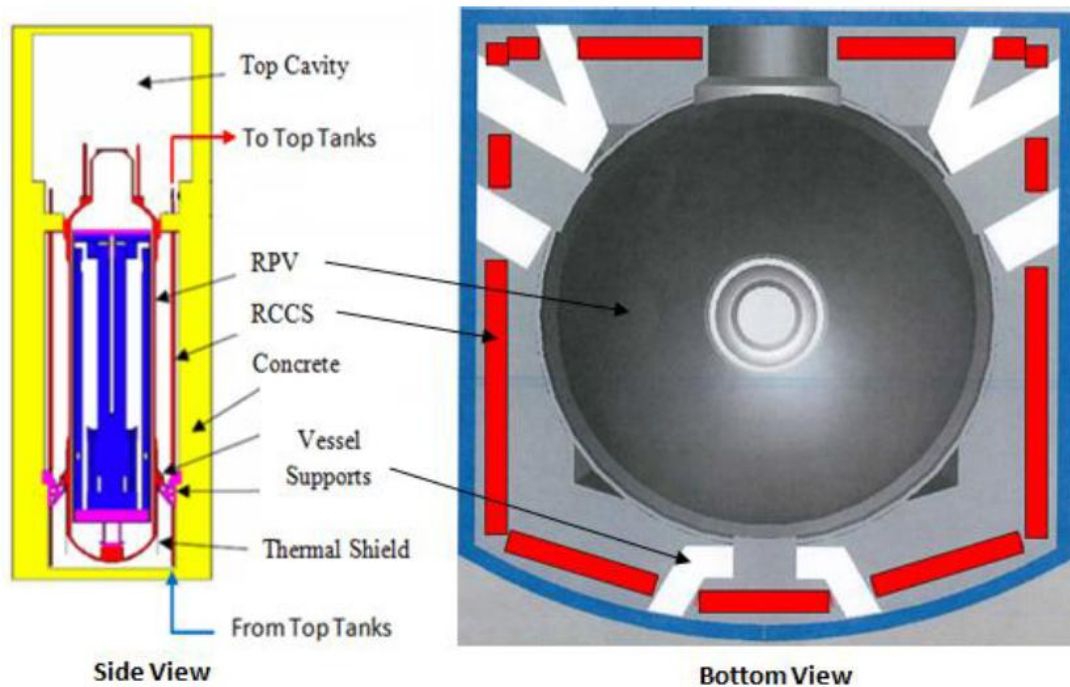


**Figure 12. Typical Reactor Cavity Internals and RCCS Layout**

This configuration may be assumed valid for the water-cooled RCCS, where risers' ducts (red blocks in Figure 12, right) are replaced by vertical pipes. The approach adopted for the design of the cooling system of the High Temperature Engineering Test Reactor (HTTR) built in Japan [21], has confirmed the necessity of organizing the riser's tubes into panels to optimize the heat removal from the cavity. In this particular case, eighteen vertical pipes were organized into two riser's panels. Only one of the two panels was considered in operation, keeping the second circuit for redundancy and backup heat removal.

A comprehensive feasibility study conducted by Argonne National Laboratory (ANL) on a heat removal system for the Natural Convection Shutdown Heat Removal Test Facility (NSTF) [22] provided the guidelines for the scaling procedures to be adopted for the experimental facility under consideration during the phases of the experiment (steady-state, transient).

Previous studies [15] and experimental activities conducted on similar facilities [23], supplied important information on the heat transfer mechanisms in the reactor cavity that were accounted during the scaling of the experimental facility.

## CHAPTER V

### PHASE 2: SCALING APPROACH

The scaling approach was based on the procedure and calculations performed for other similar experimental facilities [22, 24], and developed and elaborated to accomplish the desired scope and features of the proposed experimental activity. The non-dimensional similarity approach was adopted to calculate the main dimensions and other features of the experimental facility. The following similarity condition will be used throughout the chapter.

$$\Psi_R = \frac{\Psi(\text{model})}{\Psi(\text{prototype})} = \frac{\Psi_m}{\Psi_p} \quad (1)$$

The first similarity condition decided for the experimental facility was the axial length scaling factor  $l_R$ , defined as the ratio between the experimental facility and power plant characteristic length. As it will be shown in this chapter, this similarity condition defines the other scaling parameters such as power, heat flux, and coolant velocity. For this study, the height of the reactor vessel was used as characteristic length. Several factors were considered when deciding the height of the reactor vessel to be used for the experimental facility. This includes:

- The space available in the university laboratory. The University Science Building (USB), where the Thermal-Hydraulic Laboratory of the Department of Nuclear Engineering is located, was designated as the area where the experimental facility will be built and operate. The roof

elevation of the building (approximately 8 m) was taken into account when defining the total height of the experimental facility.

- Power Installed. As it will be shown in this chapter, the thermal power to be applied during the phases of the experimental activity is a function of the length scaling factor  $l_R$ . Limitation on the maximum power available in the designated area was accounted when defining the maximum power to be installed and, subsequently, the length scaling factor.
- Other Laboratory Capabilities. Since the length scaling factor defines the main dimensions of the experimental facility, parameters like the total height and dimensions of the facility and supporting structures, additional scaffolds, total weight etc. had to be considered when defining the scaling factor.

The optimal experimental vessel height was calculated to include all the considerations and limitations previously listed. This dimension was defined to be equal to 1 m.

$$h_{model}^{vessel} = 1 \text{ m} \quad (2)$$

Given the total height of the reactor vessel in the power plant of 23.7 m (as defined in Chapter V, Figure 11), the axial length similarity condition was determined.

$$l_R = \frac{h_{model}}{h_{prototype}} = \frac{1 \text{ m}}{23.7 \text{ m}} = 0.042 \quad (3)$$

Another similarity condition was defined by simply writing the energy balance in the reactor cavity. The total heat transfer through the cavity  $Q_{cavity}$ , is the sum of the heat

transferred by radiation  $Q_{rad}$ , and the heat transferred by convection  $Q_{conv}$ . Assuming negligible the heat losses through the cavity walls, the total heat transferred through the cavity is responsible for the increase in the temperature of the water flowing inside the RCCS risers  $T_{out} - T_{in}$ , as stated in the equation below:

$$Q_{cavity} = Q_{rad} + Q_{conv} = Q_{risers} = Q_o = A_o U_o \rho_o C_p (T_{out} - T_{in}) \quad (4)$$

Equation 4 can be re-arranged to define the water temperature rise similarity condition  $\Delta T_{oR}$ , assuming the same properties of the water for the model and prototype. In addition, assuming the same riser's flow area for the model and prototype (as it will be explained and justified below), the temperature rise similarity condition can be simplified and expressed as follow:

$$\Delta T_{oR} = \frac{Q_R}{U_{oR} A_{oR}} = \frac{Q_R}{U_{oR}} \quad (5)$$

One of the main parameters that will be preserved from the prototype plant is the temperature rise of the cooling water through the reactor cavity. In other words, a unity similarity for the condition defined in Equation 5 can be imposed.

The non-dimensional Froude Number, defining the ratio between the kinetic and potential energy of the fluid [25], also desires a unity similarity relationship, preserving the ratio of the fluids inertia to the gravitational head.

$$Fr_R = \frac{U_{oR}^2 \rho_f}{g l_R \Delta \rho} = 1 \quad (6)$$

The velocity scaling factor can be calculated from Equation 6, and expressed as a function of the length scaling factor.

$$U_{oR} = \sqrt{l_R} \quad (7)$$

Under the conditions defined by Equations 5 and 7, the scaling factor for the reactor power  $Q_R$ , can be defined as a function of the velocity scaling factor.

$$Q_R = \sqrt{l_R} \quad (8)$$

The unity similarity for non-dimensional Richardson Number [26], which in the thermal convection problems defines the relative importance between of the natural circulation versus the forced convection, is automatically satisfied.

$$Ri_R = \frac{g l_R}{U_{oR}^2} = 1 \quad (9)$$

Table 1 summarizes the scaling factors calculated for the experimental facility.

**Table 1. Scaling Factors**

<b>Scaling Ratio</b>	<b>Description</b>	<b>Value</b>
$U_{oR}$	Scaled Reference Velocity	$l_R^{0.5}$
$t_R$	Scaled Time	$l_R^{0.5}$
$\Delta T_{oR}$	Scaled Reference Temperature Rise	1
$Q_R$	Scaled Thermal Power	$l_R^{0.5}$
$q''_R$	Scaled Thermal Flux	$l_R^{-0.5}$

As it will be described in the next paragraphs, the experimental facility will incorporate one of the twenty-five riser's panels of the prototype plant. The power to be applied to during the phase of the experimental activity can be calculated using the power scaling factor (Equation 8), considering only the fraction of the total power transferred to one panel.

$$P_{\text{experiment}} = P_{\text{prototype}} \sqrt{l_R} \cdot \frac{1}{25} \quad (10)$$

The values of the thermal power to be adopted during the phases of the experimental activity were calculated using Equation 10 and summarized in Table 2.

**Table 2. Thermal Power**

<b>Operating Condition</b>	<b>Prototype</b>	<b>Experiment</b>
Normal Operation (Steady-State)	0.7 MW	~ 6 kW
Accident	1.5 MW	~ 12,3 kW

Important considerations were also made when defining the main features of the experimental facility, to account for the scaling laws previously defined and preserve some of the characteristics of the prototype plant. As described above, the temperature rise of the coolant through the reactor cavity, which controls the buoyancy forces in the risers, was assumed to be preserved in the scaled facility ( $\Delta T_{oR} = 1$ ). Selected parameters of the prototype plant were also preserved in the scaled facility.

### **V.1 Number of Risers**

The number of risers was defined based on the panel configuration of the prototype plant and on the expected flow behavior in the risers and manifolds. As previously mentioned, the RCCS risers will be organized in panels, each one containing nine vertical pipes connected to a top (hot) and bottom (cold) manifold. Possible different geometries for the inlet and outlet connections are under consideration. These configurations are expected to strongly influence the behavior of the water flow through the risers and manifolds, and recirculation between adjacent risers may occur. These reasons suggested the selection of nine risers for the experimental facility which will represent a full RCCS panel of the prototype plant.

## **V.2 Pipes Dimensions**

One of the important assumptions applied to the scaling procedure involved the horizontal dimensions of the facility (radial and azimuthal directions). These dimensions were preserved in the scaled facility. This includes:

- The riser's inner diameter which was imposed to be 5.08 cm (2" nominal, Schedule 40).
- The manifolds inner diameter, assumed to be 10.16 cm (4" nominal, Schedule 40).
- The pipeline inner diameter, connecting the reactor cavity risers to and from the water tank, imposed to be 10.16 cm (4" nominal, Schedule 40).

## **V.3 Materials**

Since radiation was confirmed to be the main heat transfer mechanism in the reactor cavity, one of the most important parameters to be considered in the material selection is the surface emissivity. In order to preserve this propriety, the reactor vessel and RCCS panel will be constructed in stainless steel (SS 304) which will be the material likely selected for the same components in the prototype plant. The same material was selected for the panel fins, which will be described in the next subsection.

#### V.4 Panel Configuration

To enhance the radiation heat transfer to the risers, two different panel configurations are considered for the prototype plant. The *shield* configuration consists of a thin steel sheet welded on the back of the risers' tubes as indicated in Figure 13.

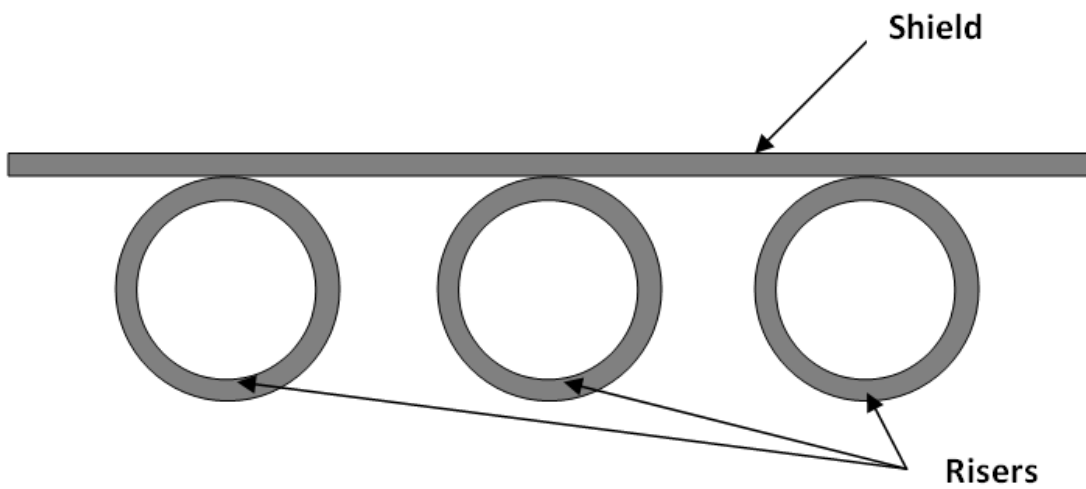


**Figure 13. Shield Configuration**

The *fin* configuration, selected for this experimental activity, consists of thin steel sheets welded along the sides of each riser, as shown in Figure 14.

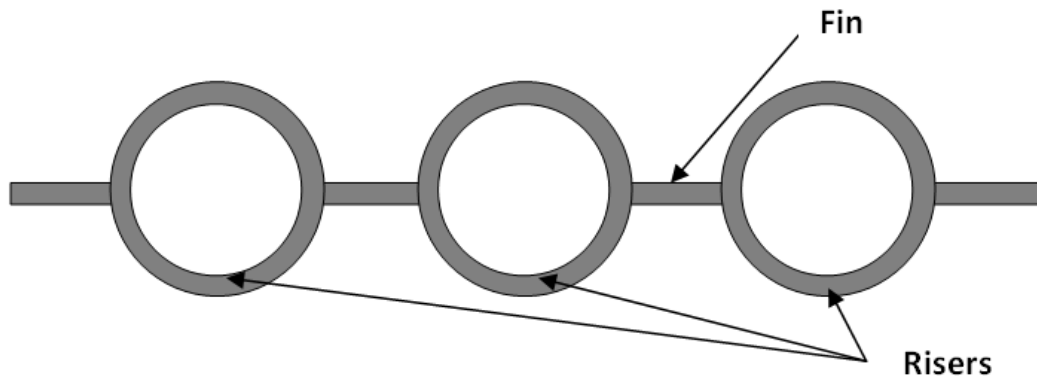


**Figure 14. Fin Configuration (Selected)**

In both configurations, the heat radiated from the reactor vessel is collected by the additional steel sheet and transferred by conduction to the risers' walls. The thickness of the fin was assumed to be 2 mm. Another factor which was preserved in the experimental facility panel is the ratio between the pitch (riser's center-to-center distance) and the risers' inner diameter which was imposed equal to 2. Possible different ratios may be imposed by simply blocking the risers with different blocking patterns as shown in Figure 15.

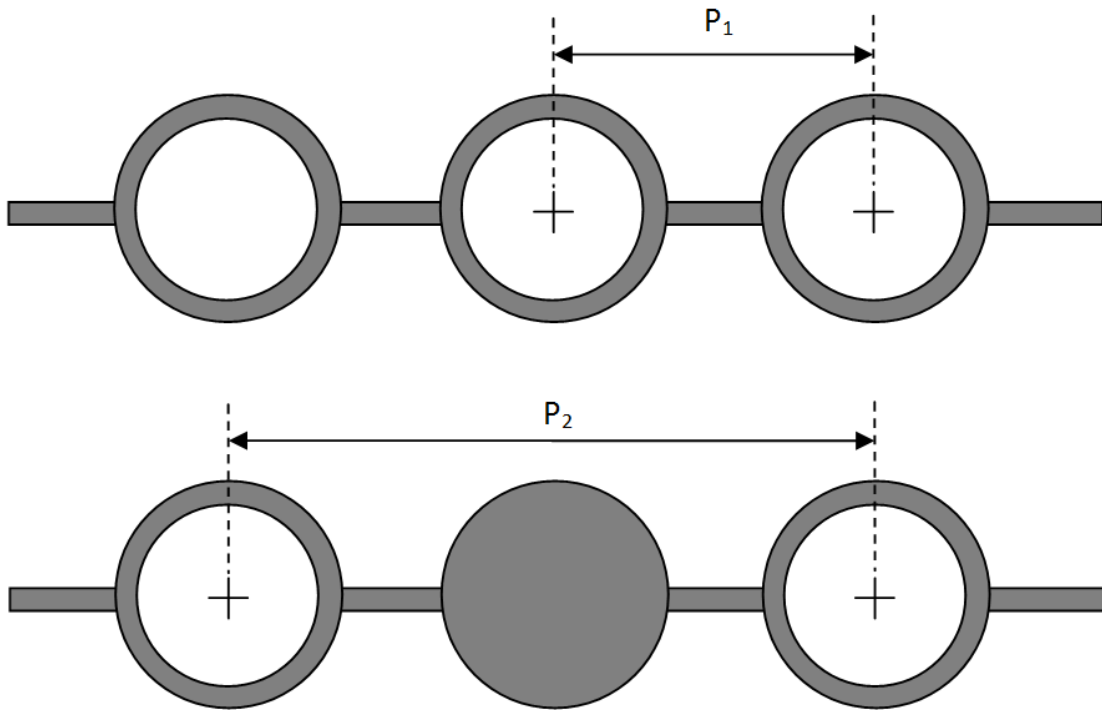


**Figure 15. Pitch Configurations (Top: Selected; Bottom: Alternative)**

### **V.5 Panel-to-Vessel Distance**

Figure 16 shows the reactor cavity floor plan of a HTGR with an air-cooled RCCS. The relative position of the risers' panels to the reactor vessel is visibly irregular due to the different shape of the reactor vessel (cylindrical) and cavity (approximately squared), and the penetrations in the cavity walls. Subsequently, the radiant view factors between the vessel surface and each riser's panel may vary. The experimental facility

will have a special design to account for the different view factors in the cavity, by changing the distance between the vessel and the panel.

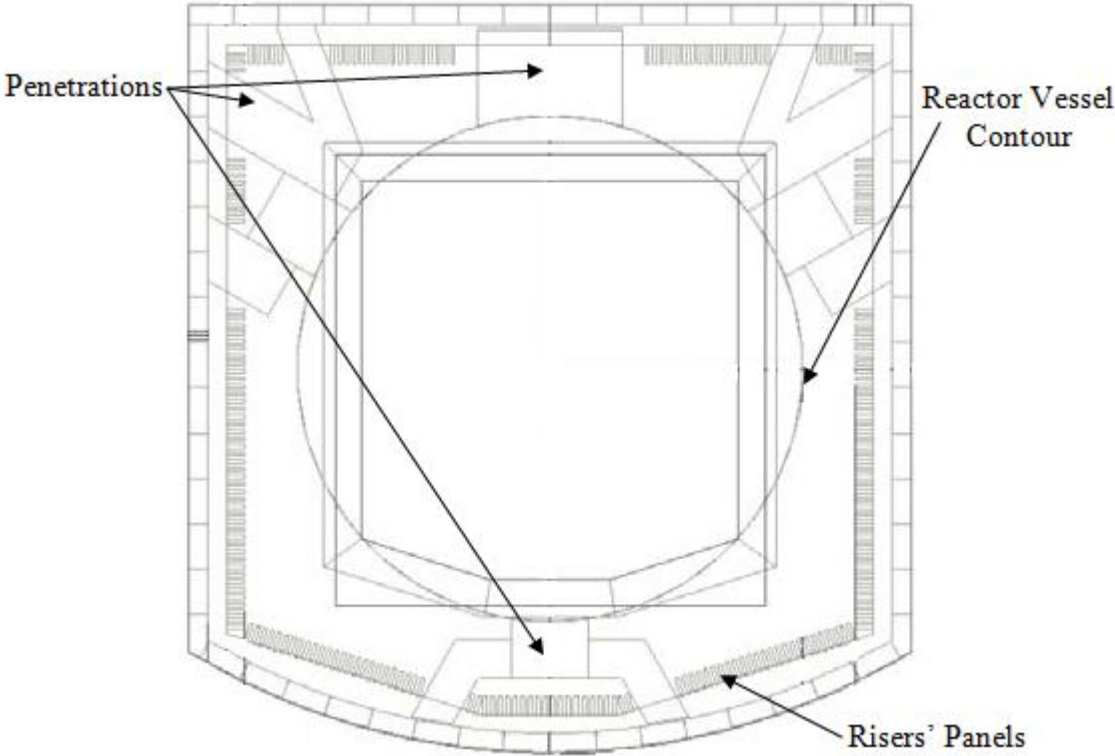


**Figure 16. Reactor Cavity Floor Plan**

## V.6 Water Tank Scaling

The water tank selection didn't follow a rigorous scaling procedure like the one adopted to define the dimensions and other features of the cavity. This was essentially due to the availability of a steel water tank donated by the Magnetic Laboratory of Texas A&M University, located at the University Science Building (USB). The calculations and additional analysis performed on the existing water tank focused on resolving the following issues:

1. Evaluating and optimizing the distance between the flow inlet pipe (coming from the cavity hot manifold), and the tank bottom level. This would avoid any disturbance of the water jet, in particular during the transient phase of the experiments, where two-phase flow conditions will be achieved.
2. Defining and test techniques to be adopted for the installation of two transparent windows to allow flow visualization in the tank during the experiments.
3. Select the proper material coating for the inner surfaces of the water tank to prevent rust under the expected operating conditions.
4. Defining a way to account for the L/D ratio (ratio between the tank height and inner diameter).

Similar experimental facilities decisions on the tank inlet pipe shape were taken under consideration when defining the characteristic of the tank water inlet for the

experimental facility (Item 1. in the bullet list). The pipe inlet (ID = 10.16 cm) was assumed to penetrate the tank wall from the side and release the flow at the center of the water tank. A 90° elbow was also considered at the end of the horizontal section to direct the water flow to the bottom of the tank, toward the water outlet nozzle. An estimation of the vertical distance between the elbow outlet and the tank bottom level was performed using Kerney correlation [27] for steam jet penetration length in water. Conservative conditions were assumed for the pool water temperature ( $T_\infty$ ), and steam flow rate ( $G_0$ ) to estimate the minimum distance of the inlet pipe location at which the jet would not impinge on the water bottom floor.

The technique and materials adopted to install the windows and to apply the coating on the tank inner surfaces (Items 2. and 3. in the bullet list respectively), will be described in detail in the next chapters.

Due to the given dimensions of the water tank, different L/D ratios (Item 4. in the bullet list) may be selected during the experiments by changing the water level in the tank, assuming it will always be located above the water inlet pipe.

## CHAPTER VI

### PHASE 3: FACILITY DESIGN AND MATERIALS SELECTION

The main characteristics of the experimental facility that were defined during the scaling phase are summarized in Table 3.

**Table 3. Experimental Facility Design Basic Characteristics**

<b>Plant Characteristic</b>	<b>Value</b>	<b>Unit</b>
Vessel Height	1	m
Cavity Height	1.1	m
Cavity Width	0.91	m
Vessel to Panel Distance	11.1	cm
Risers' ID	5.08	cm
Riser's Pitch to ID Ratio	2	-
Fin Thickness	2	mm
Manifolds and Pipeline ID	10.16	cm

The design of the experimental facility was initiated by defining dimensions, materials, and other required and desired features of the reactor cavity which can be considered as the main component of the facility. The design was then continued for the other parts of the facility based on the importance and complexity of the component. The

design phase can be subdivided into five steps listed below and described in the next paragraphs.

- STEP 1. Reactor Cavity Assembly Design
- STEP 2. Water Tank Design and Elevation
- STEP 3. Primary Structure and Scaffold Design
- STEP 4. Pipeline Design
- STEP 5. Secondary Heat Removal System Design

### **VI.1 Reactor Cavity Assembly Design**

The dimensions outer perimeter dimensions of the reactor cavity were already defined by the scaling laws previously described. The same laws allowed to establish the final dimensions of the cooling panel, at least for the its *heated section*, within the reactor cavity. The main components of the reactor cavity are:

- Reactor Vessel
- RCCS Cooling Panel
- Cavity Walls
- Manifolds

### *VI.1.1 Reactor Vessel*

A preliminary engineering evaluation of the vessel dimensions and shape, suggested the construction of a flat vessel surface instead of the real cylindrical surface. This assumption was supported by the fact that the azimuthal section of the cavity under consideration for this experimental activity is only the one facing one RCCS panel, which corresponds to

$$\delta = \frac{360^\circ}{25} = 14.4^\circ \quad (11)$$

Under these conditions, the vessel surface was assumed to be flat. This assumption drastically simplified the cavity geometry and helped in the selection of the electric heaters to be placed inside the vessel. The final drawing of the reactor vessel is displayed in Figure 17 (Front View) and Figure 18 (Back View). The reactor vessel was conceived as a steel shell, reproducing the upper and lower plena spherical shapes of the prototype reactor. The current experimental plan does not include analysis of the natural circulation of the air inside the reactor cavity but the realistic shape of the plena will allow future research activities to further investigate on this phenomenon [23]. The electric heater will be placed to fit in the back of the reactor right at the flat region, which will be the fraction of the vessel surface where most of the heat flux will be distributed. A support frame will be welded to the outer perimeter of the vessel shell to facilitate the connection of the vessel to the supporting structure. The material selected for the vessel is Stainless Steel SS304.

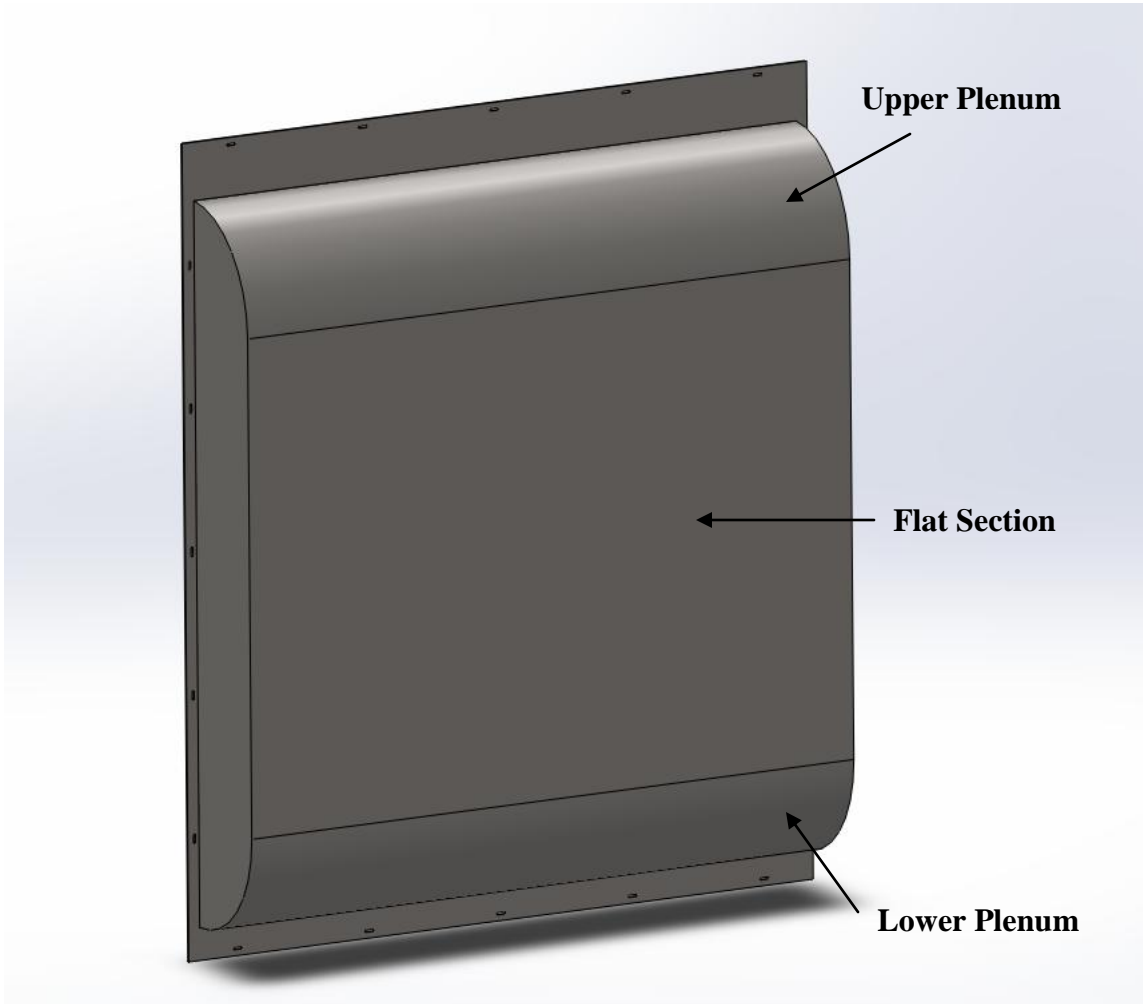


**Figure 17. Reactor Vessel (Front View)**

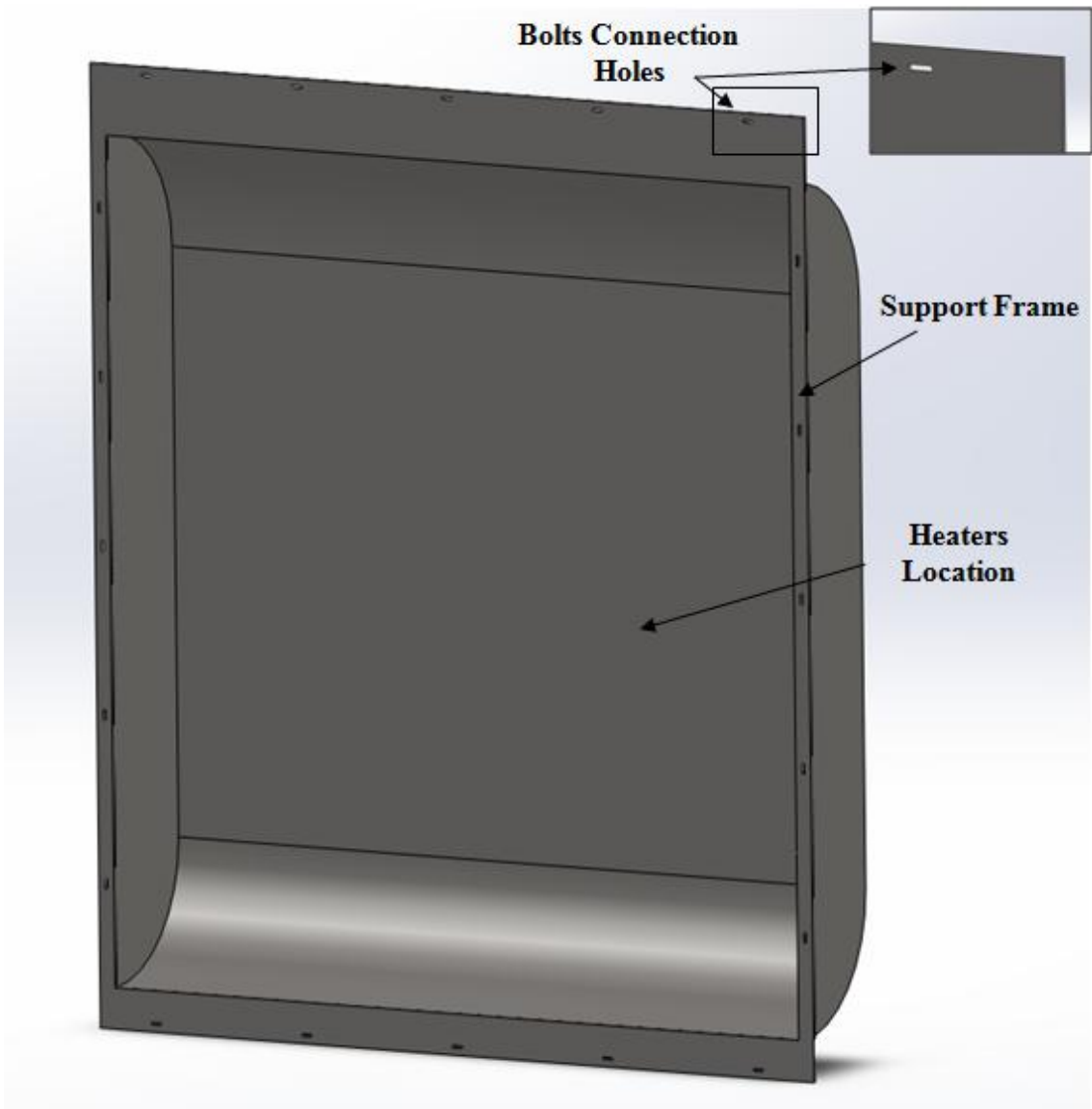


**Figure 18. Reactor Vessel (Back View)**

### *VI.1.2 RCCS Cooling Panel*

The cooling panel assembly, comprehensive of the nine risers and the fins, is shown in Figure 19. The risers' assembly consists of risers and fins which will be welded on a bottom support plate. This plate will support the panel weight and will define the reactor cavity floor. As shown in the side view, the risers were subdivided into three distinct regions:

- The heated section, laying inside the reactor cavity in front of the reactor vessel
- Two unheated extension sections at the top and bottom of the heated section, which will be located outside the reactor cavity. These two sections will be used to connect the risers to the manifolds' branches.

All the parts included in the cooling panels above mentioned will be in SS304.

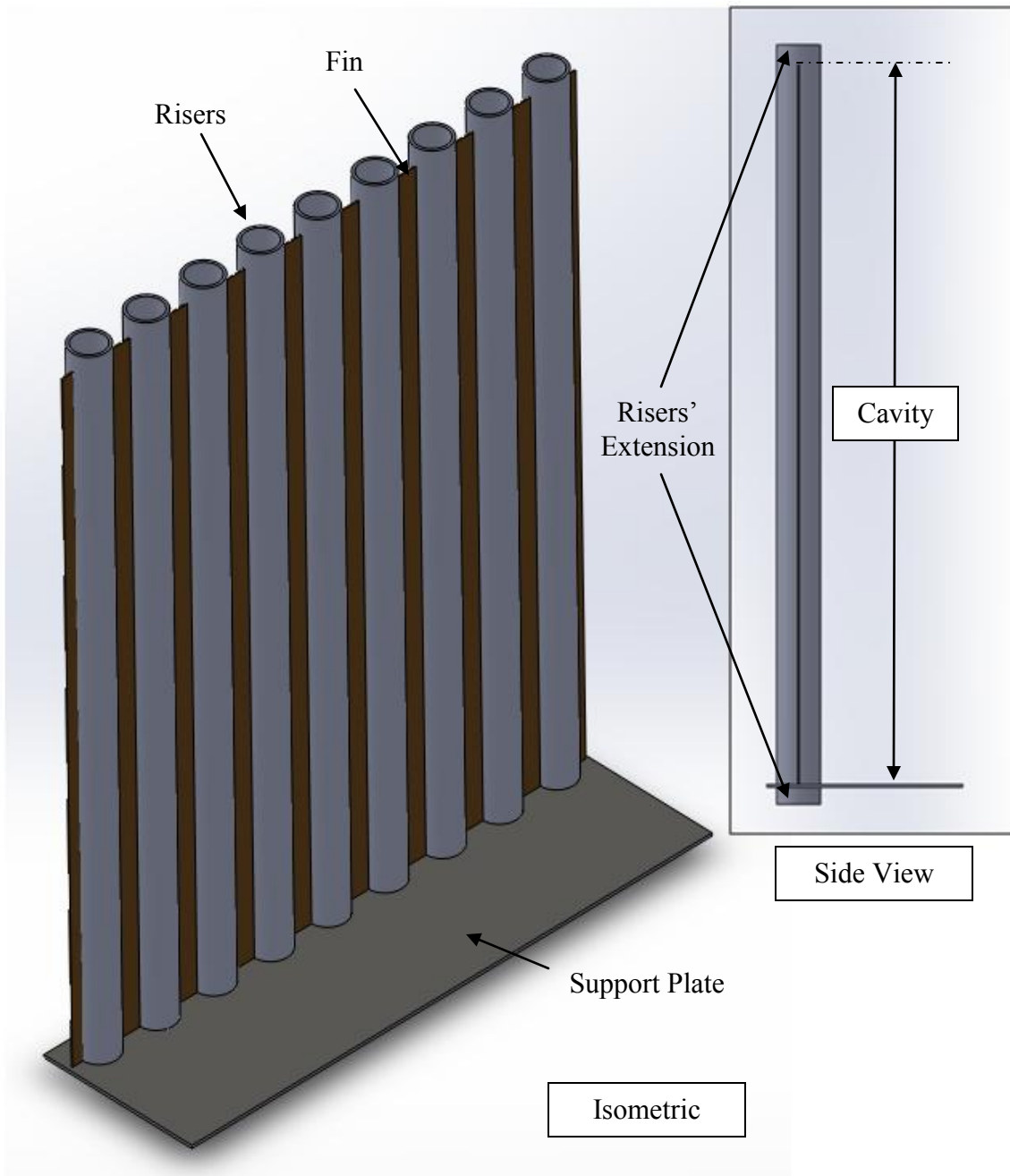


**Figure 19. RCCS Panel**

### VI.1.3 Cavity Walls

As previously mentioned, all the dimensions of the cavity perimeter and walls were defined during the scaling phase. The floor of the cavity was incorporated in the cooling panel to support its weight. All the other walls will be constructed using insulation panels. This solution helped to:

- Reduce the heat losses through the cavity walls under desired limits
- Perform maintenance inside the cavity by easily remove the panels

The selected of the thermal insulation panels was driven by different factors such as thermal conductivity and maximum operating temperature, available commercial size of the panels, maximum mechanical stress, and cost. Two different thermal insulation materials were selected as described below.

Microtherm ® Boards. These panels provide stable thermal performances for continuous exposure up to 1000 °C, excellent machineability, and very low thermal conductivity (0.0252 W/m K at 500 °C). The standard panel size is 1000 mm x 550 mm with thickness varying from 15 up to 50 mm. This material was selected to build the main cavity walls, including the ceiling, the lateral walls, the back wall cooling panel side), and the vessel side wall.

Fiberglass Mats. Different types of mats are available in the market with a wide range of thermal conductivities, densities, and cost. Two different types were selected for the reactor cavity insulation. The thermal conductivity for both types is approximately 0.6 W/m K but they have different flexibilities. The mat with the highest

flexibility was selected to fill the gaps between the microtherm panels. The one with the lowest flexibility was selected to build additional layers of insulation on top of the Microtherm panels if it will become necessary.

#### *VI.1.4 Manifolds*

Even if the manifolds are not installed inside the cavity, they are integral part of the cavity assembly, being connected directly to the riser's panel. Particular interest would be dedicated on the study of the flow behavior inside the risers and the manifolds. This suggested the use of a transparent material to allow flow visualization in the horizontal section and in through the branches (risers' extensions). There are different materials that may be selected for this scope. Due to the temperature expected during the operation of the facility (cooling water may reach saturation during the transient phase of the experiments), and to the axial thermal conduction from the heated section to the risers' extensions, the selection was limited to polycarbonate and glass tubes.

The final drawing of the manifolds is shown in Figure 20. The manifolds were conceived to allow different flow configurations. Three inlets were included in the design:

- One centered inlet at top of the manifold, facing the fifth riser, for a symmetrical flow configuration.
- Two lateral inlets, located at the edges of the manifold, to allow asymmetrical flow configurations.

These additional desired features required special mechanical properties of the material to be selected.

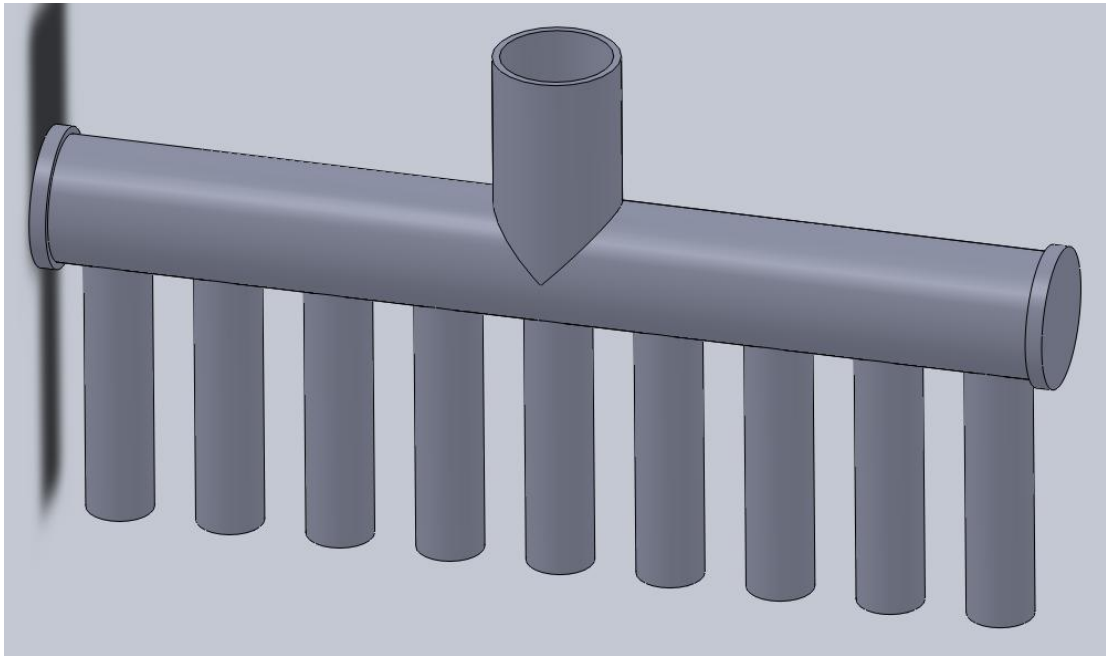


**Figure 20. Manifold**

The polycarbonate tubes can be purchased with different inner diameters and piping for the manifolds and branches (10.18 cm and 5.08 cm ID respectively) are available. Two main limiting issues were identified when considering this material:

- Welding, required to connect the nine branches to the manifold.

- Beads, necessary to connect the end caps to inlets to be closed during operation.

These issues were considered as “show stoppers” for the selection of the polycarbonate pipes.

High temperature glass (Pyrex) tubing was considered to be the best choice for to build the manifold, and include all the desired features described above. The limiting issues identified for this material are related to its thermal expansion (to be accounted when connecting the glass manifold with the stainless steel risers), and its fragility. These limitations were considered during the installation of the manifolds and the connection with the cooling panel.

## **VI.2 Water Tank Design and Elevation**

The desired features to be included in the available water tank are listed in the following bullets.

- Two transparent windows (placed at 90°) to be used for flow visualization (one to be used for the visualization and one as source of illumination).
- Lateral inlet for the main cooling water from the cavity (10.16 cm ID) located at a given distance from the bottom, as specified in Chapter V. The inlet should end with a 90 ° downward elbow at the center of the tank, as described in Chapter V.

- Bottom outlet (10.16 cm ID) to be connected to the downcomer (pipe connecting the water tank to the cavity inlet).
- Venting line, located at the top of the tank.
- Additional inlet/outlet ports for the secondary system coolant flow.

The main characteristics of the tank are summarized in Table 4

**Table 4. Tank Characteristics**

<b>Characteristic</b>	<b>Value</b>	<b>Unit</b>
Inner Diameter	62.23	cm
Total Height (Top to Bottom)	182.9	cm
Total Capacity	0.556	m <sup>3</sup>
Empty Weight (approximate)	227	kg
Total Weight (including water)	783	kg

The final drawing of the water tank is shown in Figure 21.

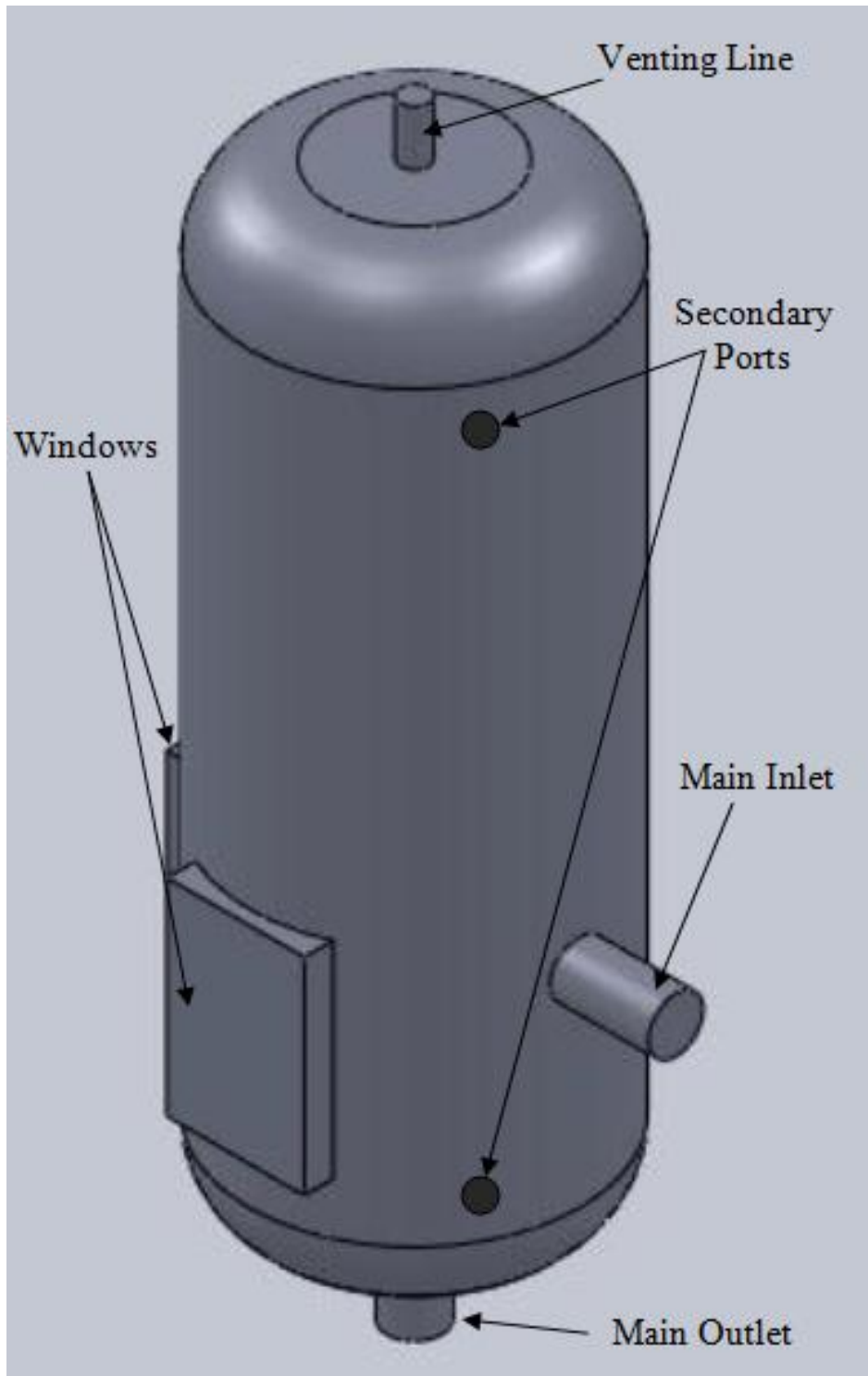


**Figure 21. Water Tank**

The final elevation of the tank was defined by scaling the elevation of the tanks of the prototype plant. The elevation of the bottom of the tank was found to be 5.63 m from the floor. This value will define the axial dimensions of the supporting structure and scaffolds.

### **VI.3 Primary Structure and Scaffold Design**

Two main structures were identified and designed for the experimental facility:

- The main structure to support the components of the facility, including the reactor cavity, the water tank, the pipelines, and the water.
- The scaffold, conceived to allow people to safely access the different components of the facility, located at different elevations.

#### *VI.3.1 Primary Structure*

Due to its modularity, relatively easy installation procedure, and cost, the Interlake ® pallet rack was selected as the primary structure of the experimental facility. The selection of the model was performed considering the weight of the components (primarily cavity and tank with water), their elevation from the floor. Conservative safety factors were applied.

### VI.3.2 Scaffold

An additional scaffold became necessary to provide:

- Access of the different components of the facility during shutdown and normal operation. In particular, cavity and manifolds, pipelines, and water tank need to be accessible for maintenance, instrumentation installation and verification (including cameras and other devices used for flow visualization), and operation (air venting, monitoring, etc.).
- Stability of the experimental facility during each phase of the activity (including two-phase and vapor generation).

Due to the dimensions and the desired location of the levels, a customized scaffold had to be design and built using steel square tubing. The size of the tubing was estimated by performing static stress calculations on the structure, assuming conservative concentrated loads at different locations of the structure. Analysis for the selection of anchors and bolts to be used to fix the scaffold to the floor were also performed.

The final drawings and dimensions of the scaffold are shown in Figure 22. Three elevations can be identified in the figure.

Elevation 0. This is the ground floor where most of the instrumentation control and operation will be conducted. The bottom manifold and the cavity (including electric heaters and risers) can be accessed from this elevation.

Elevation 1. Located at 2.89m from the floor, this elevation allows the access to the top manifold, top cavity, vertical pipeline (connecting the cavity to the tank and vice versa), and the bottom exit of the water tank.

Elevation 2. This elevation was defined to be located at 5.63 m from the floor, providing access to the water tank and all highest elevation pipelines.

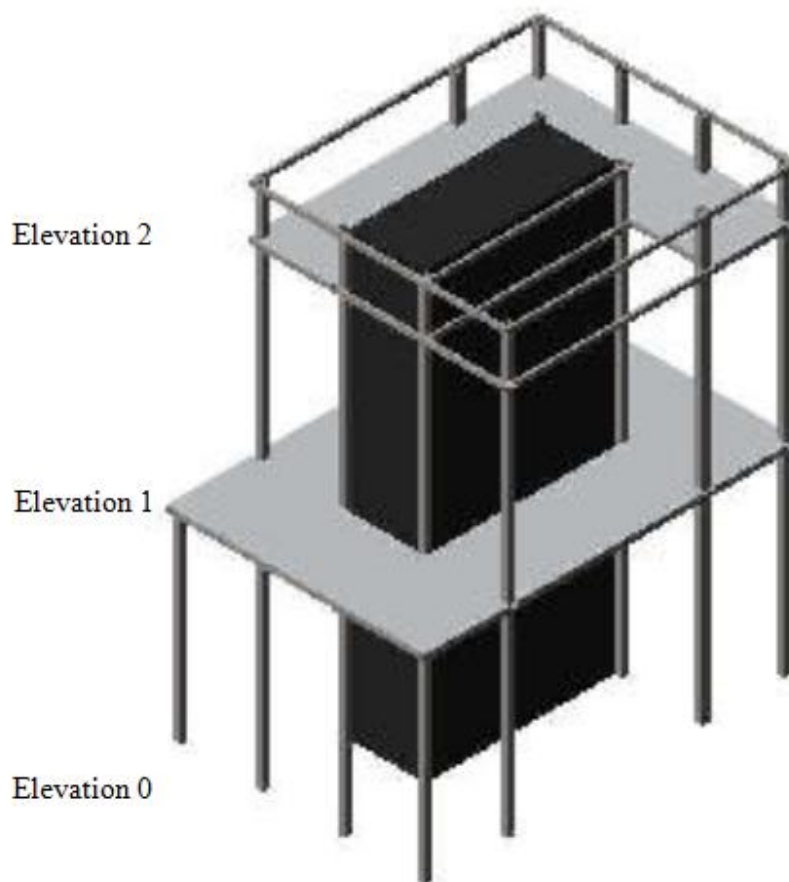


**Figure 22. Scaffold and Elevations**

## VI.4 Pipeline Design

The materials selected for the pipeline connecting the bottom and top manifolds to the water tank were chosen to allow:

- Flow visualization along the pipeline (downcomer, tank inlet).
- Instrumentation installation (flowmeters, thermocouple probes).
- Easy connection between sections.
- Safe operation at the saturation temperature and atmospheric pressure (plus gravitational head).

Polycarbonate was selected for the transparent sections. Stainless steel was selected for the other sections of the pipeline.

An overview of the facility with the final layout of the pipeline is depicted in Figure 23. The main components are marked with a number. The legend for Figure 23 is reported on Table 5, where other information is displayed.

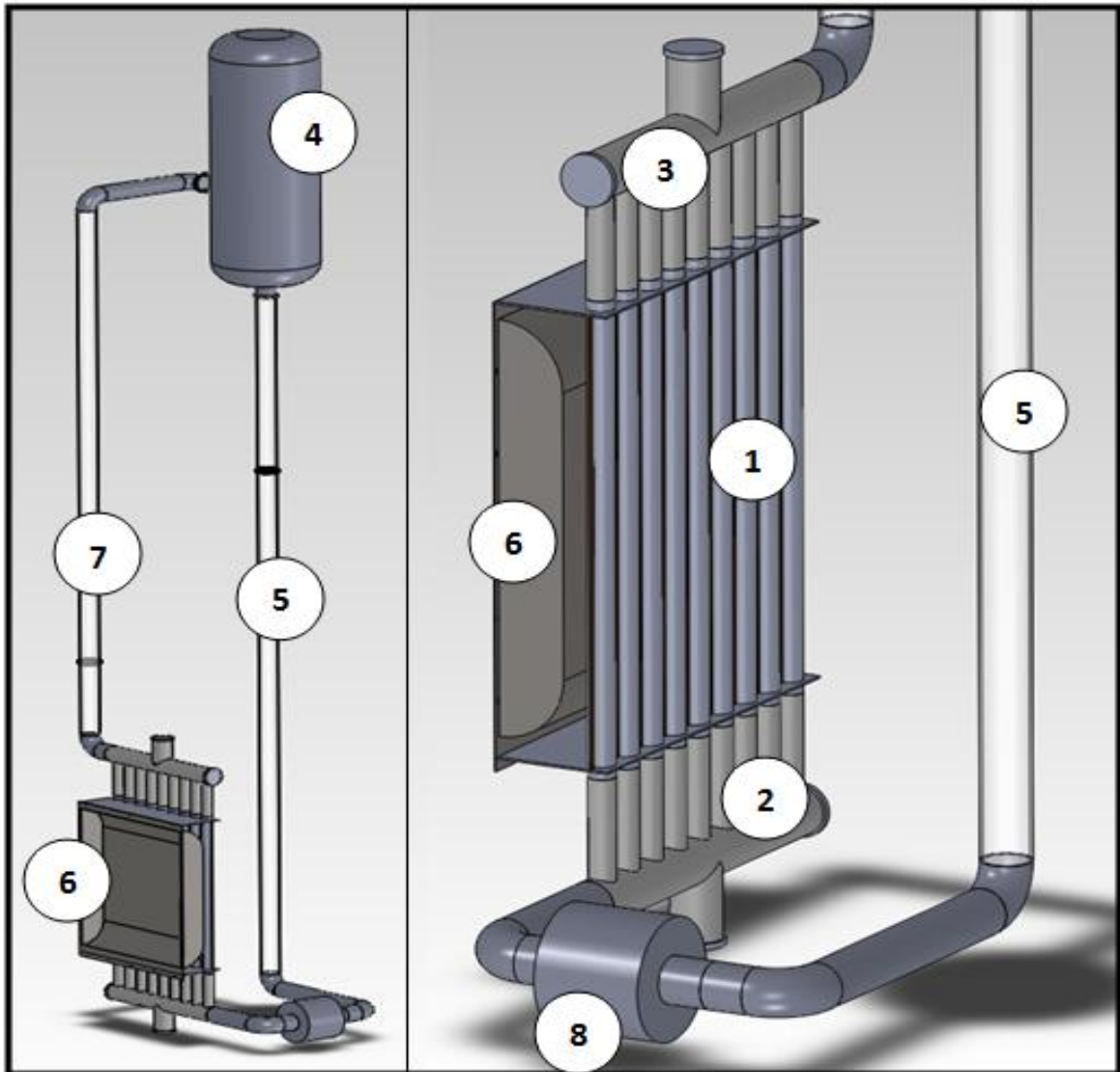


Figure 23. Experimental Facility Overview.

**Table 5. Legend of Figure 7.**

<b>Component #</b>	<b>Component Description</b>	<b>Material</b>	<b>Accessibility</b>
1	Risers' Panel	SS304	Elevation 0
2	Bottom Manifold	Glass	Elevation 0
3	Top Manifold	Glass	Elevation 0-1
4	Water Tank	Steel	Elevation 2
5	Downcomer	Polycarbonate	Elevation 0-1
5	Reactor Vessel	SS304	Elevation 0
5	Upward Pipeline	Polycarbonate	Elevation 1-2
5	Flowmeter	-	Elevation 0

### **VI.5 Secondary Heat Removal System Design**

The secondary heat removal system is required to remove the power supplied to the water in the cavity and reach the steady-state conditions at the desired temperature. Due to the unavailability of a source of cold water in the laboratory, two alternative solutions were evaluated:

- Install a heat exchanger using an AC unit as ultimate heat removal sink.
- Install a heat exchanger using a ice bath as ultimate heat removal sink.

The second solution was considered to be convenient to avoid discharging the thermal power removed from the system to the environment (causing excessive overheat of the laboratory which may interfere with other experiments), and reduce the total cost. A simplified scheme of the designed heat removal system is depicted in Figure 24.

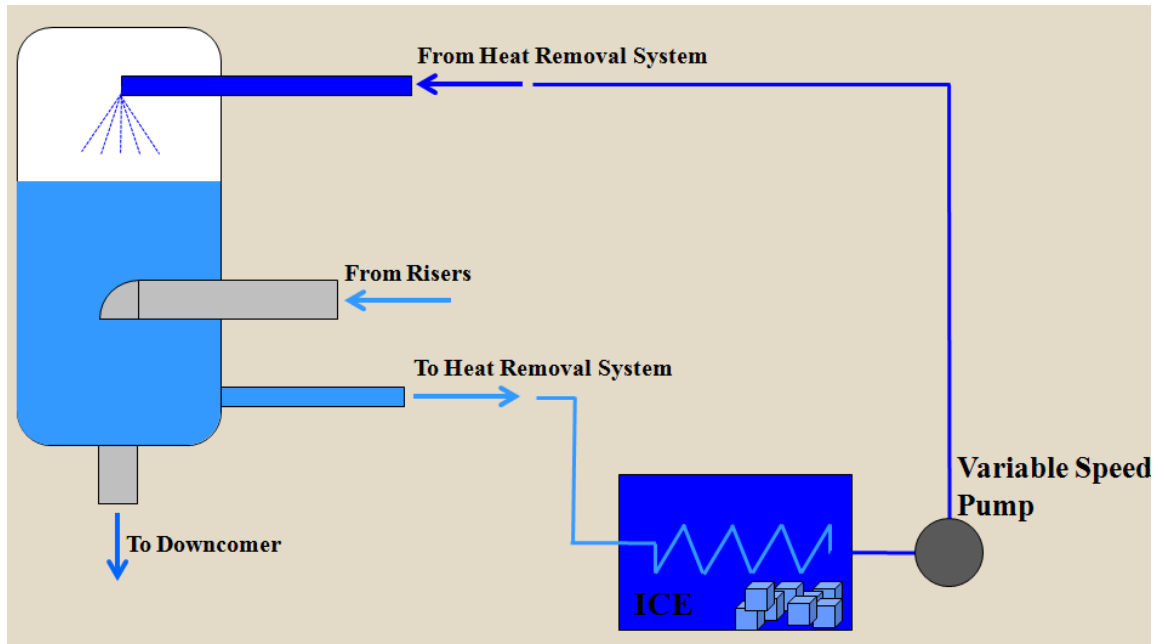


**Figure 24. Secondary Heat Removal System Schematic.**

The system consists of the following components:

- An ice container (secondary side of the heat exchanger).
- A copper coil through which the primary water to be cooled flows.
- A variable speed pump.
- Pipelines from and to the water tank.

Water is withdrawn from the outlet port located at the bottom of the water tank.

The water flows through the copper coil (which is submerged into a container where the heat is released to the melting ice. The water is pumped back to the tank and injected from the inlet port located at the top to allow uniform mixing.

## CHAPTER VII

### PHASE 4: RELAP5-3D MODEL PREPARATION AND PRELIMINARY ANALYSIS

The RELAP5 code has been developed for best-estimate transient simulation of LWR coolant systems during postulated accidents. RELAP5-3D [28] is a successor to the RELAP5/MOD3 code that was developed for the Nuclear Regulatory Commission. The code extensions in RELAP5-3D are sponsored by the Department of Energy, Office of Fusion Energy Sciences, Savannah River Laboratory, Bettis Atomic Power Laboratory, the International RELAP5 Users Group (IRUG), and the Laboratory Directed Research and Development Program at the Idaho National Laboratory (INL). RELAP5 analyzes the thermal-hydraulic behavior of light-water systems. It was originally designed to analyze complex thermal-hydraulic interactions that occur during postulated large or small break LOCAs in PWRs. However, as development continued, the code was expanded to include many of the transient scenarios that might occur in thermal hydraulic systems. Thus, the code has been successfully used to analyze not only large and small break LOCAs but operational transients in PWRs and various transients in experimental and production reactors and reactor simulators.

RELAP5-3D is one of the systems codes selected for the analysis of steady-state and transients required for the Generation IV nuclear power plants design, including the HTGR [29]. While other system codes (such as MELCOR) have been selected by other participating Universities, the selection of the RELAP5-3D for this project has been driven by different factors:

- The system code has been largely used for analysis of water systems, including systems where natural circulation phenomena occur.
- Consolidated partnership with Idaho National Laboratory (INL) where RELAP5 was designed and still maintained. This may help facilitating the resolution of possible technical issues with the code.
- The computer code is currently available at the Nuclear Engineering Department.

A RELAP5-3D model of the experimental facility was prepared in order to:

- Conduct preliminary analysis of the behavior of the coolant.
- Identify important thermal-hydraulic phenomena that could be observed during the experimental phase and that may require special experimental configurations or instrumentation.
- Select proper instrumentation and define/optimize the instrumentation layout.
- Prepare the base for the final model to be used for the final simulations that will be compared with the experimental results.

Another RELAP5-3D model of the full power plant RCCS design was also prepared and used in conjunction with the previous model to validate the steady-state scaling laws described in Chapter V.

A detailed description of the models and assumptions, and preliminary simulation results are presented in the next paragraphs.

## VII.1 RELAP5-3D Nodalization

Two different versions were assumed to prepare the RELAP5-3D models of the RCCS experimental facility:

1. *Symmetric version*, where the inlet and outlet of the coolant in the bottom and top manifolds were assumed to be at the center of the manifold. This version was originally considered to be the final configuration to be applied to the experimental facility. Other inputs received in a later phase of the analysis suggested the asymmetric version as the final configuration for the experimental facility.
2. *Asymmetric version*, where coolant inlet and outlet in the manifolds are located on the side of the collectors (bottom left and top right respectively).

Figure 25 shows the nodalization diagram for these configurations.

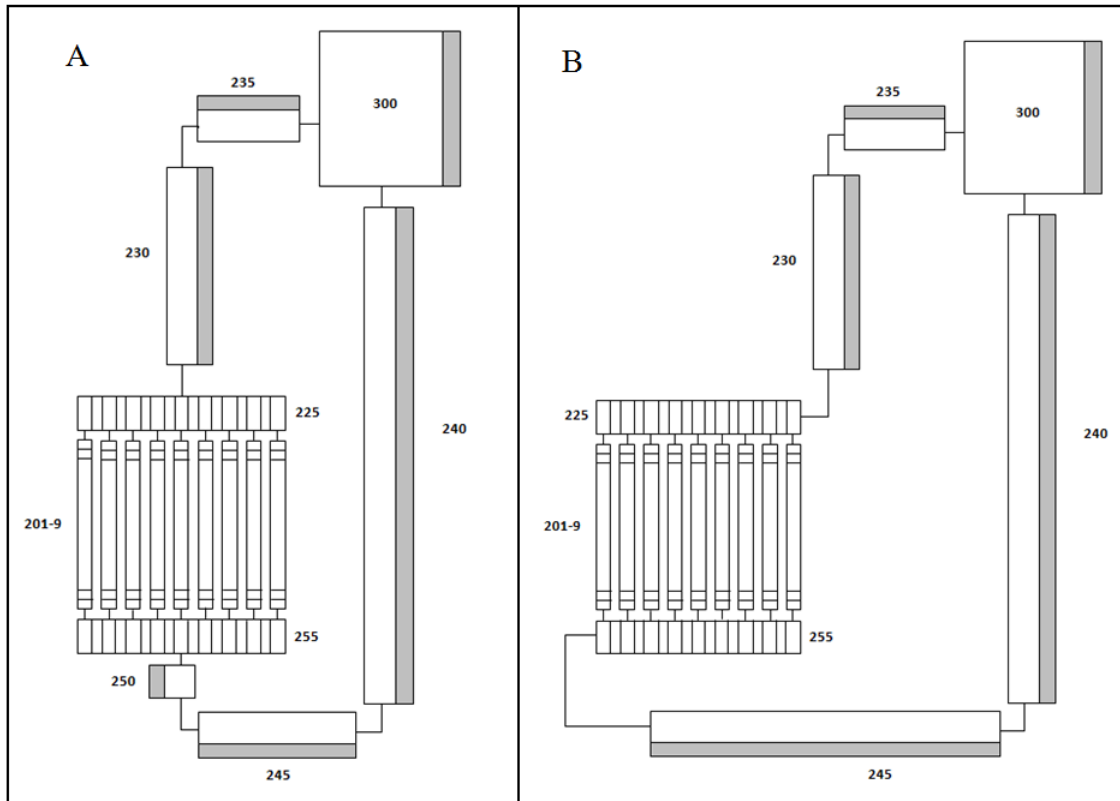


**Figure 25. RELAP5-3D Nodalization Diagrams (A: Symmetric Version; B: Asymmetric Version)**

The nodalization diagrams for the two configurations are essentially very similar and share the following features:

- The risers were simulated with nine independent vertical pipe components (201-209). Five subvolumes were defined in each pipe, one at the center, thermally connected to the cavity with heat structures, and

four (two at the top and two at the bottom) to simulate the portion of the risers outside the reactor cavity (with no heat structures).

- The front cavity (space between the reactor vessel and the risers' panel) and the back cavity (area between the risers' panel and the cavity walls) were simulated with two single volumes (100 and 400 respectively).
- The upper and lower manifolds were simulated with horizontal pipe components with fifteen subvolumes each (225 and 255 respectively). A sensitivity study was conducted to identify possible recirculation between adjacent pipes using a different nodalization for the upper manifold.
- Components 201-9 were connected to the manifolds 225 and 255 using multiple cross junctions.
- The water tank is simulated using a single volume (300). A sensitivity analysis on the water tank nodalization (using pipe component and multi-dimensional component was also performed and described in the following paragraphs).

The pressure boundary was imposed by connecting the top of the single volume 300 to a time-dependent volume where atmospheric pressure and temperature were specified. The same time-dependent volume was used to impose the boundary condition to the environment, to account for the cavity, pipes, and tank heat losses.

### *VII.1.1 Heat Structures*

Several heat structures were defined in the input deck to account for the complex heat transfer mechanisms expected in the cavity and for the heat losses between the experimental facility and the environment through walls and thermal insulation.

### *VII.1.2 Pipelines and Tank*

Heat structures were defined to account for the thermal losses of the pipelines and tank. The left boundary of the heat structures was connected to the hydrodynamic components modeling the pipeline between the cavity and the water tank. The right boundary was connected to the single volume simulating the environment.

### *VII.1.3 Reactor Cavity*

The organization of the heat structures in the reactor cavity required assumptions and additional calculations due to the complexity of the geometry, the combined heat transfer mechanisms expected to occur during the experiments, and some known constraints of the RELAP5-3D code when modeling radiation and conduction within the same heat structures. Figure 26 (left) shows a top view of the experimental cavity. Heating panel, front and back cavity (components 100 and 400), standing pipes and fin can be easily recognized in the picture.

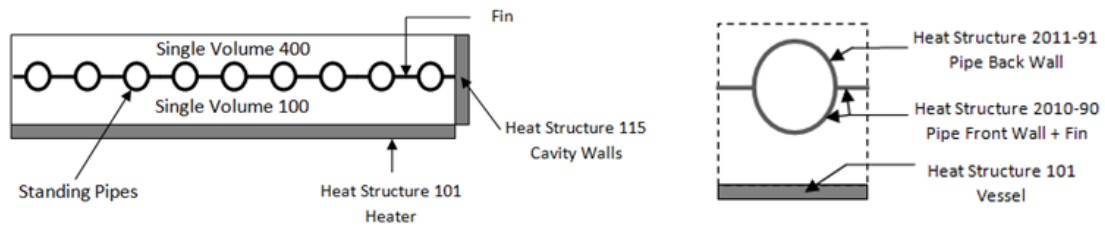


**Figure 26. Cavity Nodalization and Heat Structures Arrangement.**

Since nine independent pipe components were used to simulate the risers, the front wall of the pipes and the fin (exposed to radiation and convection heat transfer) were modeled using nine independent heat structures, each accounting for the front half of the pipe wall and two halves of the fin (left and right side of the pipe), as shown in Figure 26 (right). A summary of the heat transfer mechanisms between the vessel and the risers and the single parts of the heat structures involved is shown in Figure 27.

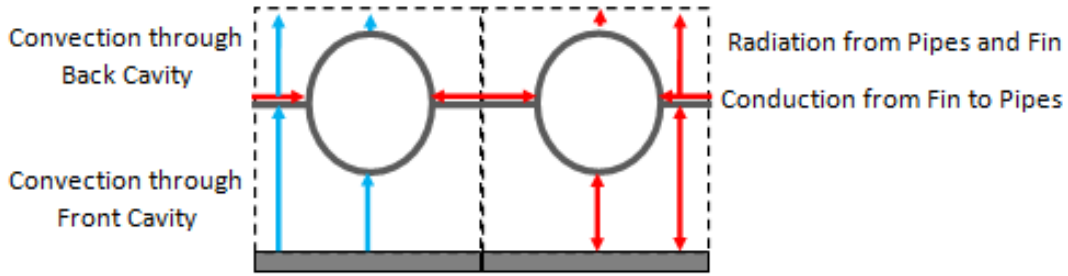


**Figure 27. Heat Transfer Mechanisms in the Cavity**

Heat is transferred from the reactor vessel (dark block at the bottom of the diagram in Figure 27) to pipes and fins by radiation and by natural convection of air through the front cavity. The heat transferred to the fins is then transferred by conduction to the pipes wall and, eventually by convection to the water flowing inside the pipes. The heat structures defined in RELAP5-3D can be grouped into *radiation or conduction enclosures* to simulate the radiation and conduction between heat structures. Since heat structures in RELAP5-3D cannot be specified in more than one enclosure, specific assumptions were necessary in order to overcome the code limitation and guarantee an accurate modeling of the cavity heat transfer mechanisms. Previous publications [15] and experimental work conducted in similar RCCS facilities [23], have shown that radiation is the predominant heat transfer mechanism in the reactor cavity, carrying almost 80% of the total heat transferred to the risers panels. For this reason the radiation enclosure was preferred and defined in the input deck to account for the radiation heat

transfer between the heat structure simulating the reactor vessel (HS 101), and the heat structures simulating the risers front pipes and fins (HS 201-9). Even if conduction between the fins and pipes was not simulated, the total energy balance within each the heat structure will be preserved. Since only one volume can be connected to each axial node of one heat structure, the left side of the heat structures 201-9 was connected only to the pipe components 201-9. Subsequently, convection heat transfer between the fins to the back cavity was ignored. Due to the small dimension of the back cavity and to the expected low temperature of the back side of the pipe walls and fin, this approximation was considered acceptable. Radiation to the back cavity was also neglected. Convection between the pipe back wall and the back cavity was instead taken into account in the model. The heat generation in the reactor vessel (HS 101) was simulated by imposing a constant heat flux as boundary condition at the left boundary of the mentioned heat structure. A convective boundary was defined on the right side of the same heat structure. As also shown in Figure 26, a dedicated heat structure was defined to account for the heat losses by convection to the environment through the cavity walls. Table 6 shows a list of all the cavity heat structures defined in the model with the heat transfer mechanisms simulated. Coolant temperatures and pressure initial conditions were assumed to be the same of the one applied in the full plant simulations during accident scenario (Depressurized Conduction Cooldown, DCC). Subcooled liquid water at 307.725 K and atmospheric pressure was imposed as initial condition in any hydrodynamic component of the water loop while air at 333.15 K and atmospheric pressure was assumed to occupy the single volumes simulating front and back cavities.

Liquid water at 296.5 K was assumed to occupy 80% of the total volume of the tank. An imposed heat flux of  $1.96 \times 10^4 \text{ W/m}^2$  was imposed to the left boundary condition of the heat structures of the vessel (HS100 series). Such as heat flux was calculated during the scaling procedure of the RCCS facility resulting from the full plant total heat produced during accident scenario of 1.5MW. The dimensions of each component and heat structures reproduced the real dimensions of the experimental facility. Realistic material properties (thermal conductivity and heat capacity) of stainless steel and thermal insulation were specified in the input file.

**Table 6. Cavity Heat Structures Summary**

<b>HS #</b>	<b>Component</b>	<b>Convection</b>	<b>Radiation</b>
101	Vessel	✓	✓
115	Cavity Walls	✓	✓
2010-2090	Pipe/Fin Front Walls	✓	✓
2011-2091	Pipes Back Walls	✓	

#### *VII.1.4 Radiation View Factors*

The radiation view factors required as input parameters for the radiation enclosures defined in the RELAP5-3D input deck were calculated using NEVADA™.

Nevada [30] is a computer code, based on Monte Carlo method [31] largely used for radiation analysis. The software allows the user to create the model by drawing the surfaces and imposing the direction of the surface normal vectors. Figure 28 presents the geometry created with Nevada. All the dimensions and relative radial and vertical position of vessel, pipes and fin were taken from the drawing of the facility. As required for any Monte Carlo calculations, the number of “rays” (histories) had to be selected and optimized in order to achieve an acceptable standard deviation with the shortest computational time.

Table 7 summarizes the final calculation results as they were applied in the RELAP5-3D input deck. The number of rays used for the simulation was  $10^9$  and the maximum standard deviation achieved in the view factor calculations was 0.07. The emissivity of the surfaces of vessel and pipes was imposed equal to 0.8 [32, 33].

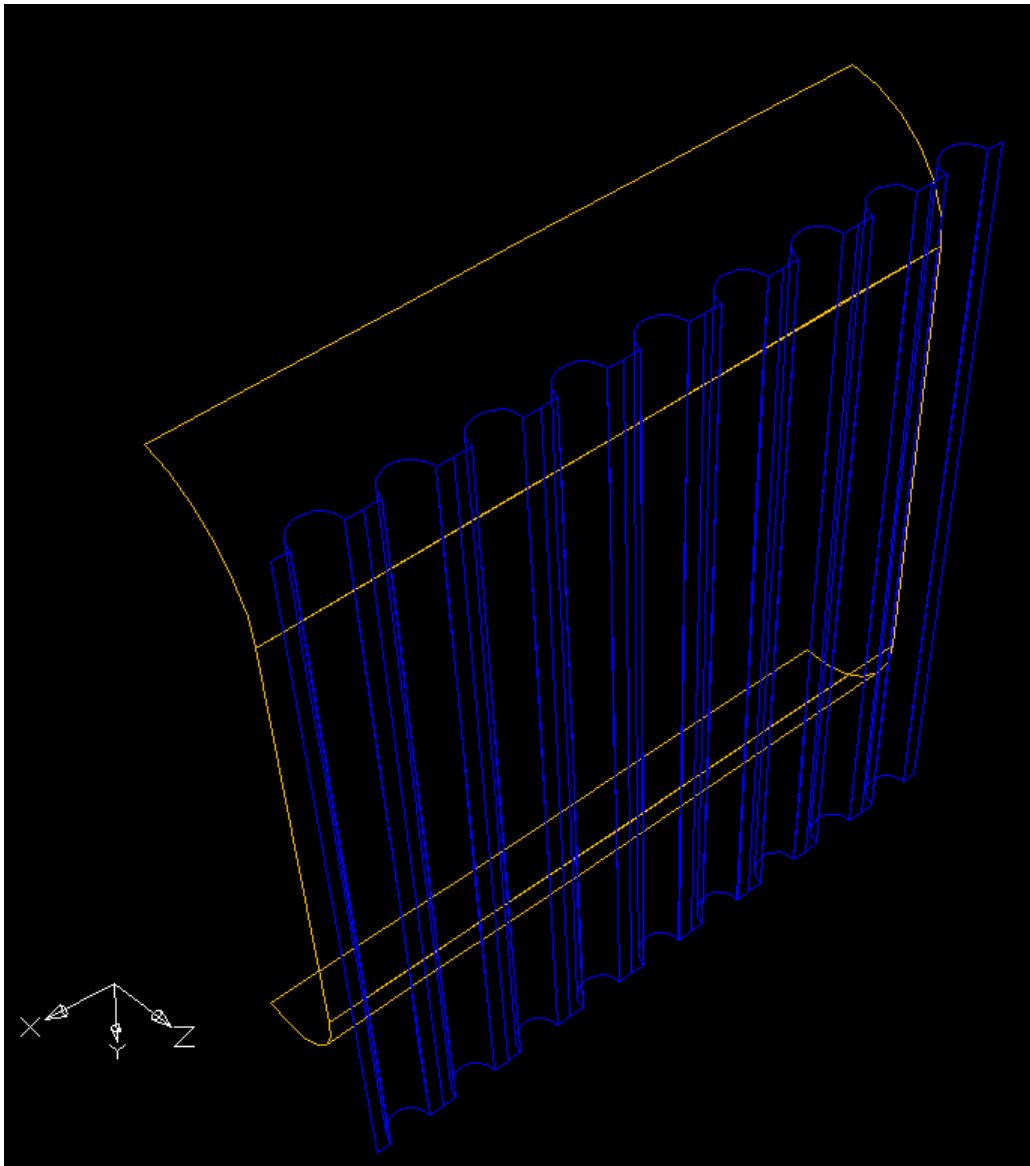


**Figure 28. NEVADA Input Geometry**

**Table 7. Radiation View Factors**

	Vessel	Pipe/Fin 1	Pipe/Fin 2	Pipe/Fin 3	Pipe/Fin 4	Pipe/Fin5	Pipe/Fin 6	Pipe/Fin 7	Pipe/Fin 8	Pipe/Fin 9	Cavity Walls
Vessel	0	0.085056	0.106983	0.109572	0.109981	0.110126	0.109981	0.109572	0.106983	0.085056	0.06669
Pipe/Fin 1	0.362298801	0.116379	0.066142	0	0	0	0	0	0	0	0.455153
Pipe/Fin 2	0.455697571	0.066142	0.116379	0.066142	0	0	0	0	0	0	0.295739
Pipe/Fin 3	0.466725501	0	0.066142	0.116379	0.066142	0	0	0	0	0	0.284561
Pipe/Fin 4	0.46846765	0	0	0.066142	0.116379	0.066142	0	0	0	0	0.282655
Pipe/Fin5	0.469085282	0	0	0	0.066142	0.116379	0.066142	0	0	0	0.282279
Pipe/Fin 6	0.46846765	0	0	0	0	0.066142	0.116379	0.066142	0	0	0.282655
Pipe/Fin 7	0.466725501	0	0	0	0	0	0.066142	0.116379	0.066142	0	0.284561
Pipe/Fin 8	0.455697571	0	0	0	0	0	0	0.066142	0.116379	0.066142	0.295739
Pipe/Fin 9	0.362298801	0	0	0	0	0	0	0	0.066142	0.116379	0.455153
Cavity Walls	0.088695504	0.1421138	0.092339506	0.0888494	0.088254248	0.088137	0.088254248	0.0888494	0.092339506	0.1421138	0

### VII.1.5 Risers' Heat Structures Settings

Figure 29 helps identifying the process followed to define the characteristics of the heat structures simulating the combined risers' front walls and fins.

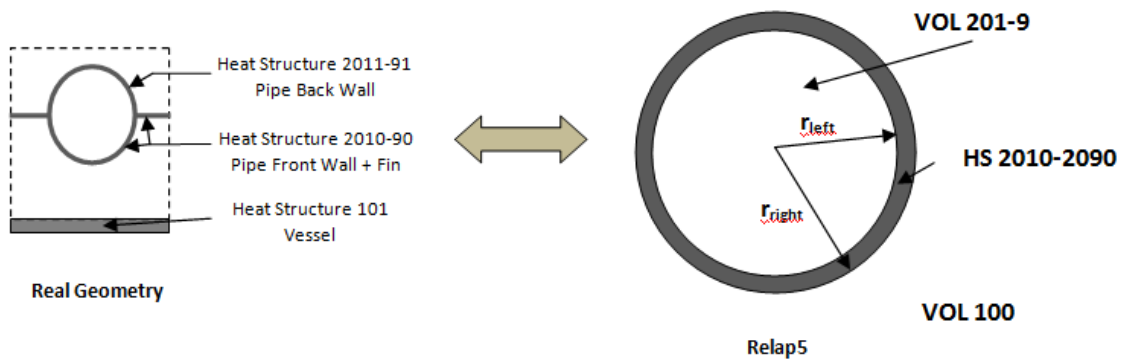


**Figure 29. Risers' Heat Structure Definition**

Cylindrical geometry was specified for the heat structure representing the pipe front walls and fins. Left and right radii are required in the geometry cards of each heat structure. In order to use the view factors as calculated and preserve the reciprocity rules, the right boundary radius was initially calculated in order to satisfy the following condition:

$$2 \pi r_{right} L = A_{wall,out} \quad (12)$$

where  $r_{right}$  is the equivalent radius of the right boundary surface (in contact with the front cavity, volume 100) and  $L$  is the axial length of the wall. The left radius was then calculated:

$$r_{left} = r_{right} - t_{wall} \quad (13)$$

In Equation 1,  $t_{wall}$  is the thickness of the wall.

Based on the way the inner and outer radii were defined, the right boundary surface area of the heat structure is equal to the real surface area of the riser/fin section. This is a required condition for the radiation enclosure, where the view factors (calculated using the real surface area of the pipes and fins) were defined. On the other hand, the left boundary surface area will be overestimated. As described above, the walls of each riser was modeled with two heat structures each one accounting for half of the total pipe wall. A correction in the heat transfer coefficient was found to be necessary to account for the difference between the area defined in the RELAP5 input deck and the real heat transfer area between pipe half wall and coolant. This was done using the Fouling factor ( $F$ ) in the additional left boundary conditions card. The factor was set up as follows:

$$F = \frac{A_{wall,in}}{A_{relap}} \quad (14)$$

where  $A_{wall,in}$  is the real surface area, and  $A_{relap}$  is the left boundary surface area defined in the RELAP5 heat structure geometry cards.

## **VII.2 Steady-State Scaling Laws Confirmation**

Minor modifications to the input model described in the previous paragraph were adopted in order to reach the steady-state conditions. This includes an additional heat structure attached to the component 300 to remove the heat from the coolant. Different methods can be used to validate the scaling laws previously described. The approach used during the design process is summarized in the diagram of Figure 30.

A Steady-State (S-S) calculation of the full power plant was performed and the temperature of the coolant at the inlet and outlet of the heated section of the risers was read. Then, the S-S calculation of the scaled facility model was conducted and the values of the temperatures at the corresponding locations were compared with full power plant S-S calculation results

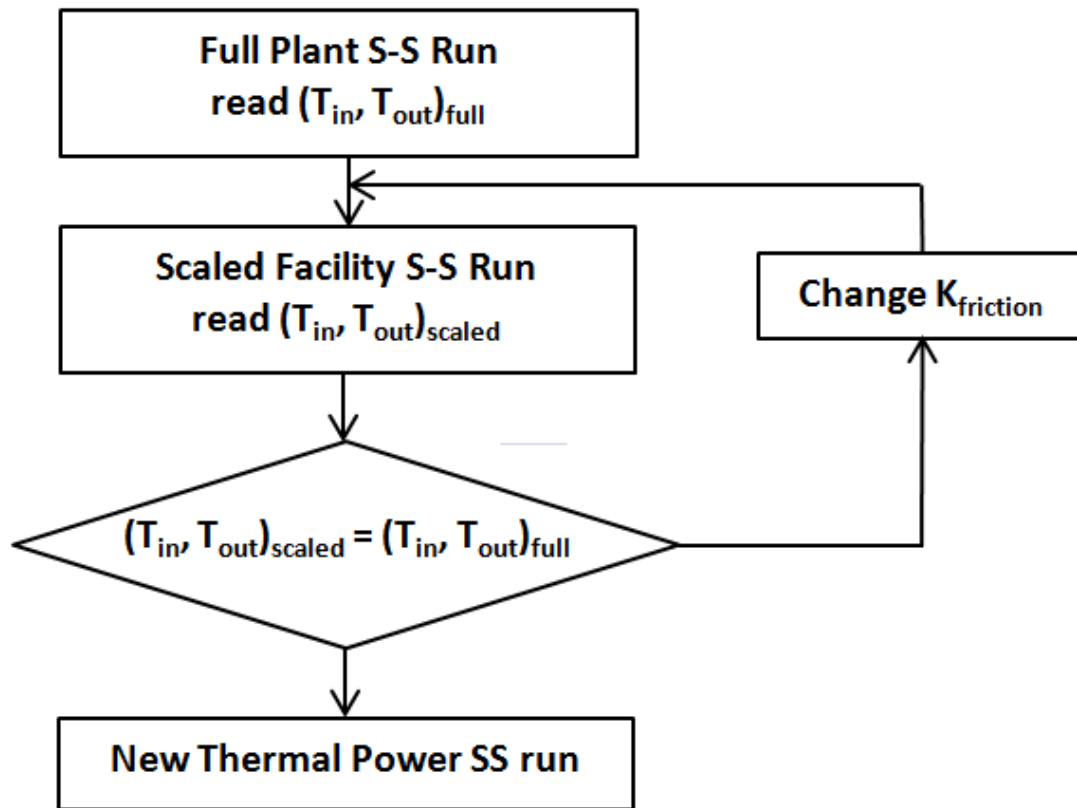


**Figure 30. Scaling Validation Method - Flow Chart**

. During the first run, a discrepancy between the two sets of temperatures was found so the scaled facility calculation was repeated by adjusting the total mass flow rate until the set of temperatures at the defined locations matched the once for the full plant simulation. This was done by changing the form loss coefficient  $K$  of some of the junctions of the model (corresponding to elbows or change in flow area in the real facility). In this approach, the coolant temperature rise in the cavity was assumed as

figure of merit. As mentioned in Chapter V, the coolant cavity temperature rise must be preserved.

The same approach was repeated for different values of the total power in the reactor vessel of the full scale plant while the power of the scaled model was changed according to the defined scaling factor for the thermal power. Table 8 summarizes the results obtained with the design steady-state RCCS thermal power (0.7MW) and the expected value during DCC (1.5MW). An additional case at 2MW was also considered.

**Table 8. Steady-State Risers Inlet/Outlet Temperatures Summary**

	0.7MW		1.5MW		2MW	
	T <sub>in</sub>	T <sub>out</sub>	T <sub>in</sub>	T <sub>out</sub>	T <sub>in</sub>	T <sub>out</sub>
<b>Full</b>	295	306	293.6 K	311.8 K	292.9 K	314.7 K
<b>Scaled</b>	294	305.2	293.6 K	311 K	293.4	314.4 K

The simulation results for the steady-state phase confirmed the validity of the scaling approach described in Chapter V, and highlighted the importance of the flow control in the experimental facility to match the coolant temperature rise through the cavity at the scaled power. This may be performed by placing an orifice plate (to

produce a fixed pressure drop) or a valve (to produce an adjustable pressure drop by changing the opening position of the valve) in selected locations of the pipeline.

### **VII.3 Transient Simulations**

The simulation of a hypothetical accident scenario was conducted to perform a preliminary estimation of the experimental facility response during the transient phase of the experimental activity, to observe the overall time behavior of the system, have a preliminary estimation of the heat removal capabilities, and follows the expected flow regimes especially in the nine risers and manifolds.

Coolant temperatures and pressure initial conditions were assumed to be the same of the one applied in the full plant simulations during accident scenario (Depressurized Conduction Cooldown, DCC). Subcooled liquid water at 307.725 K and atmospheric pressure was imposed as initial condition in the hydrodynamic components of the water loop. Air at 333.15 K and atmospheric pressure was assumed to occupy the single volumes simulating the front and back cavities. Liquid water at 296.5 K was assumed to occupy 80% of the total volume of the tank. An imposed heat flux of 1.96 104 W/m<sup>2</sup> was imposed to the left boundary condition of the heat structures of the vessel (HS100 series). Such as heat flux was scaled down from the expected power to be removed from the cavity in the full plant during a hypothetical accident (1.5MW).

For the purpose of these calculations, the tank was simulated using a pipe component with ten subvolumes, as shown in Figure 31.

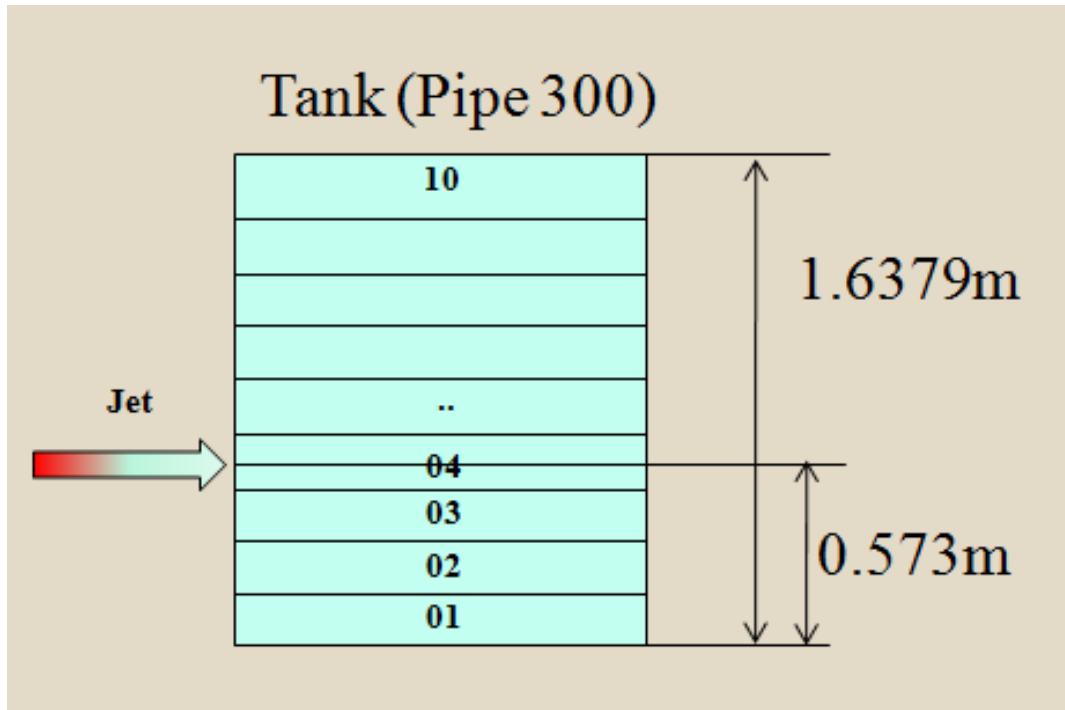


**Figure 31. Tank nodalization for Transient Analysis**

The jet was connected to the side of the subvolume 4 (cross junction) to reproduce the real geometry of the tank inlet. The tank outlet (not shown in the figure) was simulated with a single junction connected at the bottom of the subvolume 1). Another single junction was connected to the top of the subvolume 10 to simulate the discharge of vapor to the environment.

### *VII.3.1 Simulation Results: System Time Response*

The overall time response of the system was observed to be driven by void fraction evolution in the tank. Figure 32 shows the void fraction in the subvolumes of the tank as a function time. Five main time domains can be observed in the figure:

**From  $t = 0\text{s}$  to  $t = \sim 9000\text{s}$ :** The water in the system is subcooled but the temperature rises. This produced a decrease of the coolant density and, subsequently, an increase of the liquid volume in the tank (initially at the top of the subvolume 8). The void fraction in the subvolume 9 starts decreasing until vapor is generated at the liquid surface and discharged into the environment. The subvolume 10 (initially full of vapor,  $\text{voidg} = 1$ ) may see liquid entrainment when the evaporation rate increases (at saturation) at the end of this time domain.

Vapor is discharged from the top of the tank (volume 10) through the single junction connecting the pipe component 300 with the time-dependent volume simulating the ambient.

**From  $t = \sim 9000\text{s}$  to  $t = \sim 24000\text{s}$ :** The coolant has now reached the saturation temperature. The void fraction of the mixture increases to 1 starting from the top subvolumes. At the end of the period all the volumes above the jet are empty while the void fraction of the subvolume 4 where the jet is located, starts increasing at an higher rate.

**From  $t = \sim 24000\text{s}$  to  $t = \sim 27500\text{s}$ :** Void fraction of the subvolume 4 increases to 1 while a small increase in the void fraction of the volumes below the jet (1,2 and 3) is predicted. At the end of the period, volume 4 is totally empty (voidg = 1).

**From  $t = \sim 27500\text{s}$  to  $t = \sim 48000\text{s}$ :** Water in the subvolumes below the jet starts evaporating. At the end of the period the tank is totally empty. Transient is terminated at  $t=60024\text{s}$  when all the liquid in the facility is evaporated.

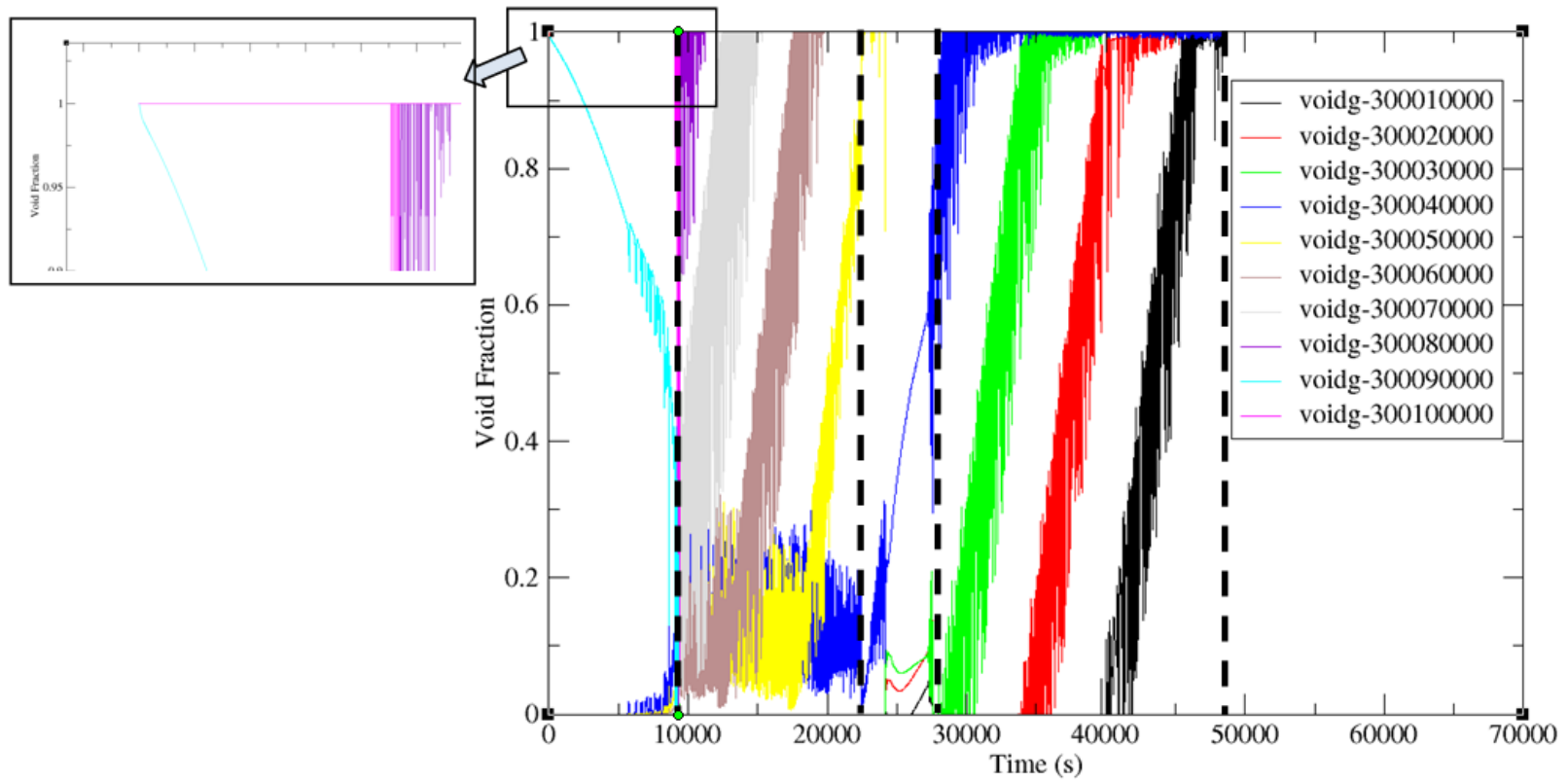


**Figure 32. Tank Void Fractions**

### *VII.3.2 Simulation Results: Flow Regimes*

For the same time domains described in the previous paragraph, the flow regimes in selected regions of the facility were extracted. Table 9 shows the prediction of the flow regimes in the risers' tubes (pipe components 201-9, subvolumes 1-5). The flow regime transition from single phase (liquid) to two-phase can be followed on the same table.

The flow regime in other selected regions of the facility is shown in Table 10.

These regions are:

- The top manifold
- The bottom manifold
- The water tank (subdivided in ten subvolumes).

**Table 9. Flow Regimes in the Risers.**

Component		Time Interval				
		0 - 9000	9000 - 24000	24000 - 27500	27500 - 48000	48000 - 60024
Pipe 1	20101	BBY	BBY	BBY	BBY	SLG/ANM/MPR
	20102	BBY	BBY	BBY	BBY	SLG/ANM/MPR
	20103	BBY	BBY	BBY	BBY	SLG/ANM/MPR/MST/MPO
	20104	BBY	BBY	BBY	BBY/SLG	SLG/ANM/MPR
	20105	BBY	BBY	BBY	BBY/SLG	SLG/ANM/MPR
Pipe 2	20201	BBY	BBY	BBY	BBY	SLG/ANM/MPR
	20202	BBY	BBY	BBY	BBY	SLG/ANM/MPR
	20203	BBY	BBY	BBY	BBY	SLG/ANM/MPR/MST/MPO
	20204	BBY	BBY	BBY	BBY/SLG	SLG/ANM/MPR
	20205	BBY	BBY	BBY	BBY/SLG	SLG/ANM/MPR
Pipe 3	20301	BBY	BBY	BBY	BBY	SLG/ANM/MPR
	20302	BBY	BBY	BBY	BBY	SLG/ANM/MPR
	20303	BBY	BBY	BBY	BBY	SLG/ANM/MPR/MST/MPO
	20304	BBY	BBY	BBY/SLG	BBY/SLG	SLG/ANM/MPR
	20305	BBY	BBY	BBY/SLG	BBY/SLG	SLG/ANM/MPR
Pipe 4	20401	BBY	BBY	BBY	BBY	SLG/ANM/MPR
	20402	BBY	BBY	BBY	BBY	SLG/ANM/MPR
	20403	BBY	BBY	BBY	BBY	SLG/ANM/MPR/MST/MPO
	20404	BBY	BBY	BBY/SLG	BBY/SLG	SLG/ANM/MPR
	20405	BBY	BBY	BBY/SLG	BBY/SLG	SLG/ANM/MPR

Component		Time Interval				
		0 - 9000	9000 - 24000	24000 - 27500	27500 - 48000	48000 - 60024
Pipe 5	20501	BBY	BBY	BBY	BBY	SLG/ANM/MPR
	20502	BBY	BBY	BBY	BBY	SLG/ANM/MPR
	20503	BBY	BBY	BBY	BBY	SLG/ANM/MPR/MST/MPO
	20504	BBY	BBY	BBY	BBY/SLG	SLG/ANM/MPR
	20505	BBY	BBY	BBY	BBY/SLG	SLG/ANM/MPR
Pipe 6	20601	BBY	BBY	BBY	BBY	SLG/ANM/MPR
	20602	BBY	BBY	BBY	BBY	SLG/ANM/MPR
	20603	BBY	BBY	BBY	BBY	SLG/ANM/MPR/MST/MPO
	20604	BBY	BBY	BBY/SLG	BBY/SLG	SLG/ANM/MPR
	20605	BBY	BBY	BBY/SLG	BBY/SLG	SLG/ANM/MPR
Pipe 7	20701	BBY	BBY	BBY	BBY	SLG/ANM/MPR
	20702	BBY	BBY	BBY	BBY	SLG/ANM/MPR
	20703	BBY	BBY	BBY	BBY	SLG/ANM/MPR/MST/MPO
	20704	BBY	BBY	BBY/SLG	BBY/SLG	SLG/ANM/MPR
	20705	BBY	BBY	BBY/SLG	BBY/SLG	SLG/ANM/MPR
Pipe 8	20801	BBY	BBY	BBY	BBY	SLG/ANM/MPR
	20802	BBY	BBY	BBY	BBY	SLG/ANM/MPR
	20803	BBY	BBY	BBY	BBY	SLG/ANM/MPR/MST/MPO
	20804	BBY	BBY	BBY	BBY/SLG	SLG/ANM/MPR
	20805	BBY	BBY	BBY	BBY/SLG	SLG/ANM/MPR
Pipe 9	20901	BBY	BBY	BBY	BBY	SLG/ANM/MPR
	20902	BBY	BBY	BBY	BBY	SLG/ANM/MPR
	20903	BBY	BBY	BBY	BBY	SLG/ANM/MPR/MST/MPO
	20904	BBY	BBY	BBY	BBY/SLG	SLG/ANM/MPR
	20905	BBY	BBY	BBY	BBY/SLG	SLG/ANM/MPR

**Table 10. Flow Regimes in other Components.**

Component		Time Interval				
		0 - 9000	9000 - 24000	24000 - 27500	27500 - 48000	48000 - 60024
Top Manifold		BBY	BBY/HST	BBY	BBY/HST	HST/MPR
Bottom Manifold		BBY	BBY	BBY	BBY/HST	BBY/HST
Tank	30001	BBY	BBY	BBY	BBY/VST	MPR
	30002	BBY	BBY	BBY	BBY/VST	MPR
	30003	BBY	BBY	BBY	BBY/VST	MPR
	30004	BBY	BBY/SLG	VST	ANM/MPR	MPR
	30005	BBY	BBY/SLG/VST	MPR	MPR	MPR
	30006	BBY	BBY/SLG/VST	MPR	MPR	MPR
	30007	BBY	VST/MPR	MPR	MPR	MPR
	30008	BBY	VST/MPR	MPR	MPR	MPR
	30009	VST	VST/MPR	MPR	MPR	MPR
	30010	MPR	MPR	MPR	MPR	MPR

*VII.3.3 Simulation Results: Flow Rate and Two-Phase Flow Oscillations*

The main coolant mass flow rate calculated at the bottom of the downcomer (junction 24002) is plotted in Figure 33. The flow behavior was found to be the water and flow conditions (saturation / two-phase) and the void fraction in the tank. When the water is subcooled, the flow in the downcomer is stable, slightly increasing with the time due to the increase in the temperature difference through the cavity. When some void is produced in the tank, small flow oscillations were observed. These oscillations became larger when the coolant reached the saturation temperature in the tank. A flow inversion [34] was predicted when void in the tank inlet (subvolume 4) started increasing. This inversion dominated the time domain up to the time when the tank inlet was completely

emptied. Larger oscillations were predicted when the tank was empty due to the large amount of vapor produced in the cavity.

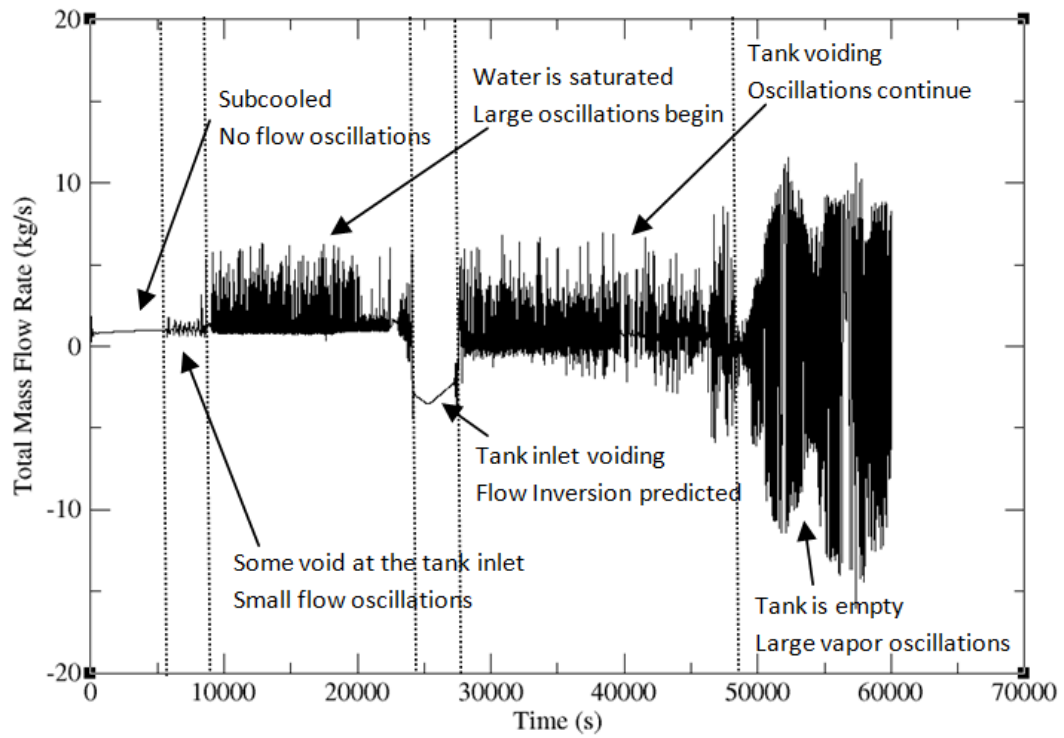


**Figure 33. Coolant Mass Flow Rate.**

A close view of the flow rate throughout the transient revealed a periodicity of the flow oscillations. The period of the flow oscillations was found to change during the time domains, as shown in Figure 34.

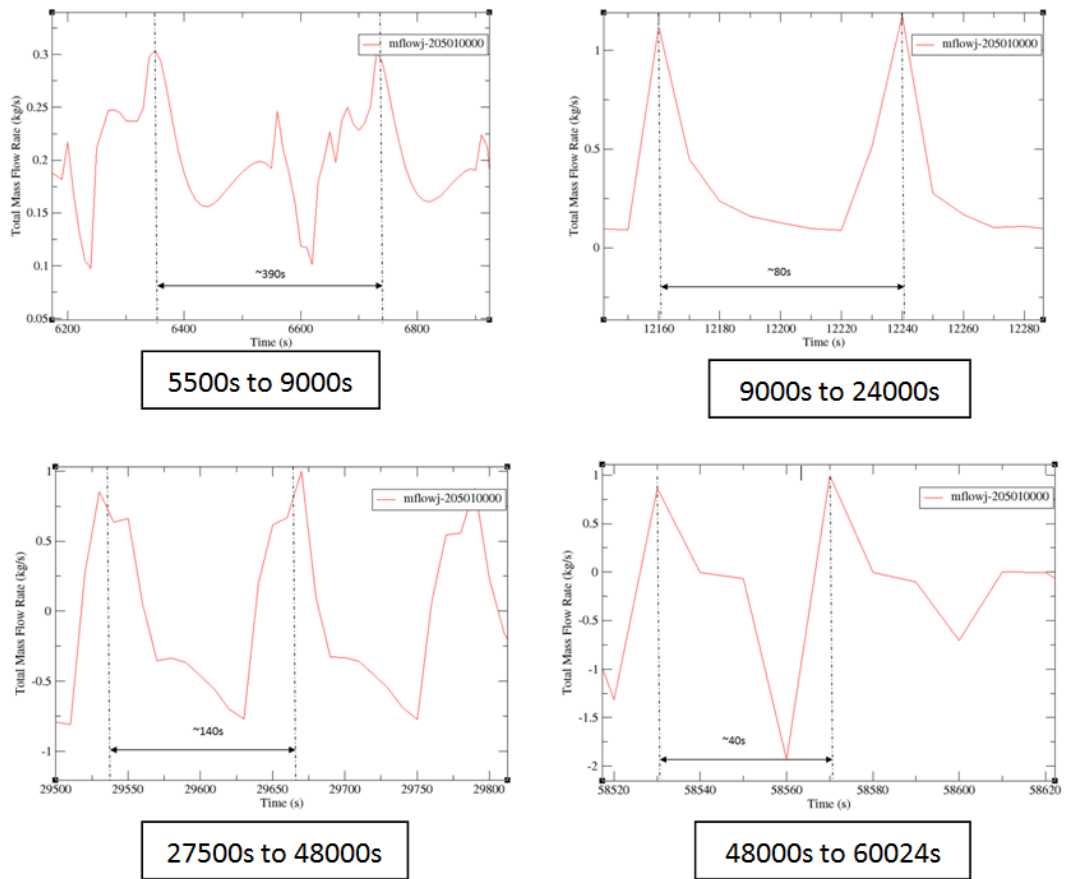


**Figure 34. Mass Flow Oscillations.**

The period of the oscillations was found to be orders of magnitude larger than the simulation time step ( $10^2$  seconds versus  $10^{-1}$  seconds). Consequently, numerical instability can be ruled out as the cause of the oscillations [35].

Similar oscillations were predicted for other thermal-hydraulic parameters such as water temperature in different locations of the facility as shown in Figure 35 and Figure 36. In particular, Figure 35 shows the temperature of the coolant in the heated section of the riser 5 (center riser).

It has to be remarked that the oscillations predicted by the RELAP5-3D simulations were not confirmed by any experimental results in this study.

Experiments conducted in the two-phase flow region in similar experimental facilities [36] have shown an oscillatory behavior of the flow rate. Nevertheless, the period of these oscillations and the time of occurrence was not compared.

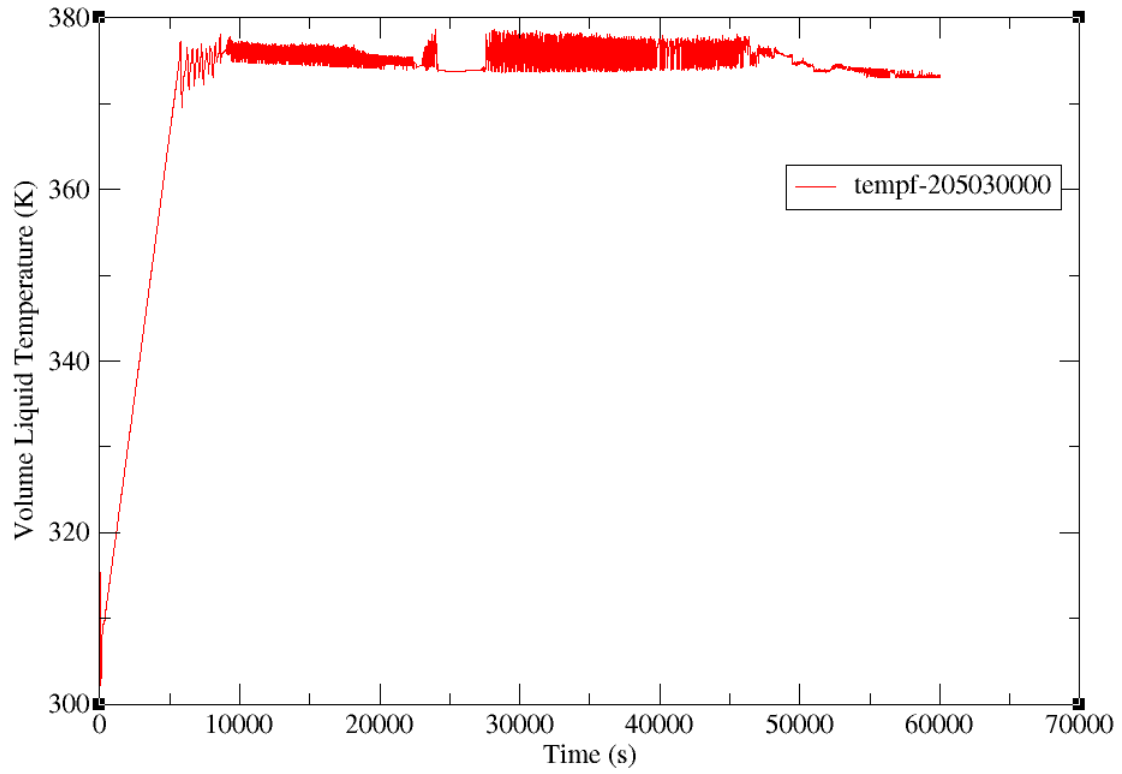


**Figure 35. Water Temperature (Central Pipe, Heated Section, Volume 20503).**

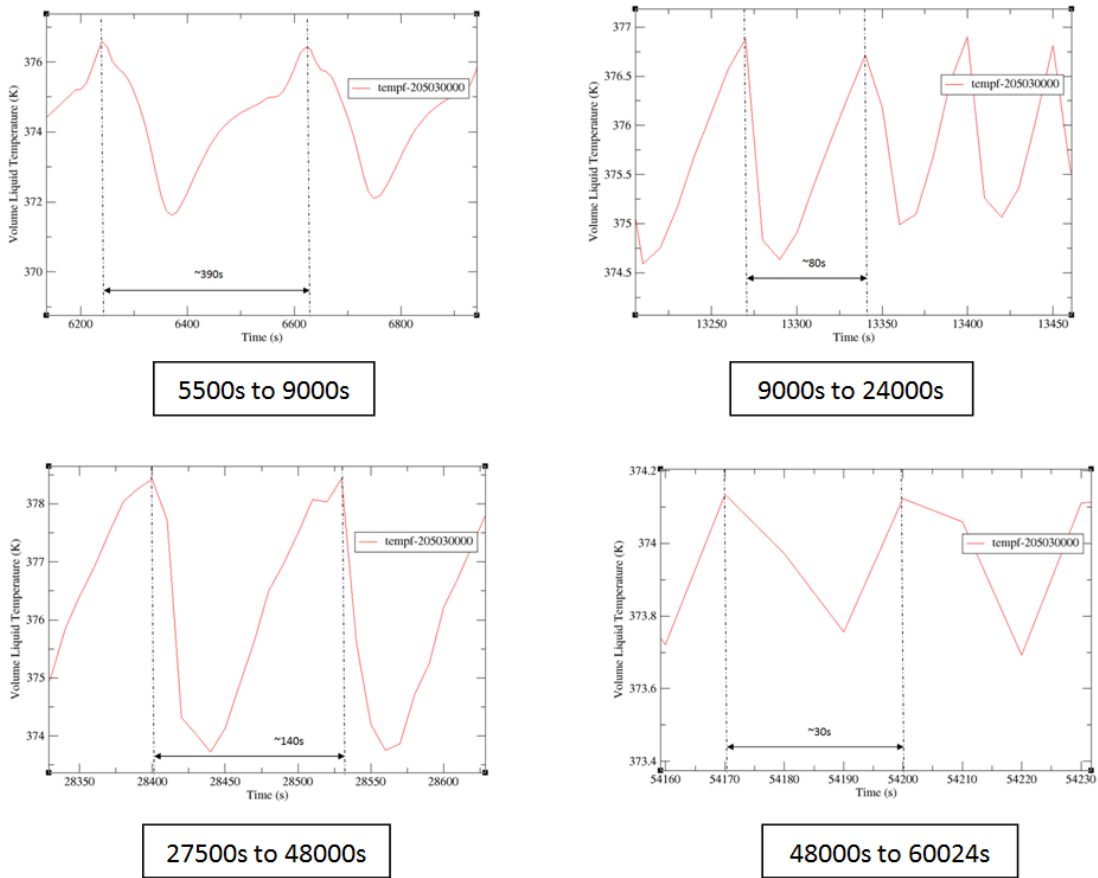


**Figure 36. Temperature Oscillations (Central Pipe, Heated Section, Volume 20503).**

### *VII.3.4 Simulation Results: Cavity Energy Balance*

The cavity energy balance was verified by reading the heat flux prediction at the heat structures of risers, vessel, and cavity walls. Table 11 shows the simulation results in terms of fraction of the energy transferred through the reactor cavity by radiation and convection as a percentage of the total energy produced in the vessel. In the same table,

the total heat loss from the cavity due to convection and radiation is shown. The estimation of the radiation heat transfer fraction (~85%) was found to be in agreement with the expectations.

**Table 11. Cavity Energy Balance.**

	<b>Power [W]</b>	<b>%</b>
<b>Total Power</b>	12509.7	100.0
<b>Convection to Pipes/Fin</b>	1352.80	10.81
<b>Radiation to Pipes/Fin</b>	10593.98	84.69
<b>Losses (rad + conv)</b>	562.92	4.50

#### **VII.4 Sensitivity Analysis**

Sensitivity analysis was conducted to study the behavior of the RELAP5-3D model and optimize the conditions (nodalization) to be applied when simulating specific thermal-hydraulic phenomena. The activity was conducted in three steps:

- Sensitivity analysis of the water tank nodalization
- Sensitivity analysis of the top manifold nodalization
- Sensitivity analysis of the tank water level

#### *VII.4.1 Sensitivity Analysis of the Water Tank Nodalization*

As mentioned in the previous paragraphs, for the steady-state simulations, the tank was modeled using a single volume component. This set of simulations was conducted in order to verify the sensitivity of the RELAP5-3D model to the nodalization adopted for the water tank component [37]. Three different nodalizations were adopted for the water tank using:

1. A single volume
2. A pipe component
3. A multi-dimensional cylindrical component

When using the multidimensional component, both three-dimensional momentum equation (option 0 for the three-dimensional flag) and normal one-dimensional momentum equation (option 1 for the three-dimensional flag) were verified. The thermal-hydraulic parameters selected for this sensitivity study were:

- Primary coolant mass flow rate (Figure 37)
- Secondary coolant mass flow rate (Figure 38)
- Primary coolant temperature (Figure 39)

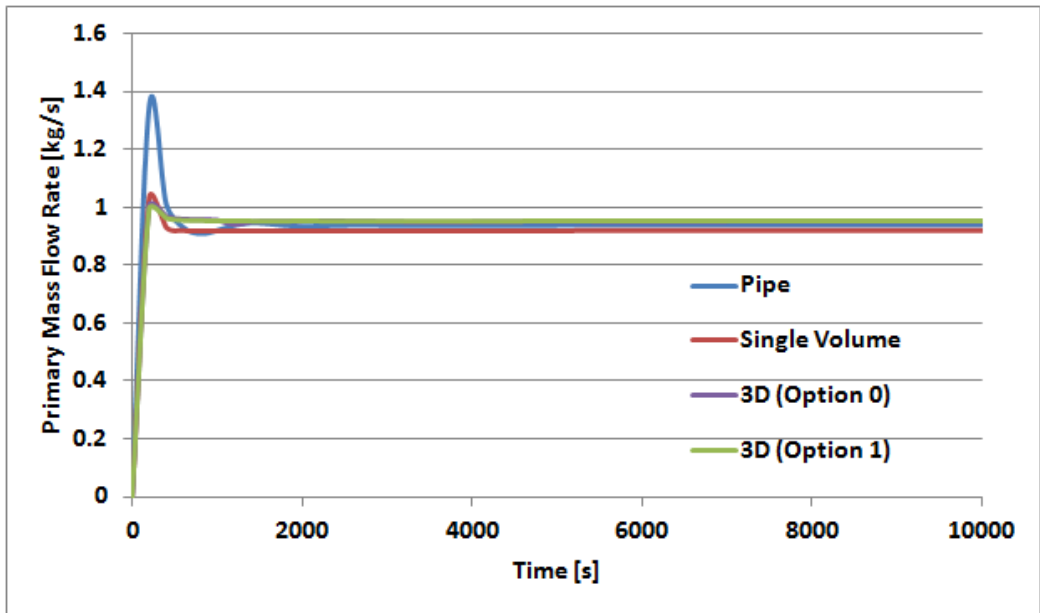


Figure 37. Primary Coolant Mass Flow Rate.

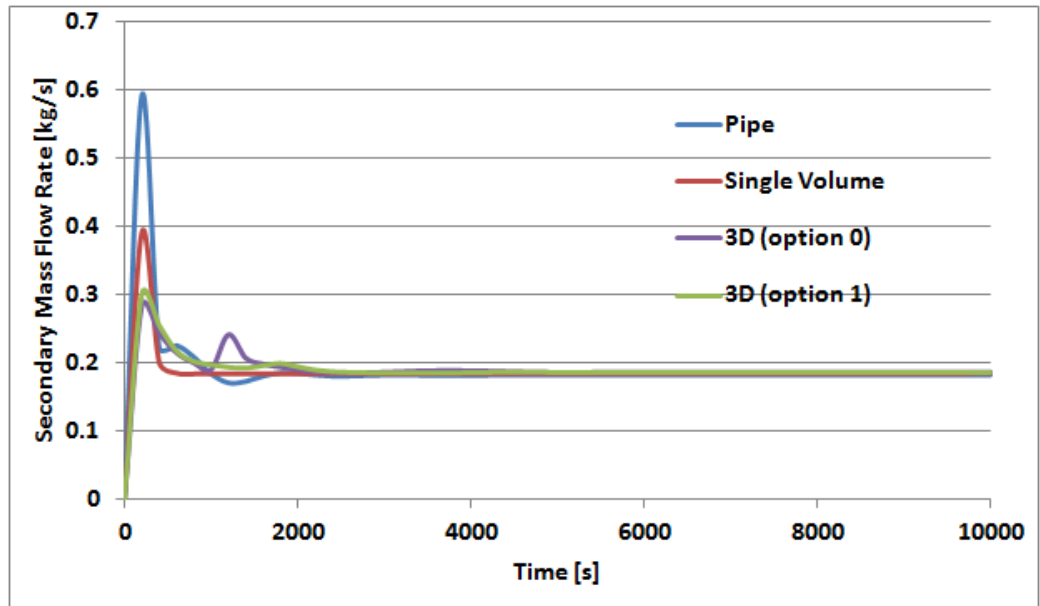
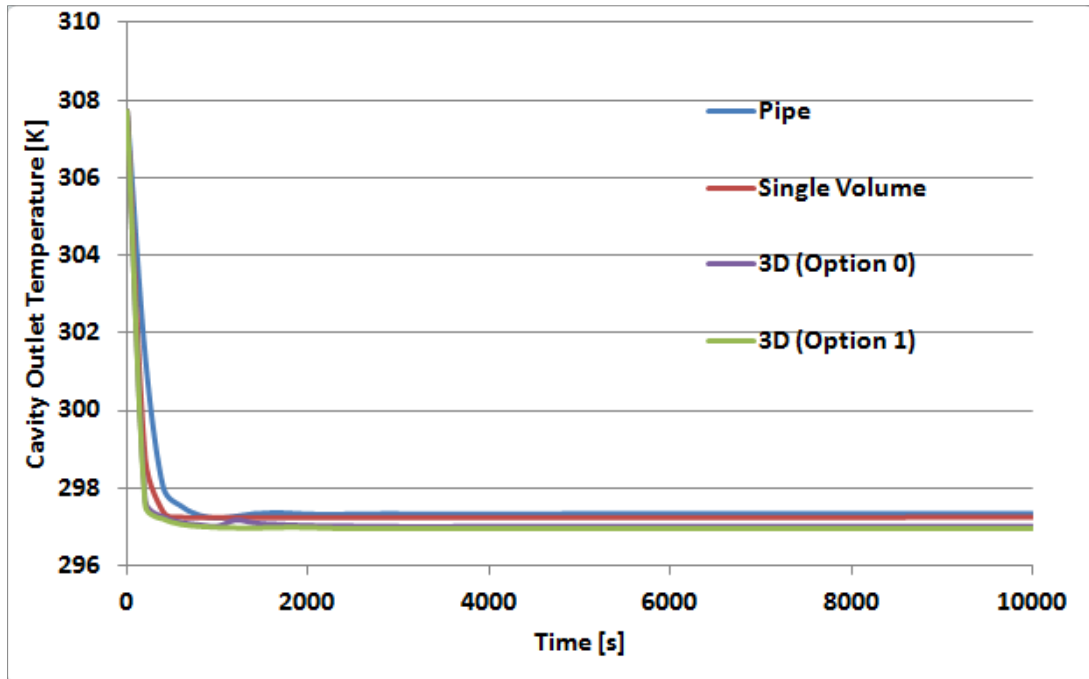


Figure 38. Secondary Coolant Mass Flow Rate.



**Figure 39. Primary Coolant Temperature (Cavity Outlet).**

Table 12 summarizes the results obtained. As it can be observed, the parameters are insensitive to the nodalization adopted for the water tank.

**Table 12. Water Tank Nodalization Sensitivity - Summary.**

	<b>Single Volume</b>	<b>Pipe</b>	<b>3D (Option 0)</b>	<b>3D (Option 1)</b>
<b>Secondary Mass Flow Rate [kg/s]</b>	0.18	0.18	0.19	0.19
<b>Primary Mass Flow Rate [kg/s]</b>	0.92	0.94	0.95	0.95
<b>Cavity Outlet Temperature [K]</b>	297.3	297.3	297.0	297.2

*VII.4.2 Sensitivity Analysis of the Top Manifold Nodalization*

A sensitivity analysis was conducted in order to verify whether recirculation of water between adjacent risers could be predicted by the system code. Recirculation was not predicted with the original nodalization described in the previous paragraphs. A different nodalization of the top manifold (originally modeled with a horizontal pipe) was considered. The following results were obtained by modeling the top manifold with three horizontal pipes connected by cross junctions as shown in Figure 40. The analysis was conducted assuming the original symmetric configuration, where inlet and outlet were located at the center of the manifolds.

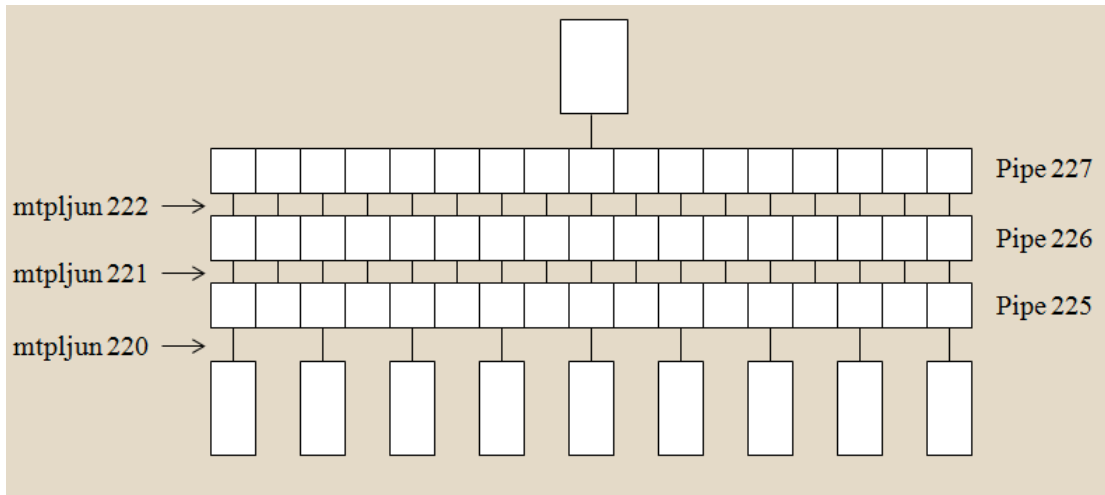


**Figure 40. New Top Manifold Nodalization.**

This configuration allowed a better simulation of the liquid stratification in the top manifold. The mass flow rate through the risers 1 to 9 with this new configuration is shown Figure 41 together with the collapsed liquid level in the top manifold. The direction of the flow rate in the risers was found to be related to the liquid level in the manifold. In particular, recirculation was found to occur when the liquid level dropped below 1 (top of the manifold). In Figure 41, recirculation can be assumed to occur when the mass flow rate of two adjacent risers has opposite sign (positive=upwards, negative=downwards) [38].

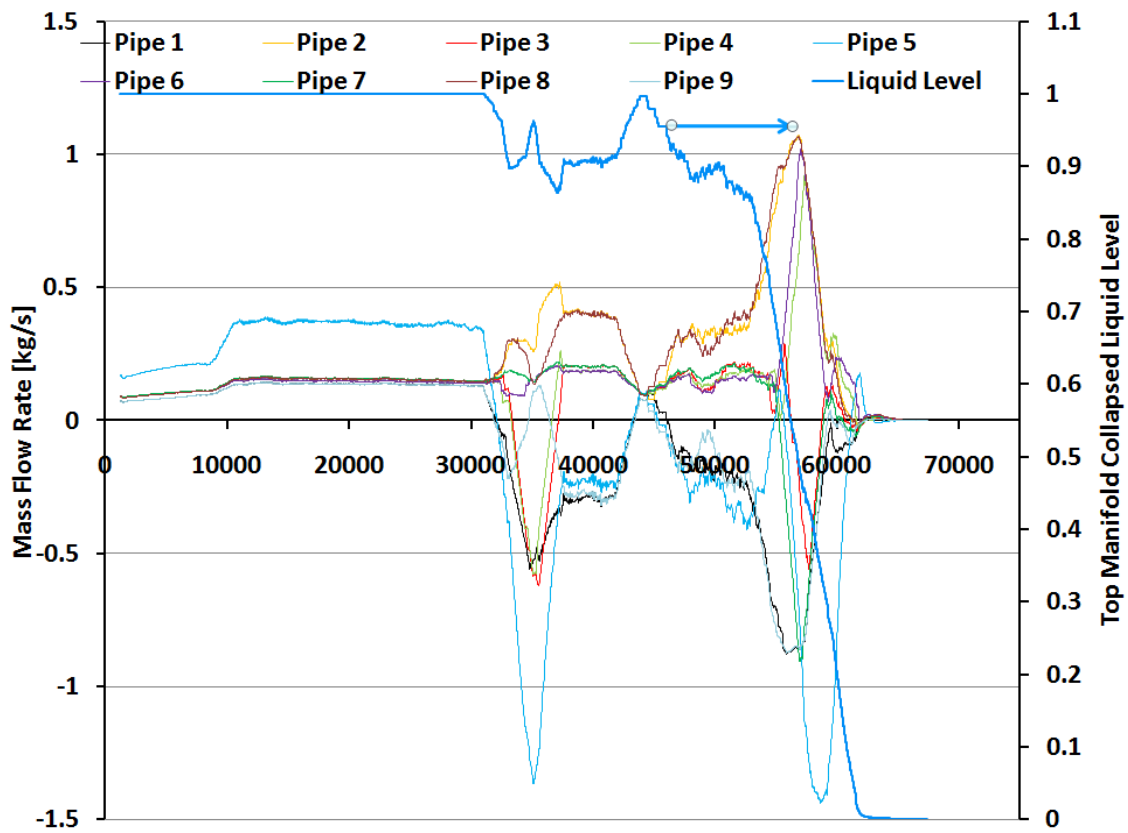


**Figure 41. Risers' Flow Rate and Manifold Collapsed Liquid Level.**

Figure 42 shows selected snapshots of the flow direction at different time intervals of the transient.

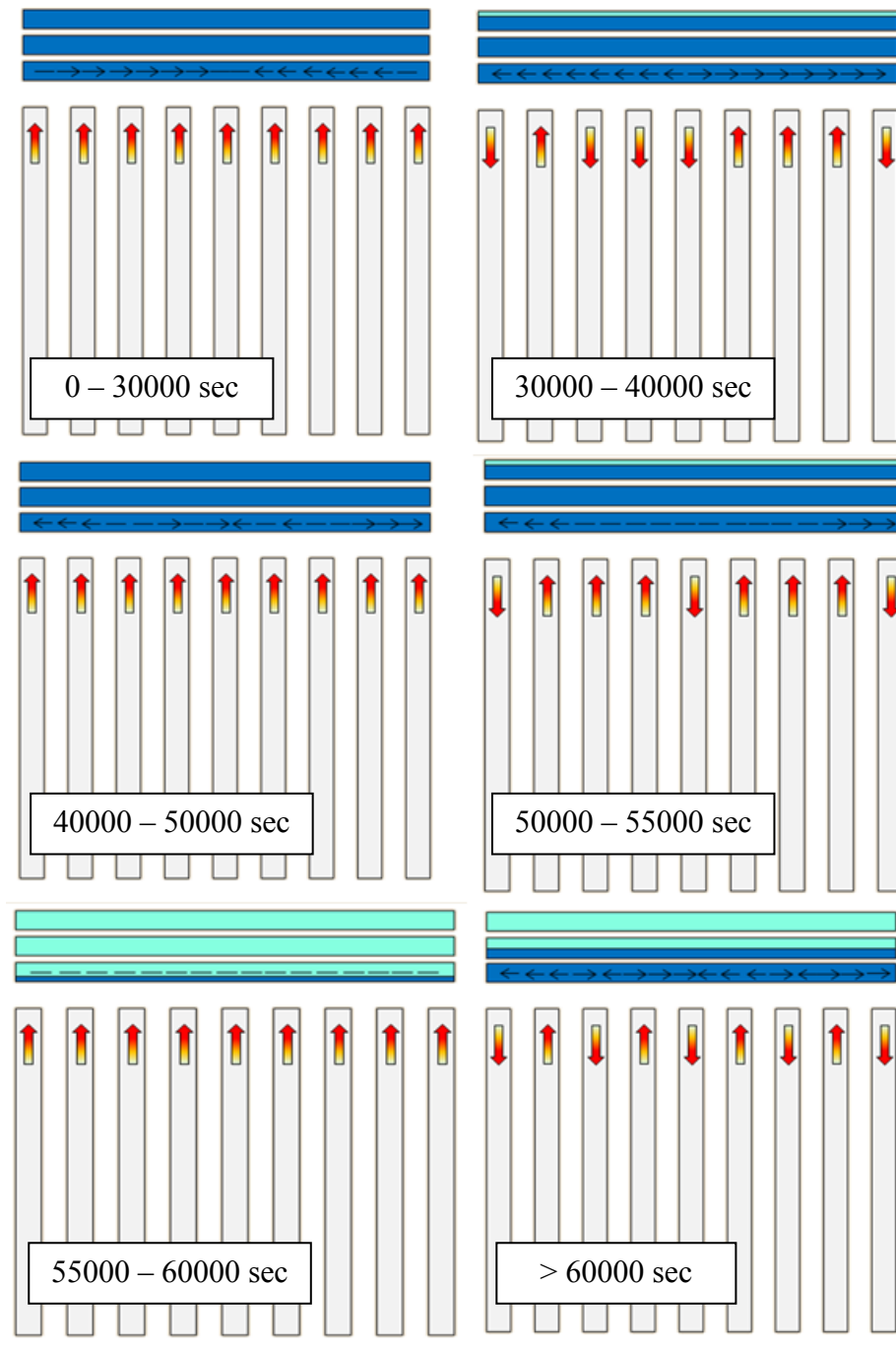


**Figure 42. Flow Direction (Snapshots).**

### VII.4.3 Water Tank Liquid Level Sensitivity Analysis

This analysis was conducted to study the system time response during the transient phase (accident conditions) under different initial water level in the tank. The simulations were conducted assuming the same configuration of the tank inlet (connected at the subvolume 04 of the pipe component 300 in Figure 43), simulating the water tank, changing the initial liquid level in the tank (at the top of subvolume 04, 05, 06, and 07).

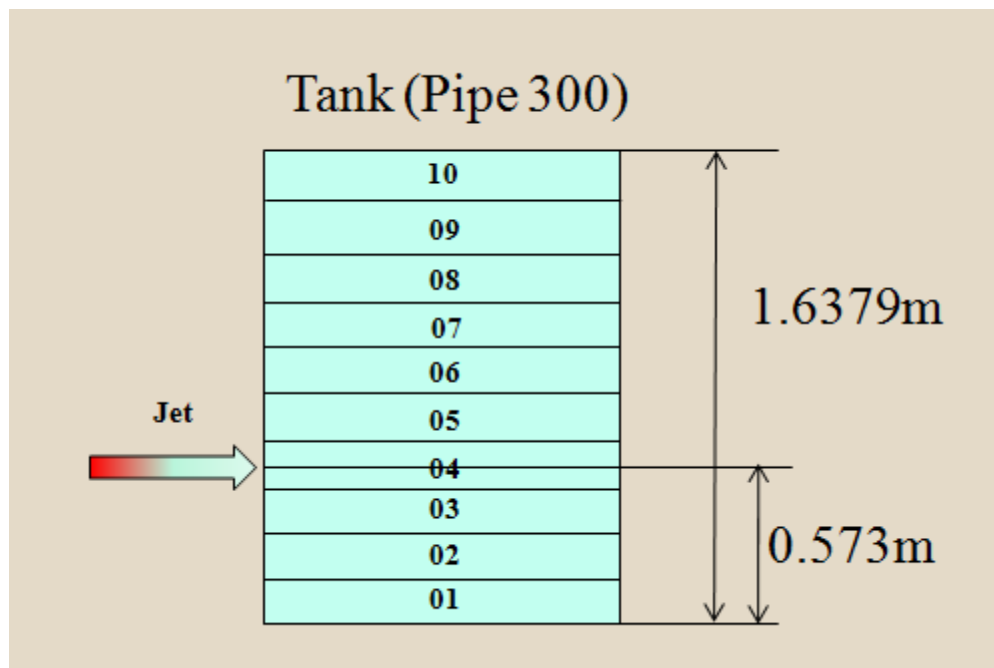


**Figure 43. Water Tank Nodalization and Initial Liquid Levels.**

The collapsed liquid level in the water tank for the four cases is plotted in Figure 44. The liquid level was found to increase during the first period of the simulation (single phase) due to the decrease of the water density and, subsequently, thermal expansion. Oscillations were found to occur when the liquid level reached the jet elevation, for all the four cases.

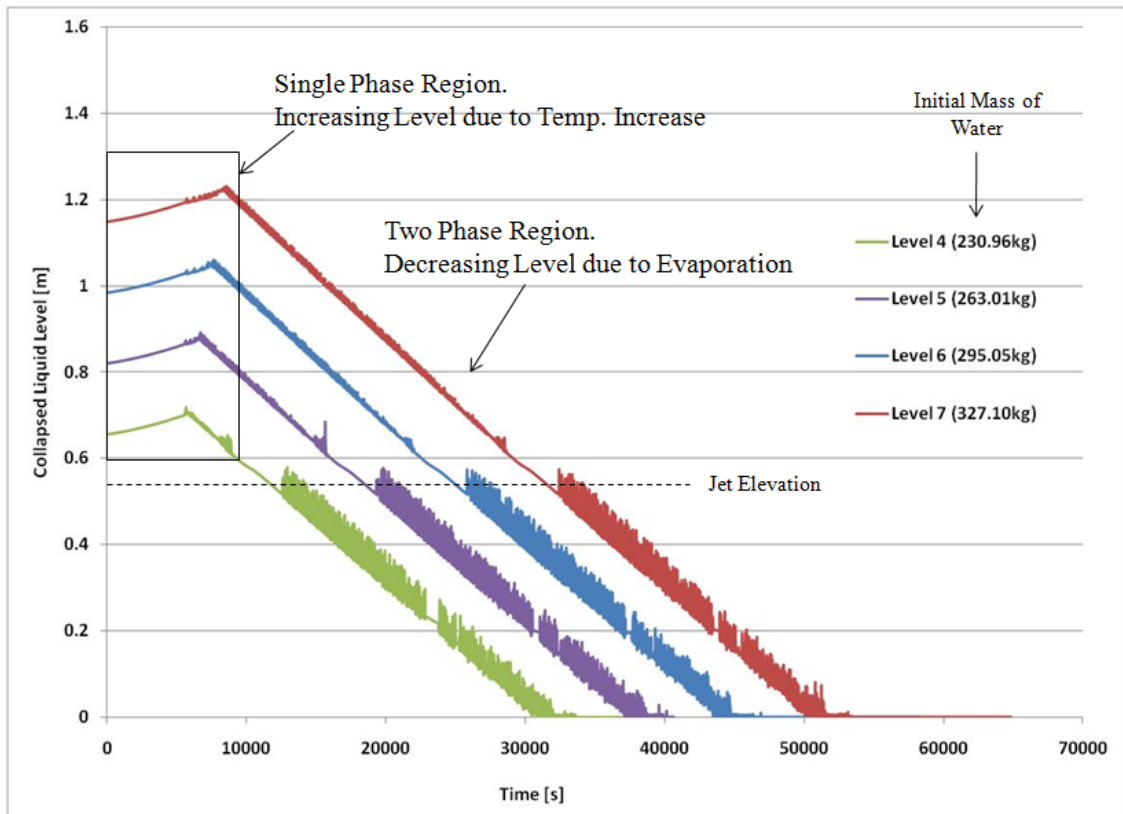


**Figure 44. Water Tank Collapsed Liquid Level.**

A sensitivity analysis was conducted to study the effect of the initial water inventory in the water tank on the system time response.

The system time response as a function of the initial water mass and water level is depicted in Figure 45 and Figure 46.

In particular, Figure 45 shows the time required for the liquid level to drop to the jet location.

Figure 46 shows the time required to empty the tank.

As can be observed in from these plots, the dependency of the time from the initial mass (or initial liquid level) is linear during the first phase, when the liquid level is above the jet.

The time required to deplete the tank after the liquid level dropped below the jet location can also be represented with a linear fitting, as can be observed in the plots showed in Figure 46.

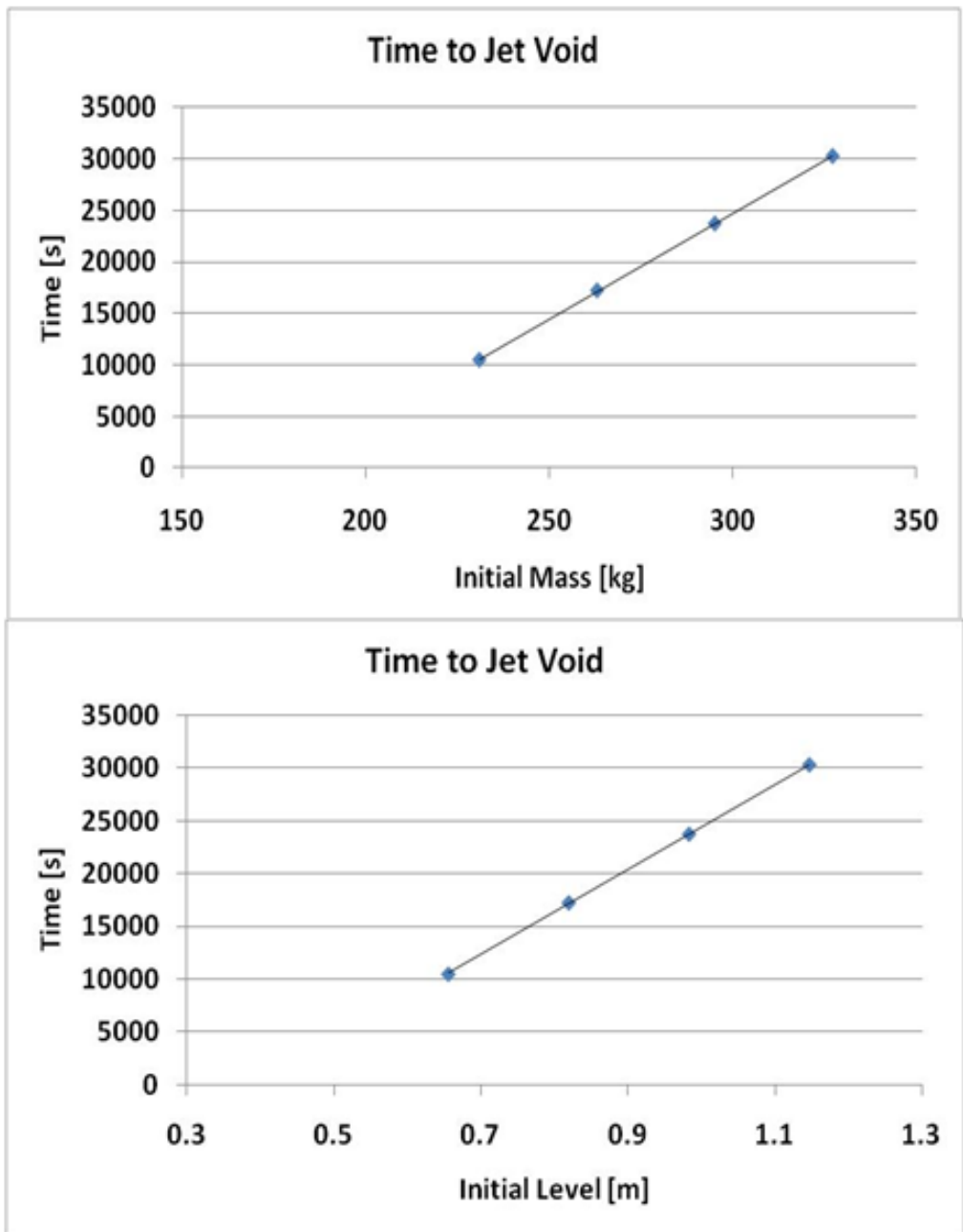


**Figure 45. Time to Liquid Level at the Jet Elevation.**

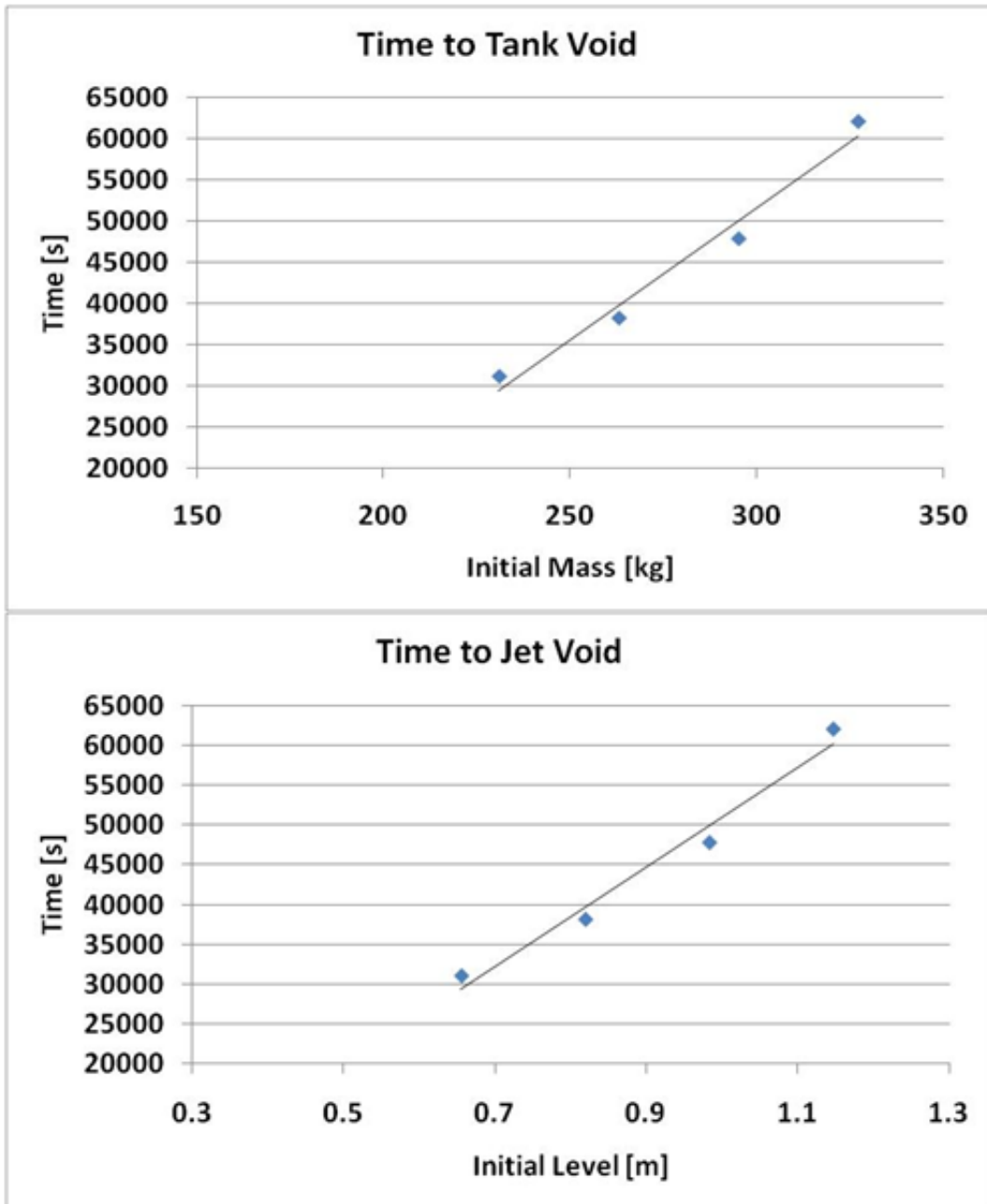


Figure 46. Time to Tank Depletion.

## CHAPTER VIII

### PHASE 5: FACILITY DESIGN COMPLETION, VENDOR SELECTION, AND CONSTRUCTION

The design of the experimental facility and the selection process of the materials to be used were driven by:

- The scaling results, which provided the main dimensions and materials of the reactor cavity, water tank capacity, and piping size;
- The preliminary steady-state and transient RELAP5-3D simulations, which helped to identify possible phenomena occurring in specific regions of the facility, including risers and manifolds.

The main features of each section of the experimental facility, including final dimensions, materials, and other fabrication requirements are described in the following paragraphs. The following facility regions will be discussed:

- Reactor Cavity, including risers' panel, vessel, and heaters.
- Manifolds
- Water Tank
- Pipeline and Pipe Connections
- Structures, including main structure, scaffolds, and supporting structures.

## VIII.1 Reactor Cavity

The final dimensions of the reactor cavity were mainly defined by the scaling procedure described in Chapter V. The main components fabricated for the reactor cavity are:

- The risers' panel, including the bottom and top cavity plates.
- The Reactor Vessel, where the electric heaters will be installed.
- The electric heaters.

### *VIII.1.1 Risers' Panel*

Figure 47 shows the final drawing of the risers' panel, as submitted to the steel shop for fabrication.

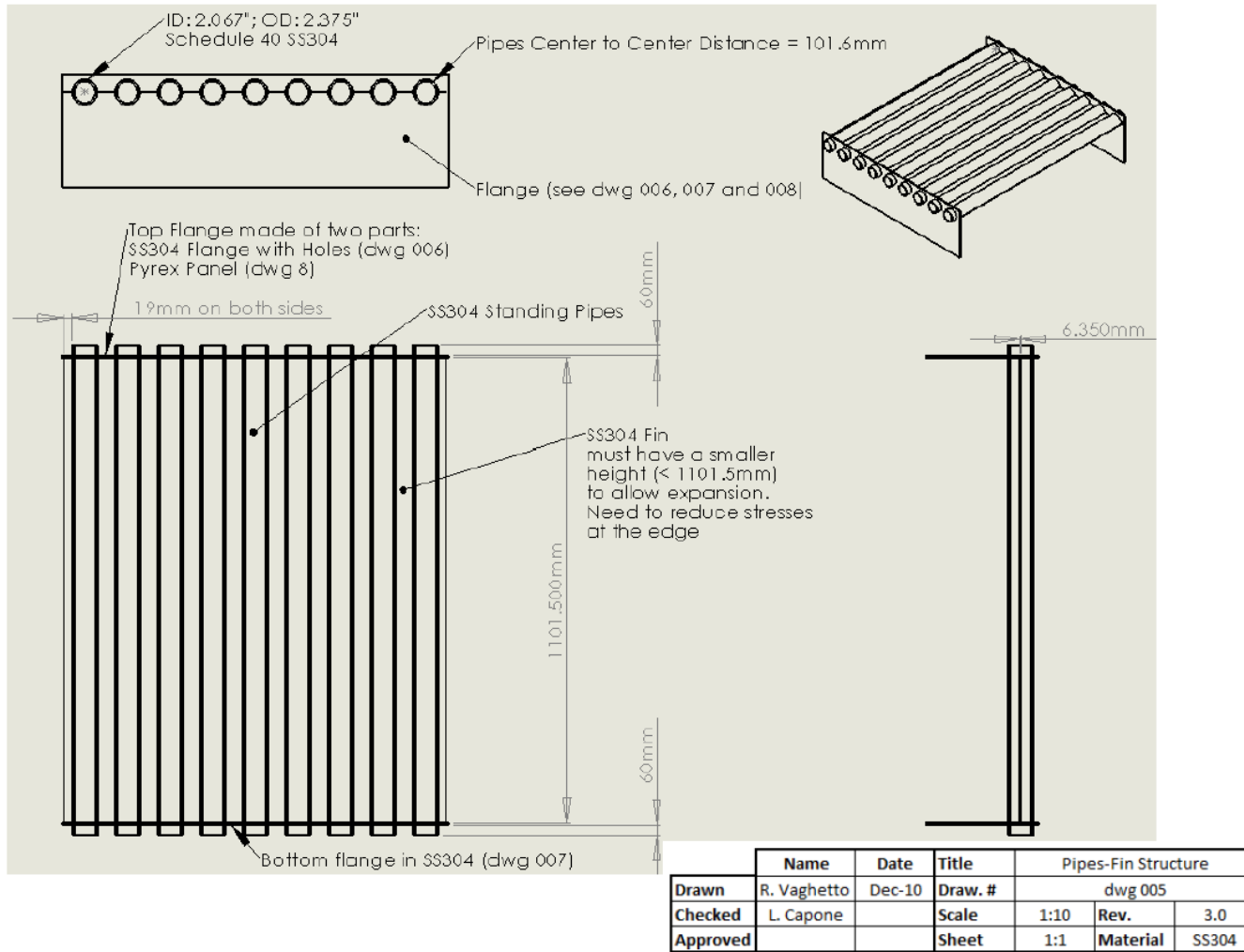


**Figure 47. Risers' Panel Drawing and Specifications.**

The active length (the portion of the risers exposed to the heat flux) of the risers was fixed to 1.1 m. The risers were extended outside the cavity top and bottom boundaries by 6 cm to allow the connection with the manifolds. Two plates were included in the panel design. The bottom plate will be welded to the risers and will be used to anchor the panel to the structure and to support the panel. The top plate was designed to be removed from the cavity to allow access into the cavity for maintenance. Nine equidistant holes will be machined in the plate to fit into the nine risers. Thermal insulation panels will be placed on top of this plate to minimize the heat losses through the cavity ceiling. Figure 48 shows a detailed of the risers' panel right after its fabrication process. One of the main challenges of the fabrication was the welding of the fin plates between the riser's tubes. As previously mentioned, the fins were conceived to enhance the radiation heat transfer to the panel by increasing the exposed surface area. The heat transferred by conduction through the fins to the risers' walls, will be ultimately removed by convection from the water. To allow a uniform conduction heat transfer through the length of the pipes, spot welding was not considered as a suitable technique to connect the fins to the risers' walls. Continuous and uniform welding technique guaranteed a uniform contact between the fin and the side of the risers'. This technique required special preparation and advanced tools to avoid plastic deformation of the pipes and fins during the welding process. The panel was fabricated by MADEWELL LCC (Houston, TX). The company is a certified machine shop with documented experience on similar work performed for large companies and institutions such as NASA. Welding certificate was provided.



**Figure 48. Risers' Panel as Fabricated.**

A detailed view of the top end of the panel with the top plate insertion and risers extensions is shown in Figure 49.

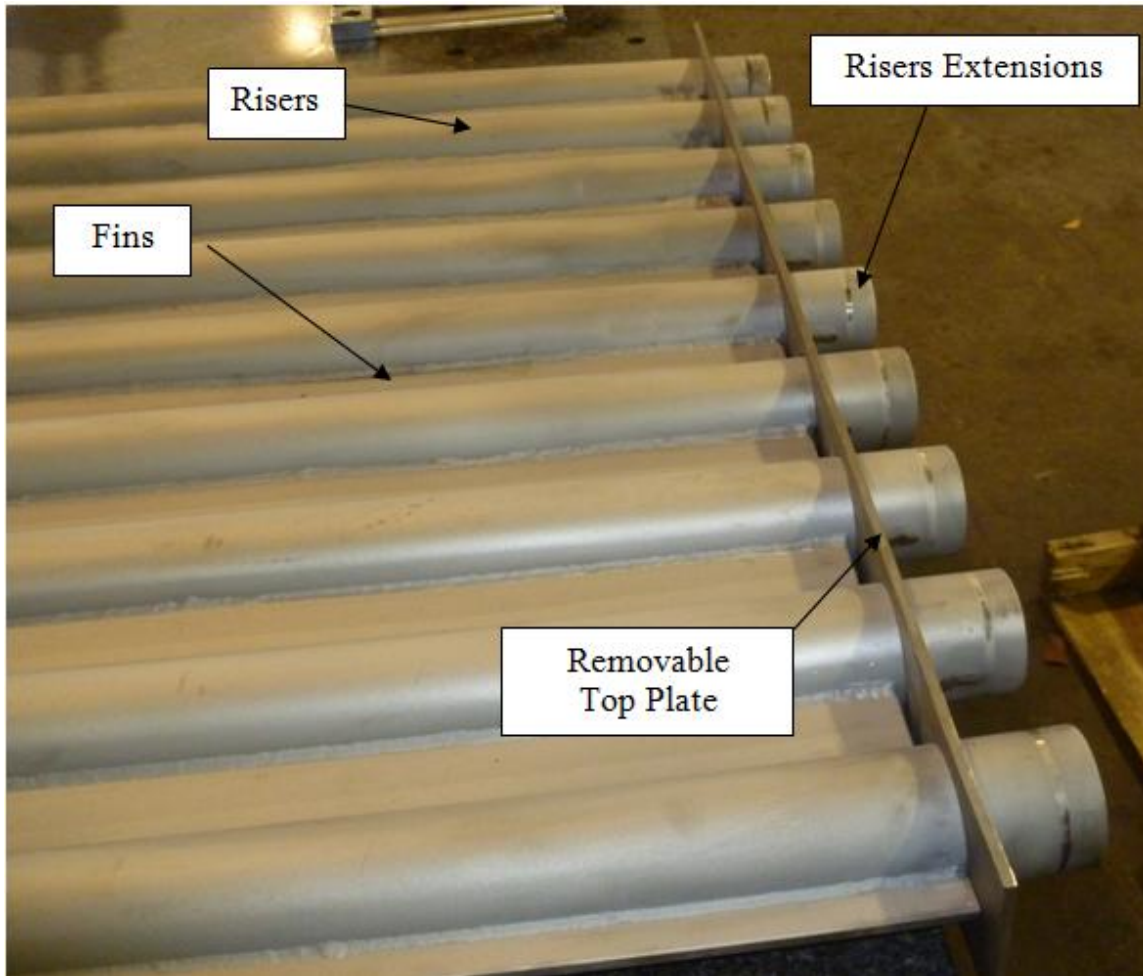


**Figure 49. Risers' Panel Top Plate**

Details of the welding in the risers' panel at the end of the welding procedure are shown in Figure 50.



**Figure 50. Risers' Panel at the End of the Welding Process**

Another view of the panel during final QA inspection is shown in Figure 51.



**Figure 51. Risers' Panel Final Configuration.**

The nine risers were constructed using SS304 piping (ID 5.08 cm, Schedule 40). The fins were cut from a SS304 plate (2mm thickness). The same material was used to fabricate the top and bottom plates.

### *VIII.1.2 Reactor Vessel*

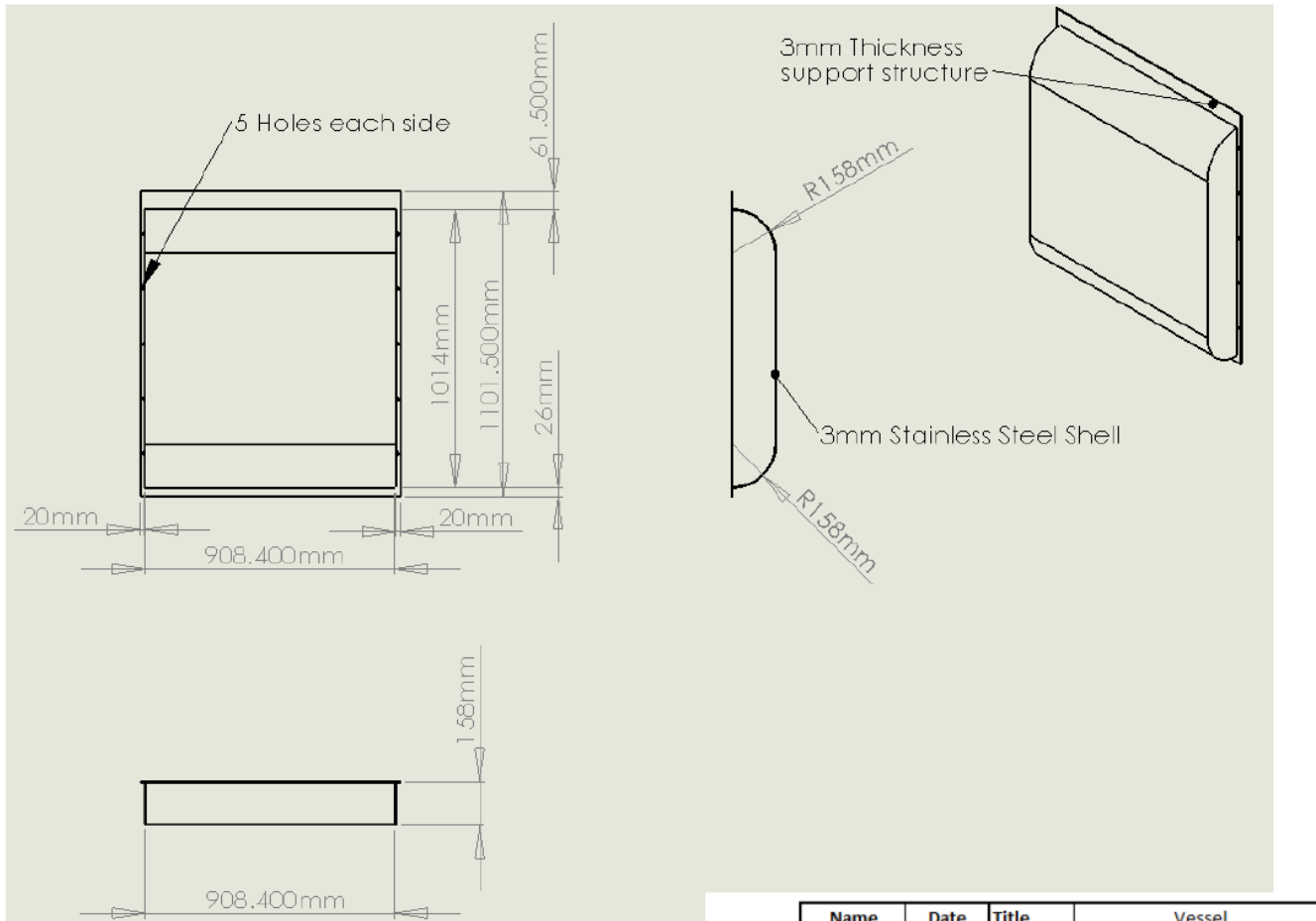
The reactor vessel was designed to:

- Contain the electric heaters.
- Incorporate the main features of the full scale vessel such as upper and lower plena hemispherical shape.

The vessel was fabricated using a 2 mm SS304 sheet. The final dimensions of the reactor vessel are reported in Figure 52.

Three main regions can be identified in the reactor vessel (Figure 53):

- The upper and lower plena, reproducing the hemispherical plena of the full scale vessel design.
- The flat region, simulating a portion of the cylindrical section of the full scale vessel (the heaters will be placed in this section of the vessel).
- The vessel frame, designed to provide support to the reactor vessel.



	Name	Date	Title	Vessel	
Drawn	R. Vaghetto	Dec-10	Draw. #	dwg 002	
Checked	L. Capone		Scale	1:10	Rev. 3.0
Approved			Sheet	1:2	Material SS304

**Figure 52. Reactor Vessel Drawing.**

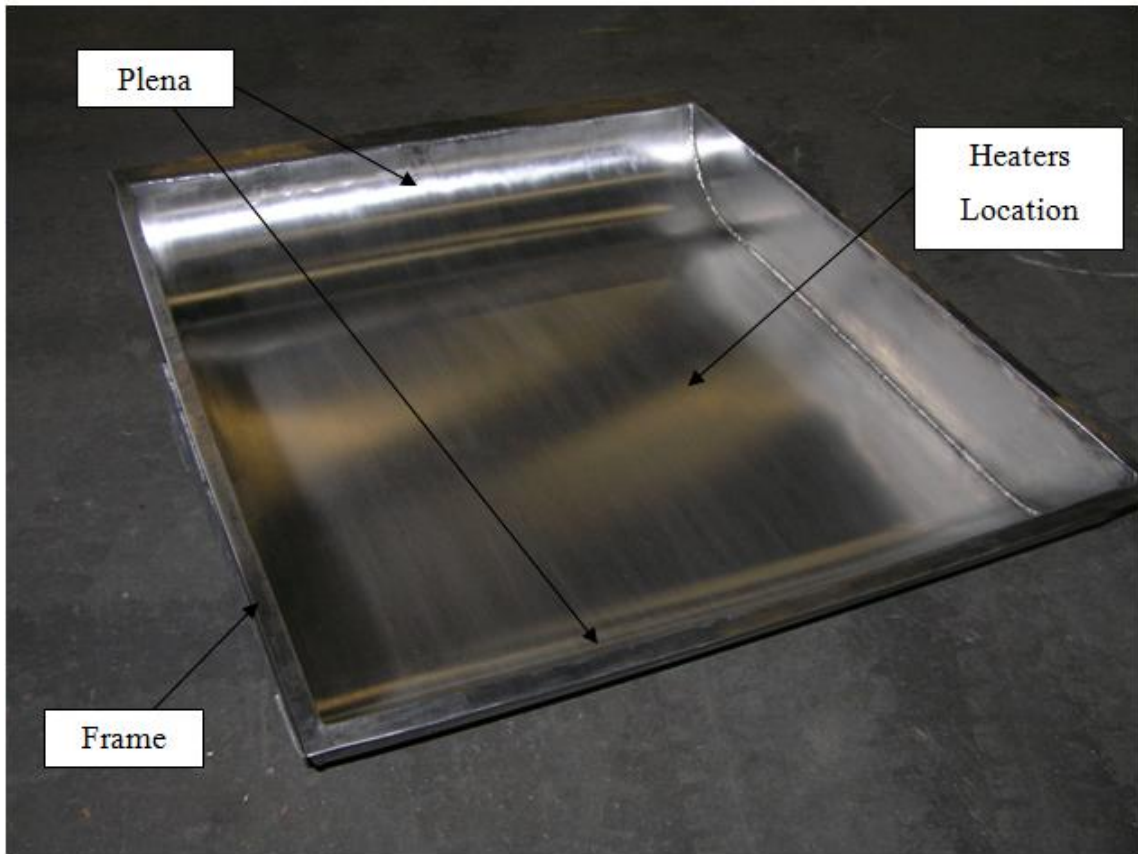


**Figure 53. Reactor Vessel**

Figure 54 shows the raw materials used to fabricate the risers' panel, and the reactor vessel.

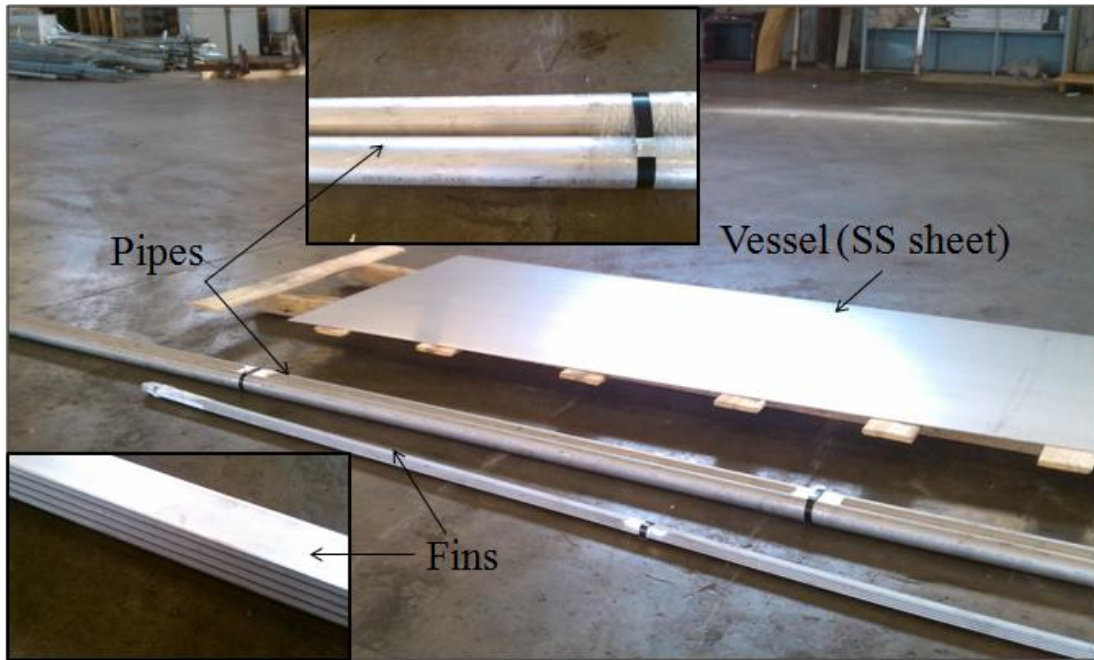


**Figure 54. Raw Materials.**

### *VIII.1.3 Electric Heaters and Controller*

The electric heaters were designed to supply the required thermal power to the system. Other important features were defined for the heaters selection:

- Preferential heat transfer to the front face, minimizing the losses from the back panel.
- Temperature and power controllable.
- Customizable size, to fit inside the reactor vessel.

The electric heaters selected for the experimental facility were supplied by Heaters, Controls & Sensors Ltd. (Ontario, Canada). The company provided

customizable radiant heaters by size and power. Three F-series radiant heater (220 V, 1 phase, 7980 W) were installed in the facility. The total power achievable with the three heaters on at maximum power is approximately 29.3 kW. Each heater (90.17 cm x 22.86 cm) was equipped with a k-type thermocouple located at the center of the emitting surface. Studs were mounted on the back of each heater to facilitate the anchoring with the external supporting frames. The heaters selected are shown in Figure 55 (front view) and Figure 56 (back view).



**Figure 55. Electric Radiant Heaters (front View).**

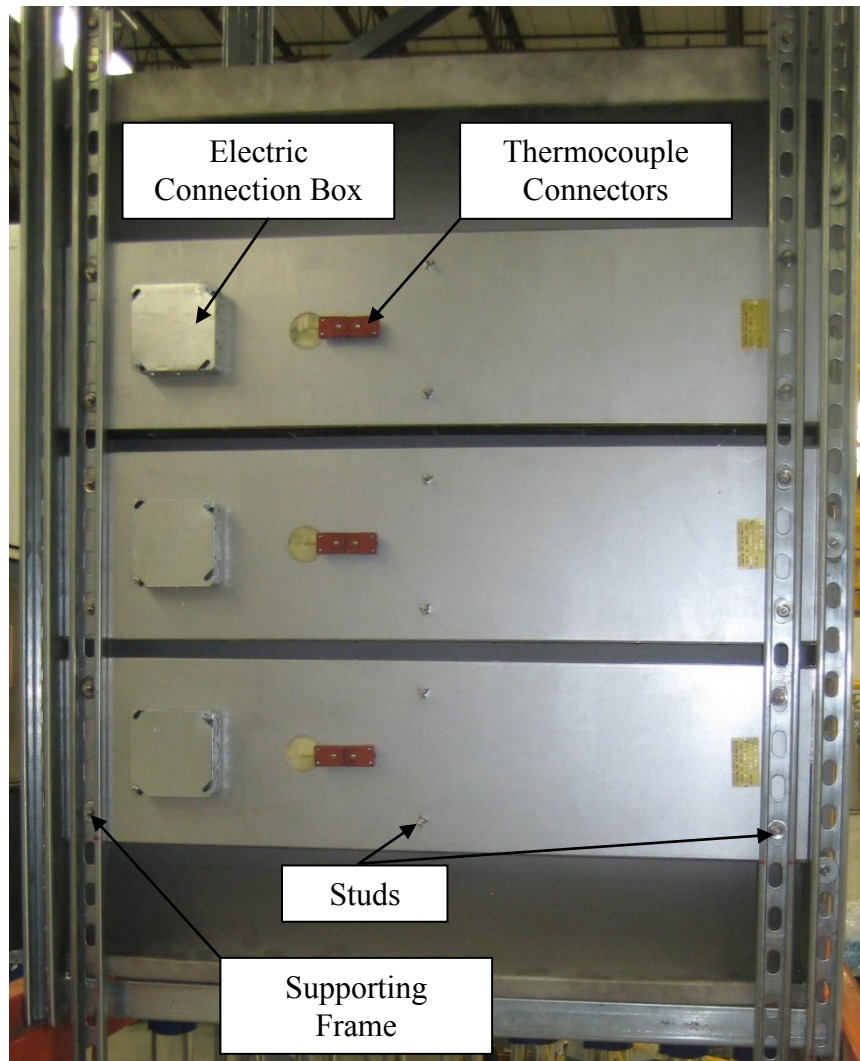


**Figure 56. Electric Radiant Heaters (back View).**

The heaters can be independently controlled by three controllers (FuzyPro 1/16 DIN). The controlled was designed to provide the following controlling features:

- Independent Temperature ramp (max temperature and time interval customizable).

- Independent Power ramp (max power and time interval customizable).
- Heaters Scram.
- Over-temperature Alarm

The power controller installed in the experimental facility is shown in Figure 57.

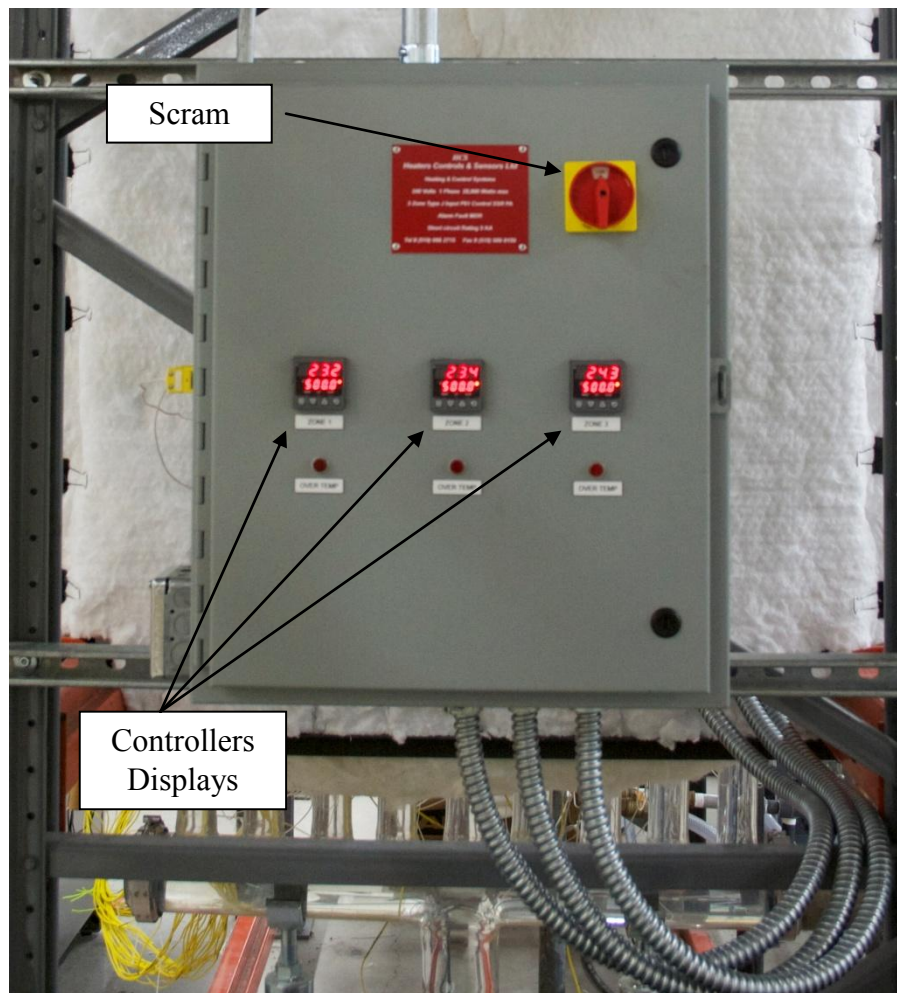


**Figure 57. Heaters Controller Panel**

## VIII.2 Manifolds

The upper and lower manifolds in the facility will collect and distribute the coolant flow from and to the cavity risers. Due to the flow asymmetries expected in panel and the mixing of the coolant streams, flow visualization in this region of the facility will be of paramount importance. Borosilicate was selected as the preferred material to manufacture the manifolds due to:

- Clear and transparent walls, allowing flow visualization using the standard light sources (including laser), and cameras.
- High working temperature (Maximum operating temp = 490 °C, Soften point = 821 °C).
- Low coefficient of expansion ( $32.5 \cdot 10^{-7}$  cm/cm °C).

The design of the manifolds was accurately conceived to provide the most flexible flow configuration and allow different flow geometries. The final drawing is shown in Figure 58. Each manifold will be constituted of:

- One horizontal section [ID: 10.56 cm (4'')] with two beaded ends.
- Nine vertical branches [ID: 50.8 cm (2'')] with flat end.
- One central branch [ID: 10.56 cm (4'')] with beaded end.
- Two end caps to be connected to the closed ends of the manifolds (Figure 58 shows the symmetric configuration where the central branch is used as inlet/outlet and the two ends of the horizontal section are closed).

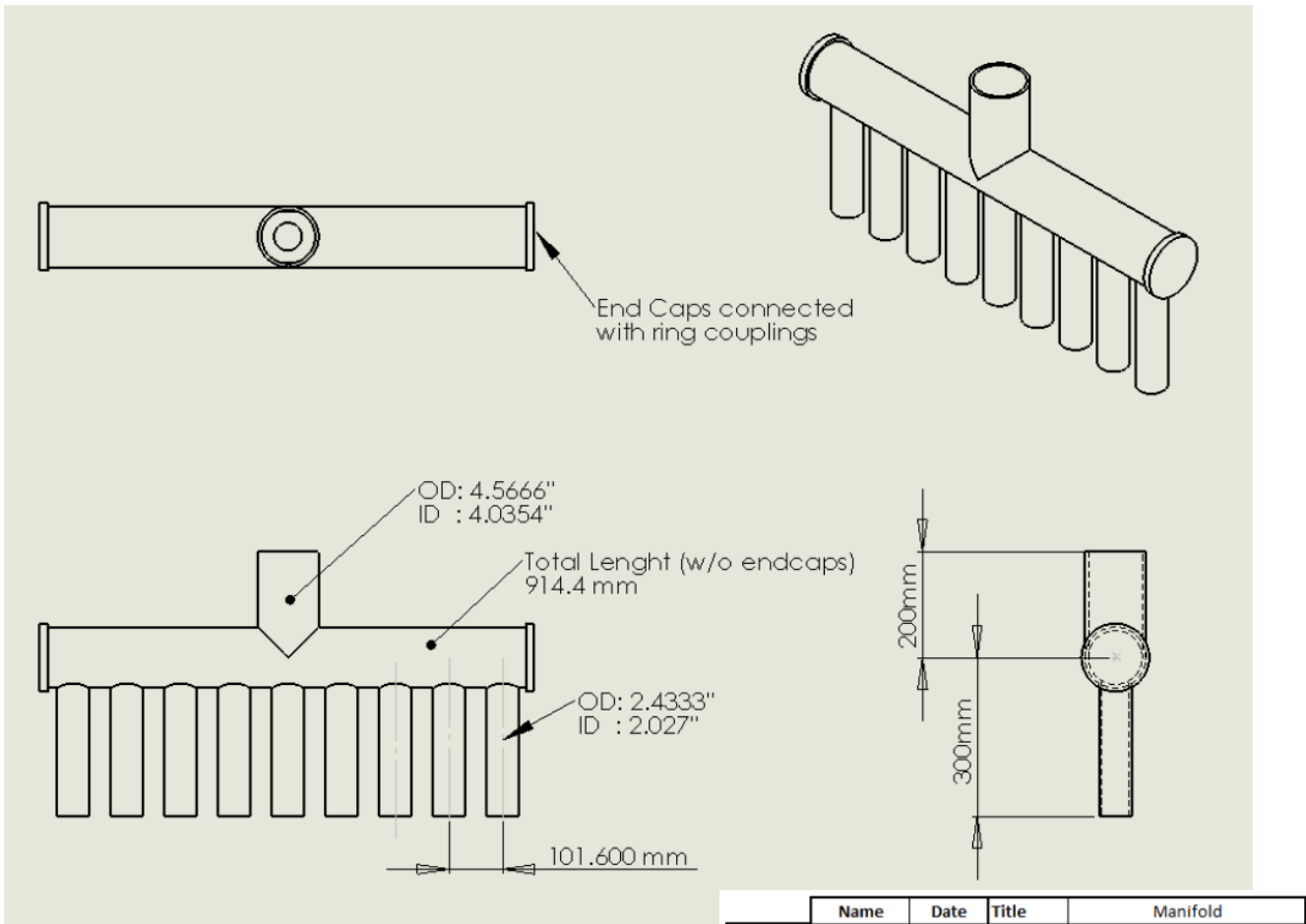


**Figure 58. Manifolds' Drawing**

Two identical manifolds were fabricated by Specialty Glass Inc (Houston, TX). The company was recommended by Schott Glass, one of the world's largest glass suppliers, as one of the specialized companies in Texas to perform custom designs using commercial glass piping. Figure 59 shows the top manifold in its final configuration and installation.



**Figure 59. Glass Manifold (top).**

### VIII.3 Water Tank

As mentioned in Chapter V, the water tank was not designed with rigorous scaling procedures, but it was accurately modified in order to guarantee its functionality during the phases of the experimental activity. A steel water tank was available at the Magnetic Laboratory of Texas A&M University and donated to the Department of Nuclear Engineering for this project. The original tank did not have inlets and outlets for the water but the overall dimensions (Table 13) were suitable for the experimental facility needing.

**Table 13. Original Water Tank - Dimensions**

	<b>Value</b>	<b>Unit</b>	
<b>Inner Diameter</b>	62.23	cm	
<b>Height</b>	182.88	cm	
<b>Volume</b>	0.556	m <sup>3</sup>	
<b>Mass (empty)</b>	~220	kg	
<b>Material</b>	steel	-	

Several modifications were planned and implemented before installation. This included:

- Two windows on the side of the tank at 90° to allow visualization.
- One side inlet port (ID 10.16 cm, 4”) with downward jet.
- One bottom outlet port (ID 10.16 cm, 4”).
- Two additional ports for the secondary side heat removal system.
- One top outlet (ID 5.08 cm, 2”) for the steam outlet (to be used during the transient analysis).
- Supporting frame.
- High temperature coating to prevent rusting of the inner surfaces.

The drawing of the tank with the modifications required is shown in Figure 60, where all the main features and additional parts of the water tank are also reported.

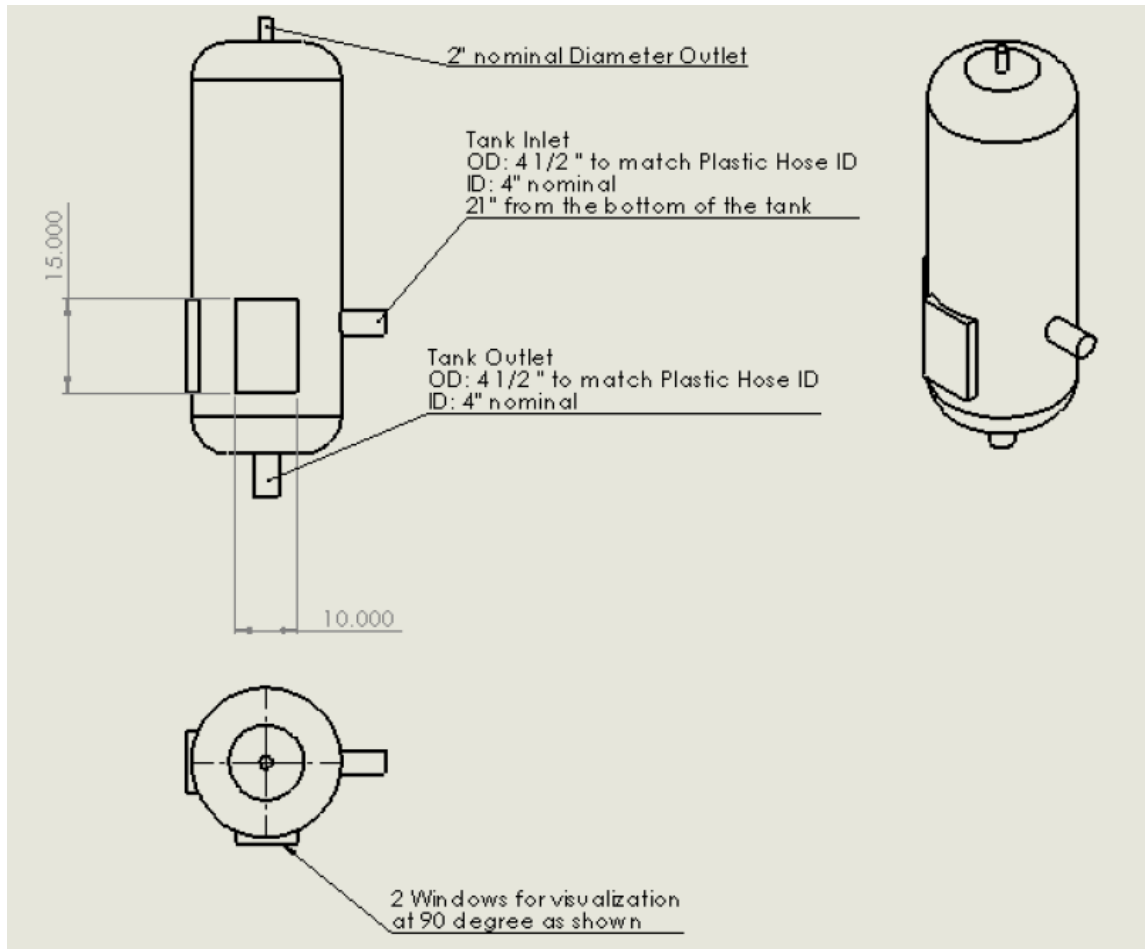


**Figure 60. Water Tank Modifications**

The windows were designed to allow flow visualization during the experiments. The location was optimized to provide the illumination source and the camera in the vicinity of the jet inlet. The two windows were created by welding a rectangular neck with flanged end as shown in Figure 61.



**Figure 61. Tank Windows.**

To guarantee the sealing, two polycarbonate sheets (0.5 cm thickness) were installed and held in place by external frames with bolted connections. Two high temperature silicon gaskets were interposed between the frame and the polycarbonate sheet and the between the sheet and the tank flange, as shown in the detail view of Figure 62. Cold leak tests were performed to verify and fix any leak from the windows before the installation of the tank.

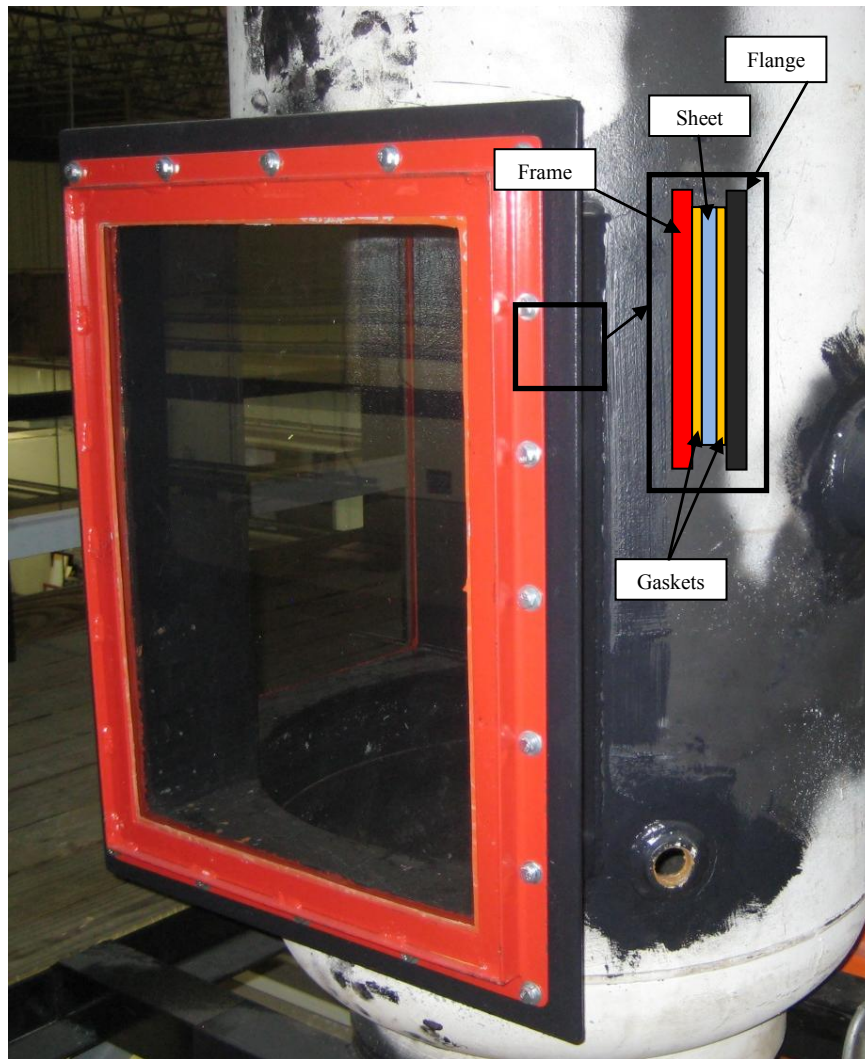


**Figure 62. Tank Windows - Final Configuration.**

The main coolant inlet and outlet pipes were welded to the side and the bottom of the tank respectively. Standard steel flanges were also welded to the external ends of the pipes to allow the connection with the other sections of the pipeline. The inner end of the

inlet pipe was attached to a 90° elbow facing downward in front of the tank bottom outlet (Figure 63).

Two 2.54 cm (1”) ports were already available in the tank. These ports were designated to be used for the secondary heat exchanger.

The 5.08 cm top outlet (centered) was also available in the water tank and selected for the accident phase steam outlet.

A support frame was also designed and manufactured to facilitate the installation of the tank on the main structure and allow fine tuning of the tank position (Figure 64).

This frame was installed on the highest operating deck of the main structure of the facility and bolted into the horizontal cross beams. To allow modifications of the location of the water tank, the tank was simply clamped to the frame, as shown in the same figure.



**Figure 63. Tank View - Internals.**



**Figure 64. Tank Supporting Frame.**

Due to the operating conditions of the experimental facility, all the internal parts of the water tank (in contact with water during the operation), were coated with a special epoxy mastic coating (Benjamin Moore & Co. M45/M46, max temp. 150 °C).

#### **VIII.4 Pipeline and Pipe Connections**

The pipeline connecting the top manifold to the water tank inlet and the water tank outlet to the bottom manifold were designed to fit the elevation changes between the connecting points and to provide room for instrumentation and visualization. A basic scheme was prepared to identify the length of the sections, select the materials base on

the section location and instrumentation to be installed, and sketch the layout of the loop.

The following sections can be identified in the loop:

- The *downcomer*, connecting the water tank bottom outlet to the bottom section.
- The *bottom section*, connecting the downcomer to the inlet of the bottom manifold.
- The *upward pipeline*, connecting the top manifold outlet to the top section.
- The *top section*, connecting the upward pipeline to the water tank inlet.

All the sections have an inner diameter of 10.16 cm (4"). The outer diameter may vary depending on the material selected and the availability. When possible, the outer diameter was selected equal to 11.43 cm (4.5").

#### *VIII.4.1 The Downcomer*

The downcomer is a vertical section connecting the water tank outlet to the bottom section. To allow flow visualization, this section was constructed using polycarbonate piping (ID: 10.16 cm, OD: 11.43 cm). The upper section of the downcomer was equipped with a polycarbonate flange to allow the connection with the tank outlet flange (Figure 65). The flange was glued to the polycarbonate pipe using Methylene chloride, a special solution which provides enough strength to the joints and cures at room temperature in approximately 24 hours. Due to the length of the

downcomer (4.87 m), the pipeline was split into two sections, and the connections built with flanges (**Error! Reference source not found.**).



**Figure 65. Downcomer - Upper Section.**

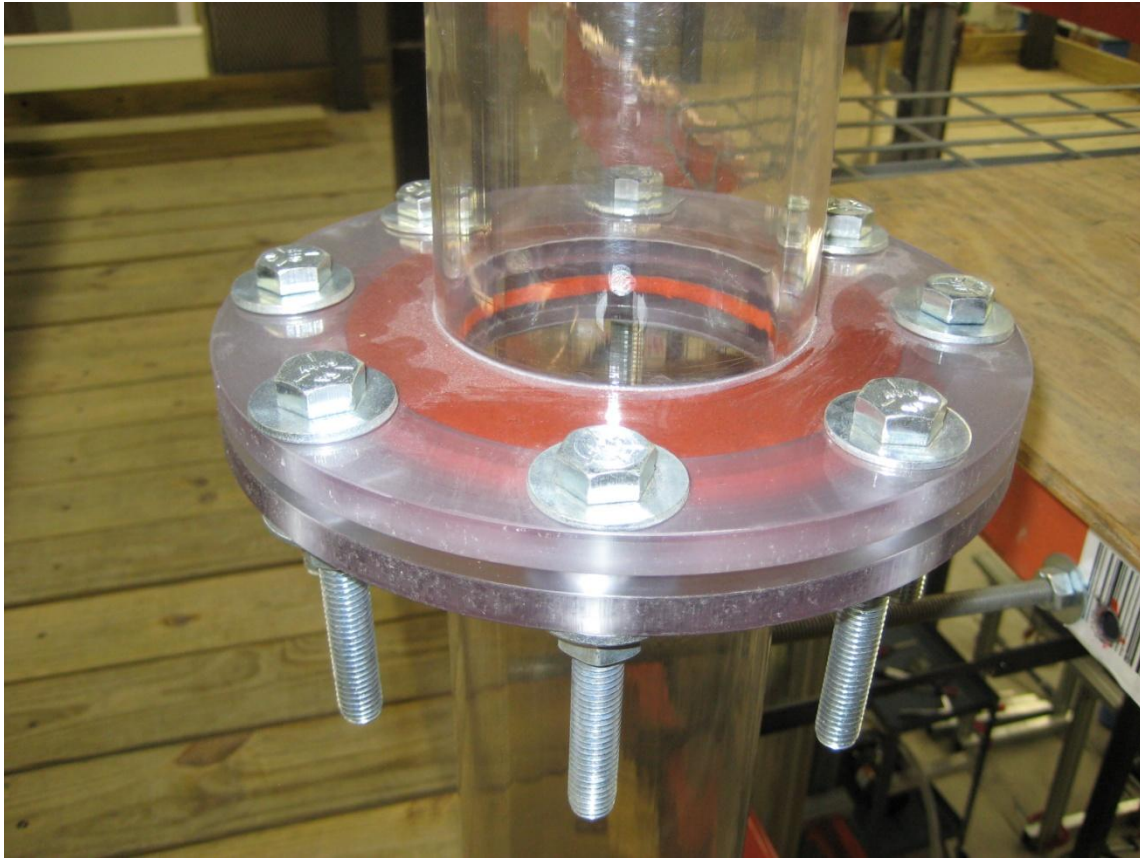


**Figure 66. Polycarbonate Flanged Connection.**

A different technique was applied to connect the lower end of the downcomer to the bottom section of the loop. This connection was specifically designed to:

- Allow differential thermal expansion between the polycarbonate pipe (thermal linear expansion =  $70 \cdot 10^{-6}$  m/m K) and stainless steel (thermal linear expansion =  $17 \cdot 10^{-6}$  m/m K).
- Provide flexibility to manage possible eccentricity between the pipes.

- Guarantee the water seal up to boiling temperature (100 °C).

The connection was realized with a high-temperature hose (McMaster-Carr 5296K641, ID = 11.43 cm, Max temperature = 175 °C) and standard hose clamps, as shown in Figure 67.

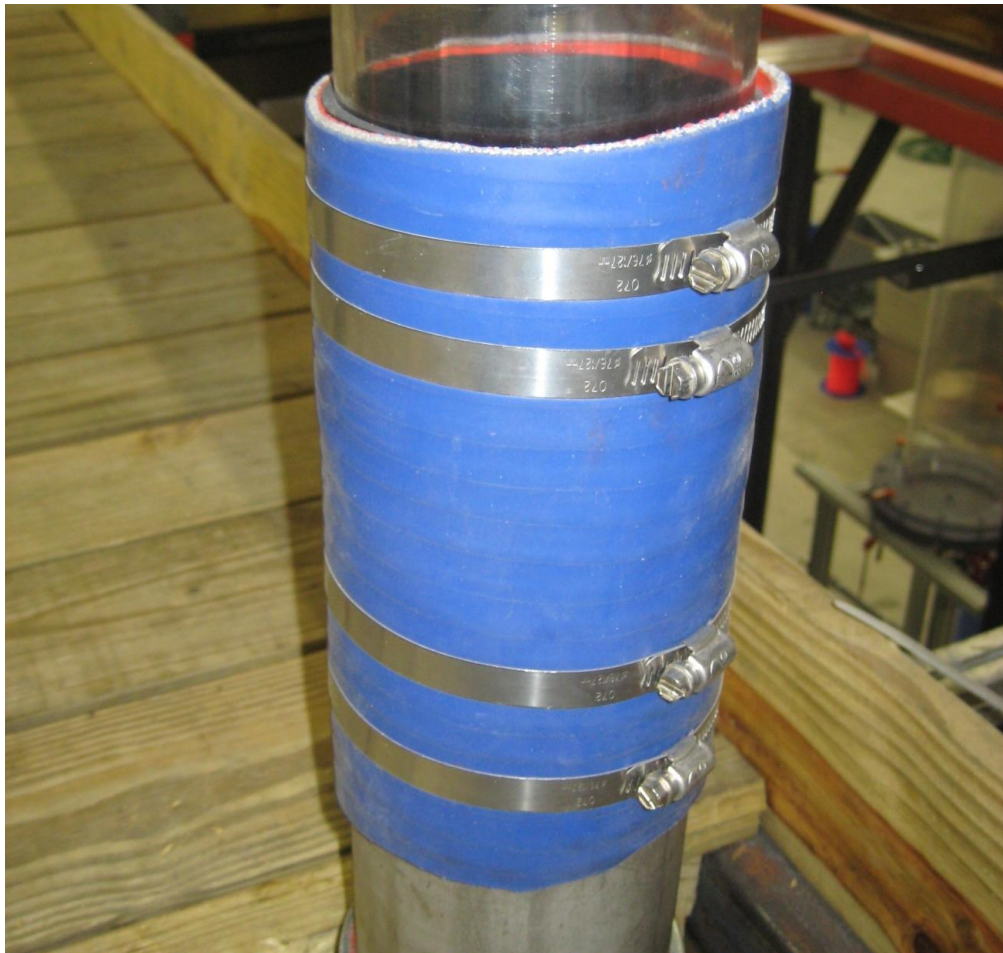


**Figure 67. Stainless Steel - Polycarbonate Connection**

#### VIII.4.2 The Bottom Section

This section connects the downcomer lower end with the bottom manifold inlet.

The section was entirely constructed with stainless steel piping due to:

- The presence of different elbows that could not be constructed with polycarbonate.
- Mechanical stress due to the weight of other piping connected to this section.
- The installation of the flowmeter.

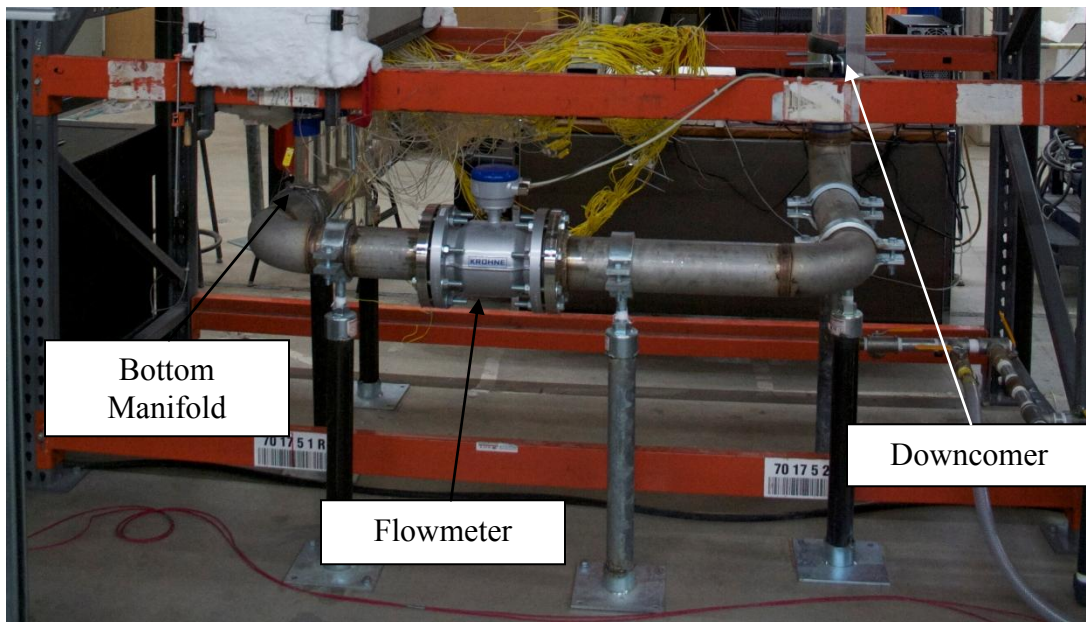


**Figure 68. Bottom Section.**

The section consists of three stainless steel elbows and three straight portions. The section was interrupted and equipped with stainless steel flanges to allocate the flowmeter (Figure 68). Part of the welding was performed at the machine shop (Custom Fabricators & Repairs Inc, Bryan TX). The different parts were finally assembled and additional welding was performed in situ.

#### *VIII.4.3 The Upward Pipeline*

The upward pipeline (Figure 69) connects the exit of the upper manifold with the top section. This part of the loop was also designed to allow flow visualization during the phases of the experiments. Polycarbonate pipes (ID=10.16 cm, OD=11.43 cm) were assembled and connected using similar techniques (flanges and high temperature hose with clamps) described in the previous sections. The high-temperature hose connection was selected to allow thermal expansion of the polycarbonate section.

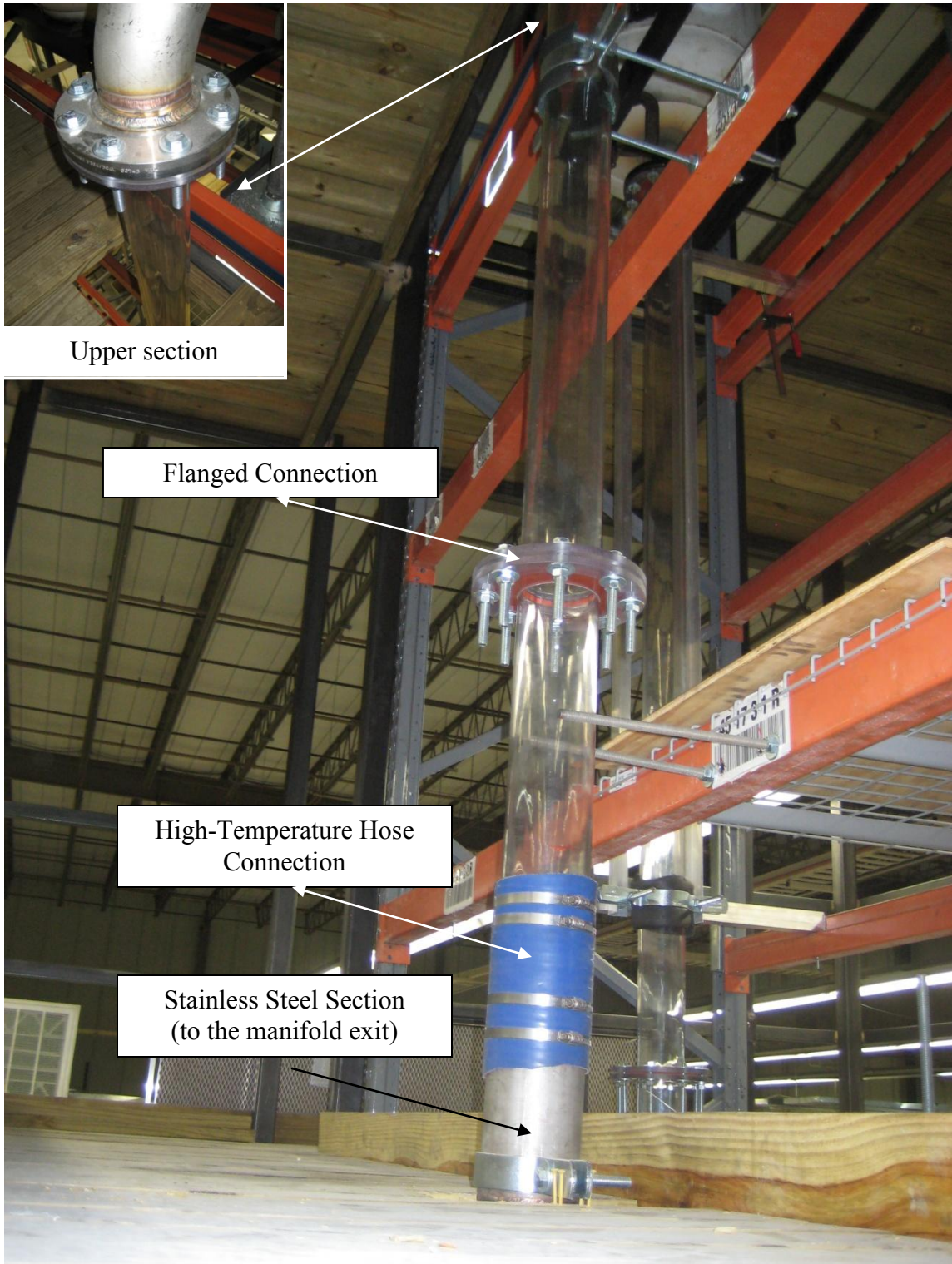


**Figure 69. Upward Pipe.**

#### *VIII.4.4 The Top Section*

The top section of the loop connects the upper end of the upward pipe with the tank inlet (jet). This section is constituted of two main parts:

- A Stainless steel section, connected to the upward pipe. Stainless steel was selected due to the presence of two elbows and to allow structural support to the entire section.
- A horizontal transparent section, connected to the tank inlet, fabricated with polycarbonate pipe.

Both sections (ID=10.16 cm, OD=11.43 cm) are shown in Figure 70.

Polycarbonate-to-steel flanged connections were used to connect the polycarbonate horizontal section to the tank and to the stainless steel piping as shown in the same figure.



**Figure 70. Top Section**

#### *VIII.4.5 Other Connections*

One of the most challenging connections between pipes was the one between the stainless steel risers and the glass branches of the manifolds. These connections were studied and engineered in order to:

- Allow the connection between the pipes of the risers' panel and the manifolds' branches, ensuring the water seal and the operating temperatures.
- Allow differential thermal expansions of steel and glass (axially and radially).

- Provide flexible connection to prevent mechanical stresses to the glass parts, also during the assembly procedures.

The connection was realized using the same technique described in the previous sections, with high-temperature hose (5.08 cm nominal ID) and hose clamps.

### **VIII.5 Structures**

Due to the size of the facility and the weight of the components to be installed, three different structures were designed and constructed:

- The *primary support structure*, to support all the components of the facility, including the water tank, and the reactor cavity.
- The *scaffolding*, designed to allow workers and researches to reach the components of the facility a different elevations, also during the experiments.
- The *secondary support structures*, conceived to provide special support and stability to selected components of the facility (piping, instrumentation, etc).

Each structure, described in the following sub-sections, was rigorously designed to comply with the safety requirements imposed Texas A&M University.

### *VIII.5.1 Primary Support Structure*

This structure was conceived to support all the main components of the experimental facility, including:

- The reactor cavity (vessel, heaters, risers' panel)
- The pipeline and manifolds
- The water tank

The Interlake Megalux ® selective pallet rack was considered as the best solution due to different reasons:

- High construction flexibility and modularity, allowing customizable working decks at different elevations.
- Large selection of sizes to match the load and space requirements.
- Relatively low cost compared with other customized structures.
- Easy assembly procedures.

The dimensions and shape of the vertical posts and the horizontal beams were selected from the manufacturer's catalogue, based on:

- 1) Desired overall length.
- 2) Total maximum load (a safety factor of 10 was applied).
- 3) The load distribution (vertical and horizontal).

Three working decks were created using pairs of horizontal beams. Additional pairs of beam were installed at selected elevations to reduce the distance between the horizontal beams under the limits suggested by the manufactures, based on the model of

the vertical posts selected and the maximum load. Figures 71, 72, and 73 show details of the pallet rack components and the support structure.



**Figure 71. Vertical Posts before Installation.**



**Figure 72. Main Support Structure - Lower Working Deck.**

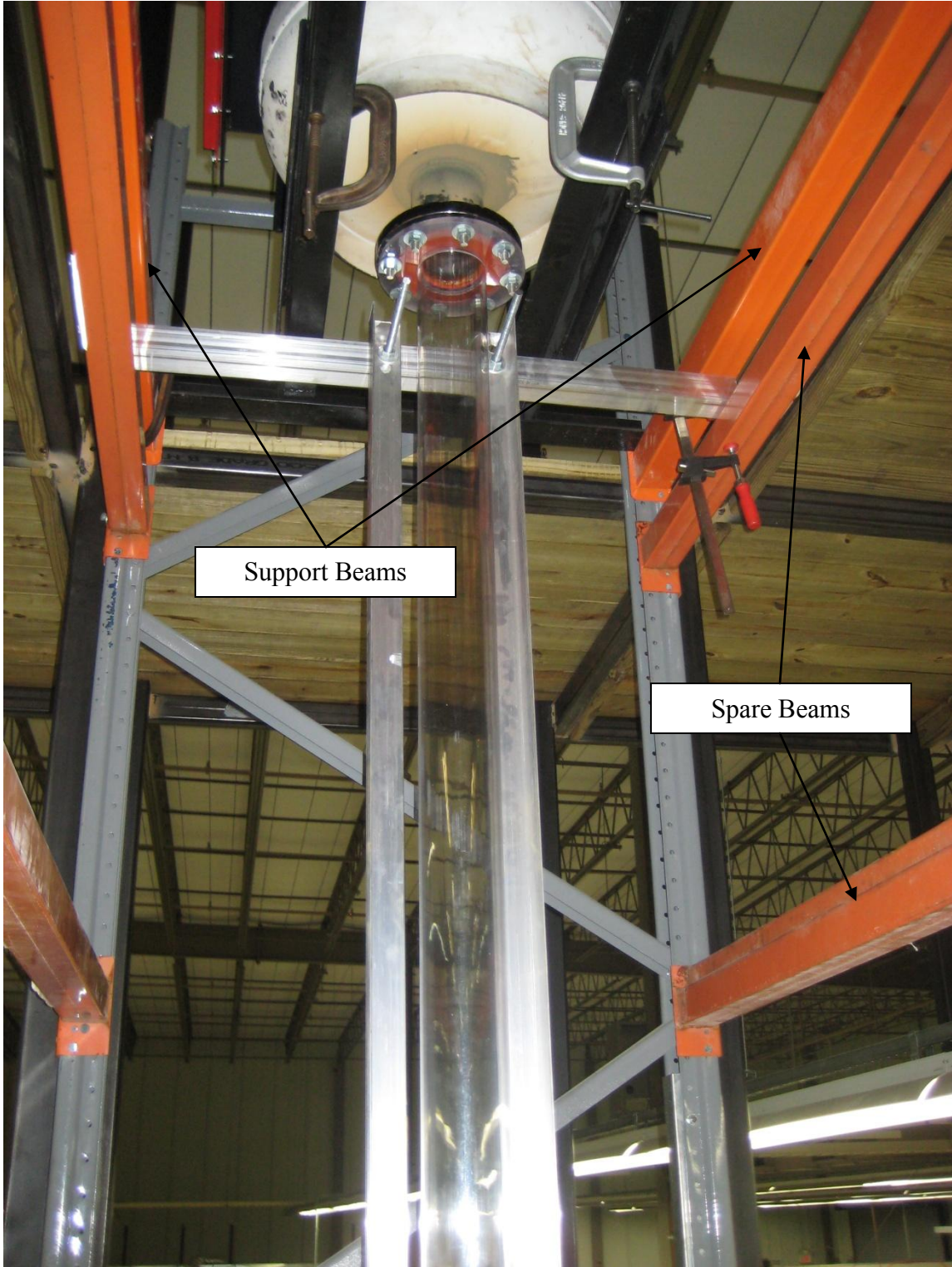


**Figure 73. Main Support Structure - Upper Working Deck.**

The vertical posts were anchored to the ground by placing two anchors with bolts on each column of the vertical posts (four locations). The size of the anchors (Diameter = 1.27 cm, Length = 5.08 cm) was estimated using the drop-in concrete anchor/fastener tables, considering the maximum load and proper safety factors.

### *VIII.5.2 Scaffolding*

Scaffolding surrounding the primary main support structure was considered to:

- Provide accessibility to the working decks and the components of the facility located at different elevations.
- Allow researchers to work safely (people are not allowed to stand on the main support structure even wearing safety harness) at different elevations, during the phases of the experiments.
- Provide stability to the main support structure.

The structure was constructed with steel tubing of different sizes. Figure 74 shows the features of the scaffolding and its dimensions (British units).

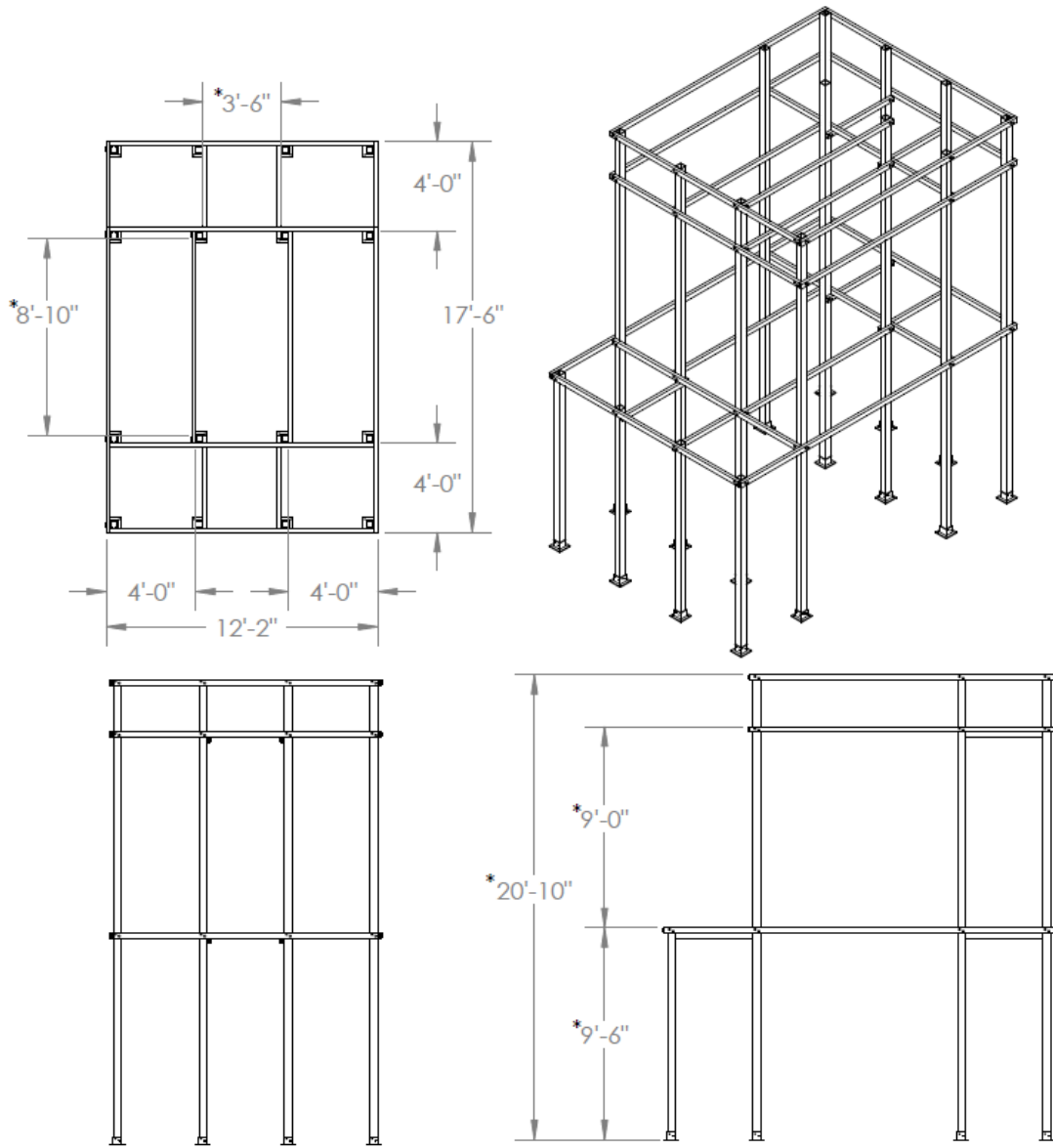


**Figure 74. Scaffolding – Dimensions (British Units).**

The size of the steel tubing, summarized in Table 14, was determined by performing a structural analysis assuming conservative static loads. The calculations were performed under the guidance of Texas A&M University Facility Services. In particular, static loads, safety factors, additional loads to railings, and load application locations, were applied after consultations with the Facility Services.

**Table 14. Parts Dimensions (British Units).**

<b>Part Name</b>	<b>Tubing Size</b>	<b>Wall Thickness</b>
Columns	4" x 4"	0.188 "
Beams	3" x 2"	0.188 "
Rainlings	2" x 2"	0.188 "
Brackets	3" x 2"	0.083 "

Flooring of the working decks were constructed using wood plates as shown in Figure 75. This helped reducing the total weight of the floors, facilitating the installation otherwise difficult using steel plates.



**Figure 75. Scaffold Flooring.**

### *VIII.5.3 Secondary Support Structures*

Some components of the facility required specific support structures in addition to the structures described above. These components are:

- Water tank
- Pipeline
- Manifolds
- Reactor cavity components

Due to its weight during the facility operation, the water tank required a special support and connection to the upper operating deck. A steel rack was constructed to support the tank, and allow fine adjustments of the position during the placement of the piping (Figure 76). The rack was designed to fit into the beams of the main structure at the upper operating deck (Figure 77).

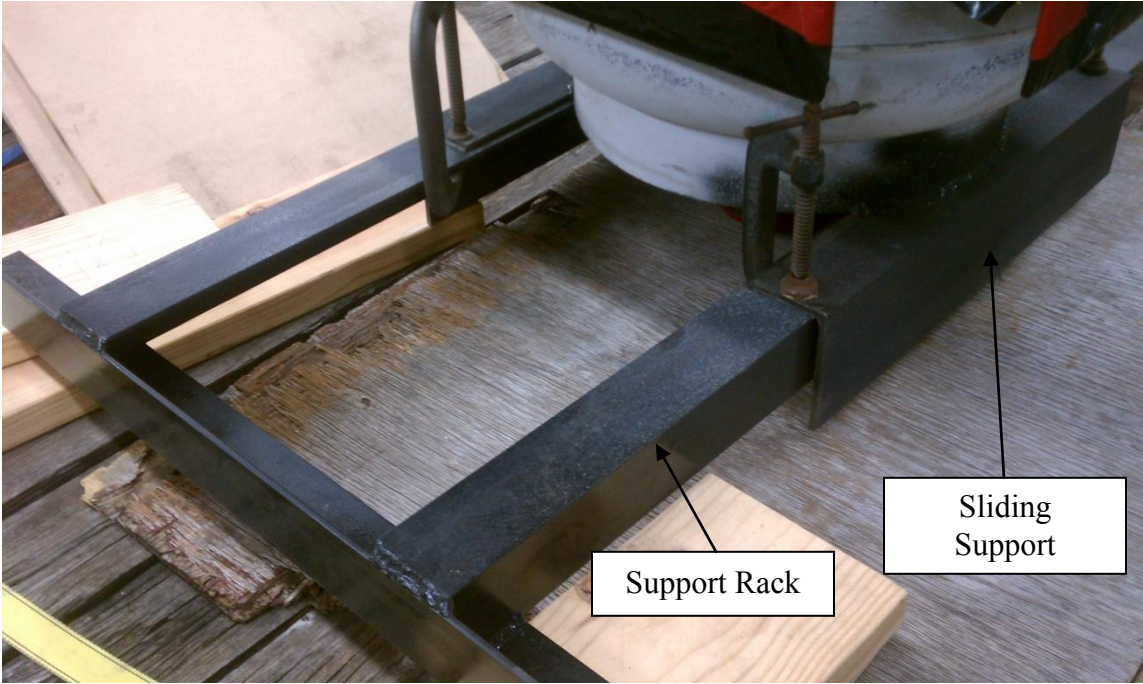


**Figure 76. Tank Support.**

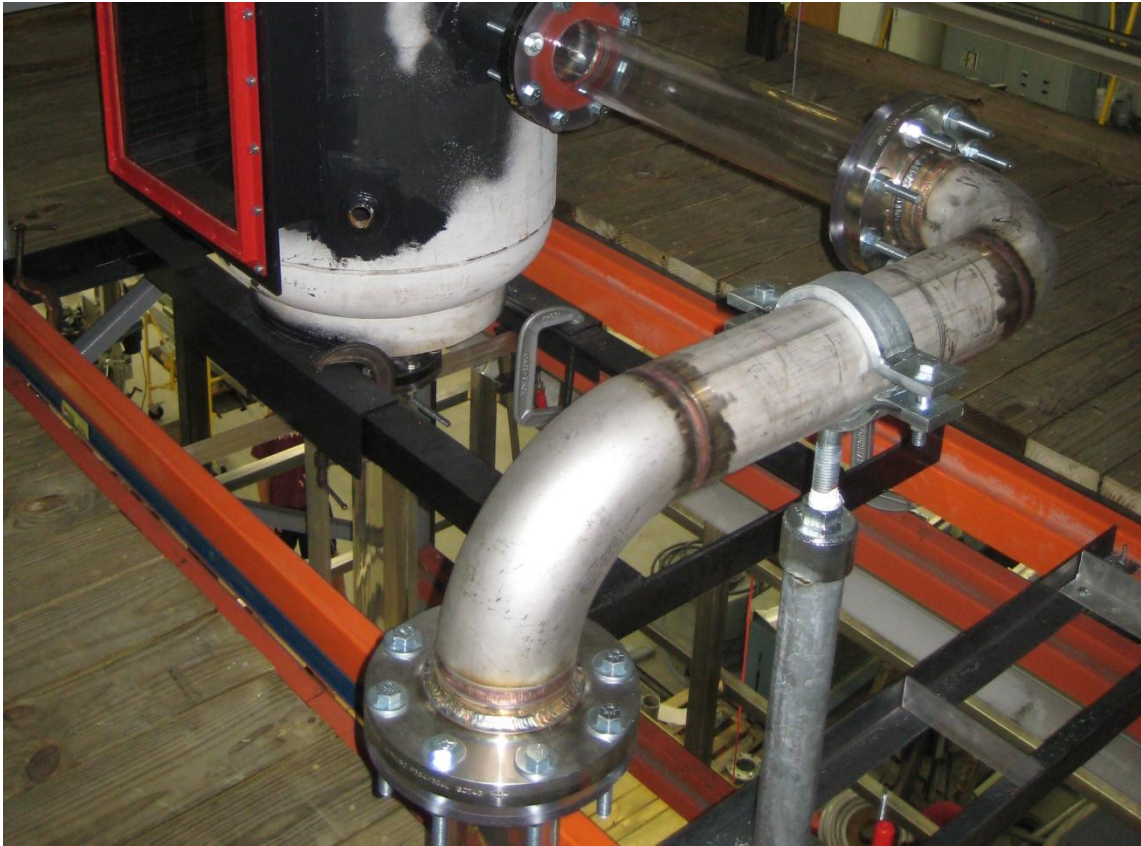


**Figure 77. Tank Support Installment.**

Proper pipeline supports were selected for horizontal and vertical pipes. Most of the vertical pipes were attached to a secondary aluminum structure with hose clamps, as shown in Figure 78.

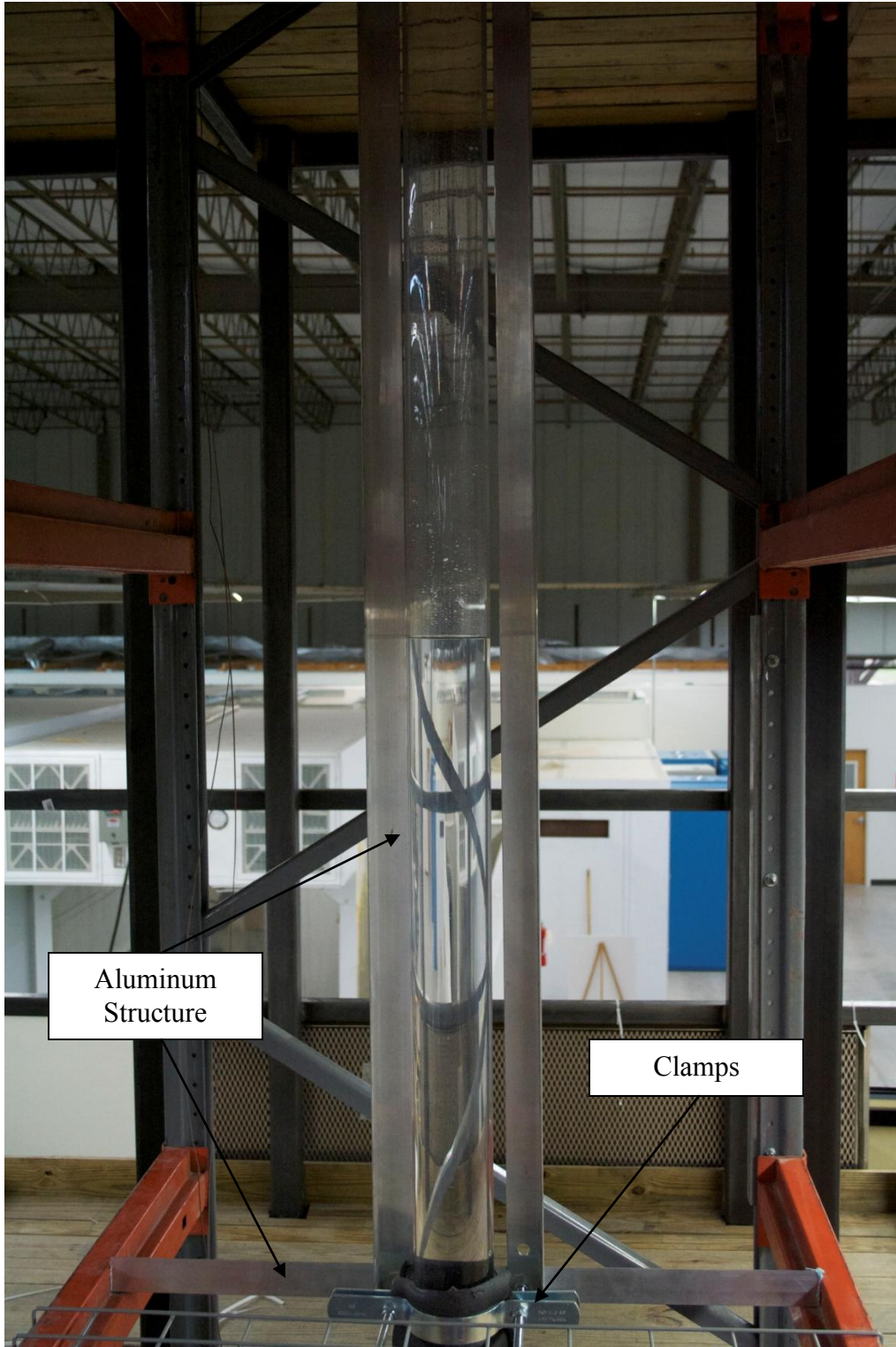


**Figure 78. Vertical Pipes Support Structure.**

Horizontal pipes were supported by support columns and clamps, as shown in Figure 79. Similar installment was used for the horizontal piping in the top section, and for the bottom manifold.

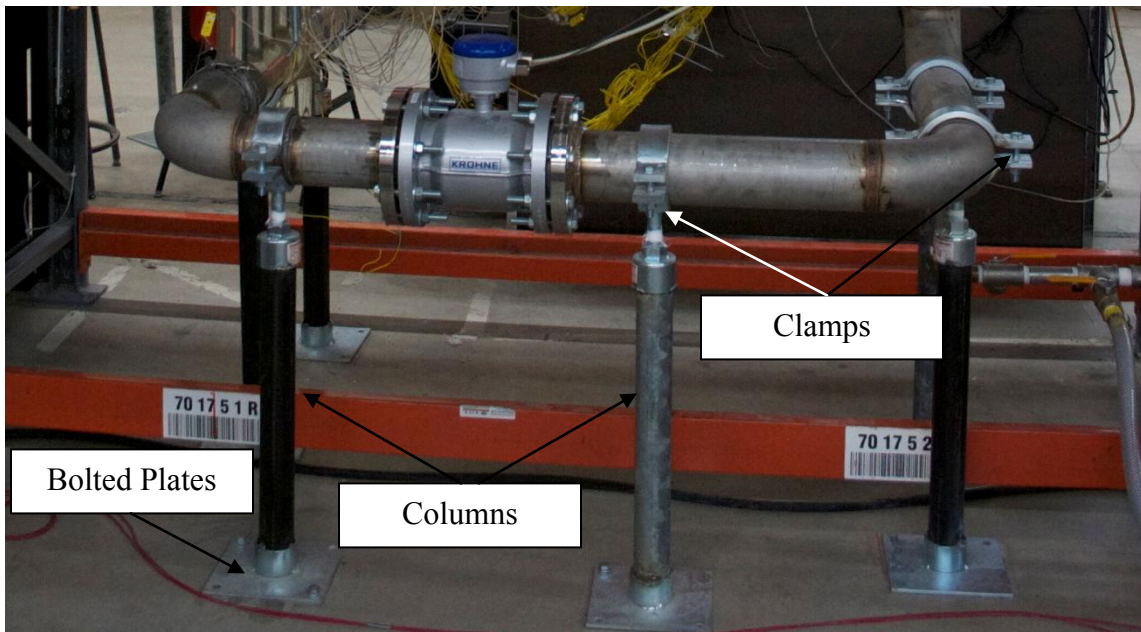


**Figure 79. Horizontal Support Columns.**

The top manifold was supported by two standard pipe ring supports as illustrated in Figure 80. This solution provided a firm, adjustable and stable support to the top manifold, preventing fixed connection which may result in mechanical stresses.



**Figure 80. Top Manifold Supports.**

The reactor cavity was installed on the beams of the first working deck. Support structures were constructed to support the reactor vessel and the heaters as shown in Figure 81.

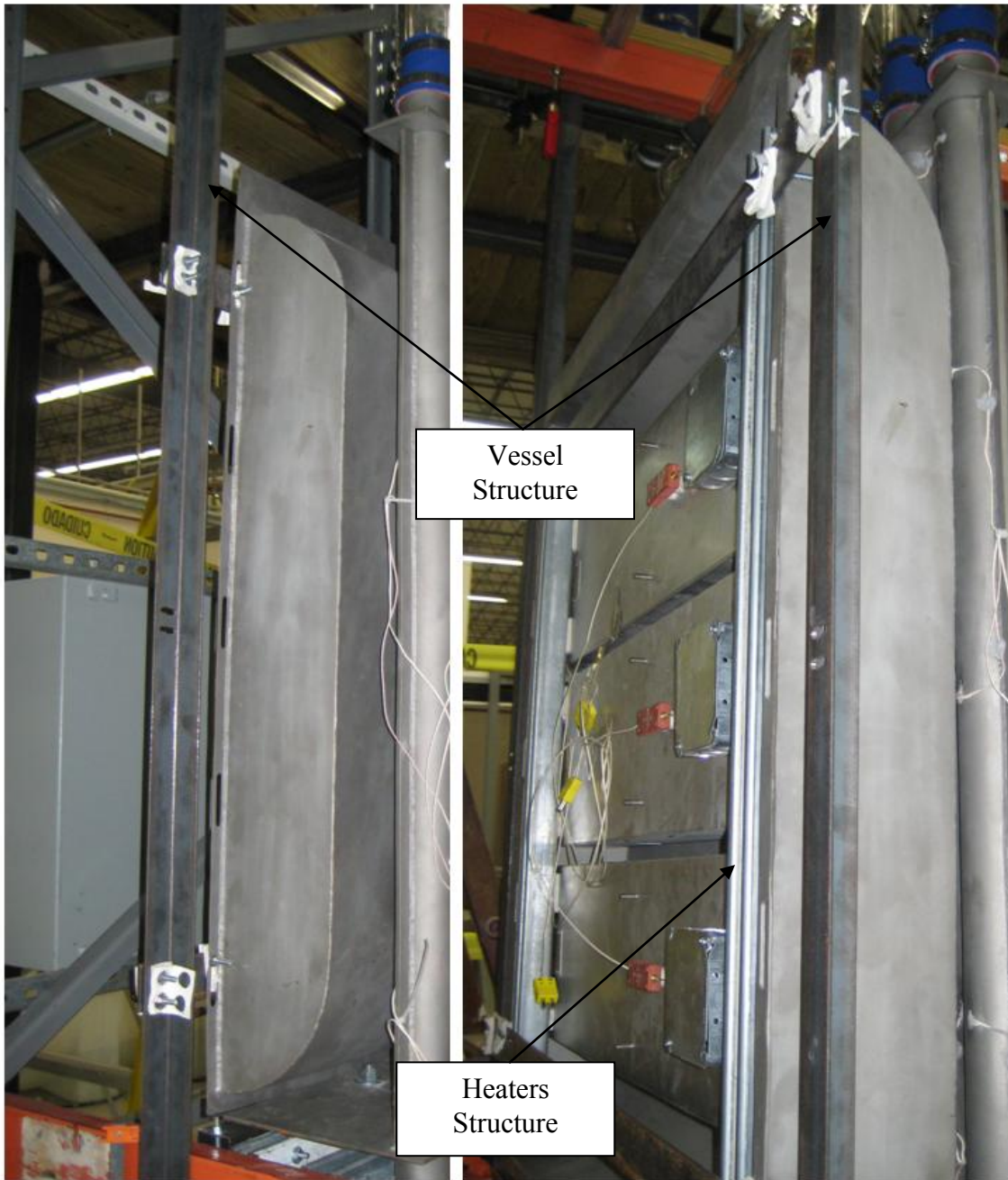


**Figure 81. Vessel and Heaters Supports.**

The risers' panel was fixed to two cross beams connected to the main working deck, by four treaded rods with bolts. The bolts were also used to adjust the vertical location of the panel to match the bottom and top manifolds and to level the horizontal angle from the bottom plate (Figure 82).

All connections, supports and techniques developed and adopted during the construction of the facility were peer reviewed and, when possible, preliminarily verified with dedicated separate tests.

The tests were especially conducted to test the connections between different materials to verify the water seal and the mechanical straight. Some of the tests (such as the leak tests conducted for the water tank), could not be conducted under realistic conditions of temperature and or pressure. These verifications were conducted during the facility shakedown and will be described in Chapter X.

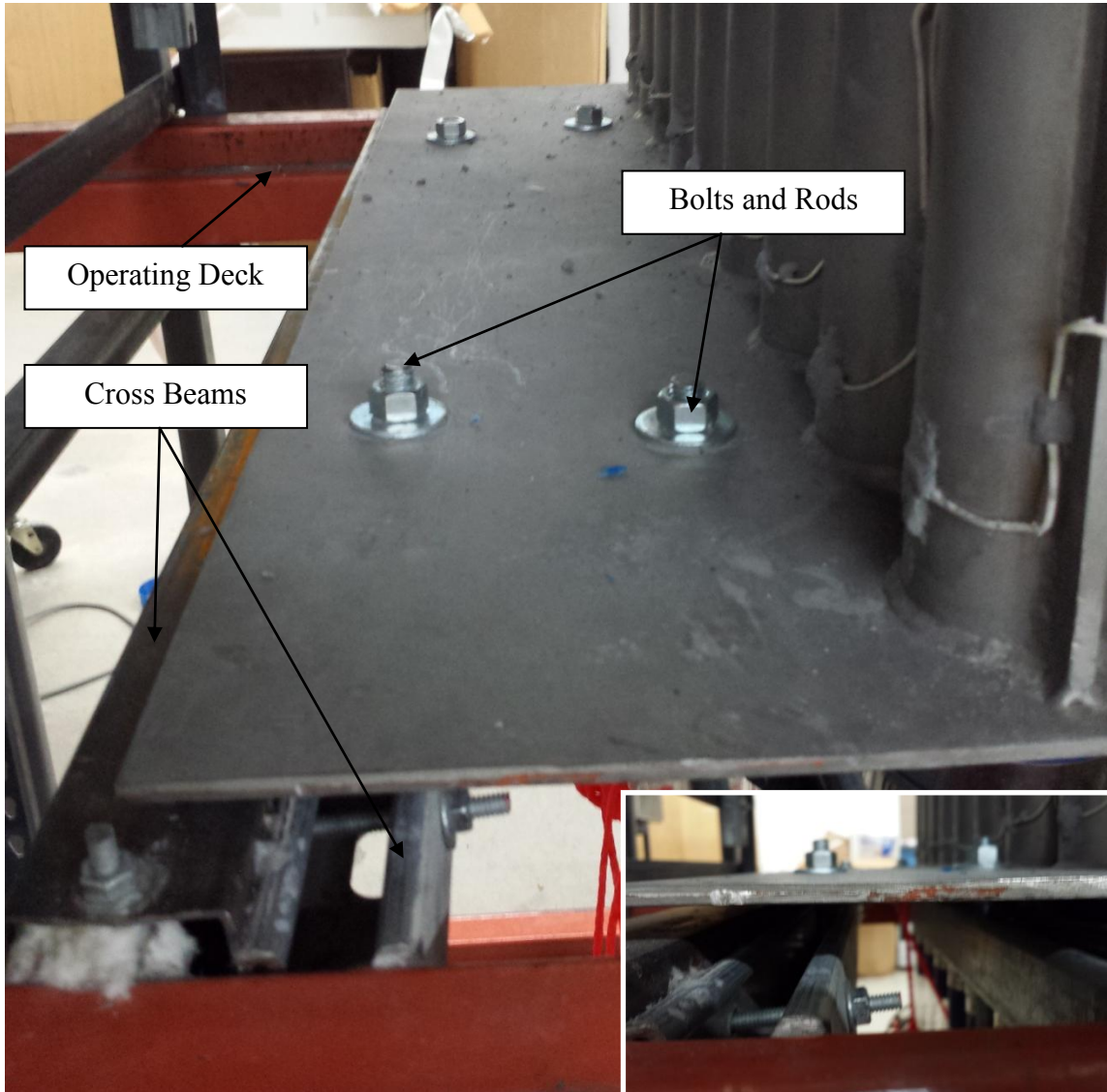


**Figure 82. Risers' Panel Support.**

## CHAPTER IX

### PHASE 6: INSTRUMENTATION SELECTION AND INSTALLATION

The instrumentation and equipment to be included in the experimental facility were selected based on the type of measurements to be performed during the experiments. The instrumentation was mainly based on the measurements requirements during the steady-state phase. Nevertheless, the majority of the instrumentation and other equipment selected will be available and can be used during the transient phase.

The main measurements to be performed during the experiments are:

- Measurement of the walls' temperature
- Measurement of the coolant temperature
- Measurement of the coolant flow rate

A schematic view of the instrumentation layout is shown in Figure 83.

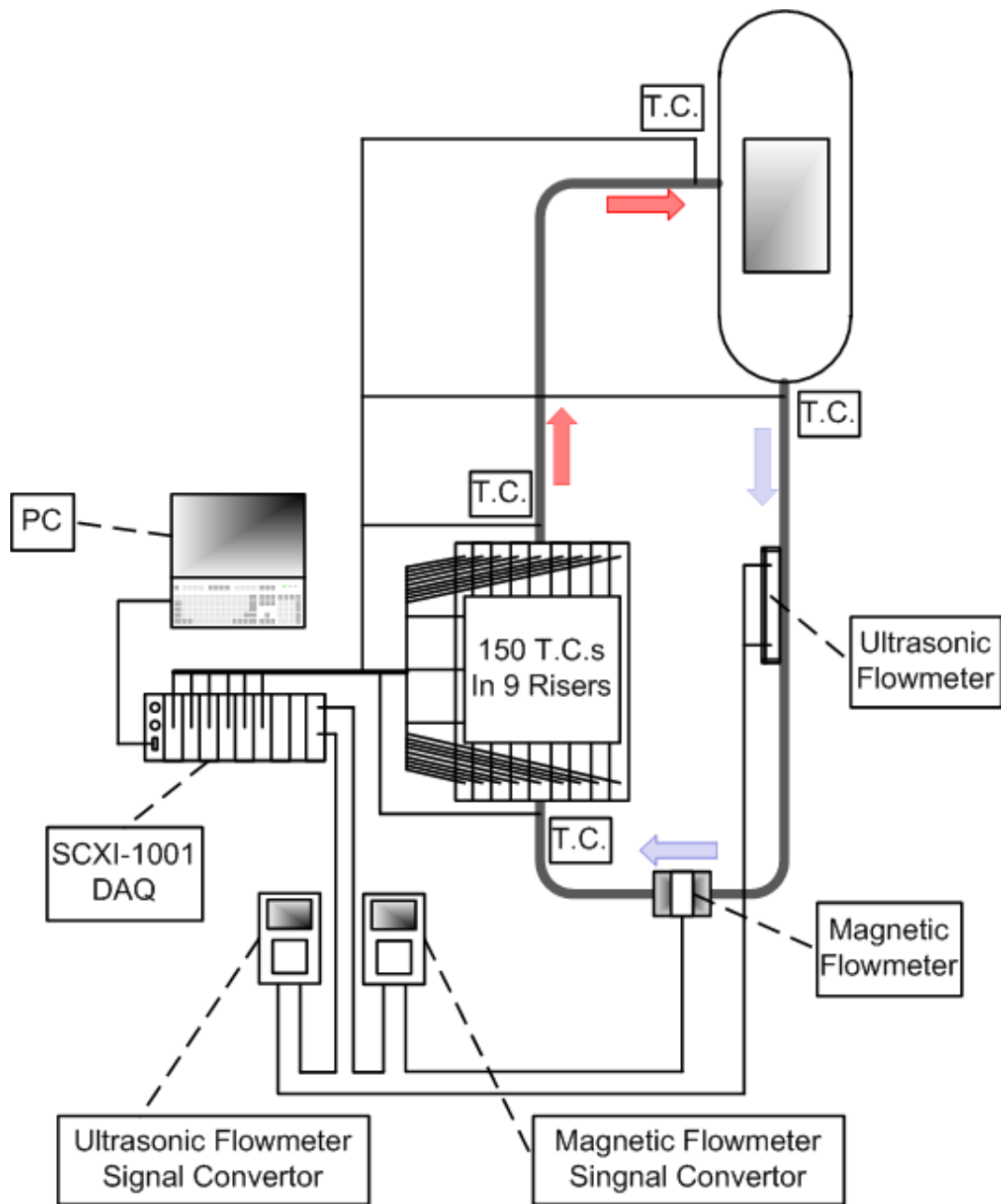


**Figure 83. Instrumentation Layout.**

## **IX.1 Measurement of the Temperature**

All the temperatures to be monitored during the experimental activity will be measured using k-type thermocouples (EN60584-2, Class1). This includes the temperature of the walls and the temperatures of the coolant in different locations.

### *IX.1.1 Temperature of the Walls*

A high-temperature glass coated thermocouple wire (Omega® HH-K-24-SLE-25, max operating temperature = 704 °C), was selected to measure the temperature of the risers panel walls (pipes and fins, front and back). The ends of the thermocouple wires were placed in selected locations of the risers' wall and fins as shown in Figure 84.

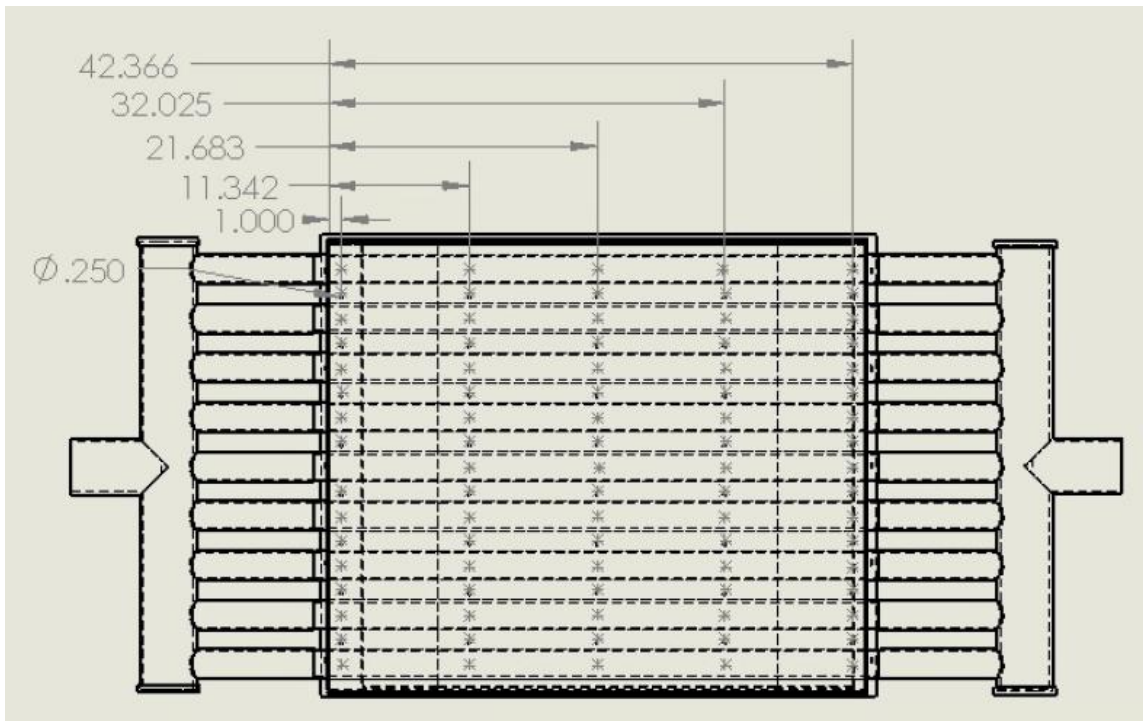


**Figure 84. Risers' Panel Thermocouples Layout.**

The measurement points for the front side of the risers' panel were organized in five equidistant rows. Each row contains:

- One measurement point on each riser (total = 9)
- One measurement point on each fin (total = 8)

The thermocouple wire was passed from the back of the panel through small holes drilled on the fins to reach the measurement points on the front surface (Figure 85).

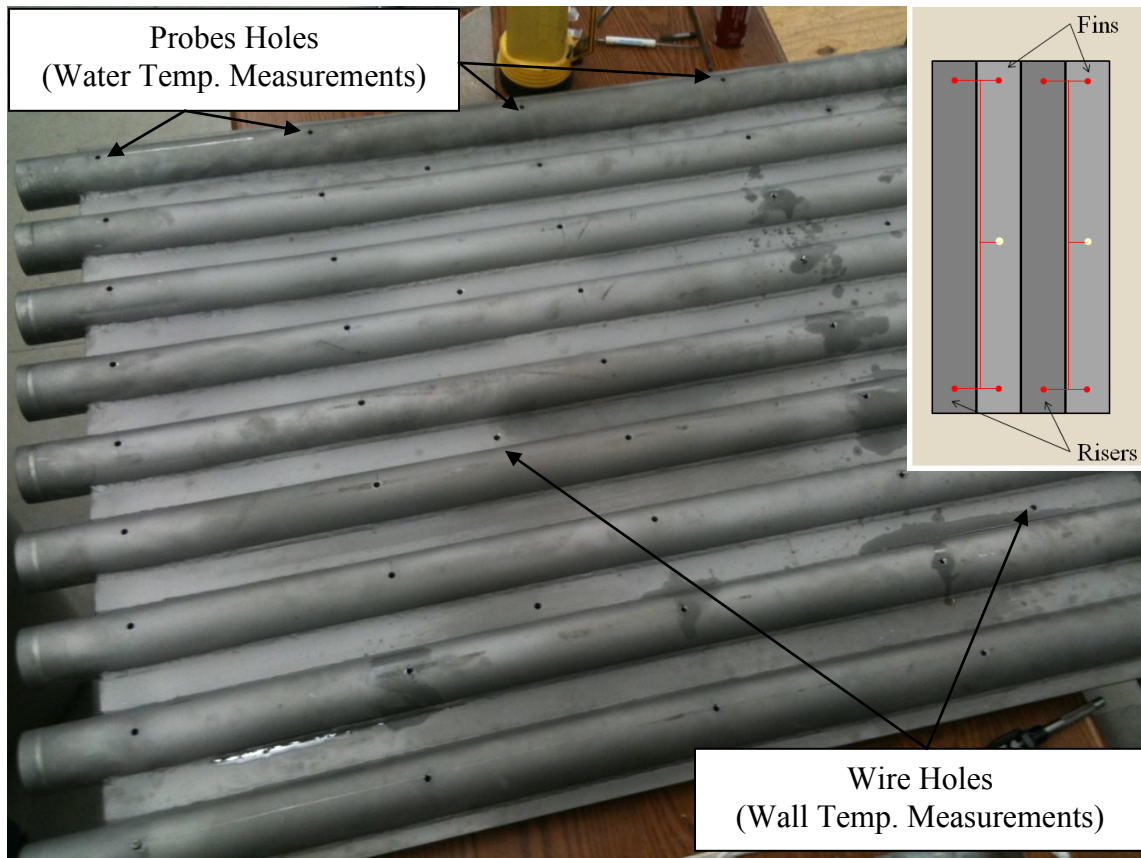


**Figure 85. Thermocouple Holes Locations.**

A similar layout was adopted for the measurements points on the back surface of the panel, where only three rows were installed (top, middle, bottom).

To fix the thermocouple junction on the selected measurement point, and maintain the contact with the steel wall, special technique was required. Due to the low accessibility of the cavity to perform the welding of the thermocouples, the search was addressed toward special glues with specific characteristics, such as:

- Resistant at high temperature ( $> 800\text{ }^{\circ}\text{C}$ )

- High thermal conductivity
- Thermal expansion comparable with steel
- Easy to prepare, install, and cure

The Cotronics Durabond™ 954Stainless Based adhesive was found to satisfy all the characteristics required. Figure 86 shows the final configuration of the thermocouples.



**Figure 86. Thermocouple Wires on the Risers' Panel (front).**

### *IX.1.2 Temperature of the Coolant*

The measurement of the coolant temperature inside the risers and in other locations of the facility will be performed using thermocouple probes (Omega® KMQXL-062G-6). The probes were inserted from the back side of the panel through holes drilled through the risers' wall (see Figure 85). Stainless steel compression fittings (Omega® SSLK-116-116) were installed to hold the probes in place and guarantee the water seal (Figure 87). The probe were placed and fixed with the measuring end at the center of the pipes.

The same technique was adopted to place the thermocouple probes in other locations of the facility such as:

1. Cavity inlet
2. Cavity outlet
3. Water tank inlet
4. Water tank outlet
5. Secondary heat removal system inlet
6. Secondary heat removal system outlet

The final configuration of the risers' thermocouple probes and the installation in selected location of the facility is depicted in Figure 88 and Figure 89.



**Figure 87. Risers Thermocouples Fittings.**

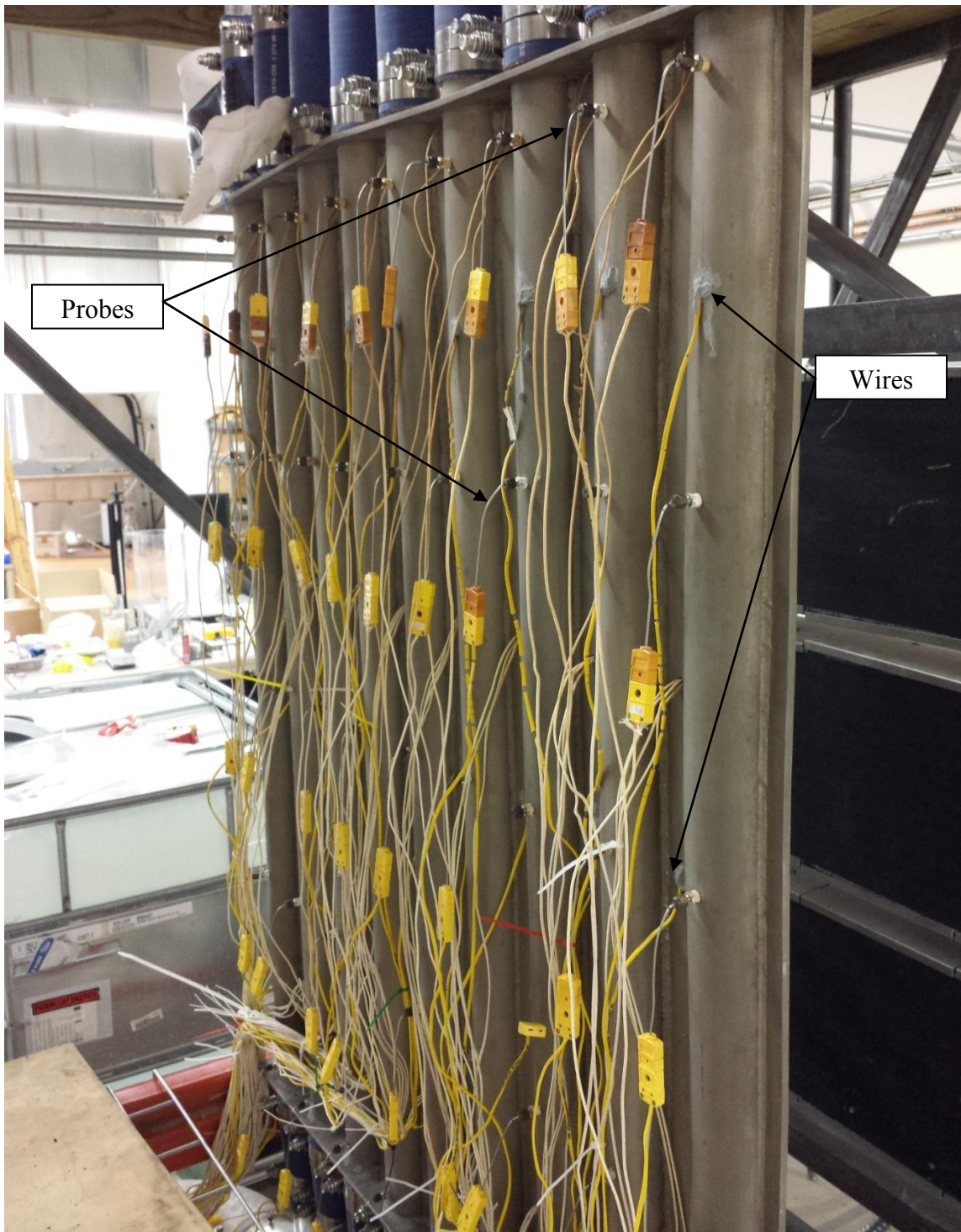


**Figure 88. Thermocouples Configuration - Risers Panel (back).**

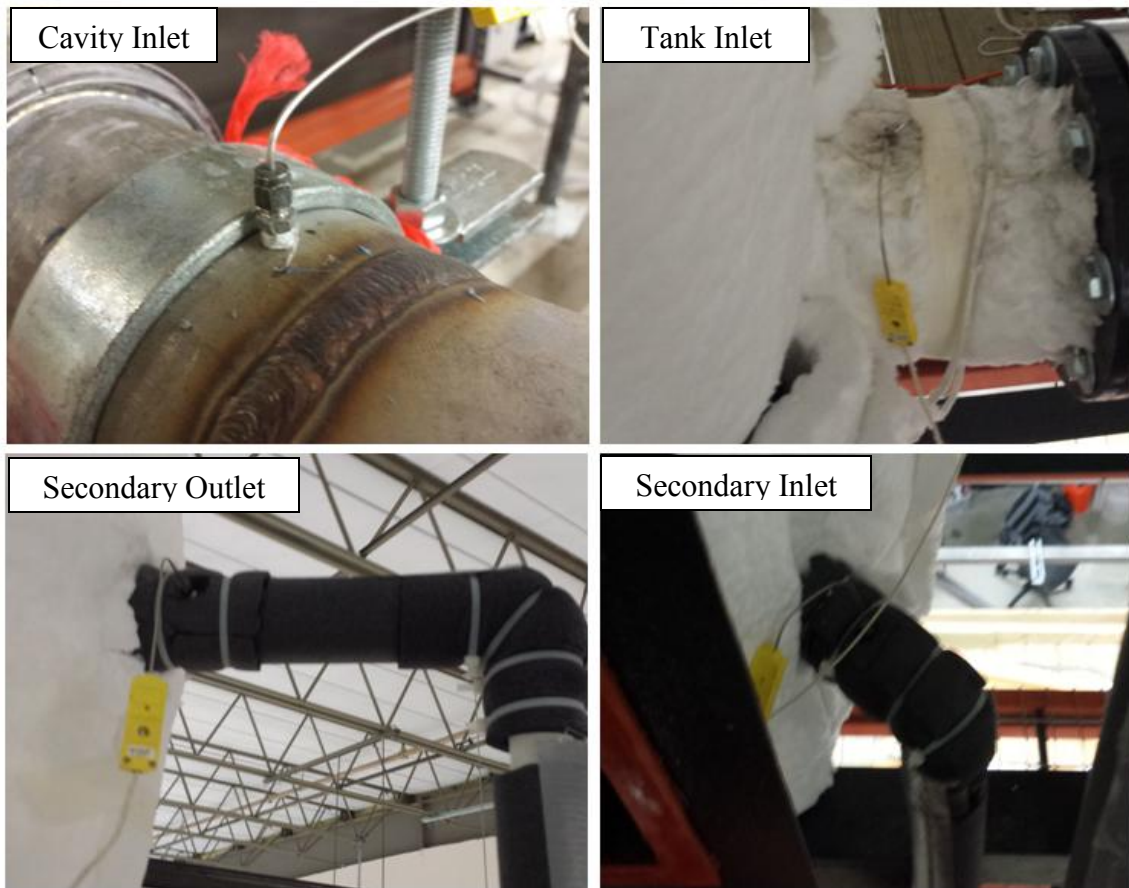


**Figure 89. Other Thermocouple Probes Locations.**

Table 15 summarizes the thermocouples type and number installed in the experimental facility.

**Table 15. Thermocouples Summary.**

<b>Location</b>	<b>Measurement</b>	<b>Number</b>	<b>Type</b>
Risers	Coolant	45	TC Probe
Cavity Inlet	Coolant	1	TC Probe
Cavity Outlet	Coolant	1	TC Probe
Tank Inlet	Coolant	1	TC Probe
Tank Outlet	Coolant	1	TC Probe
Secondary Inlet	Coolant	1	TC Probe
Secondary Outlet	Coolant	1	TC Probe
Risers (front)	Wall	85	TC Wire
Risers (back)	Wall	34	TC Wire
<b>Total Probes</b>		<b>51</b>	
<b>Total Wires</b>		<b>119</b>	
<b>Total Thermocouples</b>		<b>170</b>	

Thermocouples calibration was performed in the range of 20°C to 40°C which was the expected temperature range during the facility shakedown. For the calibration at 20°C, the system was filled with tap water and left for several hours. All the thermocouple reading and the reference temperature were recorded. For the calibration point at 40°C, the system was filled with hot water from a water heater and the calibration was performed after confirming no temperature difference between the top and the bottom manifold. The reference temperature for the calibration was measured by a thermometer and confirmed by another thermocouple reader (Fluke® 52-2, Resolution:

0.1°C, Accuracy:  $\pm 0.05\%$  of reading + 0.3°C) factory calibrated. The values measured by both devices always differed less than 0.5 °C.

## **IX.2 Measurement of the Coolant Flow Rate**

The selection of the proper flowmeter to measure of the coolant flow rate was dictated by several considerations:

- Expected minimum coolant flow rate
- Expected temperature range
- Expected max void fraction
- Flow meter desired accuracy
- Flow meter allowed location
- Cost

The magnetic flow meter was found to be one of the best selections, meeting all the requirements specified above. One of the most important limitations is related to the accuracy and response of the instrument to low flow rates, which was estimate to be approximately 8% at the lowest expected coolant flow rate. Some countermeasures could be adopted to improve the accuracy of the instrument at lower flow rates such as reducing the flow area (main pipeline ID = 10.16 cm). This solution was not adopted to avoid changes in the flow area in the pipeline. The accuracy achieved a low flow rates was also considered acceptable.

The in-line magnetic flow-meter selected was a Krohne, Optiflux® 4100, coupled with the Krohne IFC-300 signal converter. The system has an accuracy of 5.01% at 10.0 l/min and 2.15% at 25.0 l/min, and higher accuracy at greater flow rate. The flow meter signal converter provides direct reading of the flow rate on the screen, together with an analog current output signal of 4-20 mA. The flow meter was already calibrated by the manufacturer.

The flow meter was installed following the manufacturer specifications and suggestions, considering in particular:

- The entrance and exit lengths
- The minimum distances from elbows and t-junctions
- The orientation

The flow meter was installed in the bottom section of the pipeline, on the longest straight section, as shown in Figure 90. This location satisfied all the installation requirements and guaranteed the correct functionality of the instrument.

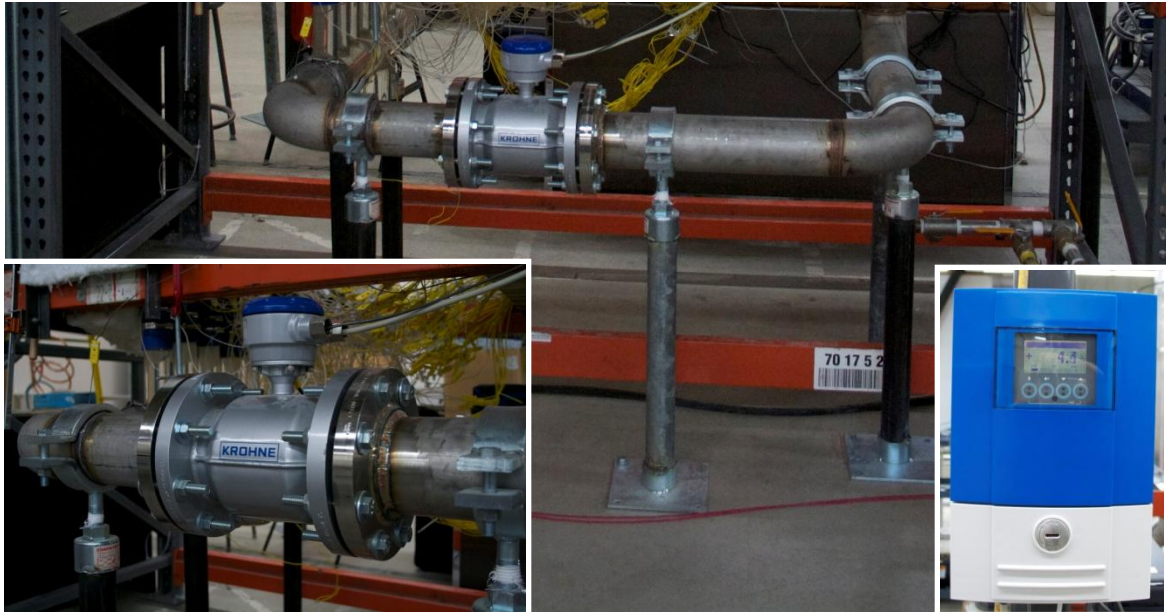


**Figure 90. Magnetic Flow meter.**

An additional clamp-on ultrasonic flow meter was also selected and planned to be used during the facility shakedown for comparison with the main flow meter. Due to its easy installation (clamp-on flow meter that can be installed on the outer surface of the pipes and set up to account for wall thickness and material), the ultrasonic flow meter can be used also during the phases of the experiments and installed at different locations. Figure 91 shows the ultrasonic flow meter installed at the downcomer.



**Figure 91. Ultrasonic Flow Meter.**

### **IX.3 Data Acquisition System**

The temperatures and flow rates were logged by a National Instrument NI SCXI-1001 data acquisition (DAQ) deck (Figure 92) with six SCXI-1303 (used for thermocouples reading) and one SCXI-1301 module (used for flow meters reading). Each SCXI-1303 is equipped with 32 channels (total number of channels available = 192). The SCXI-1301 module has also 32 channels. The number of modules can be increased up to twelve. One of the module slots was dedicated to the power supply and USB data output to be connected to a PC.

A dedicated software installed in the computer was used during the experiment to record the measurements (temperatures and flow rates) and store it into excel spreadsheets. The software allows the user to select the sampling frequency for the thermocouples and the flow meters.

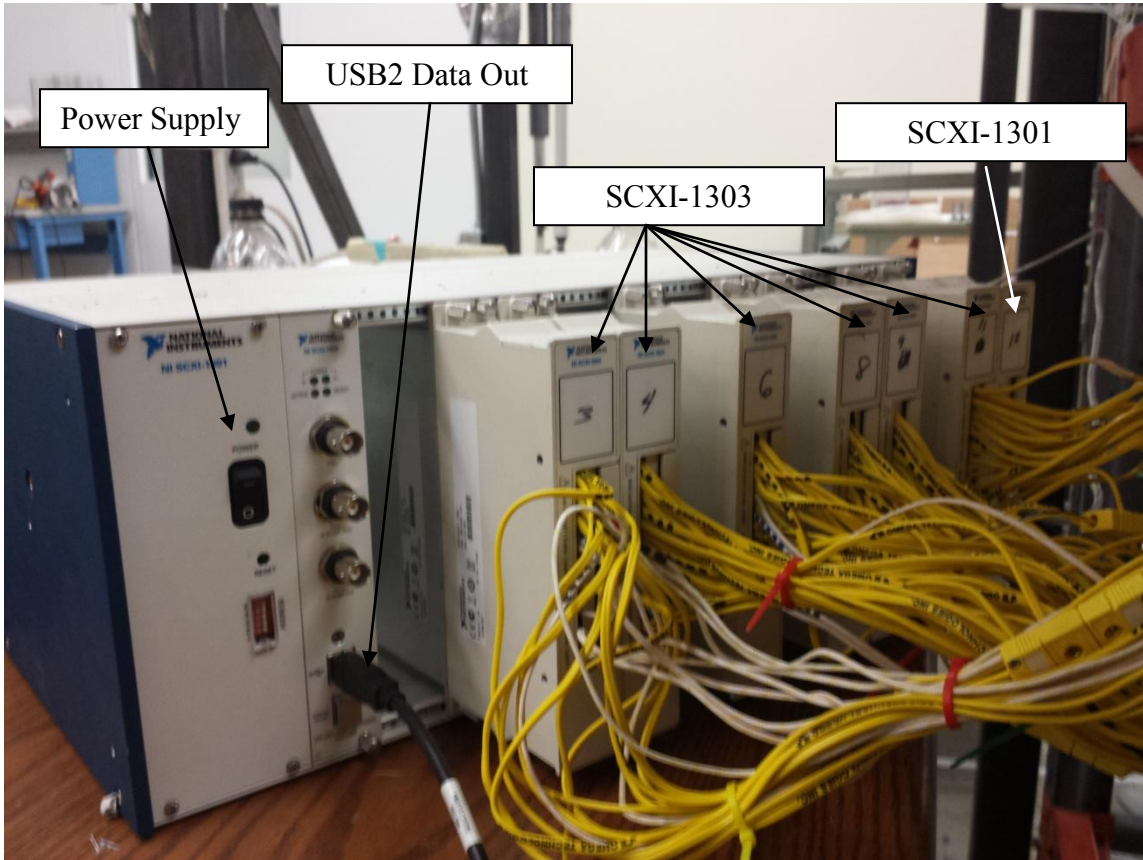


**Figure 92. Data Acquisition System.**

## CHAPTER X

### PHASE 7: FACILITY SHAKEDOWN

The shakedown of the experimental facility was conducted in order to verify the correct functionality of each component and instrumentation, and to observe the overall behavior of the facility before starting the experimental activity. This verification process was divided into five steps:

STEP 0: Facility Preparation.

STEP 1: Leak Tests (room temperature)

STEP 2: Leak Tests (final steady-state temperature)

STEP 3: Empty Test (Heat Flux Verification)

STEP 4: Thermal Insulation Installation

STEP 5: Final Tests and Test Repeatability

STEP 6: RELAP5-3D Model Refinement and Comparison with Shakedown Tests

#### **X.1 Step 0: Facility Preparation**

In preparation for the preliminary tests, additional components were selected and installed in the facility. This includes the refill and drain system, and the secondary heat removal system.

### *X.1.1 Refill and Drain System*

For safety reasons, the facility all the water in the experimental facility has to be drained at the end of each test. This special requirement was achieved by modifying the bottom section of the piping and installing a system of valves and pipe to be used during the refill phase (at the beginning of each test), and the drainage phase (at the end of each test).

To refill the facility up to the desired liquid level in the water tank (approximately 6 meters from the ground), a three-phase centrifugal water pump (Figure 93 A) was installed. The pump takes suction from a water tank (Figure 93 B) located at the ground floor, and injects the water into the experimental facility, through and 2.54 cm stainless steel pipe connected at the bottom section of the pipeline (Figure 93 C). A battery of filters was installed to remove solid particles from the tap water (Figure 93 D). A closed-loop system with valves was designed and installed in order to gradually increase the flow rate injected into the facility, avoiding overpressure in the lower section of the facility at pump startup. The system was also equipped with additional valves to be used during the facility drainage.

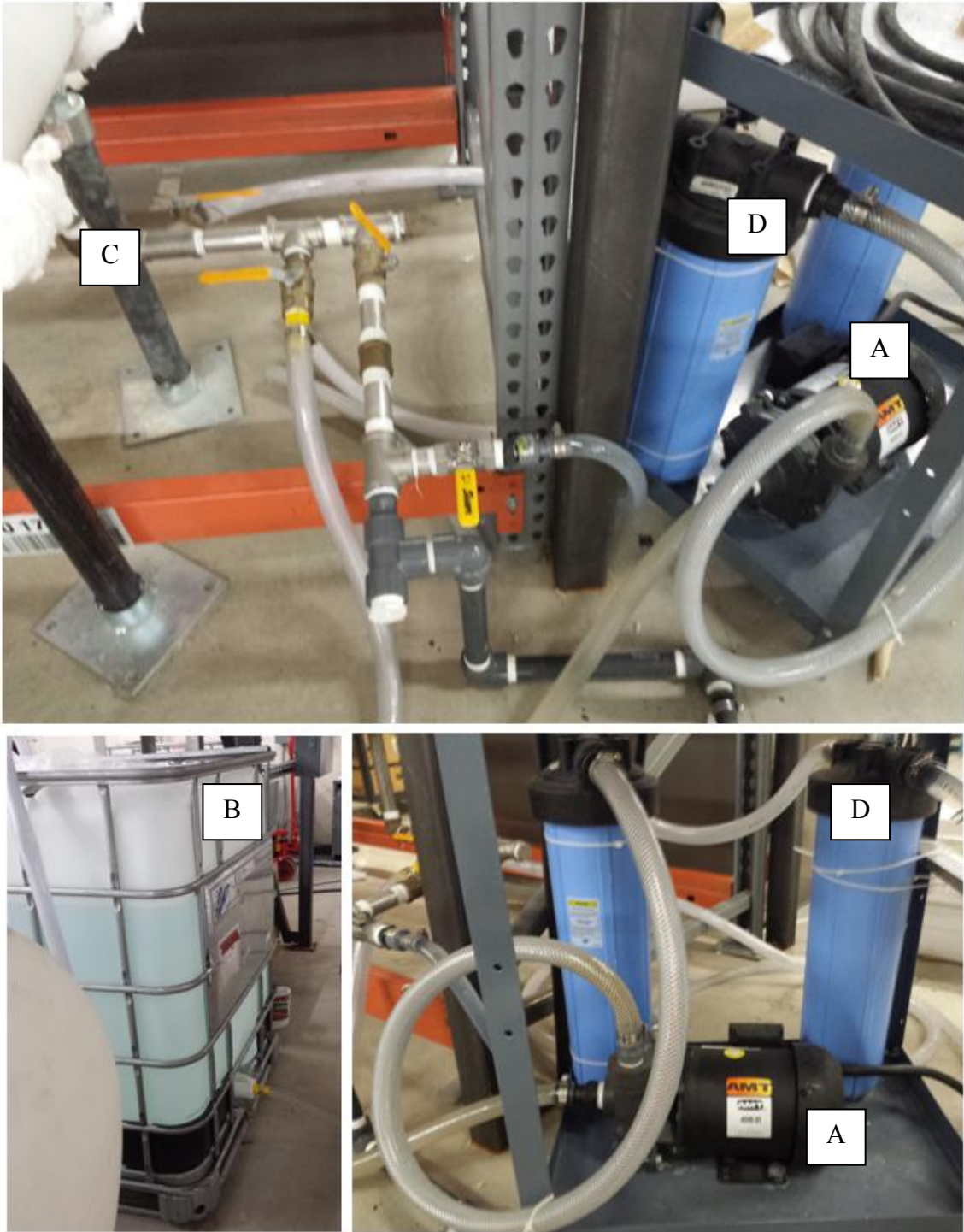


**Figure 93. Refill and Draining System.**

### *X.1.2 Secondary Heat Removal System*

During the normal operation of the nuclear reactor (full scale), a heat removal system operates inside the water tanks to remove the heat from the primary coolant and establish the natural circulation. This system is an active system which may include pumps and other active components. Although the specifications and design of the full scale heat removal system are not available, the heat removal system for the experimental facility was designed in order to remove at steady-state the power produced in the reactor cavity and released to the primary coolant. A typical design of a heat removal system would include:

- An intermediate heat exchanger where the primary coolant (higher temperature, to be cooled) releases its energy to the secondary coolant (lower temperature) through the heat exchanger walls.
- A primary circulating pump, to force the primary coolant through the heat exchanger
- A secondary circulating pump, to force the secondary coolant through the heat exchanger
- An ultimate heat sink

The selection of the heat removal system configuration among different possibilities was dictated by several considerations which include:

- The unavailability of a stable low-temperature water source in the laboratory to be used as ultimate heat sink.

- The high cost of AC units as possible ultimate heat sink
- The limited space around the experimental facility, especially on the elevated working decks (second and third floors of the scaffold)
- The limited power to be released in the laboratory environment

Different configurations were considered as possible solutions. The final configuration selected for the experimental facility proposed ice as ultimate heat sink. The configuration of the proposed heat removal system is depicted in Figure 94.

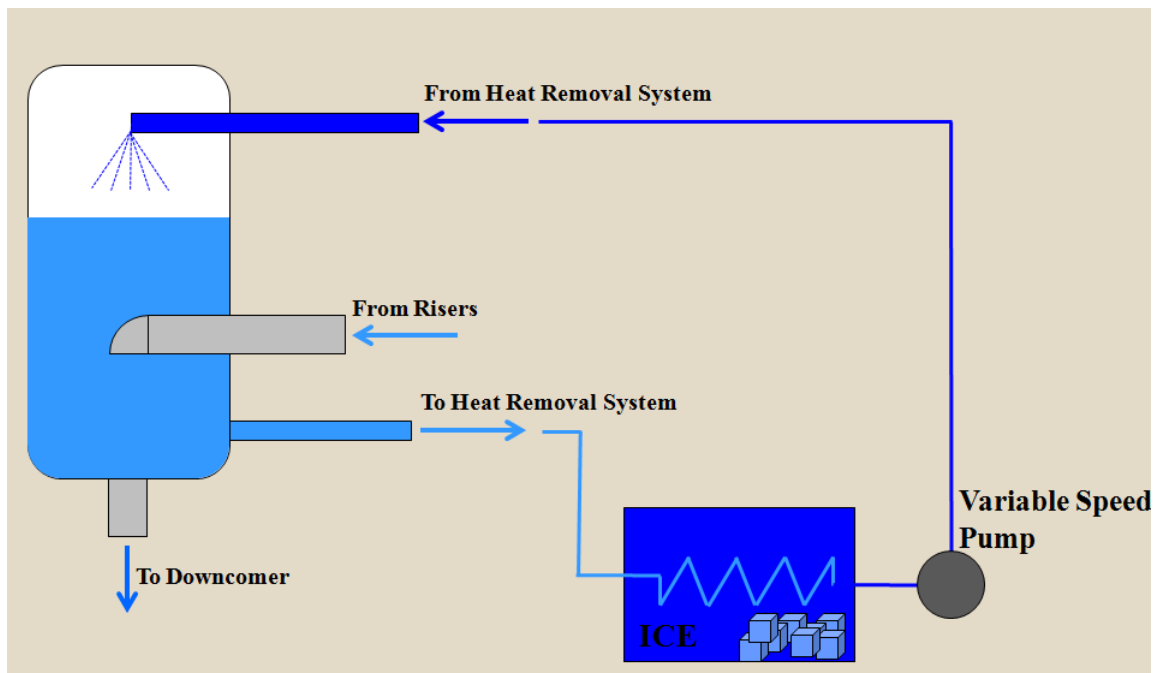


**Figure 94. Schematic Configuration of the Proposed Heat Removal System.**

The following components will be included in the system:

- An ice container (insulated), where the ice is stored.
- A copper coil submerged into the ice bath
- A primary coolant variable speed pump
- Pipelines from and to the water tank

Hot water from the water tank located on the upper working deck is drained through the lower port and flows through the inner side of the copper coil. Heat is removed through the coil and released to the melting ice. Colder water at the exit of the coil is pumped back and sprayed into the water tank through the upper port, to allow more uniform mixing in the tank. The speed of the pump can be manually varied to adjust the coolant flow rate to the desired value in order to reach the steady-state conditions at the desired primary coolant temperature. A rotameter is installed to read the volumetric flow rate supplied by the pump. The final installation of the heat removal system is shown in Figure 95.

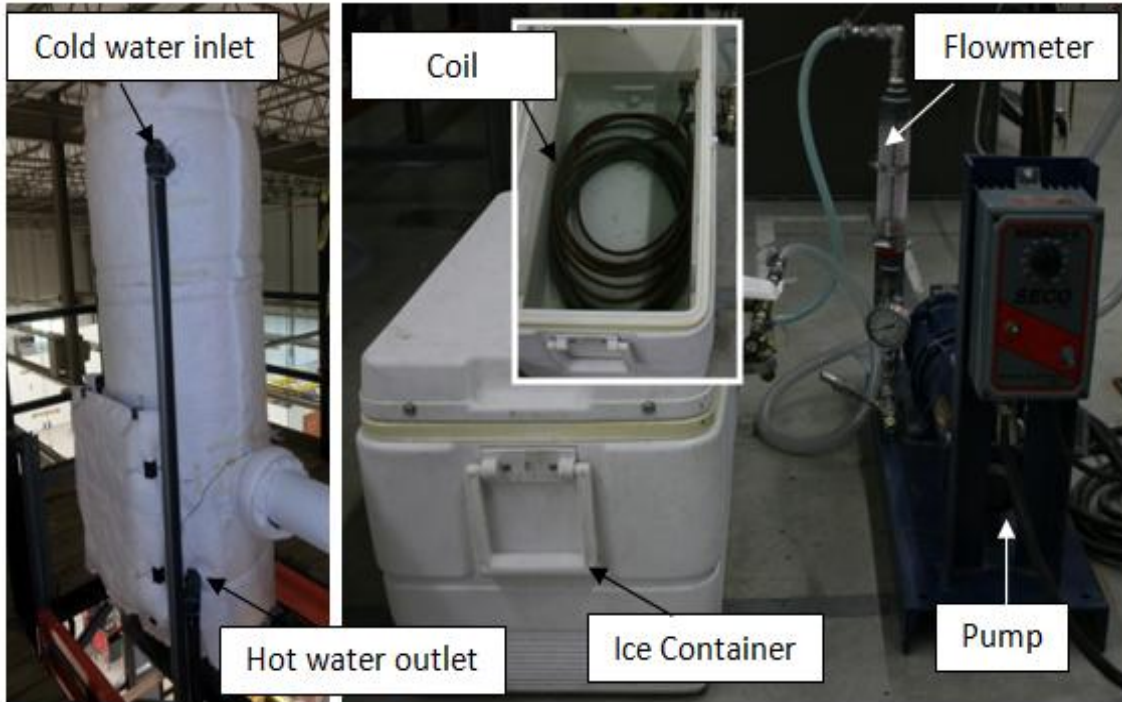


**Figure 95. Heat Removal System - Final Installation.**

The proposed heat removal system was selected also for its relatively easy installment and low cost. Special care will be required during the steady-state phase since the operation of the system is fully manual (temperature reading, pump speed/flow adjustment, ice storage in the container and water drainage from the container).

### **X.2 Step 1: Leak Tests (Room Temperature)**

Different leak tests at room temperature were required in order to verify the connection between the different sections of the facility. These tests were conducted by slowly filling the facility from the inlet port located at the bottom of the facility, as described in the previous step. All the joints, connections, valves, flanges and thermocouple ports were verified and monitored to confirm their stable water seal at room temperature. When a leak occurred, the facility was drained down to a level immediate below the leak location and the leak was fixed with technique that varied depending on the location of the leak and the type of joint under verification. This phase was assumed to be successful only when no leak was detected in any joint or connection for 24 hours with the facility filled up to a liquid level slightly above the normal liquid level expected during normal operations.

During this phase, the drainage and filing system and its operation was repeatedly tested and verified.

### **X.3 Step 2: Leak Tests (Final Steady-State Temperature)**

The phase was conducted using the same approach described in STEP 1. With the facility full, the heater were started (using default setting of power ramp) and the temperature of the coolant was slowly increased up to approximately 40 °C and then

maintained for approximately 3 hours to verify the integrity of connections and water seals.

During this phase, a preliminary verification of the following units was also performed:

- Power control unit and heaters: The control unit was confirmed to work properly, applying the desired power ramp (default) to the heaters. The power ramp was verified using a digital wattmeter connected to the heaters power lines. The thermocouple reading on the controller displays was also confirmed by comparing with an external thermocouple reader.
- Data acquisition unit: Thermocouple reading was recorder during the tests for all the thermocouples installed (wires and probes). Out of range and other improper readings were identified and corrected. The flow meter reading was monitored from the unit converter display and settings (out-of-scale value) were fine-tuned.

#### **X.4 Step 3: Empty Test (Heat Flux Verification)**

To verify the uniformity of the heat flux supplied by the heaters, an empty test was performed. The test was conducted by recording the temperatures of the thermocouple probes located inside the risers when the facility was empty. The temperature profiles were recorder and used to infer on the heaters heat flux uniformity on the horizontal direction.

The temperature profile at the upper row (row 5, risers exit), plotted in Figure 96, showed a non-uniform (non-symmetric) temperature distribution, skewed toward pipe 9 (cavity inlet).

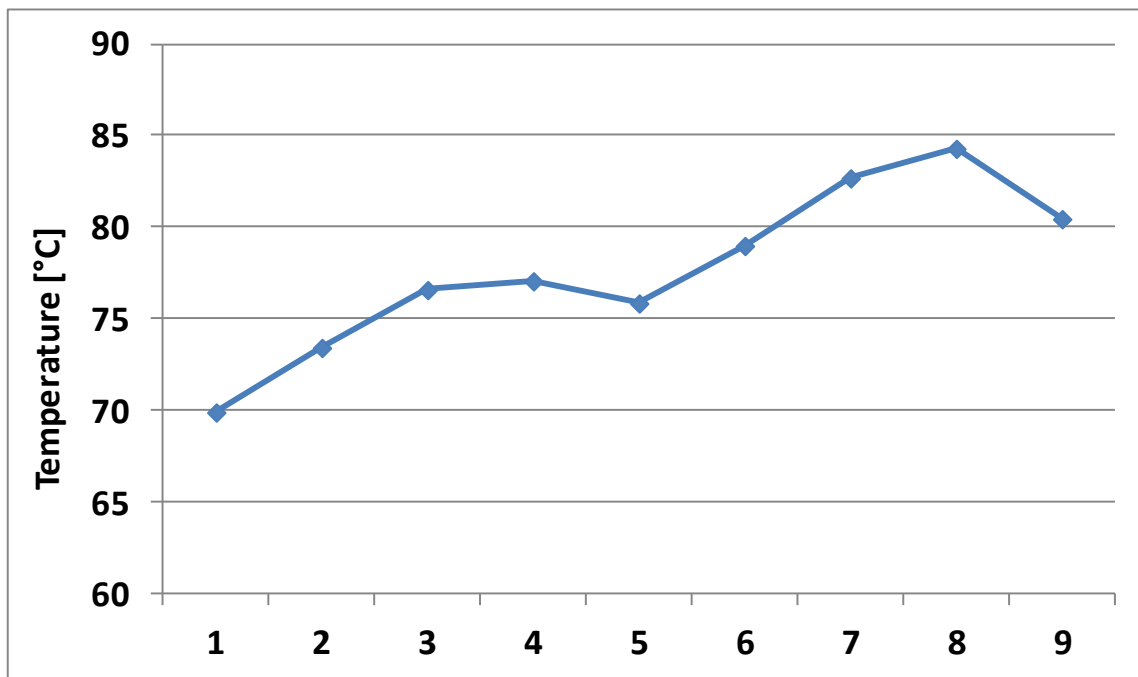


**Figure 96. Dry test - Temperature profile (Row 5).**

There are different considerations that should be done before assessing the heaters flux uniformity. This includes:

- Potential air natural circulation inside the pipes which may induce an asymmetric flow and, subsequently, an asymmetrical temperature distribution.
- The uncertainty on the thermocouple probes tip location which may differ from the desired location at the center of the risers (the temperature gradient in air is expected to be higher than the one in water so that small differences in the probe location may have a higher impact in the temperature reading.

Further investigation may be required for the two considerations listed above. No additional tests or verification were performed on this matter.

#### **X.5 Step 4: Thermal Insulation Installation**

To reduce the heat losses from the experimental facility, thermal insulation was properly selected and installed. Different insulation materials were selected based on:

- The maximum operating temperature of the component to be insulated
- The thermal conductivity
- The type of insulation suitable (rigid or flexible)
- The cost

Different types of thermal insulation were installed depending on the section of the facility to be insulated. All the insulation materials were installed after the leak tests to avoid damaging during the preliminary tests and facilitate the access to the joints and pipe connections for verification and leak correction.

### *X.5.1 Insulation of the Reactor Cavity*

The insulation of the reactor cavity was the most challenging due to:

- The high temperature expected inside the cavity, especially for heaters and vessel.
- The complex shape of the cavity with several penetrations.

The cavity was insulated with two different insulation materials. Microtherm® boards were used to produce a first layer of insulation for the main walls of the cavity, including ceiling, the back cavity, the heaters side and the cavity sides. This material is characterized by the following features:

- Low density (220 - 250 kg/m<sup>3</sup>)
- Low Thermal Conductivity (0.0233 W/m K at 400 °C mean)
- Stable thermal performance for continuous exposure up to 1000°C
- Excellent machineability.
- Different panel sizes and thickness.

The panels were cut and modified to fit on the cavity walls and fixed to secondary removable support structures. Figure 97 shows the installation of the Microtherm panels in the reactor cavity (side and back walls).



**Figure 97. Microtherm Panels in the Reactor Cavity.**

The heaters side of the cavity was also insulated using the same insulation panels. In this case, the panels were machined and customized to fit on the walls and allow the heaters electric penetrations, as shown in Figure 98 and Figure 99.



**Figure 98. Cavity Insulation - Heaters Side Panels Preparation.**



**Figure 99. Cavity Insulation - Heaters Side Complete Microtherm Panels Installation.**

The panel used to insulate the cavity ceiling was also modified and customized to fit in the risers array.

A second layer of insulation was installed to seal the gaps between the panels and to provide an additional insulation layer.

Two different type of silica were used to complete the thermal insulation of the cavity. Both types were available in mats of variable width that could be easily cut and customized on the different sides of the cavity.

Paper clamps were used to fix the second layers on the cavity structures.

A more flexible silica mat was used to fill small gaps or small areas. A relatively rigid mat was installed on larger surface areas and to wrap the entire cavity.

Figure 100, Figure 101, and Figure 102 show the different insulations applied to the cavity walls.



**Figure 100. Silica Mats Installation in the Reactor Cavity.**



**Figure 101. Cavity Final Insulation Installment (Side View).**



**Figure 102. Cavity Final Insulation Installment (Top View).**

### *X.5.2 Insulation of the Pipeline*

The insulation of the main pipeline was constructed from pre-fabricated rigid polyurethane pipe insulation (McMaster-Carr® 5431K27). This type of insulation was found to be very easy to install (thanks to their low density and the additional adhesive

jacketing. 90° elbows shapes were also installed on selected elbows of the pipeline.

Figure 103 and Figure 104 show the insulation used for the pipeline and example of installation in selected regions of the experimental facility.

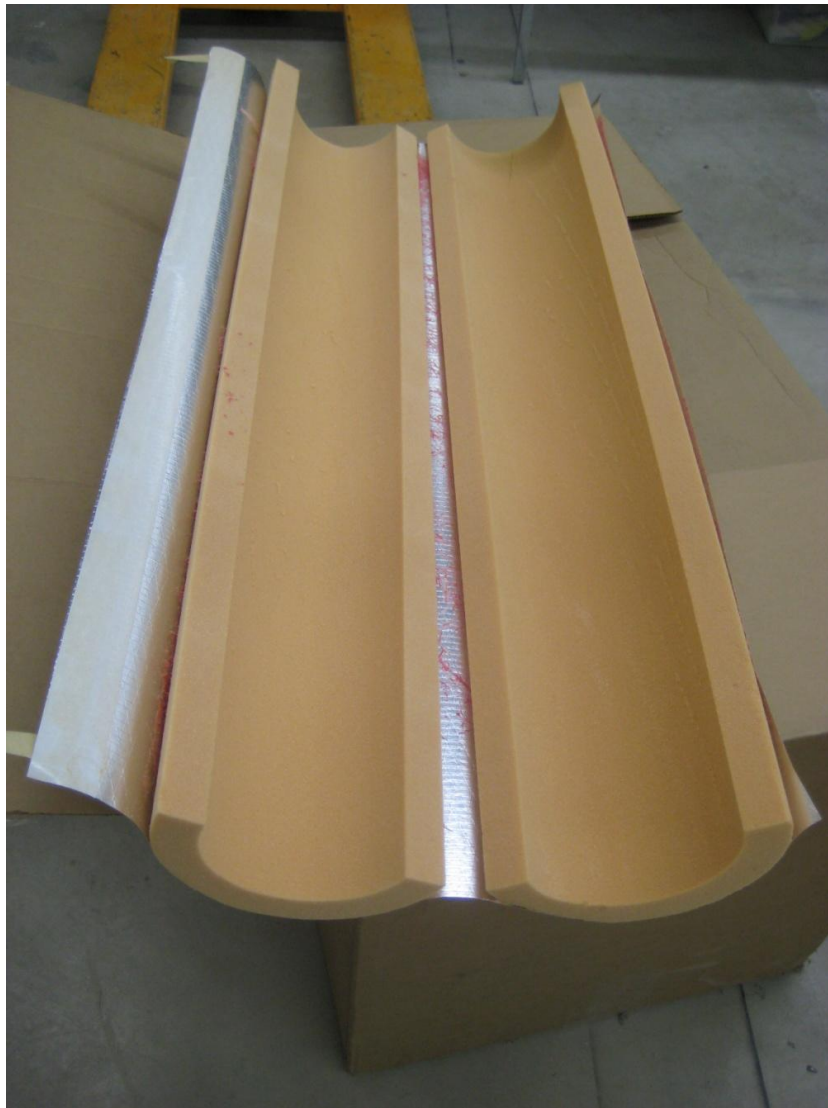


**Figure 103. Polyurethane Pipe Insulation.**

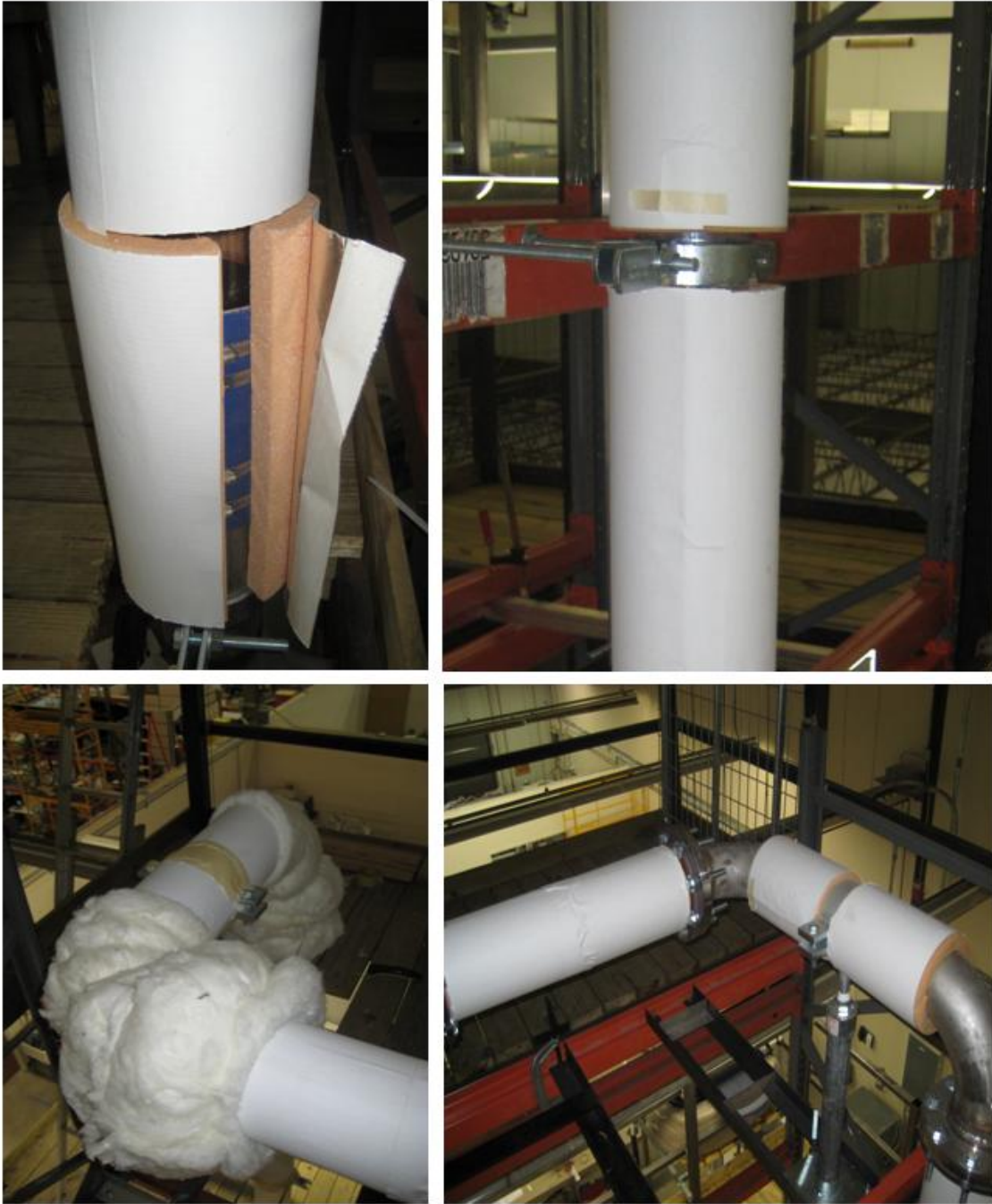


**Figure 104. Polyurethane Pipe Insulation Installation.**

The pipeline of the secondary heat removal system was insulated using flexible foam rubber pipe insulation (McMaster-Carr® 4463K131), which has simulate features of the polyurethane pipe insulation previously described (Figure 105).

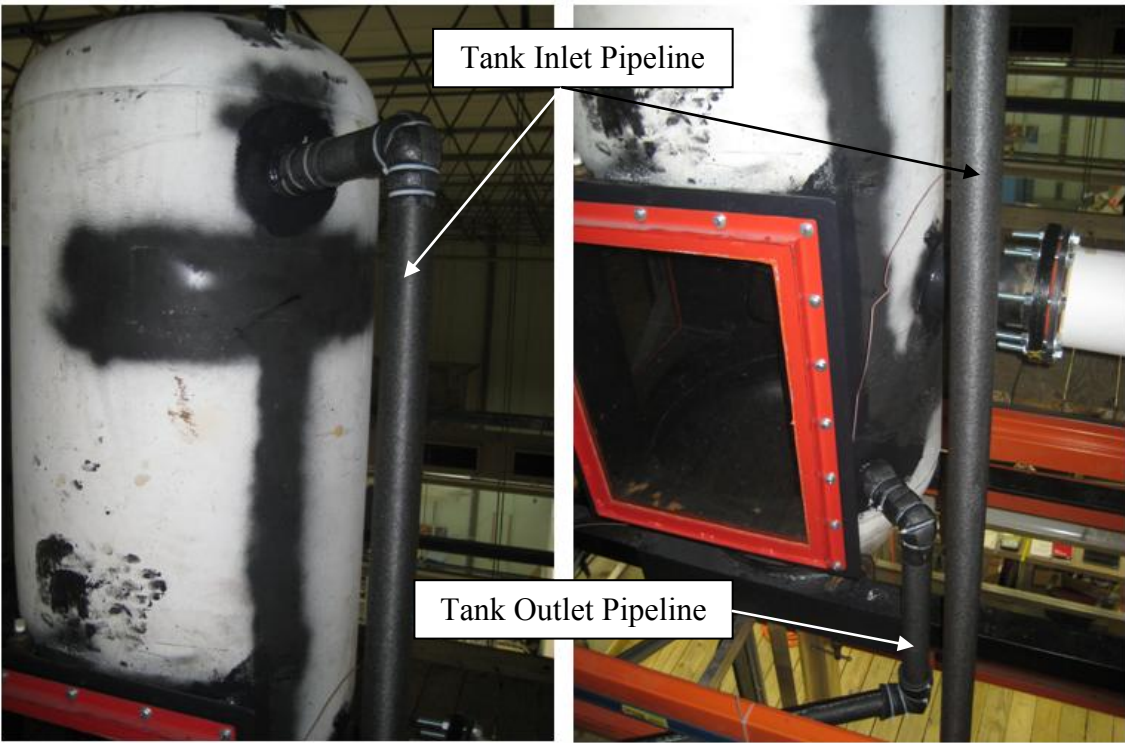


**Figure 105. Insulation of the Secondary Heat Removal Pipeline.**

### *X.5.3 Insulation of the Water Tank*

The water tank was insulated with the semi-rigid silica mat used to define the final insulation of the reactor cavity. The mat was wrapped around the tank and fixed with hose clips. The tank windows were insulated using the same material attached to the windows with paper clips for a fast and easy removal during operation (Figure 106).

Selected sections of the thermal insulation were designed and conceived to be easily removed during the operation of the experimental facility. In particular:

- The insulation of the windows was installed using paper clamps to facilitate the access of the window for internal inspection during the facility operations.
- Insulation of the inlet nozzle is accessible to allow air venting during the facility refill through the thermocouple probe port.



**Figure 106. Water Tank Insulation.**

## **X.6 Step 5: Final Tests and Test Repeatability**

After all the preliminary verifications were completed, a set of final shakedown tests were performed in order to:

- Confirm the functionality of all the components and instrumentation installed under normal operating conditions
- Confirm by observation and measurements the natural circulation of water in the facility.
- Evaluate additional required modifications to the facility before starting the experimental activity.
- Verify the repeatability of the tests, under selected initial conditions.

Four tests were performed under the same conditions. The tests were categorized as follow:

**Run 0:** Power rump to full power. Temperatures and flow rates were monitored but not recorded. Visual inspection and leak verification was performed during the test. The system response was observed. The test was stopped when full power achieved.

**Run 1:** Power rump to full power. All the instrumentations were connected to the computer and experimental data were automatically recorded during the test. Additional monitor and manual record of temperatures and flow rates. Visual inspection and leak verification was performed during the test. The test was stopped when an approximate constant flow rate was achieved.

**Run 2:** Same activity on Run 1. Prove test repeatability.

**Run 3:** Final run. Same procedure adopted for Run 1 and 2. The measurement of the flow rate was also verified with the ultrasonic flow meter. Flow visualization with dye injection was performed to confirm the natural circulation.

The procedure adopted for the tests is described on Table 16.

**Table 16. Shakedown Tests Procedure.**

<b>STEP</b>	<b>Description</b>
<b>1</b>	Turn refill pump on - suction valve open, injection valve closed, recirculation valve open.
<b>2</b>	Gradually open the injection valve and close the recirculation valve to mid position
<b>3</b>	Observe the liquid level to increase from manifolds and pipelines
<b>4</b>	Fully close the recirculation valve to provide full flow into the facility
<b>5</b>	Verify that entrapped air bubbles in the bottom section are entrained by the water flow
<b>6</b>	Monitor the water level in the tank.
<b>7</b>	Open the air relief valve located at the top section (tank inlet) to vent the air from the tank jet
<b>8</b>	Close the air relief valve when liquid starts to discharge
<b>9</b>	Gradually close the injection valve and open the recirculation valve when liquid level in the tank reaches the top edge of the window
<b>10</b>	Turn refill pump off
<b>11</b>	Wait until flow meter indicator reads 0 l/min (approximately 10 min)
<b>12</b>	Start data recording on the Data Acquisition System
<b>13</b>	Turn the main switch of the heaters controller to on (controllers were already set to the desired power ramp)
<b>14</b>	Observe heaters temperature to rise until full power
<b>15</b>	Observe coolant temperature to rise
<b>16</b>	Observe flow rate to increase
<b>17</b>	Turn the main switch of the heaters controller to off when flow rate stabilizes

The volumetric flow rate of the water measured with the magnetic flow meter plotted in Figure 107 for the runs 1 and 2. The measure uncertainty of the flow meter is also shown.

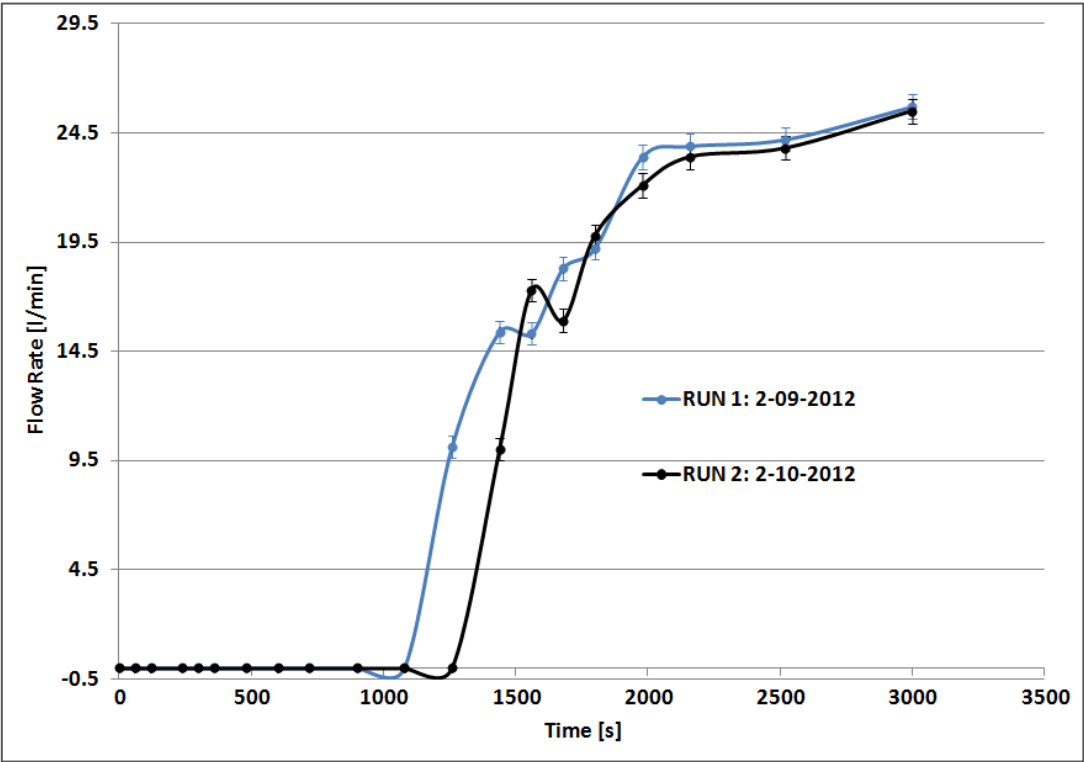


Figure 107. Coolant Volumetric Flow Rate (Run 1 and Run 2).

Two main characteristics can be observed in Figure 107:

- The volumetric flow rate steadily increases until it reaches a first plateau at approximately 24.5 l/min.
- The results of the two tests performed in two different days were in acceptable agreement (test repeatability was considered satisfactory) [39].

As mentioned above, a final shakedown run (Run 3) was performed to verify the in-line magnetic flow rate measurement with the clamp-on ultrasonic flow meter installed on the downcomer and to explain some interesting characteristics observed during Run 1 and Run 2.

The volumetric flow rate measured with the two instruments is depicted in Figure 108 (left axis) together with the heaters power ramp (right axis).

The ultrasonic flow meter showed a better response at low flow rates. A good agreement on the measurements was achieved at higher flow rates.

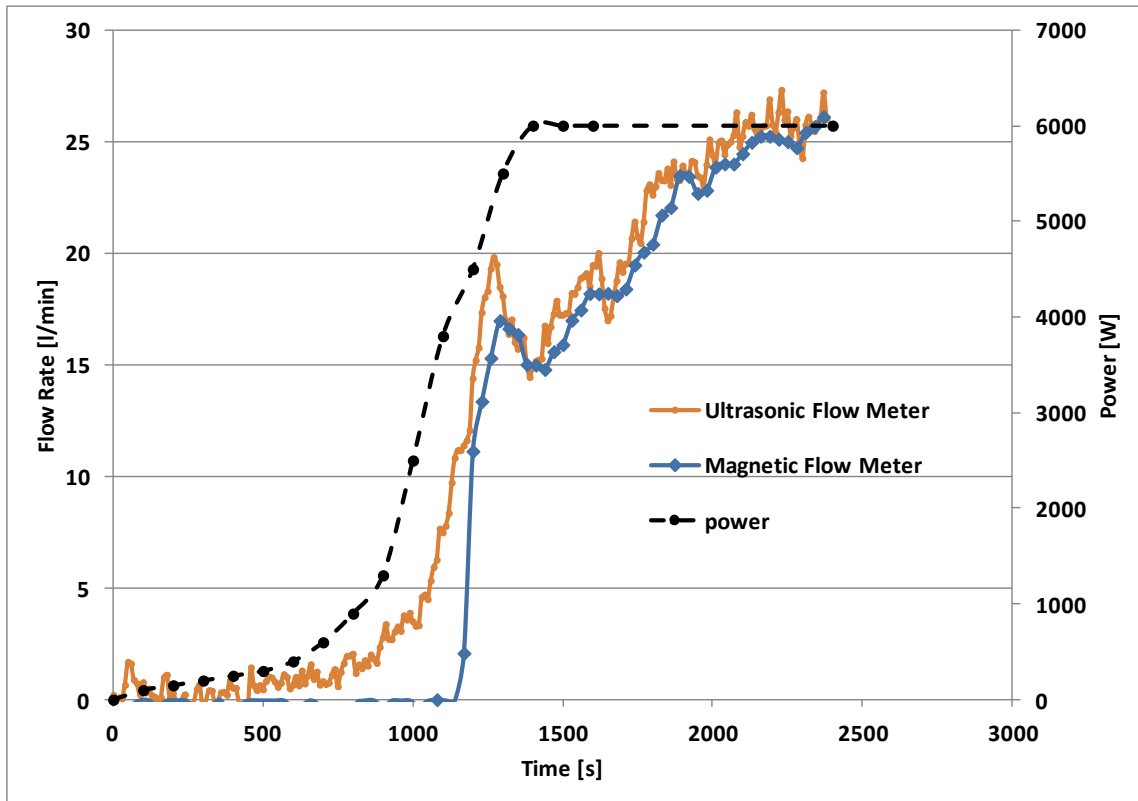


**Figure 108. Coolant Volumetric Flow Rate and Heaters Power (Run 3).**

Three main regions can be identified:

**0 s < t < ~1000 s:** The electric power ramp is applied at the beginning of the test. While the power steadily increases, the coolant starts moving approximately 500 seconds later. During this phase, the magnetic flow meter (due to its sensitivity at low flow rates and to other settings that must be verified) read zero flow. The ultrasonic flow meter showed an increase in the flow rate at approximately 500 seconds.

**~1000 s < t < ~1500 s:** During this transition phase, the coolant flow was observed to increase rapidly, reaching a peak and then decreasing. This behavior was observed in other tests at the beginning of the transient.

**t < ~1500 s:** While the power approached its maximum (6 kW), the slope of the flow rate curve was observed to gradually reduce until a quasi steady-state was achieved. The measurements of the flow rate from the two flow meters were found to be in good agreement in this phase.

During this final run, preliminary flow visualization was conducted to confirm the natural circulation in the facility and to observe the flow splitting through the bottom manifold. The visualization was performed by injecting a fluorescent dye (Rhodamine) into the flow [40] through the thermocouple port located at the cavity inlet, as shown in Figure 109.



**Figure 109. Rhodamine Injection Technique.**

A camera was installed in front of the bottom manifold to record the flow stream at the time the die was injected. Figure 110 shows three snapshots taken from the recorded movie [39].



**Figure 110. Flow Visualization at the Bottom Manifold.**

The temperatures of coolant and panel walls were also recorded during this run. For convenience, the temperature of the coolant at the cavity inlet and outlet are presented in Figure 111. The same features observed in the coolant flow rate can be highlighted in the temperature behavior.

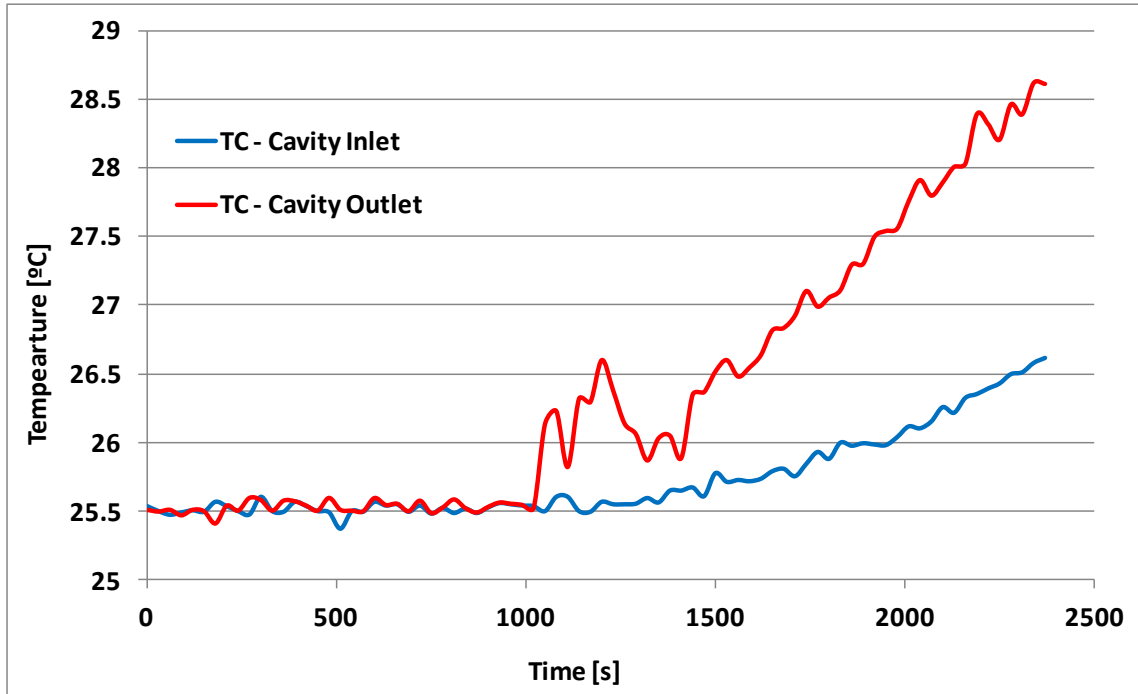


**Figure 111. Coolant Cavity Inlet and Outlet Temperatures (Run 3).**

When performing the shakedown tests, the cavity outer walls temperature was monitored in order to have a qualitative estimation of the heat losses through the cavity. The heat losses were also quantitatively estimated by calculating the net heat transfer to the cooling water in the risers. An approximate evaluation of the power released to the water was performed using the following equation:

$$P_{water} = \dot{m} C_p \Delta T_{cavity} \quad (15)$$

In equation (1),  $\dot{m}$  is the coolant mass flow rate,  $C_p$  is the specific heat of the water, and  $\Delta T_{cavity}$  is the temperature rise of the water through the reactor cavity ( $T_{out} -$

$T_{in}$ ). Using the measured values of flow rate and temperature at the end of the experiment, the power released to the water was estimated to be:

$$P_{water} = \frac{25.5(l / \text{min})}{60(s / \text{min})} \cdot 1(kg / l) \cdot 4.179(kJ / kg \cdot K) \cdot 2(K) = 3.552 kW \quad (16)$$

The total heat losses through the cavity walls can be estimated by the difference between the total power supplied by the heaters and the power released to the water (Equation 2):

$$P_{loss} = P_{heaters} - P_{water} = 6 - 3.552 = 2.448 kW \quad (17)$$

This values accounts for the losses through the glass manifolds and pipeline between the thermocouple probes locations, which were not insulated during the shakedown tests.

The runs performed during the facility shakedown were able to evidence also some issues in the connection technique adopted in the cavity, between the risers and the manifolds branches. Due to the radial thermal expansion of the stainless steel risers, the hose clamps used to hold the high-temperature hoses in place and guarantee the water seal were plastically deformed during the thermal cycles. This deformation loosened the seal and produced small leaks at the beginning of new tests. This issue was fixed by replacing the original hose clamps described in Chapter VIII, with constant-tension clamps (McMaster-Carr® 5281K19). These special clamps have Belleville springs that automatically increase and decrease the clamps' diameter to eliminate the need for retightening and prevent water leakage due to thermal cycling. Figure 112 shows the

original and new hose clamp connections installed at the top manifold. The final configuration of the clamps is shown in Figure 113.

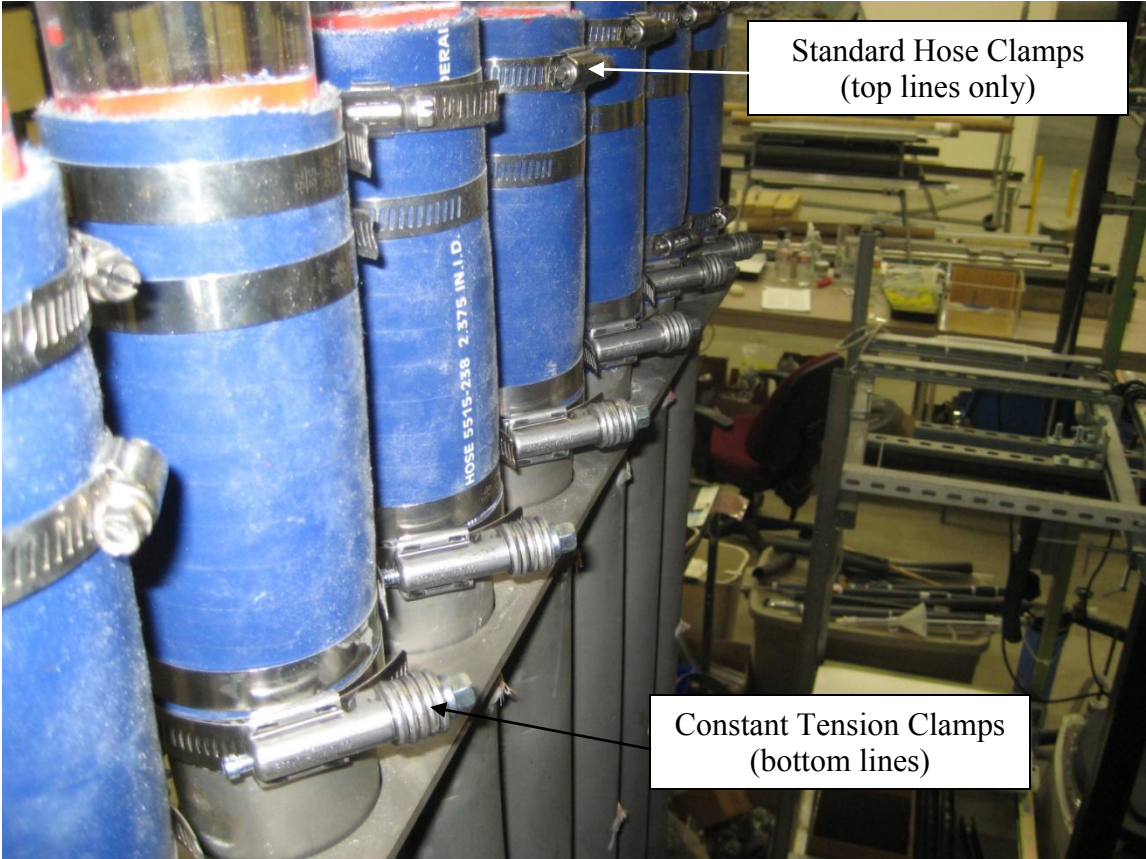


**Figure 112. New Hose Clamp Connections (Top Manifold).**

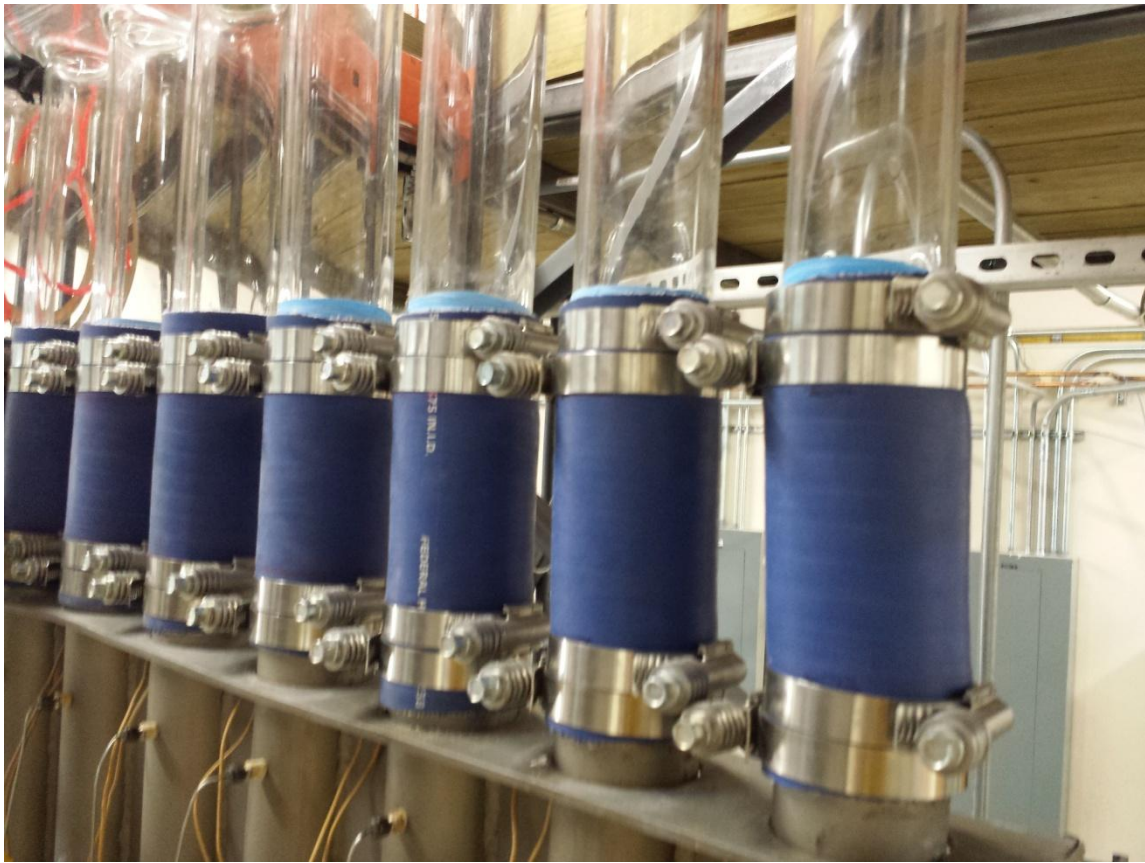


**Figure 113. Constant Pressure Hose Clamps - Final Configuration.**

To reduce thermal stresses, modifications in the draining procedures were implemented. The water in the facility was left circulating after the heaters power off until the flow meter reading showed zero flow. The facility was then slowly drained until the liquid level dropped right above the cavity and left in this location until the experimental team left the laboratory. At this time the total drainage of the water was completed.

## **X.7 Step 6: RELAP5-3D Model Refinement and Comparison with Shakedown Tests**

Due to the heat losses observed during the facility shakedown, refinements of the RELAP5-3D input file were required in order to model the losses through the cavity walls. The original model described in Chapter VII, already accounted for the heat losses through the pipeline, water tank, and part of the reactor cavity. These heat structures were slightly modified to account for the final configuration of the thermal insulation in these regions. Two important limitations were identified in the original model that needed to be fixed:

- The heat losses from the back of the heaters.
- The cavity thermal inertia, in particular for heaters and vessel

These issues were fixed by changing nodalization of the heat structure simulating the reactor vessel and heaters. Figure 114 shows the comparison between the original nodalization adopted for the cavity heat structure (left) and the new approach proposed (right).

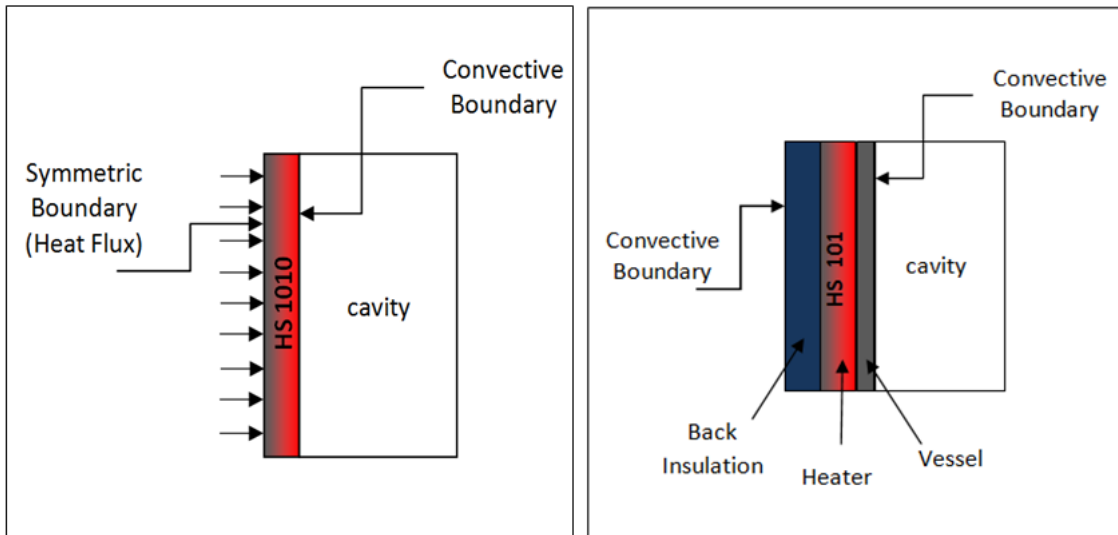


**Figure 114. Cavity Heat Structure Nodalization - Original (left), New (right).**

In the original nodalization, the reactor vessel and heaters were simulated with a heat structure having the thickness and the thermal properties (conductivity and heat capacity) of the vessel shell (stainless steel 304). The heaters were not modeled as part of the heat structure. A symmetric boundary was imposed in the left side of the heat structure where a positive heat flux was imposed (heat supplied to the heat structure). A convective boundary was imposed at the right surface of the heat structure to account for the convective heat transfer with the air in the reactor cavity. This face of the heat structure was also included in the radiation enclosure to model the radiation heat transfer with the other heat structures of the cavity (panel and walls).

The heat structure radial nodalization was improved in the new model to account for:

- Different materials in this region of the cavity (thermal insulation, heaters, reactor vessel shell)
- Heat losses at the left boundary (heaters back wall)

Three mesh intervals were defined and thicknesses and materials of vessel, heaters, and thermal insulation were specified in the input file to account for the real thermal properties of the different layers. In particular, stainless steel 304 was used for the reactor vessel, the heaters were assumed to have similar thermal properties of stainless steel. Thermal properties of the thermal insulation were retrieved from the manufacturer datasheets. A volumetric power source (total power = 6 kW) was defined in the heaters mesh interval and a power table was defined to realistically follow the power ramp used during the experiment. A convective boundary was imposed on both sides of the heat structure, the left side simulating the heat losses by convection to the environment at the heaters back walls.

The RELAP5-3D simulation results obtained with the original model and with the new (modified) model are plotted in Figure 115, together with the experimental shakedown data for the Run 3.

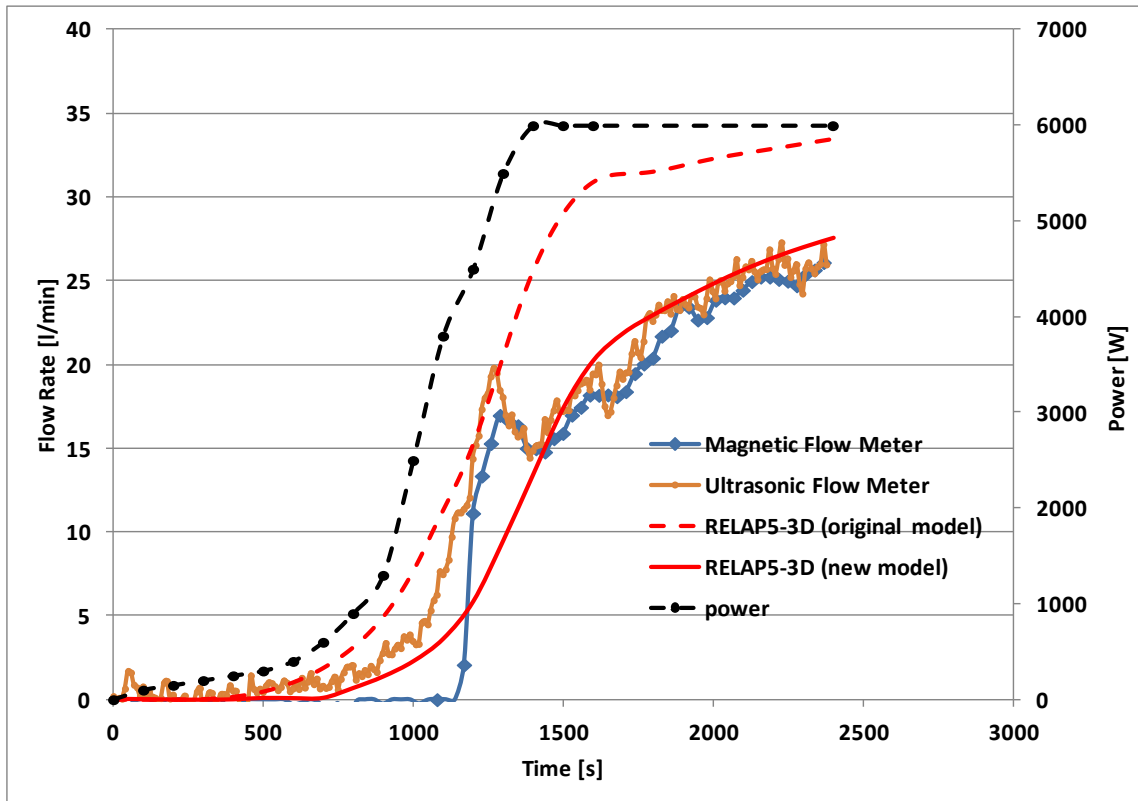


**Figure 115. Shakedown Experimental Data and RELAP-3D Simulation Results.**

As it can be noticed, the original model under-predicted the heat losses in the cavity and, subsequently, the total coolant flow rate. In both cases, the prediction of the transient phase (up to approximately 1000 seconds) was acceptable but not satisfactory. The old model over estimated the flow rate. The same parameter was under estimated by the new model. This may be related to the cavity structures thermal inertia not correctly simulated. The overall prediction of the new model was confirmed to be very satisfactory.

The comparison of the water inlet and outlet temperature experimental data with the RELAP5-3D prediction (new model only) is shown in Figure 116.

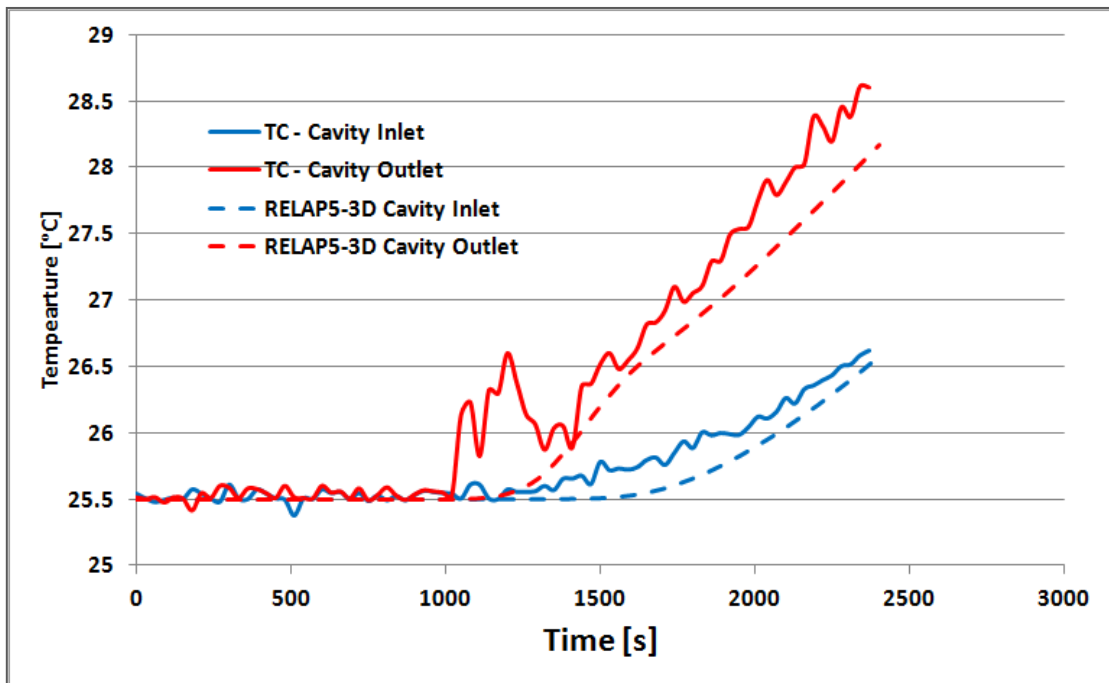


**Figure 116. Water Inlet and Outlet Cavity Temperatures and RELAP5-3D New Model Prediction.**

The prediction of the RELAP5-3D of the coolant temperatures in the regions selected were found to be in good agreement with the experimental data, confirming the validity of the modifications implemented in the RELAP5-3D model.

## CHAPTER XI

### PHASE 8: ANALYSIS OF THE EXPERIMENTAL DATA AND COMPARISON WITH SIMULATIONS

The Reactor Cavity Cooling System experimental facility was designed to study the thermal-hydraulic behavior of the water under normal operation and accident scenarios. Due to the efforts and time dedicated to the scaling, design, construction, and final verification of the facility, the test set defined for this project was limited to the steady-state phase.

The set of tests was intended to:

1. Prove the heat removal capability of the natural circulation of water under selected conditions for the geometry and configuration defined for the experiment
2. Verify that a steady-state condition can be achieved and maintained (considering the limitations of the technique adopted for to remove the heat from the system)
3. Prove the capabilities of the selected system code (RELA5-3D) to analyze this type of phenomena, identify possible techniques that should be adopted when conducting the simulations.
4. Try possible visualization techniques to study the flow in selected regions of the facility

5. Identify possible limitations of the engineered features of the experimental facility that may need to be modified in preparation of the two-phase flow (accident) analysis

The test will be performed under selected conditions summarized in Table 17.

**Table 17. Test Conditions.**

<b>Parameter</b>	<b>Value</b>
Water Temperature (test start)	room (~23 °C)
Target Water Temperature (steady-state)	~30 °C
Heaters Power (nominal)	6 kW
Steady-State Desirable Time	> 10 min

### **XI.1 Experimental Procedure**

The procedure adopted to run the final steady-state experiment was similar to the one followed during the shakedown tests, described in Chapter X.

The facility was filled with tap water at room temperature using the water pump, until the liquid level reached the top of the tank windows. Air bubbles entrapped at the bottom section of the pipeline and near the water jet were entrained and vented with the

standard procedure mentioned above. The data acquisition system was turned on approximately 30 minutes before the test started. The instrumentation (thermocouples and magnetic flow meter) was up and running at the beginning of the refill phase even if no data was recorded until the test start.

The steady state was achieved by enabling the secondary heat removal system. The quantity of ice required for the experiment was pre-determined by assuming that the total power of the heaters (6 kW) had to be removed by the melting ice (heat losses were conservatively ignored), and the steady-state maintained for approximately 10 minutes.

$$M_{ice} = \frac{P_{heaters} \cdot \Delta t}{h_{fusion,water}} = \frac{6(kW) \cdot 900(s)}{334(kJ / kg)} = \sim 17kg \quad (18)$$

To account for the losses through the ice container and the amount of ice melted during transportation and storage, the quantity of ice purchased was sensibly higher than the one estimated by Equation 18.

To minimize the main coolant flow perturbation due to the cold water injection from the secondary heat removal system at the time the target temperature was reached (approximately 30 °C), the secondary pump was turned on since the beginning of the experiment, and maintained at its nominal value of approximately 5.5 l/min (corresponding to 1.5 US gal/min read from the rotameter installed in the secondary system) but no ice was injected into the ice container. These conditions were maintained until the magnetic flow meter reading was zero in order to start the experiment with a quiescent coolant in the loop.

The initial conditions described above are summarized in Table 18.

**Table 18. Experiment Initial Conditions.**

<b>Parameter</b>	<b>Value</b>	<b>Unit</b>
Coolant Temperature	24	°C
Main Coolant Flow Rate	0	l/min
Secondary Coolant Flow Rate	5.5	l/min
Water Tank Water Level	35%	-

### **XI.2 Test Results – Main Parameters**

The test was initiated by turning on the electric heaters from the main control panel while the data acquisition system started recording the temperatures and main coolant flow rate. The main parameters that were observed during the ramp up phase were the ones monitored during the shakedown tests:

- *Primary coolant flow rate.* This parameter was easily monitored through the external converter unit located on the side of the recording station. The observation of the flow rate helped to identify the time from the test start when the coolant appreciably started flowing in the loop. The parameter was monitored also during the secondary heat removal activation phase, to observe any perturbation of the flow due to the cold water injection, and

during the later phase of the experiment, to verify that the steady-state condition was achieved

- *Heaters temperature.* The temperature of the heaters could not be recorded during the experiments since the thermocouples installed in the heaters were not connected to the data acquisition system. The temperature of the heaters was also used as an indicator for the heaters power, to confirm when the power reached the nominal value.
- *Tank outlet Temperature:* The temperature was monitored to determine the time at which the heat removal system was completely activated, by introducing ice into the ice container, previously filled with tap water to fully cover the copper coil.

When the temperature of the coolant at the cavity inlet approached the target value for the steady-state, the secondary heat removal system was fully activated. Tap water at room temperature was first introduced in the ice container tank to fully submerge the copper coil. Ice was then introduced in the ice container in batches of approximately 5 pounds (corresponding to 2.3 kg). This methodology helped to optimize and stabilize the heat removal rate from the secondary system. The observation of the secondary coolant outlet temperature showed unstable temperature of the coolant due to the ice injection batches (Figure 117).

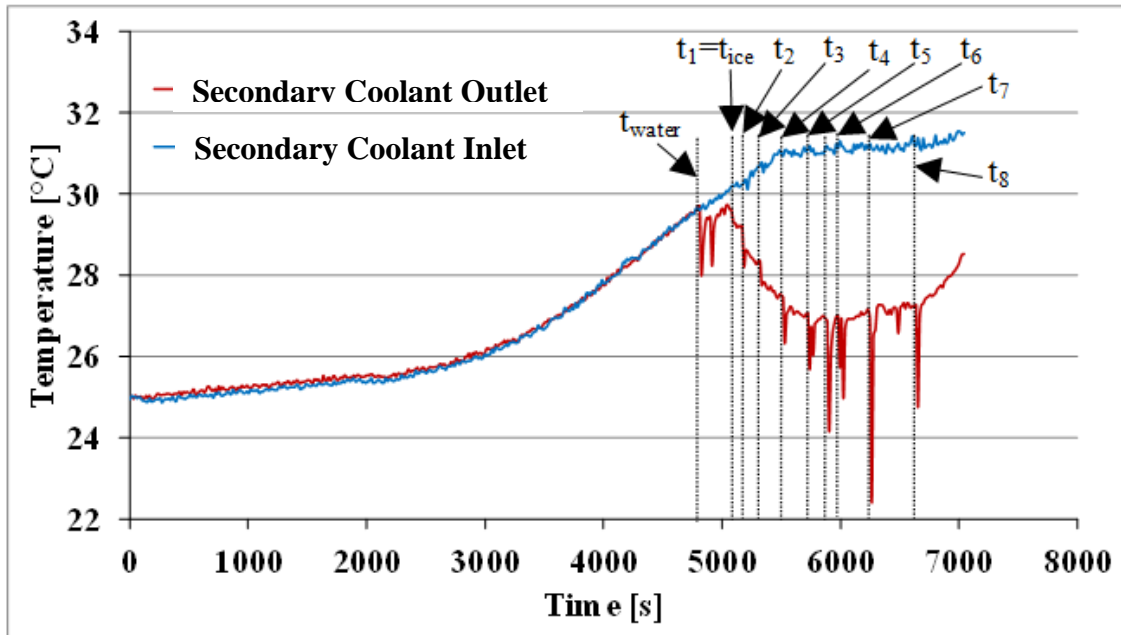


**Figure 117. Secondary Coolant Temperatures.**

In the same figure the ice batch times are also shown:

- $t_{\text{water}}$ , is the time when water was introduced into the ice container.
- $t_{\text{ice}}$  is the time when the temperature of the coolant in the tank approached 30 °C and the first batch of ice was introduced in the ice container ( $t_{\text{ice}} = t_1$ ).
- $t_2$  to  $t_9$  indicate the successive batches of ice.

The temperature of the secondary coolant injected into the water tank suddenly decreased at the time each batch of ice was introduced in the tank. This was essentially related to:

- The increase in the ice mass in the container (larger heat sink capacity)
- The enhancement of the turbulence in the water inside the ice container and subsequent increase of the convection heat transfer coefficient at the coil outer wall.

Since the secondary system was not equipped with an automatic control system to regulate the heat removal rate, the tank outlet temperature was constantly monitored to confirm that the steady state conditions were maintained. Additional ice was introduced in the ice container when the tank outlet temperature started increasing from the nominal value of 30 °C. The secondary outlet coolant temperature (corresponding to the tank injection location) was constantly monitored for the same scope. The pump speed was fine-tuned throughout the steady-state phase to compensate small differences in the temperatures (increased when the tank temperature tended to increase, or decreased in case of opposite trend). This technique helped stabilizing the temperature of the primary coolant in the water tank. The temperature of the primary coolant in the tank was observed to increase even after the first batch of ice, reaching a stable condition at approximately 31 °C. This temperature was assumed to be acceptable for the scope of the test [41].

The temperature of the primary coolant at the inlet and outlet of the cavity is plotted in Figure 118.

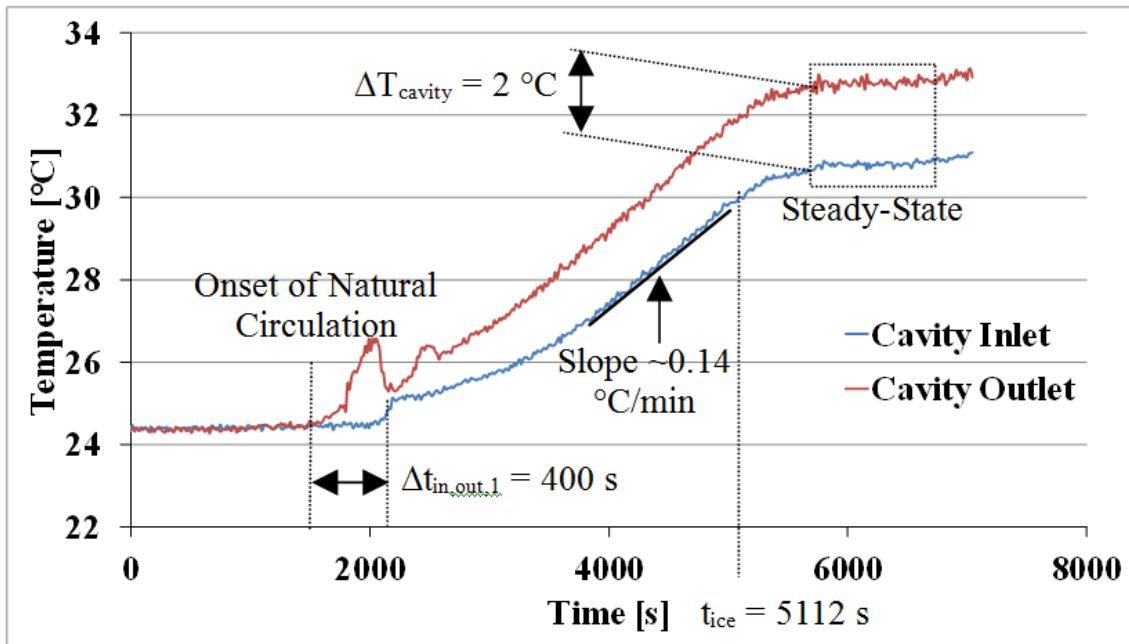


**Figure 118. Coolant Cavity Temperatures.**

In Figure 118 some of the most important timings of the experiment are also shown:

- No appreciable increase in the coolant temperature was observed until the onset of natural circulation which occurred at about 1700 s from the power on. At this time, a sudden increase in the coolant temperature was recorded which can be correlated to a similar behavior of the coolant flow rate (onset of natural circulation). A similar behavior was observed during the facility shakedown tests.

- The increase in the cavity inlet coolant temperature was observed with a delay of approximately  $\Delta t_{in,out,1} = 400$  s. This delay could be related to the time required to the coolant to flow through the entire loop at the established flow rate.
- After the natural circulation was established, the inlet and outlet cavity coolant temperatures increased steadily ( $\sim 0.14$  °C/min), while the temperature rise through the cavity stabilized at  $\Delta T_{cavity} = 2$  °C.
- When the coolant cavity inlet reached 30 °C ( $t_{ice} = 5112$  s), the heat removal from the water tank was fully activated by introducing ice into the ice container. This effect showed in the coolant inlet temperature as a decrease in the slope. The same behavior in the coolant outlet temperature was observed with a delay of  $\Delta t_{in,out,2} = 230$  s. The lower delay in the coolant outlet response is now due to the higher coolant flow rate.
- The steady-state was achieved when both inlet and outlet temperatures were stabilized. The final cavity inlet temperature achieved in this experiment was 31 °C. The steady-state condition was maintained for approximately 1000 s.
- At the end of the experiment, no more ice was introduced into the ice tank, causing the temperature of the coolant to increase before the complete facility shutdown.

An identical behavior was observed in the water coolant temperature in the tank, as shown in Figure 119. The effect of the onset of natural circulation on the coolant temperature is still evident in the water tank inlet temperature (water coming from the

cavity). Due to the mixing of the inlet water with the cold water in the tank, this effect was not observed in the water tank coolant outlet temperature.

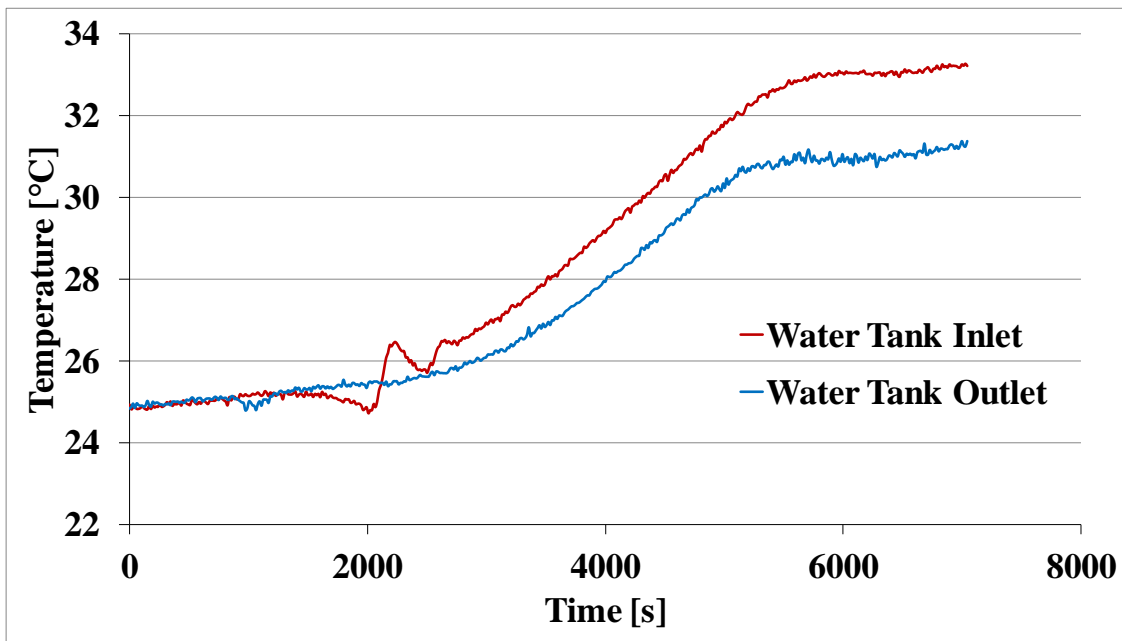


**Figure 119. Water Tank Coolant Temperatures.**

The volumetric flow rate of the water measured with the magnetic flow meter is plotted in Figure 120.

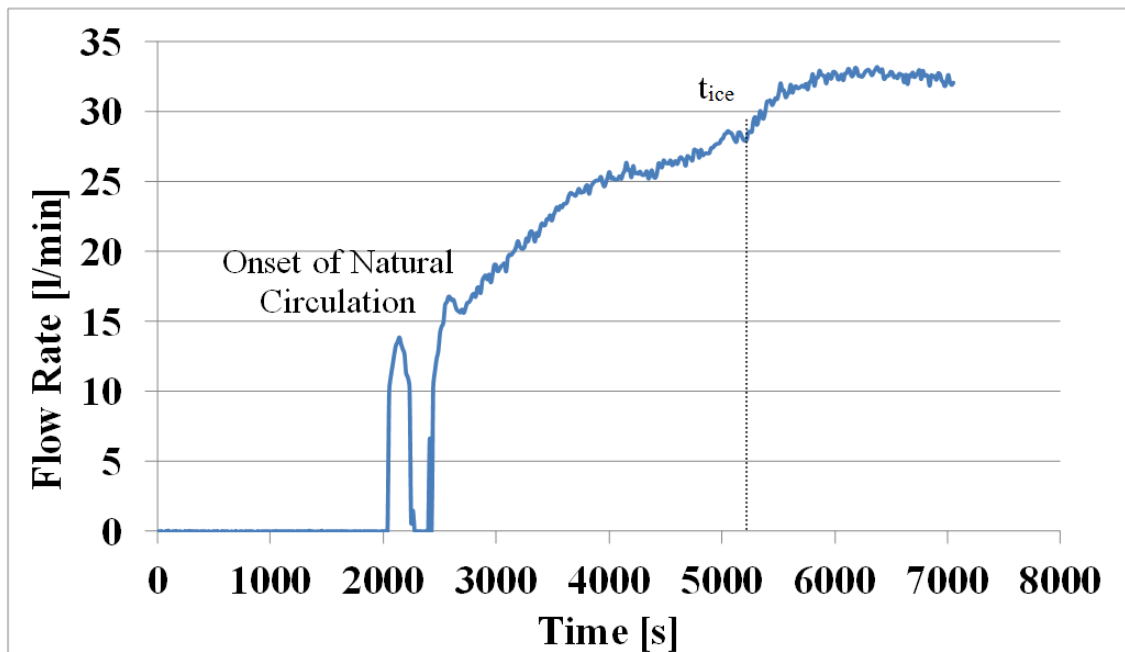


**Figure 120. Primary Coolant Volumetric Flow Rate.**

As it can be observed, the coolant flow rate starts increasing at approximately 2000 seconds. This behavior was essentially related to the flow meter low sensitivity at low flow rates for the flow range selected for this experiment. This was confirmed during the shakedown tests by comparing the results with the ultrasonic flow meter output. The measure of the flow rate using the ultrasonic flow meter during the facility shakedown showed a smoother and earlier increase in the coolant flow rate.

The onset of natural circulation produced a flow oscillation which is shown at approximately 2000 seconds in Figure 120. The amplitude of this oscillation may not be realistic due to the magnetic flow meter cut-off set point that was selected for this

experiment. Revisions of this setting in future testing were found to drastically reduce the amplitude shown by the flow meter.

The oscillation in the water flow can be related to the water cavity outlet temperature fluctuation previously mentioned.

The effect of the mixing of cold water coming from the secondary heat removal system at  $t = t_{ice}$  (first ice batch in the ice container), is also visible in Figure 120 as a sudden increase in the coolant flow rate.

The flow rate reached at steady-state was found to be approximately 32 l/min.

A slight decrease in the coolant flow rate was observed after the last batch of ice was poured into the ice tank as an effect of the lower heat removal rate from the secondary system. The test termination is not shown in the figures since the data recording was stopped a few minutes after the last ice batch was used.

### **XI.3 Test Results – Other Parameters**

The temperature of the coolant in the nine risers was also recorded during the experiment. Due to the low flow rate recorded in the experiment, the temperature rise through the cavity was limited (approximately 2 °C). The temperature rise between the thermocouple probes installed in the risers' panel was found to be small and very close to the accuracy of the system measurement. All the 45 thermocouple probes outputs will be shown, but only the temperature rise between the inlet and outlet (row 1 and row 5 respectively) should be considered.

Figure 121 shows the layout of the thermocouple probes installed in the nine risers and the way risers and probe rows were labeled. This will help interpreting the water temperature profiles in the risers described below.

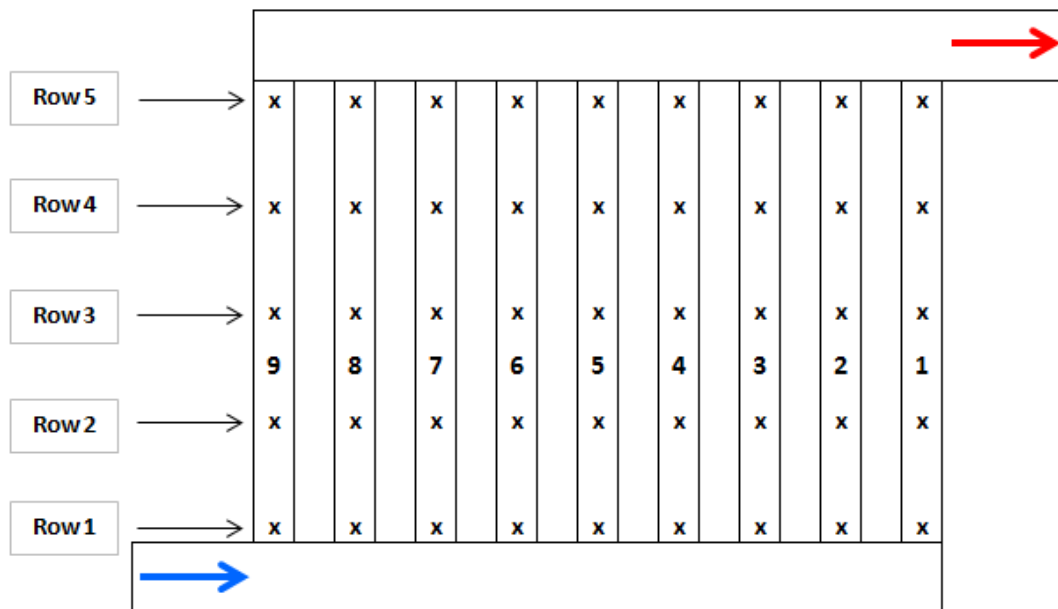


**Figure 121. Risers' Probes Layout.**

The risers were numbered from 1 to 9 (right to left) such that the closest riser to the cavity outlet is the riser 1. As mentioned in the Chapter IX, the thermocouple probes were organized in five rows, numbered from 1 to 5 starting from the bottom row as

shown in Figure 121. The inlet and outlet flow directions are also reported in the same figure.

The water temperature profile in the nine risers is presented in Figure 122. The profiles are snapshots taken at the  $t = 6000s$ , during the steady-state phase.

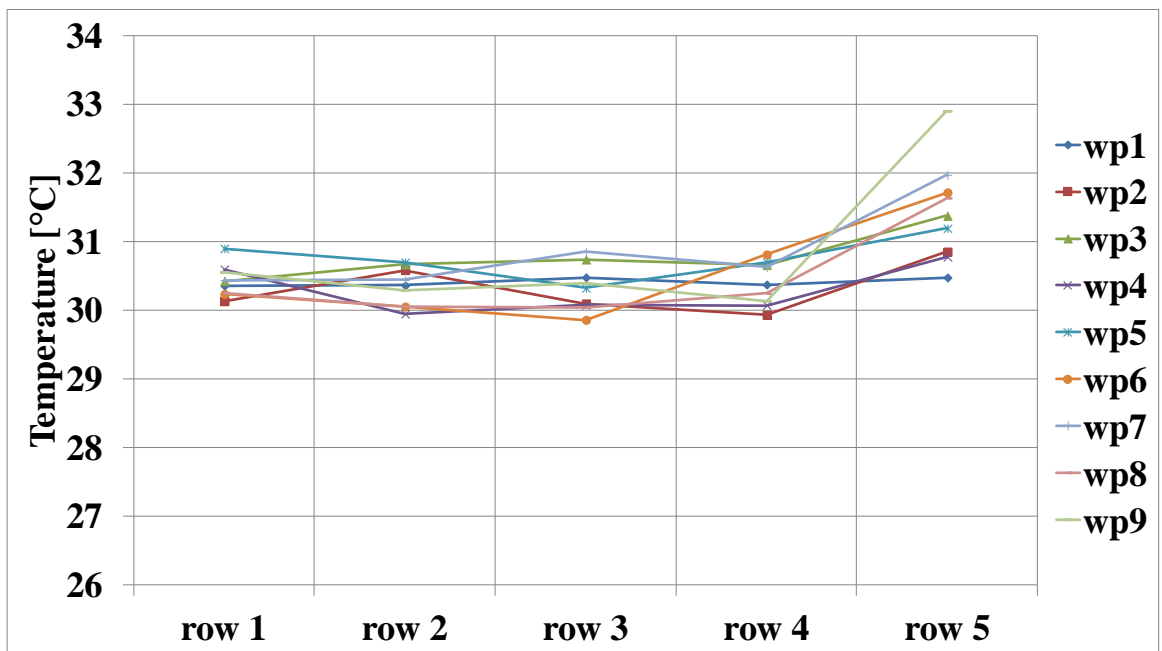


**Figure 122. Risers' Coolant Temperatures (wp = water probe).**

As can be noticed, the temperature of the water showed a complex behavior along each pipe. To better understand and interpret these results, it is necessary to

mention that the thermal behavior of the water is expected to be the result of combined phenomena such as:

- The radiation view factors, which are not uniform for the nine risers [42]. The view factors were calculated to be symmetrical respect to the riser's panel centerline as described in Chapter IV. Due to this symmetry, the radiation heat flux is expected to be higher at the center and lower toward the edge of the cavity. In particular risers 4 and 6 were found to have the biggest radiation view factor followed by the riser 5.
- The water flow distribution through the nine risers which, was estimated to be higher through the riser far from the cavity water inlet (riser 1 in Figure 121), and lower close to the cavity water inlet (riser 9 in Figure 121) [43]. This is essentially due to the different flow resistances that the inlet (horizontal) flow encounters when changing direction into the risers (vertical, upward).
- Edge effects to the heat losses (convection, conduction) through the cavity side walls.
- Possible non uniformity in the heaters heat flux, to be investigated.

Figure 123 show the temperature rise of the coolant through the nine risers as difference of the temperatures from row 5 (outlet) and row 1 (inlet). The measurement uncertainty is also plotted.

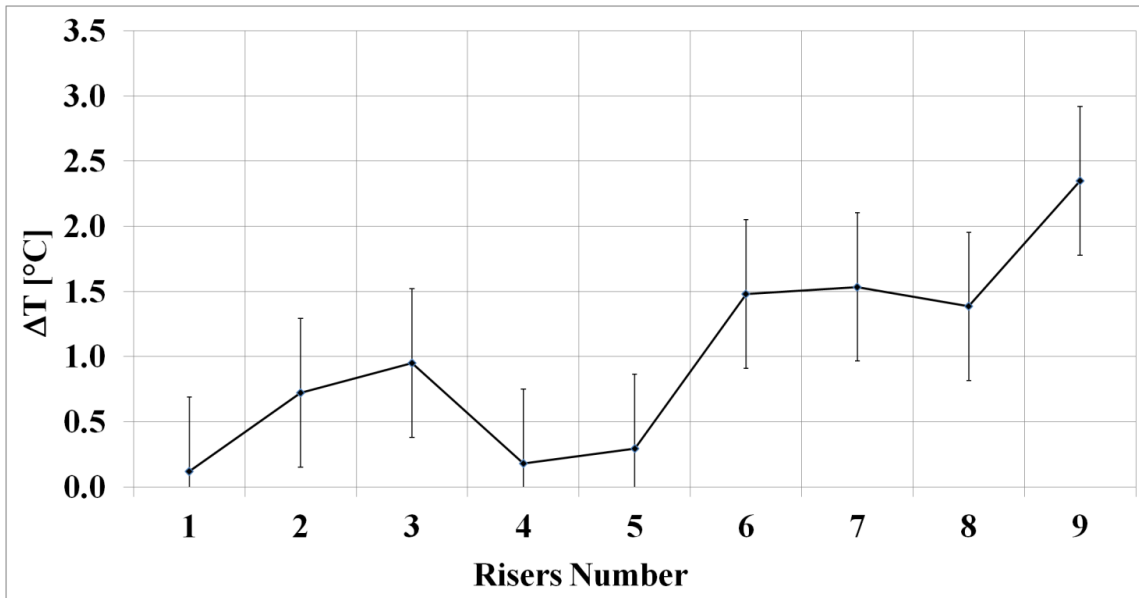


**Figure 123. Risers' Coolant Temperature Rise (row 5 - row 1).**

Riser 1 showed the lowest coolant temperature rise, while the maximum coolant temperature rise was recorded at the riser 9. This is in accordance with the calculations [43] which showed that the largest flow rate was established through riser 9, while the smallest flow rate was predicted to occur at riser 1. The behavior of the intermediate pipes (2 to 8) seems to follow the trend described for risers 1 and 9, except for the risers 4 and 5, where one of the lowest coolant temperature rises was recorded. In addition to the consideration listed above, the temperature measurements in the water may be affected by uncertainty due to the thermocouple probes location. The installation of the probes was designed to place the measuring junction of the probe at the risers' centerline. Due to the relatively high skewed radial temperature profile expected (as a

consequence of the high flux at the risers' front wall and low heat flux at the risers back wall), the uncertainty in the probe location may have a sensible impact in the measurement output. This issue will be also investigated.

#### **XI.4 RELAP5-3D Simulations and Comparison with the Experimental Data**

The RELAP5-3D model used to perform the simulations of the steady-state phase and comparison with the experimental data was the one refined during the shakedown phase (see Chapter X). Minor modifications were implemented in the model to account for:

1. The heat removal from the water tank operated by the heat removal system.
2. The reduced heat losses in the pipeline due to the thermal insulation fully installed during the steady-state phase.
3. The new heaters power profile adopted during the steady-state experiment.
4. The initial temperature of the water.

The heat removal system was modeled using a simplified nodalization with two time-dependent volumes (TV), one time-dependent junction (TJ), and one single-junction (SJ), as shown in Figure 124.

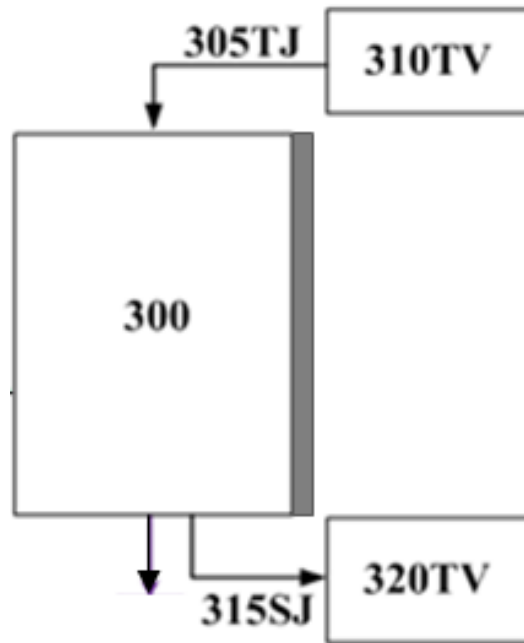


**Figure 124. Secondary Heat Removal Nodalization.**

The thermal-hydraulic conditions (pressure and temperature) of the cold water from the ice container exchanger were imposed in the time-dependent volume 310. These conditions were recorder during the experiment. The flow rate of the secondary coolant was imposed in the time-dependent junction 305. Since minor adjustments were implemented to the pump speed during the experiment, a constant flow rate was imposed in the simulation. The junction 305 was connected at the top of the component 300, simulating the water tank. Atmospheric pressure and room temperature were imposed in the discharge volume (time-dependent volume 320), which was connected to the water tank (component 300) with a single-junction (315) connected at the bottom of the

volume 300. This simplified configuration allowed accounting for the heat removal of the secondary system without modeling the ice container heat exchanger.

Figure 125 shows the secondary coolant temperature measured during the experiment at the tank inlet (upper port), and the temperature imposed in the time-dependent volume 310.

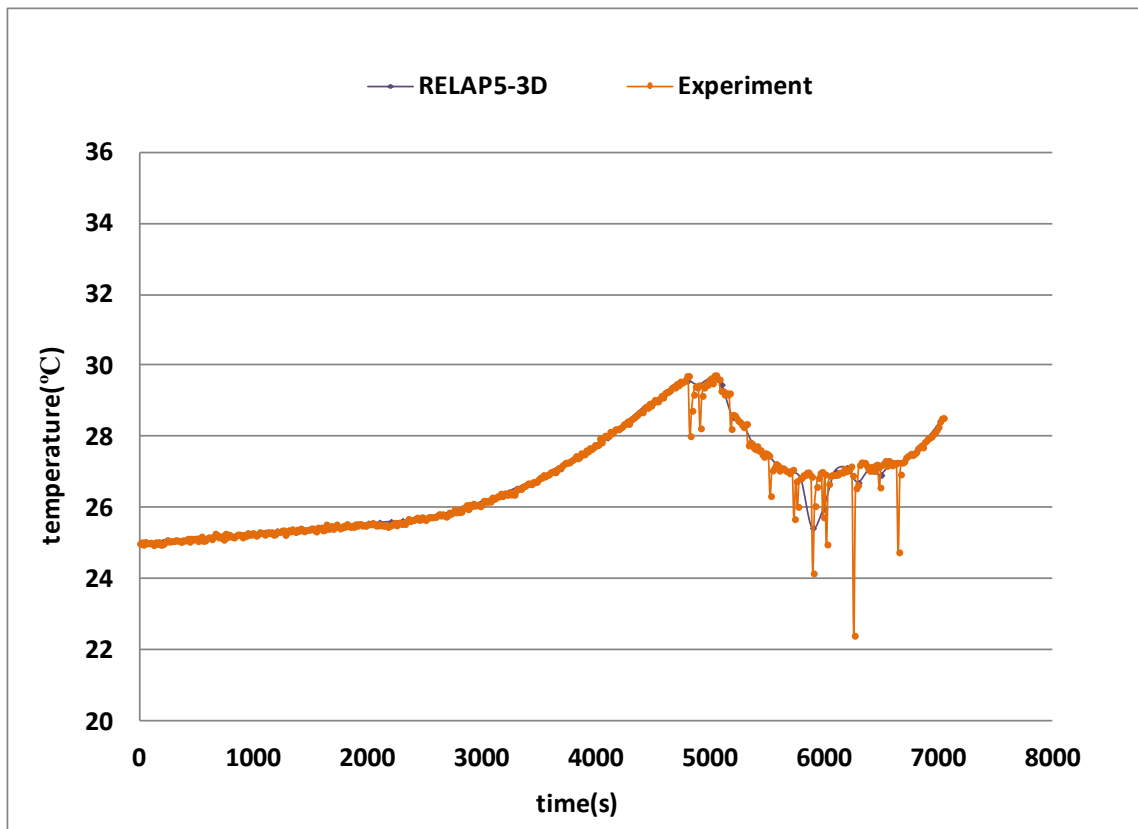


**Figure 125. Secondary Coolant Temperature.**

The plot shows the temperature spikes recorded during the experiment, due to the ice insertion, mixing, and subsequent increase of the heat transfer in the ice container.

The cavity inlet coolant temperature recorder during the experiment (black thick curve) and the RELAP5-3D predictions (orange curve) are plotted in Figure 126. The uncertainty of the thermocouple measurements is also shown (black thin curves).

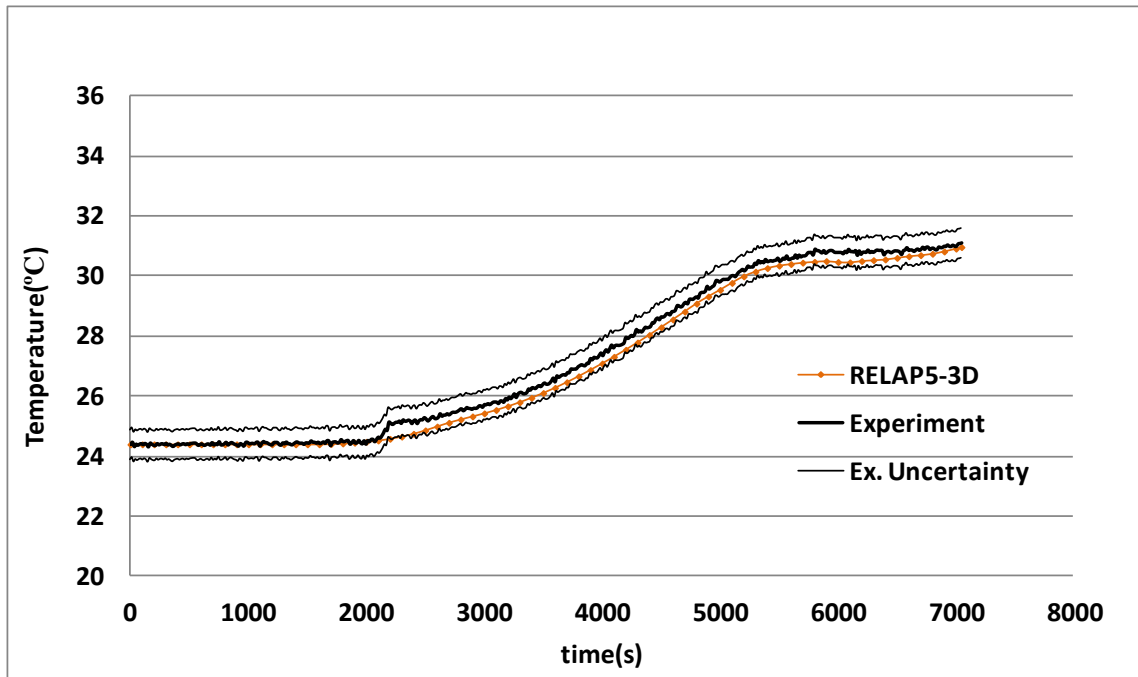


**Figure 126. Cavity Inlet Coolant Temperature.**

As can be observed, the RELAP5-3D predictions are in satisfactory agreement with the experimental data throughout the ramp up and steady-state phases.

A similar comment can be inferred to the cavity outlet coolant temperature comparison, shown in Figure 127.

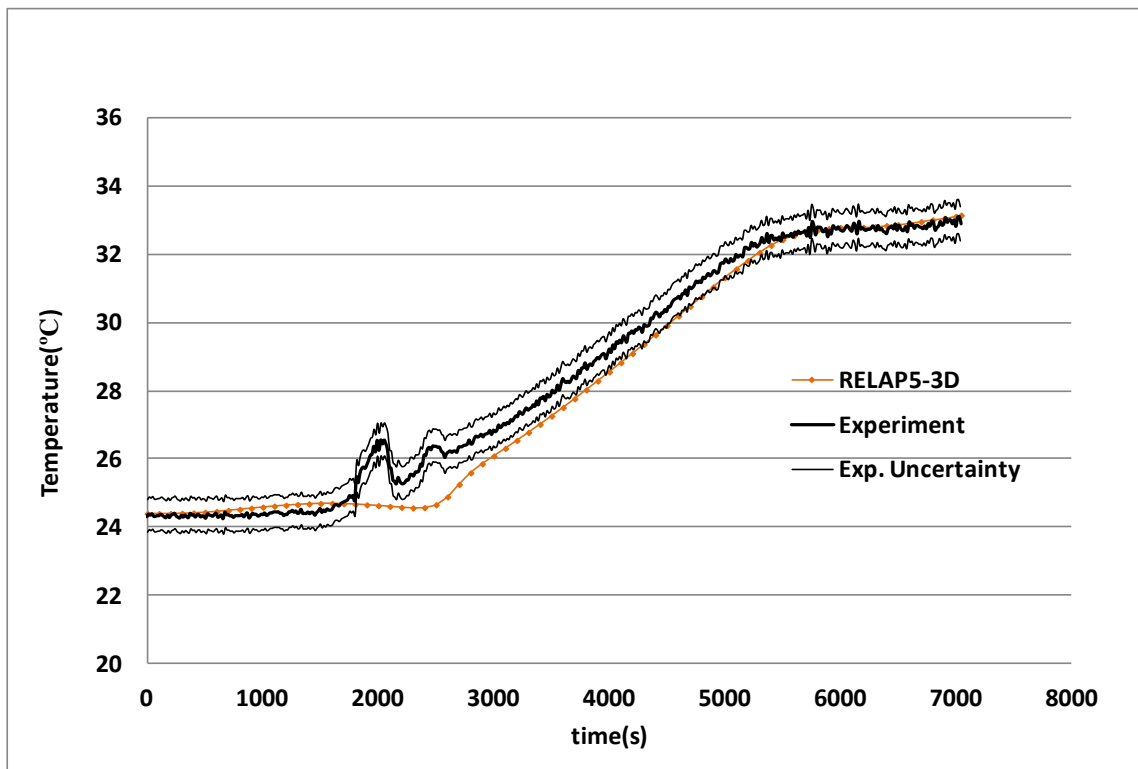


**Figure 127. Cavity Outlet Coolant Temperature.**

The overall RELAP5-3D predictions were satisfactory. At the time of the onset of natural circulation, the simulation was unable to show the temperature instability observed during the experiment.

The volumetric flow rate of the main coolant is shown in Figure 128.

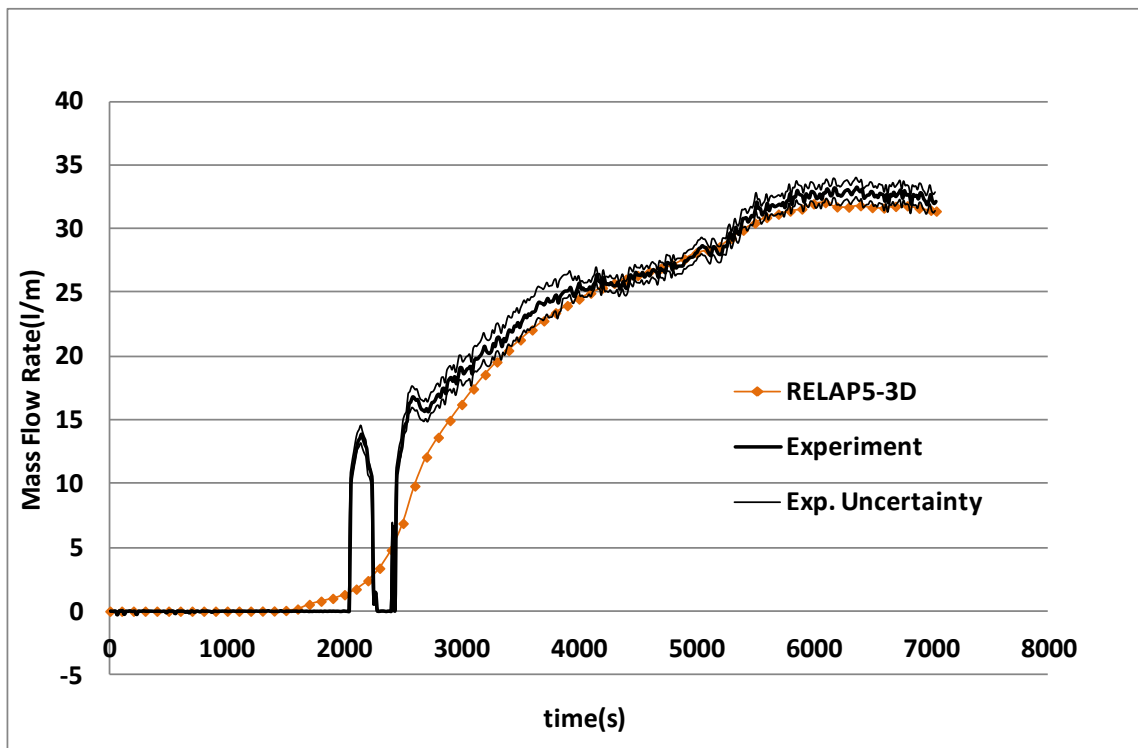


Figure 128. Main Coolant Volumetric Flow Rate.

Also in this case the predictions of the RELAP5-3D model are within the uncertainty of the flow measurement recorded during the experiment. The simulation showed a satisfactory prediction of the flow ramp up, considering the comments on the flow meter settings described in the previous subsection.

## CHAPTER XII

### ISSUES RESOLUTION PLAN

The high level of complexity of the experimental facility, due to the size, shape factor, arrangement, type of materials, and number of pipes connections, increased the chances of technical issues that were not properly addressed during the design and construction phase. These issues were identified during the continuous observations and inspections to the facility conducted during the construction, shakedown tests, and steady-state run. These technical problems can be classified in three main categories, depending on the type of components of the facility where they were identified:

- Issues directly inherent to the experimental facility (piping, connections, heaters, etc.).
- Issues related to the support structures.
- Issues in the facility instrumentation.

Even though the scope of the present work was to identify and report the technical issues for future activities, it is crucial to highlight the important of their resolution to conduct the experimental activity in a safe and productive manner during the steady-state phase, and especially for the two-phase activity. The technical issue will be described in the next paragraphs. Due to the attention in identifying and resolving these issues, a proposed solution or workaround will be proposed for each of the issues listed. Some of the technical issues have been already fixed, and the relevant improvements will be described.

## **XII.1 Issues Directly Inherent to the Experimental Facility**

The technical issues belonging to this category are mainly issues found in the pipelines and the techniques applied to connect pipes of different materials. This includes flanged connections and pipe-to-pipe connections.

### *XII.1.1 Flanged Connections*

Flanged connections between polycarbonate and steel sections experienced leaks developed in a later phase due to crack observed in the joint region between the pipe and the flange of the polycarbonate section. The cracks were essentially attributed to the vibrations of the main structure and scaffold induced by the operators' movements at the different working decks. The vibration of the scaffold and main structure will be discussed in details in the next paragraph. The cracks were observed to develop on the polycarbonate pipe wall at the point of contact with the polycarbonate flange. The continuous vibration induced the cracks to propagate front the flange connection. The final effect was an increasing leak rate which prevented the use of the experimental facility. Similar issues were found at different times after the construction in the following flanged connections:

- Connection at the bottom of the water tank (steal-polycarbonate)
- Connection at the downcomer (polycarbonate-polycarbonate)

- Connections at the upward pipeline (polycarbonate-polycarbonate and steal-polycarbonate)

The use of low-viscosity silicon helped to stop the leaks and was used as a temporary solution.

A modification of the flanged connection is required in order to prevent any leak at any time. A new technique for this type of connections has been already implemented and all the polycarbonate flanged connections were replaced.

The following figures show examples of flanged connections modifications recently implemented in the experimental facility. In particular:

- Figure 129 shows the old and new connection at the bottom of the water tank.
- Figure 130 shows the old and new connection in the pipeline.
- Figure 131 shows the old and new connection in the upward section.

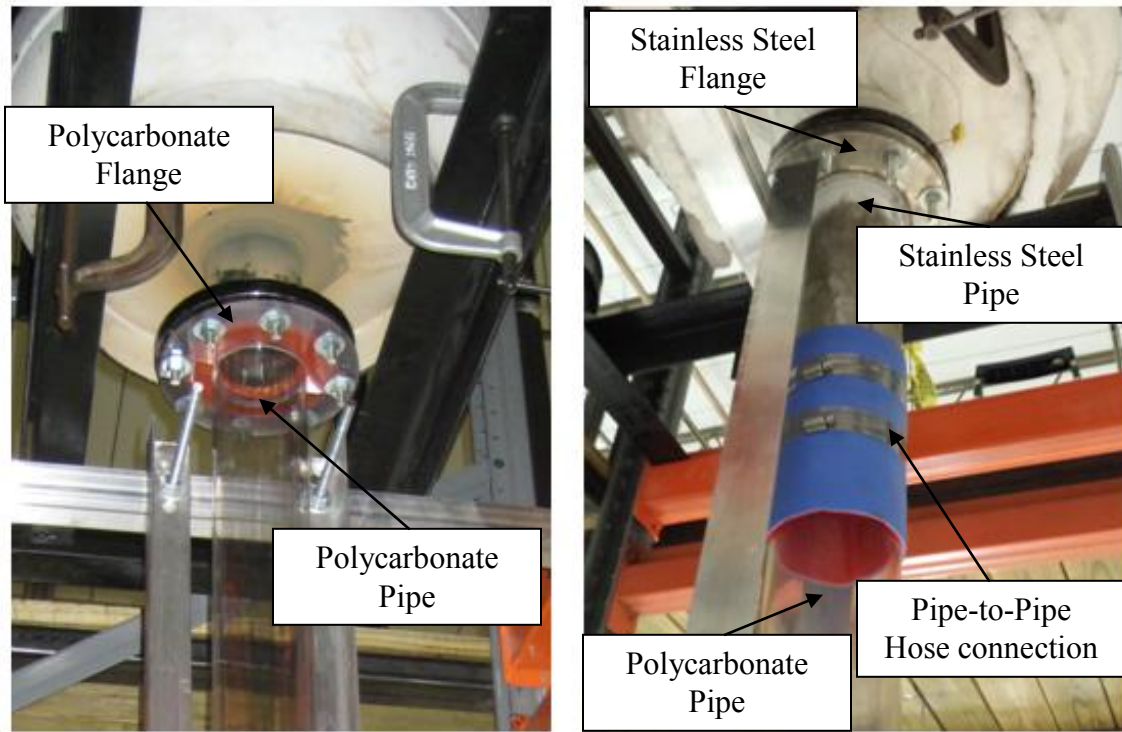


**Figure 129. Tank Outlet Flange Modification (Original: Left; Modified: Right)**



**Figure 130. Upward Pipe Mid-Section Flange Modification (Original: Left; Modified: Right)**

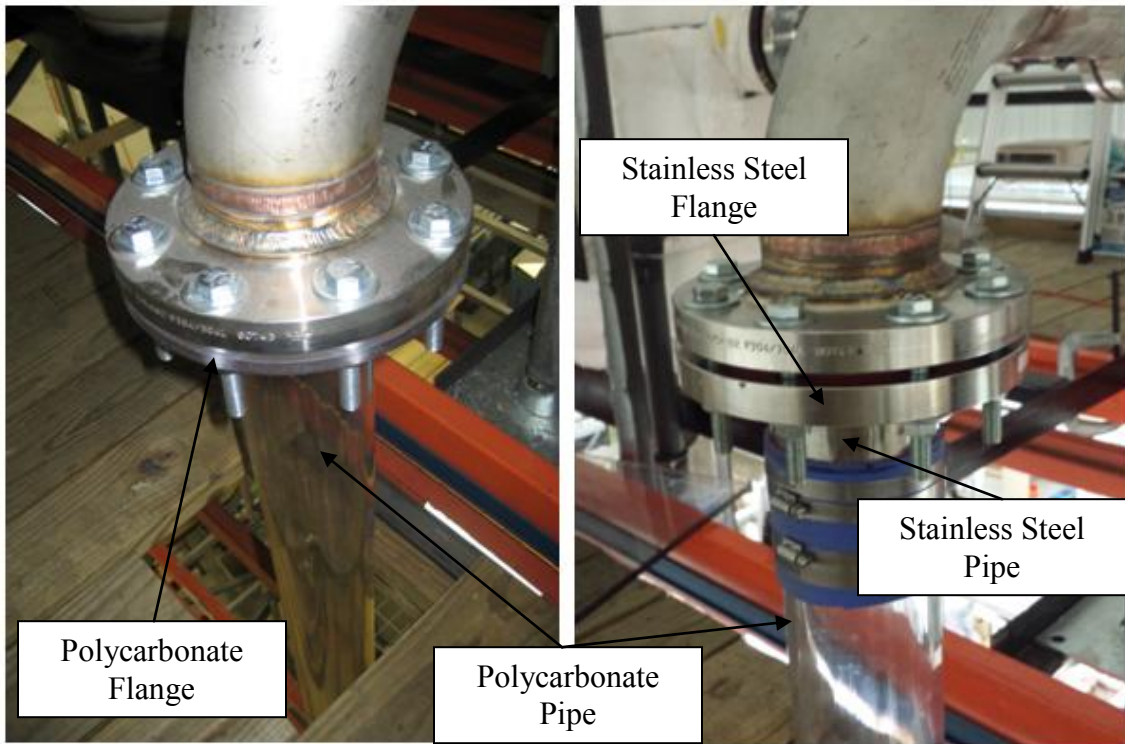


**Figure 131. Upward Pipe Top Flange Modification (Original: Left; Modified: Right)**

### *XII.1.2 Pipe-to-Pipe Connections*

This type of connections were partially replaced after the shakedown tests, especially in the region connecting the risers' ends with the glass manifolds branches. A recent complete replacement of the hose clamps in the lower and upper manifolds' connections was completed, using constant torque hose clamps to guarantee the seal during thermal cycles and high temperatures (Figure 132).



**Figure 132. Manifold-to-Panel Connection Replacement (Original: Top; Modified: Bottom).**

## **XII.2 Issues Related to the Support Structures**

The main issue observed in the main structures is the vibration induced by the access to the elevated working decks by operators and researches. Due to the shape factor of the structure (the facility has a slender configuration with a total height of 6.75 m and a shape factor H/L of 1.73), vibrations were enhanced when accessing and walking at highest operating deck. As mentioned in the previous paragraph, vibrations were identified to be the root cause of the polycarbonate damages (cracks generation and propagation) and would certainly be critical to the operation of the facility during the transient phase, when two-phase flow and bubble generation is expected to occur.

Two different solutions were found to minimize the vibrations of the main structure:

- **Welded Braces.** These braces were already placed at the corners of the structure below the second floor and third floor. The braces were welded diagonally between approximately the midpoints of the horizontal and vertical beams (Figure 133). Additional horizontal beam were also installed at the top ends of the inner scaffold perimeter for the same purpose (Figure 134).
- **Tension Cables.** Tension cables (Figure 135) will be placed at each corner of scaffold and connected to four of the closest main support columns of the University Science Building. This solution would provide

stability to the structure, avoiding fixed connections to the building structure (not allowed by Texas A&M safety department).



**Figure 133. Welded Braces (Corner).**



**Figure 134. Welded Braces (Top)**

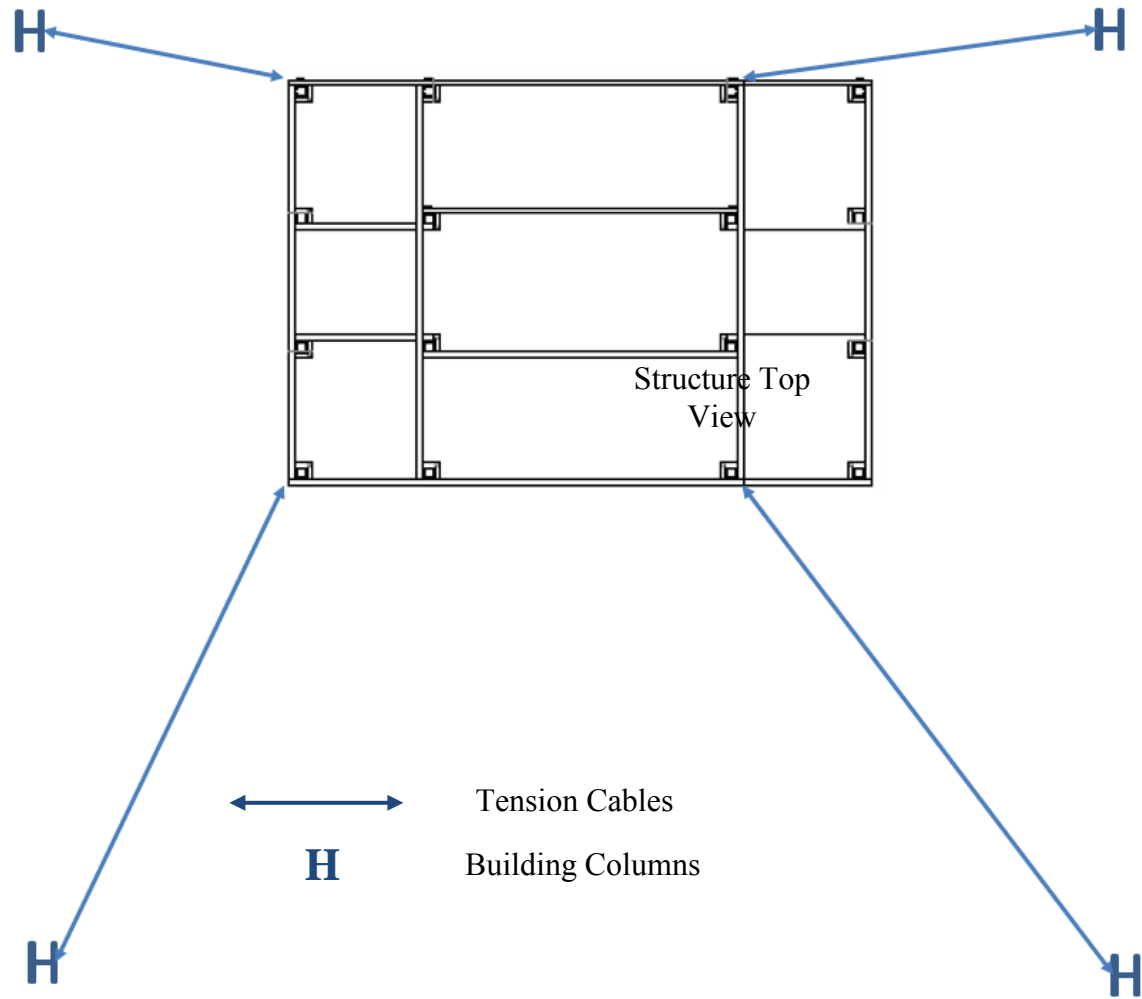


**Figure 135. Tension Cables Layout.**

### **XII.3 Issues in the Facility Instrumentation**

The main issues observed in the facility instrumentation were related to the thermocouples' installation. These issues may be resolved with different techniques for the thermocouple probes and thermocouple wires, due to the different installation procedures and requirements.

#### *XII.3.1 Thermocouple Probes*

A revision of the thermocouple probes put in evidence a high uncertainty in the location of the tip, which ideally must be placed at the center of the pipe or in a well-known location. Differences in the location of the probes within the same riser, or within the same measurement row, would induce a skewed and unrealistic temperature profile (with higher temperatures detected by the probes installed closer to the front risers' wall).

This effect was first observed when analyzing the water temperature profiles in the risers for the steady-state run and described in Chapter XI.

A closer inspection of the thermocouple probes is required to verify the exact location of the probes.

### *XII.3.2 Thermocouple Wires*

The wires installed at the inner wall of the risers' panel were affected by two different problems:

- Wall detachment after thermal cycles
- Junction separation after thermal cycles

The wall detachment was detected since the very first experimental runs as a higher temperature reading, in comparison with other thermocouples in adjacent regions. The wire detached from the wall gets closer to the radiating vessel and exposed to a higher temperature.

The thermocouple junction separation was also detected as an open circuit in the data acquisition system. This was essentially due to the technique adopted to create the junction. The two wire tips were simply twisted and no additional bonding was provided (welding).

Improvements in the thermocouple installation (using the same epoxy glue described in Chapter IX) and junction preparation are currently being implemented in the experimental facility.

## **XII.4 Other Issues to Be Addressed**

The water temperature rise through the cavity at steady-state was found to be approximately 2 °C. This value is lower than the design specification (approximately 10 °C) described in the scaling procedures (Chapter V). To perform a scaled steady-state run, this thermal-hydraulic parameter has to match the design specifications since the temperature rise similarity number was set to unity.

A technique that could be adopted to increase the temperature rise would consider the reduction of the coolant flow rate by increasing the pressure losses. The optimum solution would consider the installation of a manual valve that can be maneuvered during the steady-state phase to find the best opening ratio to establish the desired flow rate and, subsequently, the design temperature rise between cavity inlet and outlet.

Other solutions, using orifices, may be difficult to use since they may require continuous facility shutdowns and start ups to replace the orifice until the optimum flow is achieved.

The proposed technique was also modeled with the RELAP5-3D simulations, during the scaling laws validation described in Chapter V.

## CHAPTER XIII

### CONCLUSIONS

A small scale water-cooled Reactor Cavity Cooling System experimental facility was designed, built, and brought to operation to conduct experimental investigations on the behavior of the water in system.

The shakedown phase of the activity confirmed that the main features of the system meet the expectations:

- The natural circulation of water is established by the buoyancy forces caused by the power released to the coolant in the reactor cavity.
- The instrumentation installed is properly working to record the main thermal-hydraulic parameters (temperatures and flow rates) required for the investigation.
- Flow visualization in specific regions of the facility was tested and proved to be a potential tool to be used for quantitative estimation of the velocity of the fluid in the manifolds and risers.

The basic steady-state run performed at given initial and boundary conditions, confirmed the ability of the water natural circulation to remove the heat produced in the reactor vessel. The manual technique put in place to remove the heat from the system (secondary heat removal system) was proven to be capable to bring the system to steady-state conditions (stable flow rate at a given coolant temperature). Its operation required special care in handling the ice and coolant flow rate, resulting in a limited maintained

steady-state time, and flow oscillations. Nevertheless, these conditions did not impact the facility functionality and the analysis to be performed during the experiments.

A RELAP5-3D model of the experimental facility was prepared and refined during the shakedown test. The comparison of the simulation results for the steady-state case with the experimental data produced during the steady-state experimental run confirmed the ability of the system code to predict the phenomena related to the natural circulation of water in closed loops, with satisfactory prediction of coolant flow rates and temperatures. This computational task highlighted the importance of:

- Performing preliminary simulations using system codes as validation method for the scaling laws, and as optimization tool.
- Sensitivity analysis to define the optimum nodalization scheme and models to be adopted, based on the actual features of the facility.

The observations conducted during the experimental runs (shakedown + steady-state) helped identifying technical issues that need to be addressed in order to conduct the experimental activity through the next phases. These issues can be classified into three main categories:

- Issues directly inherent to the experimental facility (piping, connections, heaters, etc.).
- Issues related to the support structures.
- Issues in the facility instrumentation.

Even though the resolution of these issues is not part of the scope of this work, they will be described in detail in the next chapter and possible solutions will be provided.

Table 19 summarizes the project objective (listed and described in Chapter II) with the main achievements and conclusions.

**Table 19. Project Resolution Summary.**

	<b>Objective</b>	<b>Project Resolution</b>
1	Scale down, design, build, and shakedown a small scale water-cooled RCCS experimental facility to support the analysis of the thermal-hydraulic behavior of the coolant in the system and its cooling capabilities.	The facility was scaled down, designed, and assembled. The shakedown tests were successfully conducted, confirming the capabilities of the facility
2	Conduct scaled test to study the thermal-hydraulic behavior of a water-cooled RCCS under steady-state conditions	A steady-state run was conducted. Important parameters such as temperatures and flow rate were recorded to study the system behavior during the steady-state phase.
3	Identify and Analyze specific phenomena occurring during the single-phase stage of the experiments	Possible flow asymmetries through the nine risers were observed and related to the different temperature rise through the nine pipes.
4	Develop and refine computational models (systems codes and Computational Fluid Dynamics codes) to analyze these phenomena	A RELAP5-3D model was created and refined to perform simulations of the experimental facility during steady-state and transient scenarios. CFD models were also prepared (not part of this work)
5	Produce experimental data to be used for computational codes validation	The shakedown tests results and the steady-state run data were recorded and compared with the RELAP5-3D simulation results confirming the capability of the code to predict this type of phenomena, considering that the main features of the system are correctly represented and modeled.
6	Identify possible technical issues and technique to fix them, also in preparation for the two-phase (accident) stage	Issues were identified and correction actions were proposed.

## REFERENCES

- [1]. Generation IV International Forum, "Introduction to Generation IV Nuclear Energy Systems and the International Forum", (2008).
- [2]. Carbon Mitigation Initiative, "Stabilization Wedges Game" Princeton University (2004).
- [3]. S. Pacala, R. Socolow, "Stabilization Wedges: Solving the Climate Problem for the Next 50 Years with Current Technologies", Science 13 (August 2004).
- [4]. A. McDonald, "Nuclear Power Global Status", IAEA Bulletin, Vol.49-2 (2008).
- [5]. T. Abram, S. Ion, "Generation-IV Nuclear Power: A Review of the State of the Science", Energy Policy, 36 (2008).
- [6]. Generation IV International Forum, 2002 "A Technology Roadmap for Generation IV Nuclear Energy Systems" GIF-002-00 (2002).
- [7]. Generation IV International Forum, <http://www.gen-4.org/index.html>
- [8]. H. D. Gougar, D. A. Petti, R. N. Wright, W. E. Windes, R. R. Schultz, J. S. Herring, P. Sabharwall, P. Humrickhouse, "Current Status of VHTR Technology Development," Proceedings of HTR 2010 Prague, Czech Republic, October 18-20, 2010 Paper 048 (2010).
- [9]. D.A. Dilling, "Passive Decay and Residual Heat Removal in the MHTGR", IAEA-TECDOC-757, Juelich (1982).
- [10]. General Atomics, "Gas Turbine-Modular Helium Reactor (GT-MHR) Conceptual Design Description Report," GA-A910720, Project (1996).

- [11]. J. Thielman, P. Ge, Q. Wu, L. Parme, "Evaluation and Optimization of General Atomics' GT-MHR Reactor Cavity Cooling System using an Axiomatic Design Approach," Nuclear Engineering and Design Vol.235 (2005).
- [12]. D. Hittner, "RAPHAEL, A European Project for the Development of HTR/VHTR Technology for Industrial Process Heat Supply and Cogeneration," Proceedings of HTR 2006, 3rd International Topical Meeting on High Temperature Reactor Technology, October 1–4, Johannesburg, South Africa (2006).
- [13]. L.J. Lommers, F. Shahrokhi, J.A. Mayer III, F.H. Southworth, "AREVA HTR Concept for Near-Term Deployment", Nuclear Engineering and Design, Vol.251 (2012).
- [14]. IAEA-TECDOC-1163, "Heat Transport and Afterheat Removal for Gas Cooled Reactors under Accident Conditions," International Atomic Energy Agency (2000).
- [15]. J. Antwerper, G.P. Greyvenstein, "Evaluation of a Detailed Radiation Heat Transfer Model in a High Temperature Reactor Systems Simulation Model", Nuclear Engineering and Design Vol. 238 (2008).
- [16] R.W. Schleicher, A.C. Lewis, "Modular High Temperature Gas-Cooled Reactor Heat Source for Conversion", IAEA Workshop on High Temperature Applications of Nuclear Energy, October 19-20,1992, Oarai-mhi, Ibaraki-ken, Japan (1992).
- [17] INEEL/EXT-03-00141, "Very High Temperature Reactor (VHTR), Survey of Materials Research and Development Needs to Support Early Deployment" (2003).
- [18]. C. H. Oh, E. S. Kim, R. R. Schultz, D. Petti, "Computational Fluid Dynamics Analyses on Very High Temperature Reactor Air Ingress", Proceedings of ICONE 17

International Conference on Nuclear Engineering July 12–16 2009, Brussels, Belgium, Paper 75863 (2009).

[19]. C. Oh, E. Kim, R. R. Schultz, M. Patterson, D. Petti, “Thermal Hydraulics of the Very High Temperature Gas Cooled Reactor”, The 13th International Topical Meeting on Nuclear Reactor Thermal Hydraulics (NURETH-13) Kanazawa, Japan. September 27-October 2, 2009 (2009).

[20]. DOE-HTGR-90016 “450MWt Reactor Cavity Cooling System- System Design Description”, Bechtel National ,Inc (1993).

[21]. A. Saikusa, “Data on Test Results of Vessel Cooling System of High Temperature Engineering Test Reactor”, JAERI-Data/Code 2002-027 (2003).

[22]. C.P. Tzanos, M. Farmer, ‘Feasibility Study for Use of the Natural Convection Shutdown Heat Removal Test Facility (NSTF) for Initial VHTR Water-Cooled RCCS Shutdown”, Technical report, Nuclear Engineering Division, Argonne National Laboratory, ANL-GenIV-079 (2006).

[23]. R. Vaghetto, L. Capone, Y. A. Hassan, “Experimental Study of the Effect of Graphite Dispersion on the Heat Transfer Phenomena in a Reactor Cavity Cooling System (RCCS)”, Nuclear Technology, Vol. 177, number 2 (2012).

[24]. D. D. Lisowski, S. M. Albiston, R. M. Scherrer, T. C. Haskin, M. H. Anderson, A. Tokuhiro, M. L. Corradini, “Experimental Studies of NGNP Reactor Cavity Cooling System with Water”, Proceedings of ICAPP 2011 Nice, France, May 2-5, 2011, Paper 11116 (2011).

- [25]. R. B Bird, W. E. Stewart, E. N. Lightfoot, "Transport Phenomena", John Wiley & Sons, Inc., New York (1960).
- [26]. F. P Incropera, D. P DeWitt, "Fundamental of Heat and Mass Transfer", John Wiley & Sons, USA . Fourth Edition.
- [27]. P.J. Kerney, G.M. Faeth, D.R. Olson, "Penetration Characteristics of Submerged Jet". American Institute of Chemical Engineering Journal Vol. 18, number 3 (1972).
- [28] RELAP5-3D Code Manuals, INEEL-EXT-98-00834, Rev. 2.4 (2005).
- [29]. INL/EXT-06-01362, "Development of Safety Analysis Codes and Experimental Validation for a Very High Temperature Gas-Cooled Reactor" (2006).
- [30]. TAC Technologies, "NEVADA Software Package Quick Reference Series", TAC Technologies, USA (2000).
- [31]. F. B Brown, "MCNP - A General Monte Carlo N-Particle Transport Code, Version 5 Volume I: Overview and Theory," LA-UR-03-1987, Los Alamos National Laboratory (2003).
- [32] C.H.Oh, G.C. Park, C.Davis, "RCCS Experiments and Validation for High-Temperature Gas-Cooled Reactor", Nuclear Technology, Vol.167 (2009).
- [33]. A. Sala, "Radiant Properties of Materials", Elsevier Science Publishing Co., Inc. New York (1986).
- [34]. P.K. Vijayan, "Experimental Observations on the General Trends of the Steady State and Stability Behaviour of Single-Phase Natural Circulation Loops", Nuclear Engineering and Design, Vol. 215 (2002).

- [35] NUREG/CR-6285, "Severe Accident Natural Circulation Studies at the INEL". INEL-04/0016 (1995).
- [36] D. Lisowski, O. Omotowa, A. Tokuhiko, M. Anderson, M. Corradini, "Power Investigations on the Two-Phase Behavior and Instability in an Experimental Reactor Cavity Cooling System with Water", The 15th International Topical Meeting on Nuclear Reactor Thermal - Hydraulics, NURETH-15, Pisa, Italy, May 12-17, 2013, Paper 492 (2013).
- [37]. R. Vaghetto, W. Huali, Y.A. Hassan, "RELAP5-3D Simulations of the Reactor Cavity Cooling System Experimental Facility" ANS Annual Meeting, Chicago, IL, June 24-28 2012, Paper 979 (2012).
- [38] R. Vaghetto, H. Wei, Y.A. Hassan, "Simulation of a Simple RCCS Experiment with RELAP5-3D System Code and Computational Fluid Dynamics Computer Program", The 14th International Topical Meeting on Nuclear Reactor Thermal-Hydraulics, NURETH-14, Toronto, Ontario, Canada, September 25-30, Paper 352 (2011).
- [39]. R. Vaghetto, S. Lee, Y. A. Hassan, "Reactor Cavity Cooling System Facility Shakedown and RELAP5-3D Model Validation", Proceedings of the 20th International Conference on Nuclear Engineering, ICONE 20, July 30-August 3, 2012, Anaheim, California, USA, Paper 55276 (2012).
- [40]. W. Merzkirch, "Flow Visualization", Academic Press Inc, Second Edition (1987).
- [41]. R. Vaghetto, S. Lee, Y. A. Hassan, "Analysis of the Steady-State Phase of the Reactor Cavity Cooling System Experimental Facility", ANS Annual Meeting, San Diego, CA, November 11-15 2012, Paper 6593 (2012).

[42]. J. C. Chato, "Natural Convection Flows in Parallel-Channel Systems", J. Heat Transfer 85(4), 339-345 (1963)

[43] H. Wei, R. Vaghetto, Y.A. Hassan, "CFD Simulations of Mesh Sizes and Turbulent Models Sensitivity Study for a Reactor Cavity Cooling System of the Very High Temperature Reactor". The 9th International Topical Meeting on Nuclear Thermal-Hydraulics, Operation and Safety NUTHOS-9, Kaohsiung, Taiwan, September 9-13, (2012).

## APPENDIX A – SCAFFOLDING CAPACITY VERIFICATION

	RCCS STRUCTURE CAPACITY Author: Jacob Peterson Revised by: Rodolfo Vaghetto	Page 1 of 6

### RCCS SCAFFOLDING CAPACITY VERIFICATION

#### Factor of Safety (FoS) Analysis

All pieces are 3/16" thick, the vertical beams are 3x3", and the horizontal are 2x3" load bearing beams. The 2x2" railings are not load bearing, and thus weren't factored in to the calculations. The structure was entered into SolidWorks® for analysis as one solid piece made of Plain Steel. The FoS with 2000 lb loaded at each level came out to 11.

Analysis was also done considering the main water tank falling. This extra 2000 lb (added laterally at the top) caused the FoS to drop to 2.5.

#### Force on Anchors - Normal Situation

Total weight of scaffold:  $W_{SCAF} = 5700$  lb

Projected maximum total load applied:  $W_{LOAD} = 2000$  lb

Center of Mass (CoM) very nearly in center (10 in skewed). Weight almost evenly distributed among 16 feet. Thus the 4x4 array of vertical beams can be considered as 4 roughly equivalent 4x1 arrays. Figure 1 shows one of these.

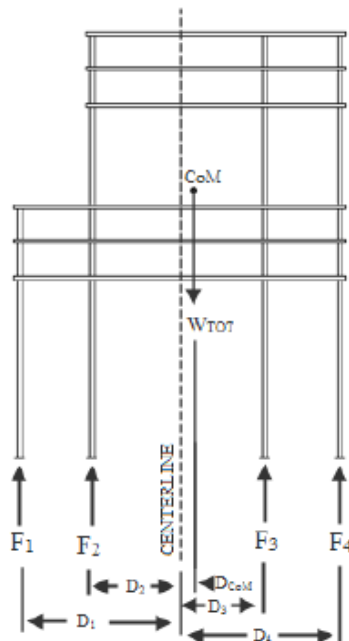


Figure 1. Force Diagram in Normal Situation

$$W_{TOT} = (W_{SCAFF} + W_{LOAD}) / 4 = (5700 + 2000 + 2000) / 4 = 2425 \text{ lb}$$

FORCE AND MOMENT BALANCE EQUATIONS:

$$F_1 + F_2 + F_3 + F_4 = W_{TOT}$$

$$F_1D_1 + F_2D_2 - F_3D_3 - F_4D_4 = W_{TOT}D_{CoM}$$

SYMMETRY:

$$F_1(D_1 + D_{CoM}) = F_4(D_4 - D_{CoM})$$

$$F_2(D_2 + D_{CoM}) = F_3(D_3 - D_{CoM})$$

SOLUTION:

$$F_{MAX} = F_3 = 714 \text{ lb (All stresses are into concrete, not pulling on bolts)}$$

#### Force on Anchors - Tank Falling Situation

$$\text{Tank weight: } W_{TANK} = 2000 \text{ lb}$$

$$\text{Distance tank to CoM} = 115 \text{ in} \times 40 \text{ in} \times 0 \text{ in} = 122 \text{ in}$$

$$M_{TANK} = 2000 \text{ lb} \times 122 \text{ in} = 244,000 \text{ in-lb}$$

$$\text{Moment from structure} = 700,000 \text{ in-lb}$$

$$\text{Distance foot to CoM} = 150 \text{ in} \times 70 \text{ in} \times 115 \text{ in} = 200 \text{ in}$$

Since the scaffold is secured only in the corners and is symmetric we can divide the moment in half to get the total moment

$$M_{TOT} = (244,000 + 700,000) / 2 = 472,000 \text{ in-lb}$$

Since the structure is only tipping one direction, it can simplify to one reaction force, as shown in Figure 2.

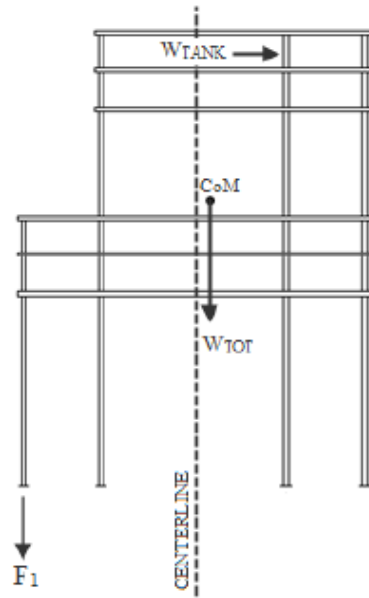


Figure 2: Force Diagram in Tank Falling Situation

$F_1 = M_{TOT} / 200 = 2360$  lb. Since each foot has 2 bolts, there is **1180 lb** pulling force at each bolt.

**Drop-In concrete anchor/fastener - Technical Data:**

Anchor Size	Overall Length	Drill Bit Diameter	Internal Thrd. Length	Bolt Dia.	Pull-Out 3000 psi concrete
1/4"	1"	3/8"	1/2"	1/4"	2,200 lb.
3/8"	1-9/16"	1/2"	5/8"	3/8"	4,400 lb.
1/2"	2"	5/8"	3/4"	1/2"	7,040 lb.
5/8"	2-1/2"	7/8"	7/8"	5/8"	11,880 lb.
3/4"	3-3/16"	1"	1-1/4"	3/4"	12,960 lb.

**Table 1. Anchor Manufacturer Specification (Max Load).**

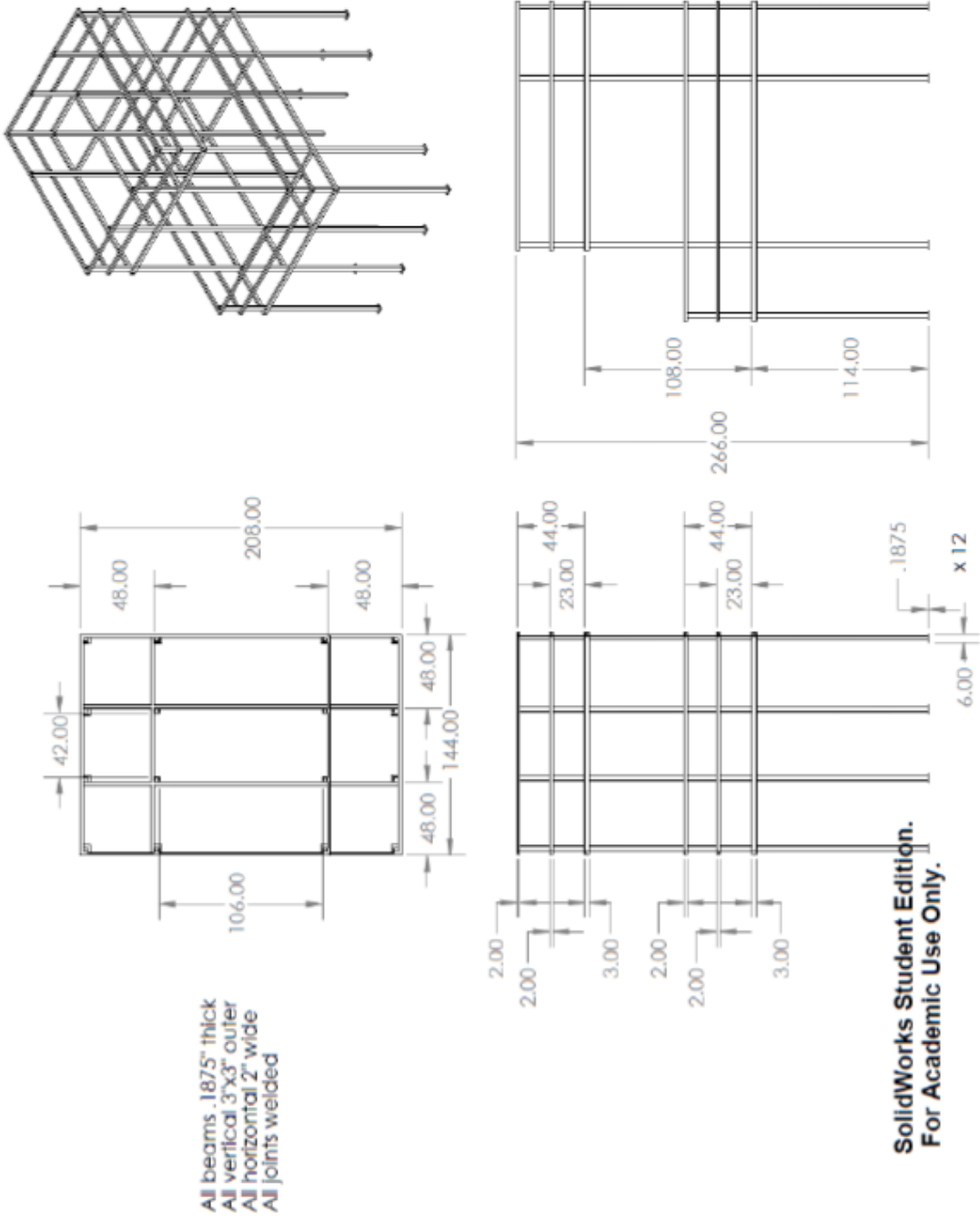
From the table the average force withstood by the anchor is 7,040 lb. (FoS = 5.9)

To shear the bolt, a force of 10,000 lb is required. (FoS = 8.5)

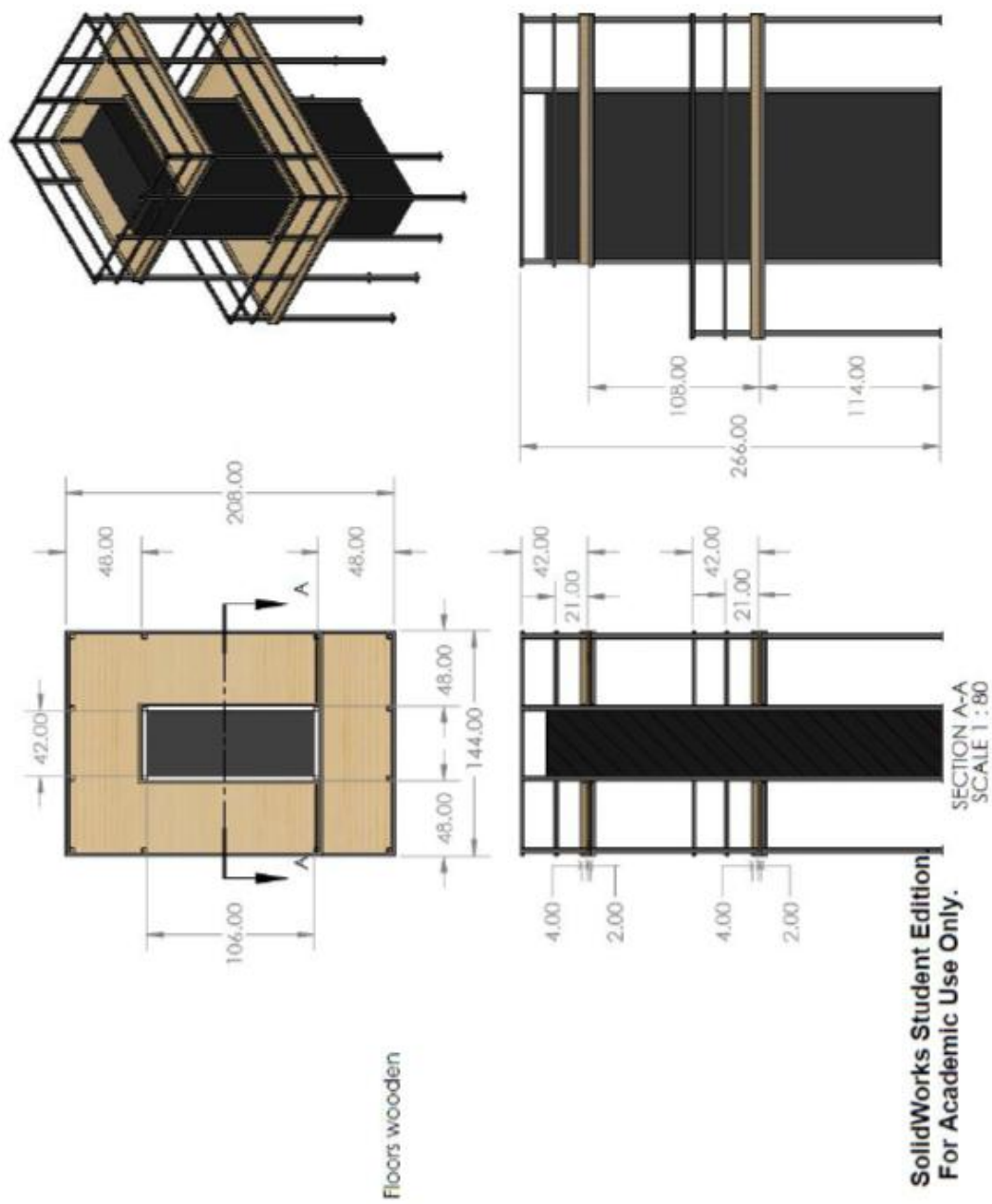
By SolidWorks<sup>®</sup> analysis on the foot plate, the safety factor for the bolt pulling through the hole in the plate is 4.1.

Thus the overall FoS for the bolt in the tank falling situation is **4.1**.

**Appendix I - Bare View**



**Appendix II - Real View**



## APPENDIX B – ANCHORS CAPACITY VERIFICATION

	RCCS STRUCTURE CAPACITY Author: Colton Hermes Revised by: Rodolfo Vaghetto	Page 1 of 2

### RCCS MAIN STRUCTURE ANCHORS CAPACITY VERIFICATION

#### Water Tank Dimensions

$$M_{TANK} = 500 \text{ lb}$$

$$D = 24.5'' \quad H=72'' \quad \rightarrow \quad V=0.556 \text{ m}^3$$

$$M_{WATER} = 600 \text{ kg} = 1322 \text{ lb (Assuming tank 100% full)}$$

$$M_{TOT} = 1322 + 500 = 1822 \text{ lb} \rightarrow 2000 \text{ lb}$$

#### Force on Anchors

$$H = 6 \text{ m}; \quad M_{TOT} = 2000 \text{ lb}$$

$$\text{Moment}_{TANK} = 6 \times 2000 = 12,000$$

$$L/2 = \text{Horizontal Distance From Tank to Anchor} = 22'' = .559 \text{ m}$$

$$\text{Moment}_{BASE} = F \times (L/2) = 12,000 \Rightarrow F_{TOT} = 21,467$$

$$F_{ANCHOR} = F_{TOT}/4 = \underline{5,367 \text{ lb}}$$

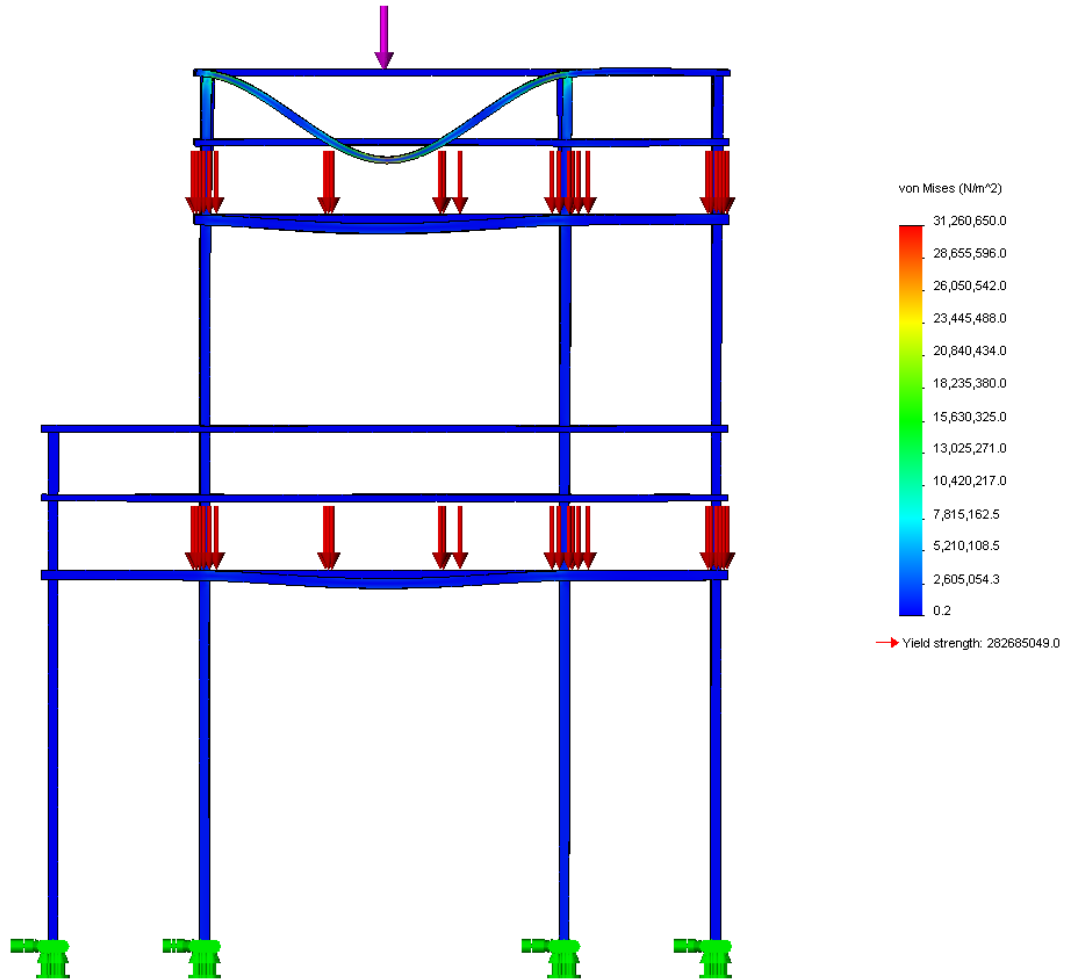
#### Drop-In concrete anchor/fastener - Technical Data:

Anchor Size	Overall Length	Drill Bit Diameter	Internal Thrd. Length	Bolt Dia.	Pull-Out 3000 psi concrete
1/4"	1"	3/8"	1/2"	1/4"	2,200 lb.
3/8"	1-9/16"	1/2"	5/8"	3/8"	4,400 lb.
1/2"	2"	5/8"	3/4"	1/2"	7,040 lb.
5/8"	2-1/2"	7/8"	7/8"	5/8"	11,880 lb.
3/4"	3-3/16"	1"	1-1/4"	3/4"	12,960 lb.

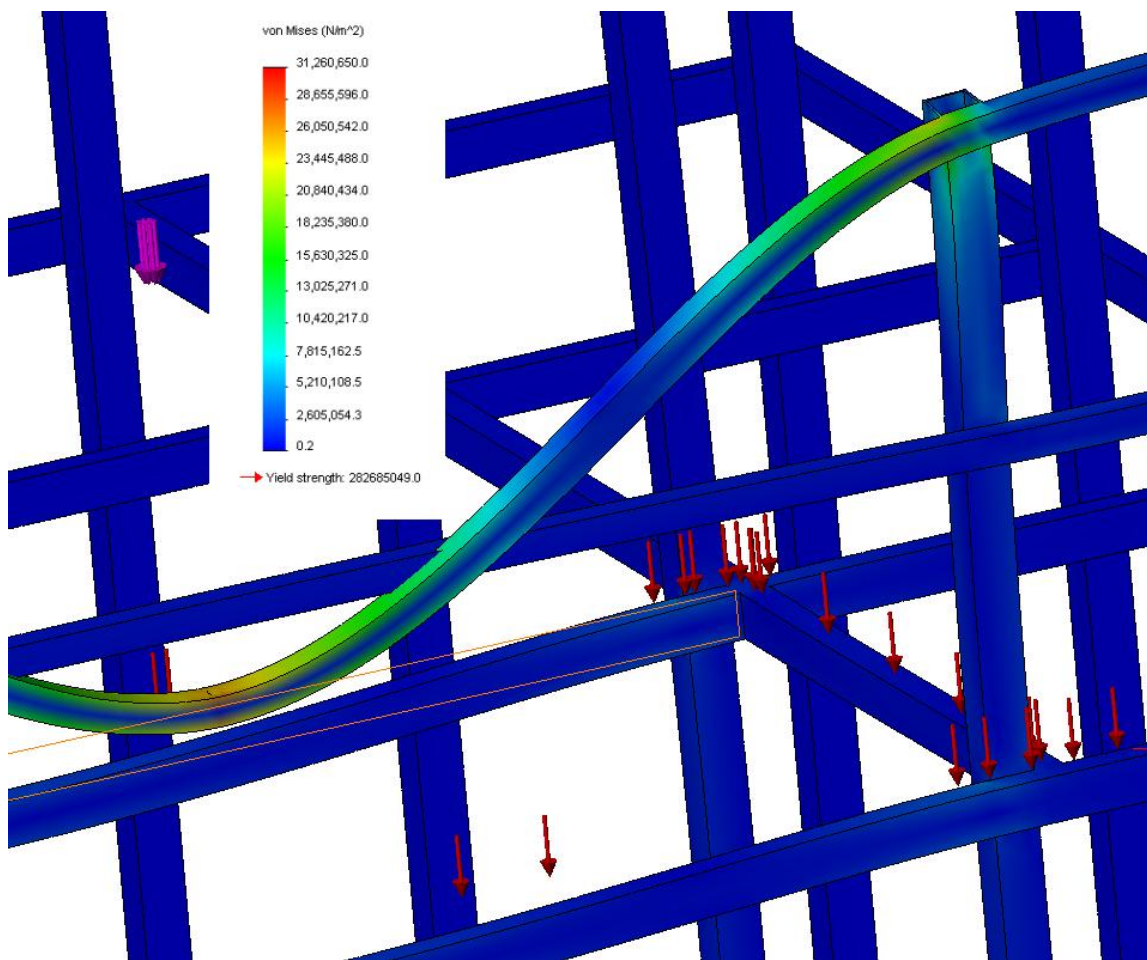
**Table 1. Anchor Manufacturer Specification (Max Load)<sup>1</sup>.**

From the table, we can read the average force withstood by the anchor is 7,040 lb, allowing margin for each anchor.

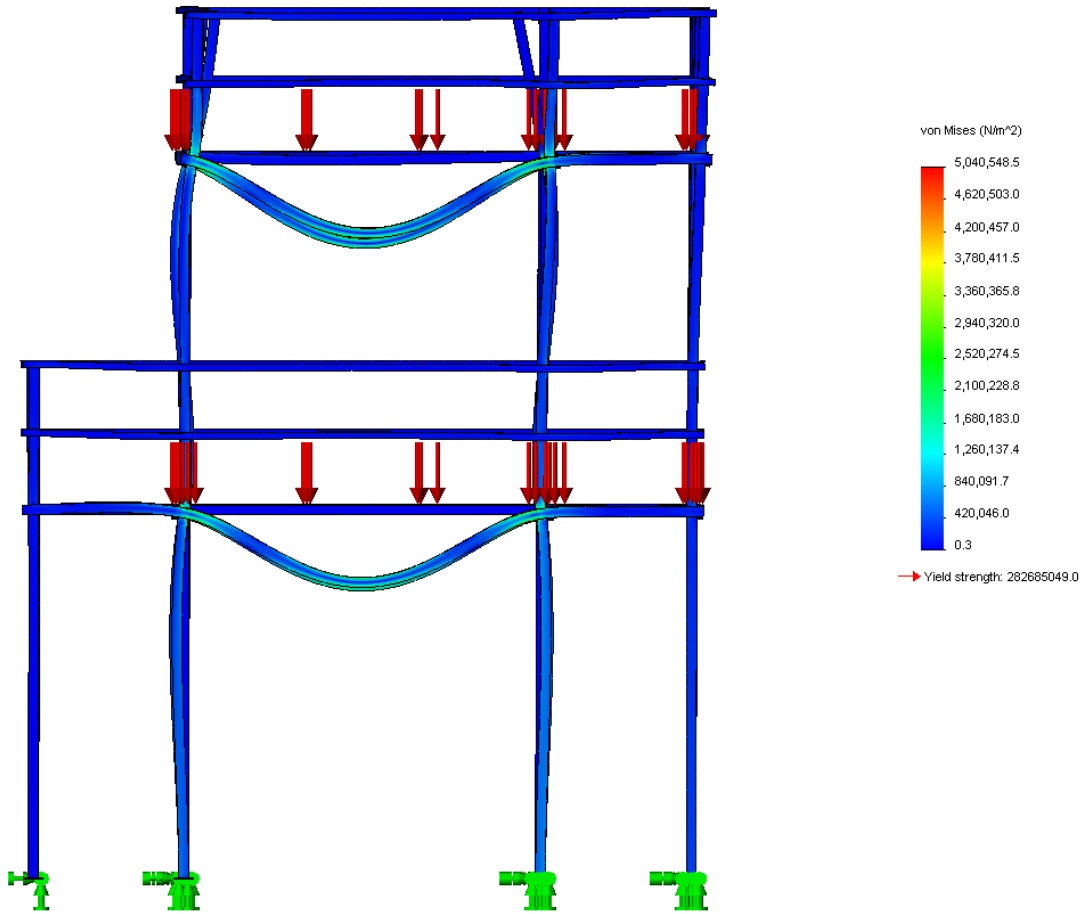
## APPENDIX C – SOLIDWORKS STRUCTURE ANALYSIS



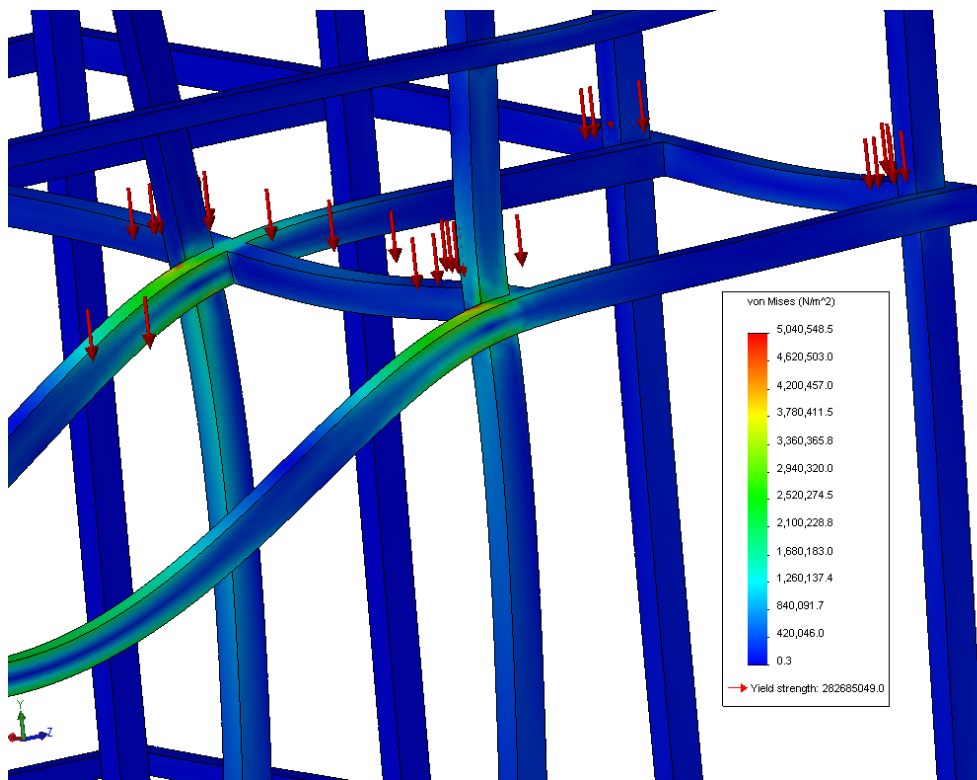
**C. 1 – Distributed Load + Point Load (Side View).**



**C. 2 – Distributed Load + Point Load (Zoom)**

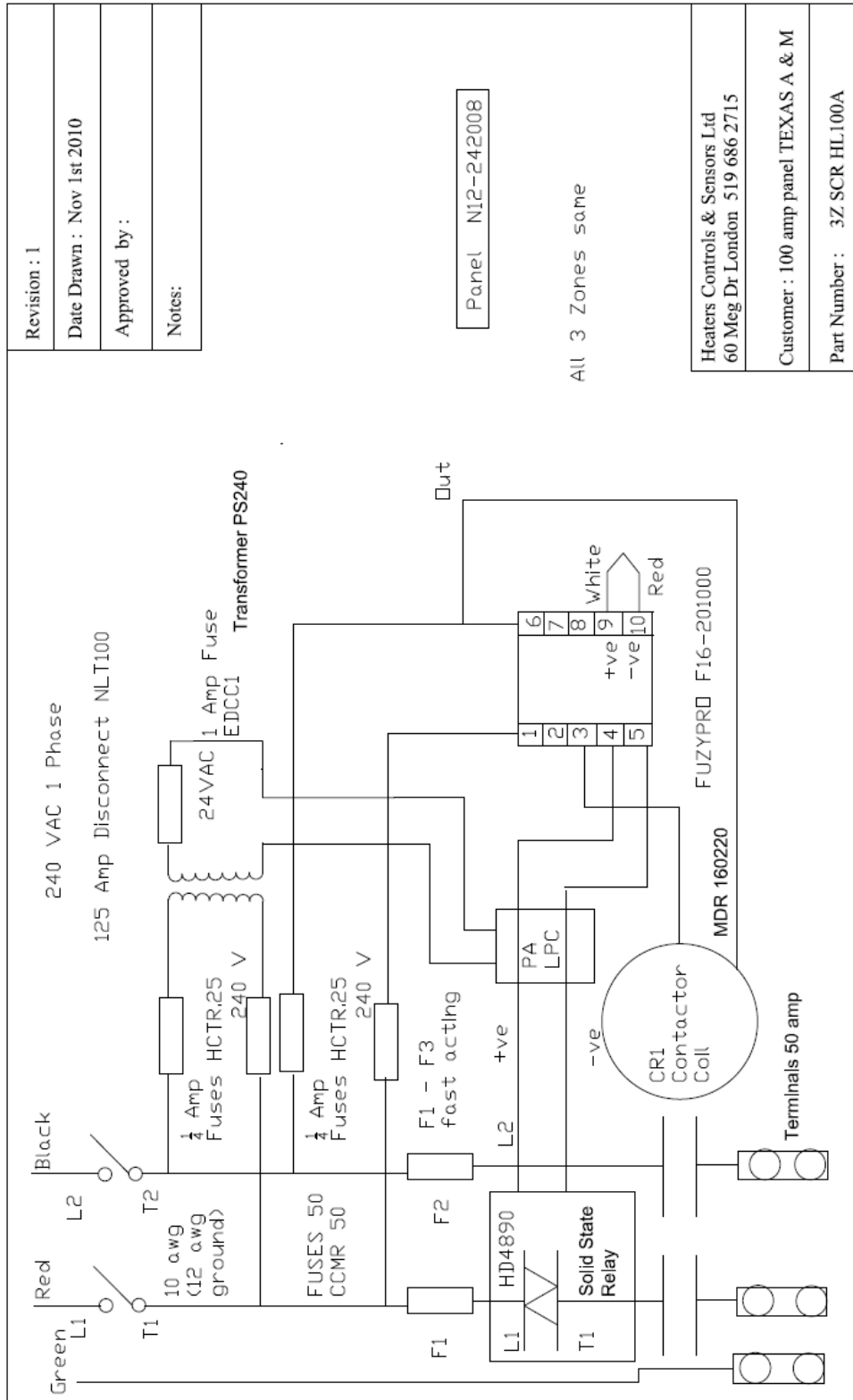


**C. 3 – Distributed Load (Side View)**



**C. 4 – Distributed Load (Zoom)**





Revision : 1

Date Drawn : Nov 1st 2010

Approved by :

Notes:

Heaters Controls & Sensors Ltd  
60 Meg Dr London 519 686 2715

Customer : 100 amp panel TEXAS A & M

Part Number : 3Z SCR HL100A



Titanium Dioxide								
Y	N	35.3	013463-67-7	10 mg/M3	10 mg/M3	N/E	N/E	N/A
-----								
Diatomaceous Earth								
Y	N	12.9	061790-53-2	10 mg/M3	5 mg/M3	N/E	N/E	N/A
-----								
2-Propoxyethanol								
Y	Y	2.3	002807-30-9	N/E	25 ppm	N/E	N/E	1.3@20C
-----								

\*\*\*\*\*  
 This product contains one or more reported carcinogens or suspected carcinogens which are noted NTP, IARC, or OSHA-2 in the other limits recommended column.  
 \*\*\*\*\*

Note: This product contains pigments which may become a dust nuisance when removed by abrasive blasting, sanding, or grinding.  
 This product may contain small amounts of materials known to the State of California to cause cancer and reproductive harm.

-----  
 SECTION III PHYSICAL DATA  
 -----

BOIL RANGE: 116.0 to 343.0 WT/GL: 11.2 to 13.3 %VOL/VOL: 18.1 to 24.9  
 EVAPORATION RATE: SLOWER THAN ETHER VAPOR DENSITY: HEAVIER THAN AIR  
 -----

SECTION IV FIRE AND EXPLOSION HAZARD DATA  
 -----

D.O.T. FLAMMABILITY CLASS.: COMBUSTIBLE FLASH POINT: 105 F PMCC  
 LEL %: 0.6  
 EXTINGUISHING MEDIA: FOAM CO2 DRY CHEMICAL WATER FOG  
 UNUSUAL FIRE AND EXPLOSION HAZARDS:  
 Toxic gases may form when product burns.  
 Closed containers may burst if exposed to extreme heat or fire.  
 SPECIAL FIRE FIGHTING PROCEDURES:  
 Cool exposed containers with water. Use self-contained breathing apparatus.  
 Do not use water stream on burning liquid. Use self-contained breathing apparatus.  
 -----

SECTION V HEALTH HAZARD DATA  
 -----

IMPORTANT: Designed to be mixed with other components. The resulting material will have the hazards of all its components.  
 EFFECTS OF OVEREXPOSURE - ACUTE:  
 Inhalation - Harmful if inhaled. May affect the brain or nervous system causing dizziness, headache or nausea.  
 Contact - Causes eye burns.  
 Contact - Causes skin irritation.  
 Skin Absorption - Hazardous ingredients contained in this product have the capacity to be absorbed through the skin in sufficient quantities to cause systemic toxicity. See Safe Handling and Use Information (Section VIII).  
 Ingestion - Irritation of the digestive tract and nervous system depression (drowsiness, dizziness, loss of coordination and fatigue). Aspiration Hazard - This material can enter lungs during swallowing or vomiting and cause lung inflammation and damage.  
 EFFECTS OF OVEREXPOSURE - CHRONIC:  
 Contains: Crystalline Silica which has been determined to be carcinogenic to humans (1) by IARC when in respirable form. Risk of cancer depends on duration and level of inhalation exposure to dust from sanding the dried  
 -----

paint or spray mist.

NOTICE: Reports have associated permanent brain and nervous system damage with repeated, prolonged overexposure to solvents among persons engaged in the painting trade. Intentional misuse by deliberately concentrating and inhaling the contents may be harmful or fatal.

IARC has classified Ethyl Benzene as possibly carcinogenic for humans (2B). May cause allergic skin reaction.

MEDICAL CONDITIONS PRONE TO AGGRAVATION BY EXPOSURE:

None expected when used in accordance with Safe Handling and Use Information (Section VIII).

Material is extremely destructive to tissue of the mucous membranes and upper respiratory tract, eyes and skin.

Inhalation - May be fatal as a result of spasm, inflammation and edema of the larynx and bronchi, chemical pneumonitis and pulmonary edema.

PRIMARY ROUTE(S) OF ENTRY: DERMAL INHALATION INGESTION

EMERGENCY AND FIRST AID PROCEDURES :

Inhalation - Remove from hazard area, maintain breathing, call physician.

Skin Contact - Remove with soap and water.

Eye Contact - Flush immediately with large amounts of water. Call physician

Ingestion - Drink 1 or 2 glasses of water to dilute.

DO NOT induce vomiting. Call physician.

-----  
SECTION VI REACTIVITY DATA  
-----

STABILITY: STABLE under normal conditions

HAZARDOUS POLYMERIZATION WILL NOT OCCUR

HAZARDOUS DECOMPOSITION PRODUCTS:

Burning may produce carbon dioxide and carbon monoxide.

CONDITIONS TO AVOID: Elevated temperatures and build up of vapors

INCOMPATIBILITY (MATERIALS TO AVOID): None reasonably foreseeable.  
-----

SECTION VII SPILL OR LEAK PROCEDURES  
-----

STEPS TO BE TAKEN IN CASE MATERIAL IS RELEASED OR SPILLED:

Remove all sources of ignition. Avoid breathing vapors. Use non-sparking tools to return materials to container. Absorb residue with Fullers earth.

WASTE DISPOSAL METHOD:

Conventional procedures in compliance with local, state and federal regulations. Do not incinerate sealed containers.  
-----

SECTION VIII SAFE HANDLING AND USE INFORMATION  
-----

RESPIRATORY PROTECTION:

Wear a properly fitted vapor/particulate respirator approved by NIOSH for use with paints during application or sanding and until all vapors and spray mist are exhausted. In confined spaces or in situations where continuous spray operations are typical, or if proper respirator fit is not possible, wear a positive-pressure, supplied air respirator approved by NIOSH.

VENTILATION:

Adequate to maintain working atmosphere below T.L.V. and L.E.L.

(See Sect. II for ingredient data and concentrations). Mechanical exhaust may be required in confined areas.

Discharge exhaust only in area away from ignition sources.

PROTECTIVE GLOVES: Solvent impermeable gloves are required.

EYE PROTECTION : Splash goggles or safety glasses with side shields.

OTHER PROTECTIVE EQUIPMENT: Clothing adequate to protect skin.

**HYGIENIC PRACTICES:**

Remove and wash clothing before reuse. Wash hands before eating, smoking or using the washroom.

-----  
**SECTION IX SPECIAL PRECAUTIONS**  
-----

**PRECAUTIONS TO BE TAKEN IN HANDLING AND STORAGE:**

Flammable - Keep away from heat, sparks and flames.

**OTHER PRECAUTIONS :**

Corrosive

Use only with adequate ventilation. Avoid prolonged contact with skin and breathing of vapor spray mist or sanding dust.

Close container after each use. Keep out of reach of children. Do not take internally.

-----  
**SECTION XX**  
-----

HMIS (Hazardous Materials Identification System) (R) NPCA

HMIS is a recognized workplace Hazard Communications System as required by OSHA (29 CFR 1910.1200). Information on establishing a compliant hazardous communication program using HMIS is available from:

American Labelmark Co., Inc., Labelmaster Division  
5724 N. Pulaski Rd., Chicago, IL 60646  
1-800-621-5808

The ratings assigned by Benjamin Moore & Co. are only suggested ratings; the contractor/employer has ultimate responsibility for HMIS rating where this system is used.

**PERSONAL PROTECTION:** This code is left blank on Benjamin Moore & Co. MSDS's as it depends on application technique and the workplace ventilation. Please read Sections II through IX of this MSDS before deciding on appropriate protective equipment and beginning work. There are codes available for this section which can be obtained from Labelmaster. This product contains at least one toxic chemical listed in Section II that is subject to the reporting requirements of section 313 of the Emergency Planning and Community Right-To-Know Act of 1986 and 40 CFR 372.

-----  
**DISCLAIMER**  
-----

The information contained herein is presented in good faith and believed to be accurate as of the effective date shown above. This information is furnished without warranty of any kind. Employers should use this information only as a supplement to other information gathered by them and must make independent determination of suitability and completeness of information from all sources to assure proper use of these materials and the safety and health of employees. Any use of this data and information must be determined by the user to be in accordance with applicable federal, state and local laws and regulations.

**NOTICE:** Removal of old paint by sanding, scraping or other means may generate dust or fumes which contain lead. Exposure to lead dust or fumes may cause adverse health effects, especially in children or pregnant women. Controlling exposure to lead or other hazardous substances requires the use of proper protective equipment, such as a properly fitted respirator (NIOSH approved) and proper containment and cleanup. For additional information, contact the USEPA/Lead Information Hotline at 1-800-LEAD-FYI.



## M45 / M46 Epoxy Mastic Coating

### Features

- Self-priming
- High build
- Exceptional adhesion
- Apply over tightly adhering rust
- Good flexibility
- Good impact resistance
- Good wetting properties
- Reduced undercutting at damaged areas
- Reduced number of coats required
- High solids
- Low VOC content
- Reduced pinholing
- No lifting of conventional coatings
- Immersion in fresh or salt water
- Interior or exterior application
- High traffic floors

### Recommended For:

- Bulk storage tanks
- Structural and support steel
- Off-shore rigs
- Roof decks
- Bar joists
- Piping
- Catwalks
- Water and waste treatment plants
- Dairies
- Bottling plants
- Power generating plants
- Food processing
- Hospitals
- Schools
- Performs well as an encapsulating coating

### General Properties

This two-component high build epoxy is self-priming and has exceptional adhesion even over tightly adhering rust. It also has good flexibility and impact resistance, plus good wetting properties, almost eliminating undercutting at damaged areas. The high solids provide exceptional coverage and the low solvent reduces pinholes and lifting of conventional coatings. May be used as a high build primer, an intermediate coat or single coat interior applications. Minimum two coats for exterior applications. For immersion use in fresh or saltwater.

### Limitations:

- Not for immersion in low pH liquids
- Not for immersion in strong solvents
- Not for application on high abuse floors
- Tendency to yellow on exterior surfaces
- Limited low temperature cure
- Limited gloss retention on exterior surfaces

### Product Information

#### Mixing Instructions:

This two-component product is mixed as a 1 to 1 ratio by volume of components "A" to "B." First, mix each component separately until uniform, then combine components "A" & "B" and mix thoroughly (5 minutes) or until homogeneous. For best results, use a spiral mixing blade in a variable speed (400-600 rpm) electric drill. Place the spiral mixing blade at the bottom of the container before turning on the mixer. This will help avoid inducting air into the material. Inducted air will cause "bubbles" in the coating when applied. Gently move the mixer head up to the surface while running. Do not remove the head while it is still spinning. Allow the combined components to sit for an induction time of 30 minutes, then lightly stir again to ensure uniformity. This product has a workable pot life of 6 hours at 70° F. Applying the material immediately after the 30 minute's induction time will provide best results. **Note:** Higher air and mixture temperatures will decrease the pot life and working time.

#### Colors: ALL MUST BE MIXED WITH M46-84 CATALYST

—Tint Bases: M45-90 Tintable White  
M45-91 Deep Base  
M45-92 Clear Base

—Special Colors: Contact your Benjamin Moore & Co. Representative

#### Certification:

Master Painters Institute MPI #108.  
Formulated without lead, mercury, or chromates.  
Does not contain any ozone-depleting substances, either Class I or Class II.

#### Analysis:

M45-90 F. ac/ml/mix M46-84 E	Vehicle: 60.0%
Pigment: 36.0%	Amido Amine Epoxy Resin: 74.0%
Titanium Dioxide: 20.2%	Solvents & Additive: 25.4%
Inhibitive Pigments: 41.3%	100.0%
Inert Pigments: 100.0%	

#### Technical Data

Generic Type	Amido Amine Epoxy
Pigment Type	Titanium Dioxide & Corrosion Inhibitors
Volume Solids (mixed as recommended)	78%
Theoretical Coverage	315 Sq. Ft. @ 4 Mils
Film Thickness – Wet	3.8 – 10 mils
– Dry	3 – 5 mils
Dry Time @ 70° F – To Touch	4 Hours
– To Recoat	8 Hours
Dries By	Chemical Cure
Dry Heat Resistance – Intermittent	350° F
Viscosity @ 70° F (mixed as recommended)	90 ± 5 KU
Flash Point (Seta)	102° F
60° Specular Gloss – Semi-Gloss	30% – 50%
Surface Temperature At Application – Min.	40° F
– Max.	90° F
Surface must be dry and at least 5° above the dew point.	
Reducer	M95
Reduction – Brush	5%
– Roller	5%
– Spray	10%
Clean Up Thinner	M95
Mixing Ratio (by volume)	1:1
Induction Time @ 70° F	30 Minutes
Pot Life @ 70° F	6 Hours
Weight Per Gallon (mixed as recommended)	12.8 lbs
Storage Temperature – Min.	40° F
– Max.	90° F

#### Volatile Organic Compounds (VOC)

**Unthinned	Grams/Liter	199
	Lbs./Gal.	1.66

\*\*Contact Benjamin Moore & Co. for actual levels, which may or may not be substantially less than stated.



## M45 / M46 Epoxy Mastic Coating

### Primer Selection

#### Technical Information

	Ferrous Metal Hot or Cold Rolled Steel	Masonry Walls Poured, Cast or Brick	Block Walls Concrete-Cinder or Lt. Weight
Primer Product Code	M45/M46	CM36-00/M37-84	M31/M32
Generic Type	Amido Amine	Polyamide Epoxy	Waterborne Epoxy Block Filler
Pigment Type	Titanium Dioxide, Corrosion Inhibitors,	Clear	Organic Fibers and Select Inerts
Volume Solids	78%	54%	46%
Theoretical Coverage at Recommended Film Thickness	315 sq. ft.	430 sq. ft.	75 sq. ft.
Film Thickness - Wet - Dry	5.1 mils 4.0 mils	3.7 mils 2.0 mils	22 mils 10 mils
Dry Time - To Touch - To Recoat	4 hours 8 hours	1.5 hours 4 hours	2 hours 16 hours
Dries By	Chemical Cure	Chemical Cure	Chemical Cure
Dry Heat Resistance	300° F	300° F	260° F
Viscosity	85 KU ± 5	70 ± 5 KU	Mastic
Flash Point (Seta)	82° F	84° F	None
60° Specular Gloss	30-50%	85-95%	10% max.
Surface Temperature - Min. At Application - Max. <small>Surface must be dry and at least 5° above the dew point.</small>	40° F 90° F	60° F 90° F	60° F 95° F
Reducer	M95		Clean Water
Reduction - Brush - Roller - Spray	5% 5% 10%	do not thin do not thin do not thin	5% 5% 5%
Clean Up Thinner	M95	M95	Water followed by Xylol
Mixing Ratio (by volume)	1:1	1:1	1:1
Induction Time	30 minutes	30 minutes	30 minutes
Pot Life @ 70° F	6 hours	8 hours	8 hours
Weight Per Gallon	12.8 lbs.	8.5 lbs.	12.0 lbs.
Storage Temperature - Min. - Max.	40° F 90° F	40° F 90° F	40° F 90° F

Note: For additional information regarding primer selection — reference the primer selection chart in the product manual or in the product catalog.

### Primer Information

#### M45 / M46

Self-Priming

#### CM36-00 / M37-84

Can also be used for penetrating concrete floors, wood, and wood floors. Accepts a wide variety of high performance finish coats.

#### M31 / M32

Provides the bonding properties needed to support any two component product when used on high abuse surfaces, high moisture areas or below grade applications. Excellent for areas subjected to repeated cleaning with high pressure water. Protects surfaces in food processing plants, water & waste treatment plants, pulp and paper plants, dairies, bottling plants, and a host of others.

## Surface Preparation

### Bare Steel

All surfaces shall be free of loose rust, millscale, and contaminants such as oil, grease, dirt, and salts. Before any surface preparation is attempted, oil and grease must be removed by employing SSPC-SP1 Solvent Cleaning. For large areas, use Oil & Grease Emulsifier (M83).

### For Mild Exposures

Use Commercial Blast Cleaning to SSPC-SP6 to remove millscale, rust, and other contaminants and leave a roughened surface.  
Use Power Tool Cleaning to Bare Metal SSPC-SP11 to remove millscale, rust and other contaminants and leave a roughened surface.

### For Severe Exposures

Use Near-White Blast Cleaning to SSPC-SP10 to remove millscale, rust, and other contaminants and leave a roughened surface.

**WARNING!** If you scrape, sand or remove old paint, you may release lead dust. **LEAD IS TOXIC. EXPOSURE TO LEAD DUST CAN CAUSE SERIOUS ILLNESS, SUCH AS BRAIN DAMAGE, ESPECIALLY IN CHILDREN. PREGNANT WOMEN SHOULD ALSO AVOID EXPOSURE.** Wear a NIOSH-approved respirator to control lead exposure. Carefully clean up with a HEPA vacuum and a wet mop. Before you start, find out how to protect yourself and your family by contacting the National Lead Information Hotline at 1-800-424-LEAD or log on to [www.epa.gov/lead](http://www.epa.gov/lead).

## Application Information

Due to the rapid dry of this coating, only small areas may be coated by brush, applicator pad, or roller. Generally, this paint is best applied by spray. Care must be taken to achieve the specified wet and dry film thicknesses. Uniform, even coats must be obtained.

## Application Equipment

Conventional or airless spray, brush or roller. Certain colors may require two coats depending on method of application and color of the primer or intermediate coat.

### Conventional Spray

Equipment Recommendations: Binks Model 62 Spray Gun or equivalent.

Fluid Nozzle	Air Nozzle	Atomizing Air Pressure (Measured at gun inlet)	Fluid Pressure
66 (.070")	66 SK	60 PSI	40 PSI

Notes: Airless atomization strongly recommended. Do not exceed pot life.

Low temperatures or longer hoses require higher pot pressure. Proper atomization is necessary to obtain a smooth finish.

### Airless Spray

Equipment Recommendations: Binks Airless 1 Spray Gun or equivalent.

Airless Tip Orifice	Fluid Pressure	Binks Tip No.
.018" – .026"	2,500 – 3,000 PSI	9 – 1860/9 – 2680

Notes: Do not exceed pot life. Requires higher pressure pump.

CAUTION! Use 100 mesh manifold filter and gun with 100 mesh tip strainer. Use appropriate tip and atomizing pressure for equipment, applicator technique and weather conditions.

### Roller

Use a ¼" nap synthetic cover. Do not use medium or long nap roller covers.

## Clean Up Instructions

Clean all equipment immediately after use with Epoxy Thinner (M95). At the same time, flush out all fluid lines and carefully clean pressure pots. Use clean solvent only. It is also good practice to periodically clean the spray tip or the fluid tip/air cap combination during the course of the working day or shift.



## M45/M46 Epoxy Mastic Coating

### Performance Standards

All test results are for Safety White unless otherwise noted.

Description	Test	Results
<b>Adhesion</b>	ASTM D 3359 Cross Cut Tape Test Elcometer Adhesion	5B 400 P.S.I.
<b>Abrasion Resistance</b>	ASTM D 4060 C17 Wheels, 1000 gm Load, 1000 cycles	85 mg/1000 Cycles
<b>Impact Resistance</b>	ASTM D 2794 Gardner Impact, 7 Day Air Dry at 77° F	Direct 20 inch pounds, reverse 4 inch pounds
<b>Flexibility</b>	ASTM D 522 Conical Mandrel Apparatus	14%
<b>Chemical Resistance</b> ASTM D1308 24 Hour Covered Watch Glass Spot Test	5% NaOH	No Effect
	5% H <sub>2</sub> SO <sub>4</sub>	No Effect
	100% Xylene	No Effect
	100% Mineral Spirits	No Effect
<b>Hardness</b>	ASTM D3363 Pencil Hardness 7 Day Cure	6H
<b>Exterior Durability</b>	ASTM G53 Accelerated aging via exposure to fluorescent, ultraviolet, and condensation.	Yellows
<b>Salt Fog Resistance</b>	ASTM B117	500 Hours - No effect, 800 Hours - M#6 Blisters
<b>Immersion</b>	Ambient	1500 Hours - No effect
<b>Graffiti</b>	Resistance: Crayon: Good Litter: Good Lipstick: Good Marker: Good Ink Pen: Poor Shoe Polish: Good	
<b>Hot Water Immersion</b>	180° F	1500 Hours - No effect

### Environmental, Health & Safety Information

**WARNING!** COMBUSTIBLE LIQUID AND VAPOR! HARMFUL IF INHALED OR SWALLOWED

Contains xylene (xylo), n-butyl alcohol, tetraethylenepentamine, epoxy resin and crystalline silica: HARMFUL IF INHALED. MAY AFFECT THE BRAIN OR NERVOUS SYSTEM CAUSING DIZZINESS, HEADACHE, OR NAUSEA. MAY CAUSE EYE, SKIN, NOSE, AND THROAT IRRITATION. MAY CAUSE ALLERGIC SKIN REACTION.

**IMPORTANT:** Designed to be mixed with other components. Mixture will have hazards of both components. Before opening packages, read all warning labels. Follow all precautions.

**NOTICE:** Repeated and prolonged exposure to solvents may lead to permanent brain and nervous system damage. Eye watering, headaches, nausea, dizziness, and loss of coordination are signs that solvent levels are too high. Intentional misuse by deliberately concentrating and inhaling the contents may be harmful or fatal. Cancer Hazard: contains crystalline silica which can cause cancer when in respirable form.

Keep away from heat and flame. Close container after each use. Use only with adequate ventilation. Do not breathe vapors, spray mist, or sanding dust. Do not get in eyes or on skin.

WEAR A PROPERLY FITTED VAPOR/PARTICULATE RESPIRATOR APPROVED BY NIOSH for use with paints, eye protection, gloves, and protective clothing during application (or sanding) and until all vapors and spray mist are exhausted. In confined spaces or in situations where continuous spray operations are typical, or if proper respirator fit is not possible, wear a positive-pressure, supplied air respirator. In all cases, follow respirator manufacturer's directions. Do not permit anyone without protection in the painting area.

**FIRST AID:** If affected by inhalation of vapors or spray mist, remove to fresh air. In case of eye contact, flush immediately with plenty of water for at least 15 minutes and call a physician. For skin, wash thoroughly with soap and water. In case of ingestion, DO NOT induce vomiting. Get medical help immediately.

**IN CASE OF: FIRE** – Use foam, CO<sub>2</sub>, dry chemical, or water fog.

**SPILL** – Absorb with inert material and dispose of in accordance with applicable regulations.

**DISPOSAL:** Use completely or dispose of properly. This product contains organic solvents which may cause adverse effects to the environment if handled improperly. Disposal of waste containing either organic solvents or free-liquids in landfills is prohibited. Dry, empty containers may be recycled in a can recycling program. **Local disposal requirements vary; consult your sanitation department or state-designated environmental agency on disposal options.**

**FOR PROFESSIONAL USE ONLY KEEP OUT OF REACH OF CHILDREN**

Refer to Material Safety Data Sheet available from your retailer for further safety and handling information.

### Warranty & Limitation of Sellers Liability

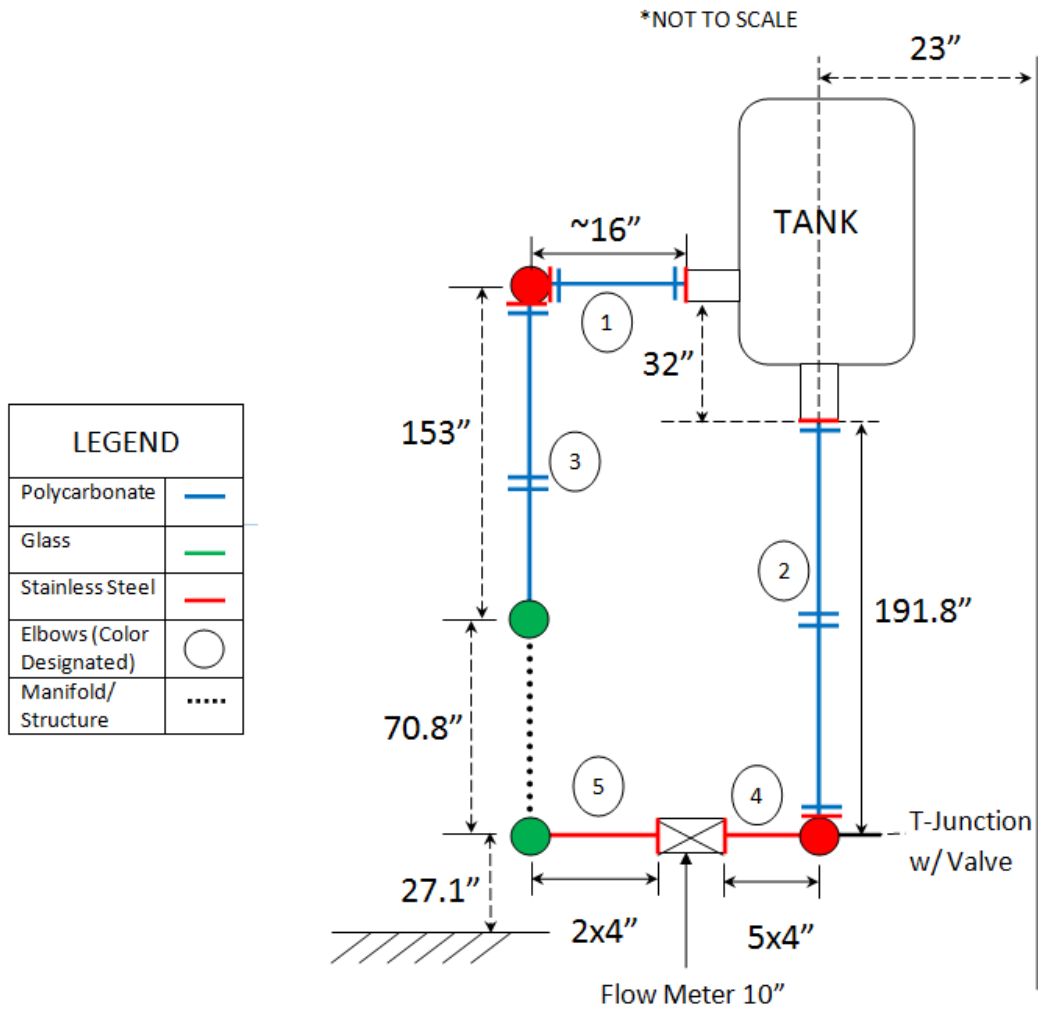
All statements made on any product label, product manual, product data sheets, technical data charts or specification charts contained herein, are accurate to the best of our knowledge. The products and information are intended for use by persons having skill and know-how in the industry at their own discretion and risk. Benjamin Moore & Co. warrants only that its coatings represented herein meet the formulation standards of Benjamin Moore & Co. NO OTHER WARRANTY OR GUARANTEE OF ANY KIND IS MADE BY THE SELLER, EXPRESSED OR IMPLIED, STATUTORY, BY OPERATION OR LAW, OR OTHERWISE INCLUDING MERCHANTABILITY AND FITNESS FOR A PARTICULAR PURPOSE. Workmanship, weather, construction equipment, quality of other materials and other variables affecting the results are beyond our control. No agent, employee or representative of seller has any authority to bind seller to any affirmation, representation or warranty except as stated above.

Benjamin Moore & Co., 51 Chestnut Ridge Road, Montvale, NJ 07645 Tel: (201) 573-9600  
The triangle "M" device is a registered trademark, licensed to Benjamin Moore & Co.

Fax: (201) 573-9046 www.benjaminmoore.com  
© 2000, 2005 Benjamin Moore & Co. All rights reserved

M73 M4500 8/05  
Litho in USA

## APPENDIX F – PIPING LAYOUT CALCULATIONS





## Materials Data

Part	Material	Length
1	Polycarbonate	~16"/.41m
2	Polycarbonate	172"/4.37m
3	Polycarbonate	139.3"/3.54m
4	Stainless Steel	20"/.51m
5	Stainless Steel	8"/.2m
6	Stainless Steel	33"/.838 m
7	Glass (Attached to Manifold)	10"/.38m
8	Glass (Attached to Manifold)	14"/.38m
9	Polycarbonate	32"/.838 m

\* Thermal expansion for above piping was determined to be negligible.

### Thermal Expansion for Structure

Thermal Expansion Coefficient for Stainless Steel (304) =  $\kappa$  = 17.3

Vertical Expansion = 2.08 mm

Horizontal Expansion = 1.64 mm

Expansion between Pipes = .176 mm

### Ring Clamp

OD 4.5"

Total Rings: 20 (16)

ID# 8946K36 (mcmaster.com)

OD 2.875"

Total Rings 40 (36)

ID# 5443K29 (mcmaster.com) 20 (18)

ID# 8946K52 (mcmaster.com) 20 (18)

Item	Specifications	Quantity
Polycarbonate Pipe	ID 4", OD 4.25" x 96"	5
Polycarbonate Flange		13
Stainless Steel Pipe	61"	
Stainless Steel Flange		9
Stainless Steel Elbow	ID 4" , OD 4.25"	3

**Flange Specifications:**

33142829D

4" ANSI B16.5 4501b A105N

171954 TDU264-TS

**Final Notes:** Parts 7 and 8 are measured from edge of manifold to center of elbow. Elbow will come attached to actual piping.

Outer diameter of stainless steel is variable, only critical value is that pipe, flange, and elbow all match.

For specifications of flanges, see Solid Works drawing.

APPENDIX G – RISERS' PANLE WELDING CERTIFICATE

**Madewell LLC**

Page 1 of 4

**Welding Procedure Specification**

MW.GTAW.PQ.-001

---

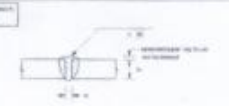
WPS No. MW.GTAW.PQ.-001 Revision 0 Date 12/14/2010 By Tim Shaw AWS/SCWI

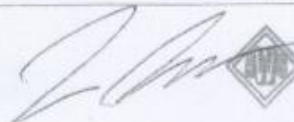
Authorized By Armando Cepeda Date 12/14/2010 Prequalified

Welding Process(es) GTAW Type: Manual  Machine  Semi-Auto  Auto

Supporting PQR(s) n/a

---

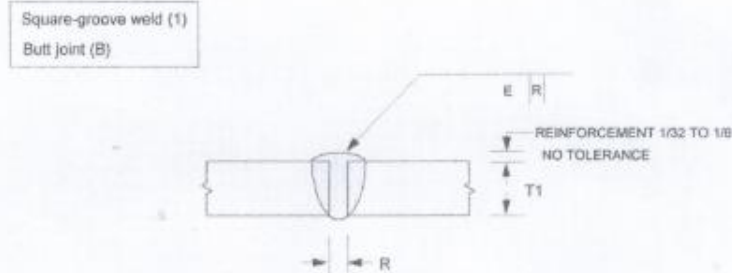
<p><b>JOINT</b></p> <p>Type <u>Grooves/Filletts [as detailed]</u></p> <p>Backing Yes <input checked="" type="checkbox"/> No <input type="checkbox"/> Single Weld <input checked="" type="checkbox"/> Double Weld <input type="checkbox"/></p> <p>Backing Material <u>Memo Note 1] b)</u></p> <p>Root Opening <u>As Detailed</u> Root Face Dimension <u>As Detailed</u></p> <p>Groove Angle <u>As Detail</u> Radius (J-U) <u>As Detail</u></p> <p>Back Gouge Yes <input checked="" type="checkbox"/> No <input type="checkbox"/></p> <p>Method <u>Air Arc and/or Grind</u></p>	<p><b>Sample Joint 1</b></p>  <table border="1" style="width: 100%; border-collapse: collapse; margin-top: 10px;"> <thead> <tr> <th>Layer</th> <th>Process</th> <th>Filler Metal Class</th> <th>Diameter</th> <th>Cur. Type</th> <th>Amps or WFS</th> <th>Volts</th> <th>Travel Speed</th> <th>Other Notes</th> </tr> </thead> <tbody> <tr> <td>All Passes</td> <td>GTAW</td> <td>308L, 309L, 316(L), 347</td> <td>.063, .095, .125 (in.)</td> <td>DCEN</td> <td>60-250</td> <td>10-19</td> <td>4-12 ipm</td> <td>3/32" electrode</td> </tr> <tr> <td>All Passes</td> <td>GTAW</td> <td>308L, 309L, 316(L), 347</td> <td>.093, .125 (in.)</td> <td>DCEN</td> <td>100-350</td> <td>11-22</td> <td>4-12 ipm</td> <td>1/8" electrode</td> </tr> </tbody> </table>	Layer	Process	Filler Metal Class	Diameter	Cur. Type	Amps or WFS	Volts	Travel Speed	Other Notes	All Passes	GTAW	308L, 309L, 316(L), 347	.063, .095, .125 (in.)	DCEN	60-250	10-19	4-12 ipm	3/32" electrode	All Passes	GTAW	308L, 309L, 316(L), 347	.093, .125 (in.)	DCEN	100-350	11-22	4-12 ipm	1/8" electrode
Layer	Process	Filler Metal Class	Diameter	Cur. Type	Amps or WFS	Volts	Travel Speed	Other Notes																				
All Passes	GTAW	308L, 309L, 316(L), 347	.063, .095, .125 (in.)	DCEN	60-250	10-19	4-12 ipm	3/32" electrode																				
All Passes	GTAW	308L, 309L, 316(L), 347	.093, .125 (in.)	DCEN	100-350	11-22	4-12 ipm	1/8" electrode																				
<p><b>BASE METALS</b></p> <p>Material Spec. <u>Groups A &amp; B</u> to <u>Groups A &amp; B</u></p> <p>Type or Grade <u>As Listed in</u> to <u>Groups A &amp; B</u></p> <p>Thickness: Groove ( ) Ref. Memo- <u>--1]a)</u></p> <p>Fillet ( ) Ref. Memo- <u>--1]a)</u></p> <p>Diameter (Pipe, in ) <u>.250" min</u> - <u>Unlimited</u></p>	<p><b>POSITION</b></p> <p>Position of Groove <u>F,H,V,OH</u> Fillet <u>F,H,V,OH</u></p> <p>Vertical Progression: <input checked="" type="checkbox"/> Up <input checked="" type="checkbox"/> Down</p>																											
<p><b>FILLER METALS</b></p> <p>AWS Specification <u>A 5.9</u> <u>A5.9</u></p> <p>AWS Classification <u>ER308L</u> <u>ER316(L)</u></p> <p><u>ER309L</u> <u>ER347</u></p>	<p><b>ELECTRICAL CHARACTERISTICS</b></p> <p>Transfer Mode (GMAW):</p> <p>Short-Circuiting <input type="checkbox"/> Globular <input type="checkbox"/> Spray <input type="checkbox"/></p> <p>Current: AC <input type="checkbox"/> DCEP <input type="checkbox"/> DCEN <input checked="" type="checkbox"/> Pulsed <input checked="" type="checkbox"/></p> <p>Other <u>CC / DCEN only, Pulsed Optional.</u></p> <p>Tungsten Electrode (GTAW):</p> <p>Size <u>3/32-1/8X7</u> Type <u>2% Thoriated A5.12</u></p>																											
<p><b>SHIELDING</b></p> <p>Flux <u>n/a</u> Gas <u>Argon</u></p> <p>Composition <u>100%</u></p> <p>Electrode-Flux (Class) <u>n/a</u> Flow Rate <u>15-35 CFH</u></p> <p><u>n/a</u> Gas Cup Size <u>.375"- .500"</u></p>	<p><b>TECHNIQUE</b></p> <p>Stringer or Weave Bead <u>Both</u></p> <p>Multi-pass or Single Pass (per side) <u>Both</u></p> <p>Number of Electrodes <u>1</u></p> <p>Electrode Spacing: Longitudinal <u>n/a</u></p> <p>Lateral <u>n/a</u></p> <p>Angle <u>n/a</u></p> <p>Contact Tube to Work Distance <u>.5" - .75"</u></p> <p>Peening <u>none</u></p> <p>Interpass Cleaning <u>Memo Note 1] e).</u></p>																											
<p><b>PREHEAT</b></p> <p>Preheat Temp., Min. <u>Memo 1] d)</u></p> <p>Thickness Up to 3/4" Temperature <u>32F</u></p> <p>Over 3/4" to 1-1/2" <u>n/a</u></p> <p>Over 1-1/2" to 2-1/2" <u>n/a</u></p> <p>Over 2-1/2" <u>n/a</u></p> <p>Interpass Temp., Min. <u>Memo 1] d)</u> Max. <u>350F</u></p>	<p><b>POSTWELD HEAT TREATMENT</b> PWHT Required <input type="checkbox"/></p> <p>Temp. <u>n/a</u> Time <u>n/a</u></p>																											
<p><b>WELDING PROCEDURE</b></p>																												
<table border="1" style="width: 100%; border-collapse: collapse;"> <thead> <tr> <th>Layer/Pass</th> <th>Process</th> <th>Filler Metal Class</th> <th>Diameter</th> <th>Cur. Type</th> <th>Amps or WFS</th> <th>Volts</th> <th>Travel Speed</th> <th>Other Notes</th> </tr> </thead> <tbody> <tr> <td>All Passes</td> <td>GTAW</td> <td>308L, 309L, 316(L), 347</td> <td>.063, .095, .125 (in.)</td> <td>DCEN</td> <td>60-250</td> <td>10-19</td> <td>4-12 ipm</td> <td>3/32" electrode</td> </tr> <tr> <td>All Passes</td> <td>GTAW</td> <td>308L, 309L, 316(L), 347</td> <td>.093, .125 (in.)</td> <td>DCEN</td> <td>100-350</td> <td>11-22</td> <td>4-12 ipm</td> <td>1/8" electrode</td> </tr> </tbody> </table>		Layer/Pass	Process	Filler Metal Class	Diameter	Cur. Type	Amps or WFS	Volts	Travel Speed	Other Notes	All Passes	GTAW	308L, 309L, 316(L), 347	.063, .095, .125 (in.)	DCEN	60-250	10-19	4-12 ipm	3/32" electrode	All Passes	GTAW	308L, 309L, 316(L), 347	.093, .125 (in.)	DCEN	100-350	11-22	4-12 ipm	1/8" electrode
Layer/Pass	Process	Filler Metal Class	Diameter	Cur. Type	Amps or WFS	Volts	Travel Speed	Other Notes																				
All Passes	GTAW	308L, 309L, 316(L), 347	.063, .095, .125 (in.)	DCEN	60-250	10-19	4-12 ipm	3/32" electrode																				
All Passes	GTAW	308L, 309L, 316(L), 347	.093, .125 (in.)	DCEN	100-350	11-22	4-12 ipm	1/8" electrode																				



 Timothy A Shaw  
 SCWI 10010038  
 QC1 EXP. 1/1/2013

**Madewell LLC**  
**Welding Procedure Specification**

**Sample Joint 1**



Welding Process	Joint Designation	Base Metal Thickness (U=unlimited)		Groove Preparation			Permitted Welding Positions	Weld Size (E)	Notes
		T1	T2	Root Opening	Tolerances				
					As Detailed (see 3.12.3)	As Fit Up (see 3.12.3)			
GTAW	B-P1a	16 gauge min. .75" max.	-	R = 0 to T/2	+T/2, -0	±T/2	F	3/4	8.0.0

**MEMO**

1] This WPS is prequalified and exempt from testing per AWS/D1.6 [2007]. Requirements for prequalification have been met as set forth in Clause 3.0. All references to Clauses, Sub-Clauses, Tables, and Figures here-in are in reference to ANSI/AWS D1.6, 2007 edition. Notes 1) a) through e) are basic requirement clarifications for the intended users of this WPS. In addition, this procedure is subject to all other applicable requirements of AWS D1.6.

- a) All GTAW PJP and CJP groove configurations detailed in Fig. 3.4, Fig. 3.5, and Fig. 3.6 are permitted for use with this WPS. Fillet Joints detailed in Fig. 3.2 and Fig. 3.3 are also permitted for use. Joint configurations detailed on pages 2 and 4 of this WPS are sample configurations and prequalified limits. It is not intended to limit this WPS to these joint details.
- b) When steel backing is used it shall be made from the same base metal group (A or B). [Ref. Sub-Clause 3.8]. For additional backing requirements and options reference Sub-Clause 3.29 (9) (10) and Sub-Clause 5.6.
- c) Welding positions are F, H, V, & OH. Whenever practicable welds shall be done in the Flat position. [ Ref. Sub-Clause 3.29(5)]. Vertical downhill welding that complies with Sub-Clause 3.29 (8) may be used.

**Madewell LLC**  
**Welding Procedure Specification**

Page 3 of 4

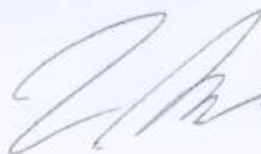
MW.GTAW.PQ.-001

**MEMO (continue)**

d) The minimum preheat shall be sufficient to remove moisture from the work. [Ref. Sub-Clause 3.29(3)]. Additional preheat and interpass temperatures requirements are listed in Sub-Clause 5.1.2.1. Maximum Interpass is 350F. Additionally, proper techniques are required to avoid excessive preheat and interpass temperatures for each type of joint configuration.

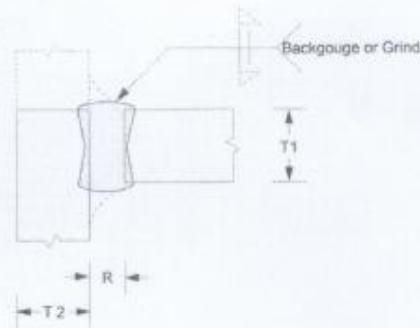
e) Where brushes are used, the brush wires shall be made of stainless steel materials. Grinding shall be done with iron free abrasive wheels. [Ref. Sub-Clause 5.10].

2] This WPS is the sole property of Madewell LLC. Any disturbance, use, or alterations of this WPS is not permitted without prior consent of Madewell LLC.

  Timothy A Shaw  
SCWI 10010038  
QC1 EXP. 1/1/2013

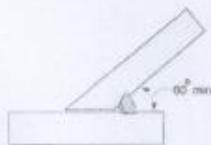
Sample Joint 2

Square-groove weld (1)  
T-joint (T)  
Corner joint (C)



Welding Process	Joint Designation	BM Thickness (U=unlimited)		Root Opening	Groove Preparation Tolerances		Permitted Welding Positions	Notes
		T1	T2		As Detailed (see 3.13.1)	As FR Up (see 3.13.1)		
		GTAW	TC-L1b		16 gauge min. .75" max.	U		

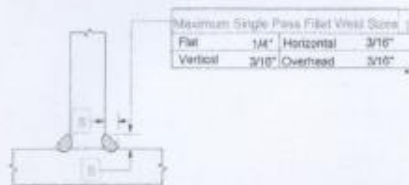
D1.6 PQ Limits



Acute Angular Limit  
For Proqualiflat Skewed T-Joints  
(Ref. Figure 3.3 (note 4))

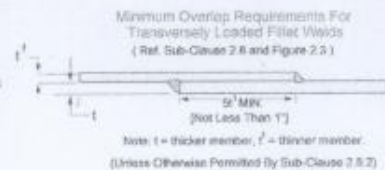
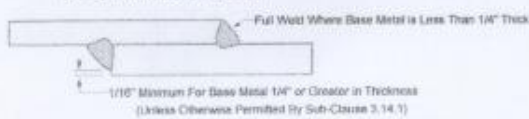


Weld Pass Dimensions (All Weld Types and Positions)	
R	Max. Root Pass Thickness = 1/4"
T	Max. Fill Pass Thickness = 1/8"
W	Max. Single Pass Layer Width = 1/2"

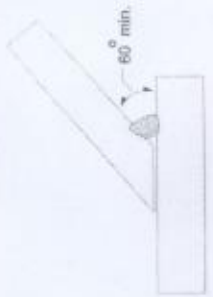


Maximum Single Pass Fillet Weld Sizes	
Flat	1/4"
Horizontal	3/16"
Vertical	3/16"
Overhead	3/16"

Maximum Fillet Weld Size Along Edges of Lap Joints  
(Ref. Sub-Clause 3.14 and Figure 3.2)

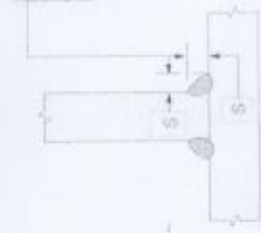


# AWS D1.6 [2007] GTAW Prequalified Limits



Acute Angular Limit  
For Prequalified Skewed T-Joints  
(Ref. Figure 3.3 (note 4).)

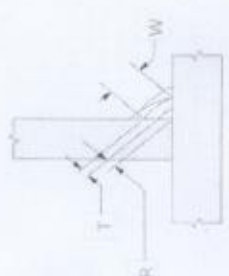
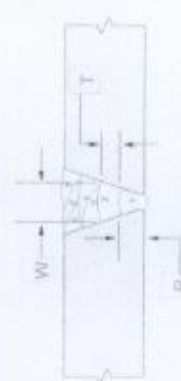
Maximum Single Pass Fillet Weld Sizes S	
Flat	1/4" Horizontal 3/16" Overhead
Vertical	3/16"



Maximum Fillet Weld Size Along Edges of Lap Joints  
(Ref. Sub-Clause 3.14 and Figure 3.2)

Full Weld Where Base Metal is Less Than 1/4" Thick

Weld Pass Dimensions (All Weld Types and Positions)	
R	Max. Root Pass Thickness = 1/4"
T	Max. Fill Pass Thickness = 1/8"
W	Max. Single Pass Layer Width = 1/2"

Minimum Overlap Requirements For  
Transversely Loaded Fillet Welds  
(Ref. Sub-Clause 2.8 and Figure 2.3)



Note: t = thicker member, t' = thinner member.  
(Unless Otherwise Permitted By Sub-Clause 2.8.2)

  
**Timothy A. Shaw**  
 SCWI 10010038  
 QC1 EXP. 1/1/2013

## APPENDIX H – EPOXY GLUE SPECIFICATIONS

### UNIQUE METALLIC ADHESIVES AND PUTTIES High Bond Strength, Thermal Shock and Impact Resistance

#### DURABOND™ 950 - 952 - 954 2000°F Metallic Adhesives

Durabond Adhesives and Putties were specially formulated to bond metals, ceramics and dissimilar materials for use to 2000°F.

These metallic composite adhesives overcome the brittle bonds obtained with ceramics and offer some of the ductility and impact resistance associated with soldering and welding. Durabond adhesives can be drilled, tapped, machined, etc.

They do not contain Epoxies or Silicones which would limit their use to 600°F.

These composites are inorganically bonded and chemically cured.

They are safe and easy to use. No odors. No VOC's.

Just mix, apply and cure at room temperature.

**Fast Setting Durabond Composites (type FS)** are now available. These smooth, creamy, putties are ideal for repairs, patching, casting, potting, etc.

DURABOND	950	952	954
Use Temp °F	1200	2000	2000
Base	Aluminum	Nickel	Stainless
Color	Grey	Grey	Grey
Density (# / ft <sup>3</sup> )	120	180	180
Thermal Expansion (10 <sup>-6</sup> /°F)	10	4	10
Pot Life (Hours)	2	2	2
Bond Strength @ 200°F (psi)	500	400	600
Bond Strength @ 1200°F (psi)	1000	1200	1400
Components	2	2	2
Mixed Ratio (A / B)	100/60	100/120	100/25
Cure (@ R.T.)	24	24	24

#### Aluminum Durabond 950 - Usable to 1200°F

This adhesive was developed for high strength and high temp. bonding. Its easy to apply and cures at low temp. Use with steel, cast iron, aluminum, copper, etc.

Its easily machinable. Can be ground, sanded or polished.

#### Nickel Durabond 952 - Usable to 2000°F

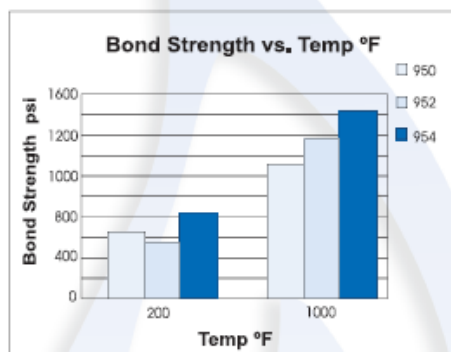
952 was specially formulated to be a low expansion, metallic adhesive for bonding 400 series Stainless Steel, low expansion high temp. alloys, metals and ceramics, etc.

#### Stainless Steel Durabond 954 - Usable to 2000°F

954 is a high expansion adhesive for high temp. bonding of 300 series Stainless, high expansion metals, ceramics, etc.

#### NEW, Stainless Steel, Sealing Adhesive - Usable to 2000°F

**954OD** bonds and seals high expansion materials. Ideal for applications requiring the minimum porosity from a ceramic adhesive. Commonly used to prevent leaks from equipment.



**Durabond 954 Bonds a Stainless Filter Cartridge for use at 1200°F**

Cat. No.	Base	Type	Size
950-1	Aluminum	Adhesive	Pint
950-2	Aluminum	Adhesive	Quart
950FS-1	Aluminum	Putty	Pint
952-1	Nickel	Adhesive	Pint
952-2	Nickel	Adhesive	Quart
952FS-1	Nickel	Putty	Pint
954-1	Stainless	Adhesive	Pint
954-2	Stainless	Adhesive	Quart
954FS-1	Stainless	Putty	Pint
954OD-1	Stainless	Sealer	Pint
954OD-2	Stainless	Sealer	Quart

**Now Available, Pre-Measured Kits  
Ideal for Field Applications**

**COTRONICS CORP. | 33**

# APPENDIX I – PROJECT SAFETY ANALYSIS (PSA)

Engineering Program  
Texas A&M University

Look College of Engineering  
Texas Engineering Experiment Station

## Guide to Project Safety Analysis (PSA)

---

### PROJECT IDENTIFICATION SECTION

Project Name:  
Computational Fluid Dynamics Model Development and Validation for High Temperature Gas-Cooled Reactor Cavity Cooling System (RCCS) Application

TEES Project Number (if applicable): 32525 / A8340 / NE

Project Description (abstract or executive summary):  
The purpose of the project will be to study the thermohydraulic phenomena in the water-cooled Reactor Cavity Cooling System with particular attention to the behavior of the coolant flow through the risers, downcomer and into the water tank. The experimental activity will produce a set of measurements (wall temperature profiles, coolant temperatures, pressures, mass flow rates etc) that will be used to validate computer codes such as RELAP5-3D and CDF.

Principal Investigator:  
Name: Hassan, Yassin A.  
Department/Division: Department of Nuclear Engineering  
Office Location: 130E Zachry Engineering Center  
Office Phone Number: 979 845-7090  
Email: y-hassan@tamu.edu

Researchers:  
(List all project personnel: Faculty, PI, Students or Staff)  
Rodolfo Vaghetto, Luigi Capone, Saya Lee, Colton J. Hermes, Dimitri MICHAELIDES  
Department/Division: Department of Nuclear Engineering  
Office Location: 129 Zachry Engineering Center  
Office Phone Number: (979) 845-4161  
Email: r.vaghetto@tamu.edu (reference)

Location of Project Facilities:  
Building No: 3400  
Building Name: USB  
Room No: Aerospace Laboratory / SSIL

Project Duration (projected dates): 10/01/2009 - 09/30/2012

---

### REVIEW & AUTHORIZATION SECTION

The attached Project Safety Analysis has been reviewed by the undersigned. Any major modifications of equipment or changes in procedures will require additional review by the Departmental Safety Committee, and/or the Departmental Safety Officer, and the Department Head. In executing this work, you must abide by the Safety Procedures of the Department and University and must inform the Departmental Safety Officer of any changes in personnel or operations outside these procedures.

Faculty/PI:



Date:

2-15-2011

Department Head:



Date:

2/14/11

Dept. Safety Officer:

Date:

Manager, Engineering Safety

Date:

---

## Guide to Project Safety Analysis (PSA)

---

### STRATEGY SECTION

#### Purpose of Project Safety Analysis:

PSA provides the Principal Investigator with the opportunity to review the environmental health, safety and security aspects of the research project to be undertaken, to identify known and potential hazards, to assess risks, and to select and implement necessary protective controls. This will help protect the researchers, graduate students, and staff involved with the project, reduce risk, ensure compliance, and conserve environmental resources, and protect facilities.

#### Scope:

All Principal Investigators shall file a written report on the safety analysis of each research project prior to the initiation of that exercise. The Project Safety Analysis (PSA) shall identify potential hazards and assess risks by the use of system safety analysis techniques, and shall detail the engineering and administrative controls that will be necessary to reduce risk to acceptable levels for the researchers, graduate students, and staff as well as the occupants of the building and the environment. The PSA will identify the costs, and the source of adequate funding, to implement necessary controls. It will identify necessary personnel training needs. The PSA will identify a plan for ultimate disposal of leftover equipment, materials and wastes, and the decontamination & clean up necessary to render the facility safe to reassign and reoccupy.

#### Extent of Applicability:

Recognizing that no activity is without some degree of risk, and that certain routine risks are accepted without question by the vast majority of persons (for example: machine shops that do not handle hazardous materials, cars used for personal transportation, etc.) the applicability of this analysis has been limited to those academic research projects that involve hazards not routinely encountered and accepted in the course of everyday living by the vast majority of the general public.

The analysis of a project which involves only hazards of a type and magnitude routinely encountered and accepted by the public will require justification which can be referenced to a recognized source.

#### Assistance in Conducting PSA

The Office of Engineering Safety is available to work with the Faculty/PI and research staff to identify hazards associated with the project, assess risks, and to identify necessary protective control measures.

---

Guide to Project Safety Analysis (PSA)

PROCEDURE SECTION

I) Apparatus Used in the Project

A) Equipment Used in the Experiment

*(List all equipment; describe it's use, and potential for injury an/or harmful exposure)*

The facility will be equipped with three electrical radiant heaters (240V, single phase, 7980W each). They will be connected and controlled by a dedicated power controller equipped with safety fuses. Electric safety switches will be installed on the wall. Water coolant flows in natural circulation inside 9 stainless steel pipes moving upward to a water tank. An electric water pumps will be installed to reach steady-state conditions and will be kept off during the experiments.

One personal computer and connected with peripherals (such as high resolution camera and temperature data acquisition system will be also installed and powered.

In a later phase of the experiment, a high speed laser (ESI® New Wave Research, Pegasus PIV, wavelength of 527 nm, maximum energy of 10 mJ per pulse) will be used as source of illumination for Particle Image Velocimetry technique. This laser is already located at USB and in use in the Nuclear Engineering laboratory for other experiments.

B) Experiments Performed in the Project

*(Attach a summary description of the project to be undertaken, research procedures, standard operating procedures (SOP), tasks, and safe work practices (SWP))*

Most of the experimental activity will focus on the measurements of the temperatures of cooling water and walls (standing pipes, fins, and vessel) and flow visualization. During the experiment water at atmospheric pressure and near the saturation point will be produced. Steam will be condensed and stored in a secondary water tank to be re-used in other experiments. No particular operating procedures are required to run the experiments in addition to the actual rules and procedures identified for the laboratory where the experimental facility will be built.

C) Chemicals Used in the Research Project:

*(List all chemicals to be used in the project)*

Required chemical inventory current and posted? <i>(Attach a copy of the current chemical inventory for this facility)</i>	N
Material Safety Data Sheets (MSDS)? <i>(Are current MSDS's available for all chemicals?)</i>	N
All stored chemicals segregated by Hazard Class? <i>(Stored chemicals must be segregated by Hazard Class.)</i>	N

II) Analysis of Potential Hazards

A) List all Physical Hazards That May Cause:

**Electrical Shock:** Electrical Heaters. Those parts of the facility will be identified and marked. During the operating phase, the area surrounding the heaters will be confined and closed. Metals structures will be grounded.

**Cuts:** Glass Panels and Manifolds only if broken. All the glass components will be protected with foam once installed

**Burns:** Hot surfaces. Surfaces will be thermally insulated during the experiments and labeled properly

**Abrasions:** N/A

**Slips:** Wet Floor if water is present. Water may leak during drainage of the facility. Water will be removed before starting any new experiment.

**Trips:** Possible Electric Cables running around the facility. Cables will be marked and covered.

**Falls:** From the ladder or any shelf of the main structure



---

Guide to Project Safety Analysis (PSA)

---

H) Personnel Training Needed for Specific Hazards

*(Identify the specific hazard and the individuals affected)*

All the individuals accessing the area and working on the experimental program will take the standard online laboratory safety training for Hazards Awareness. The laser machine will be operated only by personnel who passed the laser safety training.

Principal Investigator:  
Researcher/Lab Technician:  
Graduate Student:  
Student Workers:  
Other...

III) Potential Accidents and Responses *(What if ... ?)*

A) Utility Failure

<u>Utility:</u>	<u>Planned Response (SOP's):</u>
Electricity	Heaters will shut down
Gas	N/A
Air	N/A
Vacuum	N/A
Hot Water	It will cool down by natural circulation
Cold Water	N/A
Ventilation Hood	Not Required
Room/Lab Ventilation	Not Required

B) Leaks and Spills

MSDS Available:	N/A
Spill Kit Available:	N/A
PPE Available:	N/A
Containment Procedures:	N/A
Disposal Procedures:	N/A
Personnel Training:	N/A

C) Equipment Failure

*(Attach Documentation of All Emergency Shutdown Procedures)*

No special Procedures Required

D) Fire Prevention *(Attach the following)*

Laboratory Fire Prevention and procedures apply. No special procedures required.

Fire Extinguisher Locations:  
Building Emergency Evacuation Plan:  
Evacuation Routes:  
Emergency Response Procedure:  
Incident Reporting and Notification Procedure:

Guide to Project Safety Analysis (PSA)

---

IV) Equipment Labels

A) Utility Shut-offs labeled:

Electricity	Y
Vacuum	N/A
Gas	N/A
Air	N/A
Hot Water	N/A
Cold Water	N/A
Other...	

B) Identify all necessary Warning Signs:

Equipment:	Hot Surfaces
Instrumentation:	Laser in Use Sign
Utilities:	N/A
Personal Protective Equipment:	N/A
Reagent Bottles:	N/A
Secondary Containers:	N/A
Refrigerators and Microwaves:	N/A
Chemical Storage:	N/A
*Emergency Contact Information (ECI)	
	<i>(Must be posted on all entry door(s))</i>

V) Noise

Will the project/ generate excessive noise? N  
If yes, anticipated dBA is: \_\_\_\_\_

Type of hearing protection provided:

VI) List all Personnel Training Needs

Laboratory Safety Training *(Mandatory)*  
Hazard Communication Training *(Mandatory)*  
Shop & Tool Safety Training: N/A  
Safety Training Needs: N/A  
Standard Operating Procedures (SOP): N/A  
Safe Work Practices (SWP): N/A  
Other Project-Specific Training Needs...

---

Guide to Project Safety Analysis (PSA)

---

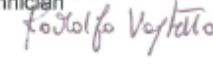
- VII) Standard Operating Procedures (SOP) for each Planned Procedure
- |  |     |
|--|-----|
| Safe Work Practices (SWP) Identified:          | N/A |
| Safe Work Practices Standardized & Documented: | N/A |
| Affected Personnel Trained on SOP's & SWP's:   | N/A |
- (Refer to training recordkeeping requirements)*
- VIII) Ultimate Disposal Plan
- {A detailed plan is required for the ultimate disposal of unused equipment, materials, chemicals and wastes following project conclusion; includes the plan for clean up and decontamination of instrumentation, equipment & facilities.}*
- The instrumentation used during the experimental activity will be uninstalled and moved in other laboratories for other activities. The metal structure will be de-assembled can be re-used for other experiments. Non-reusable parts will be wasted using the procedures required for glass, metal and plastic materials. The facility has no materials which require special treatments, clean up or decontamination.
- IX) List & attach all necessary Emergency Planning
- Refer to the Emergency Plan of the Laboratory.
- Emergency Response Plan  
Building Emergency Evacuation Plan  
Emergency Contact Information (ECI)  
*{Must be posted on entry door(s)}*  
Spill Control Plan  
Decontamination & Clean Up Plan  
Other...
- x) Internal Safety Reviews *{self-inspections to be conducted by project personnel}*
- The experimental facility will be subject to the standard safety audit and review (if available) of the laboratory.
- Procedure for Periodic Internal Safety Audit & Review:  
Schedule for Internal Safety Review:  
List all mechanism(s) to ensure compliance, abatement & accountability:

Guide to Project Safety Analysis (PSA)

---

- XI) **Safety Agreements** *(Signatures are required to document the commitment of each participant in maintaining the safe, healthful, and secure project environment)*

Signed By: \_\_\_\_\_ Location of Files: \_\_\_\_\_

Principal Investigator   
Researcher/Lab Technician  
Graduate Student   
Student Worker  
Other...

- XII) **Attachment Section** *(List all Attachments to this document, including:)*  
Refer to the Safety documents of the Laboratory.

Hazard Analysis Plan (HAP)  
Risk Assessment(s)  
Maps  
Floor Plan Drawings  
Standard Operating Procedures  
Training Plans  
Chemical Inventory  
Supplemental Information  
Other...